Exploring marine sponges and their associated microorganisms as a source of natural compounds

Margarida Costa

Thesis for the degree of Philosophiae Doctor

December 2018

UNIVERSITY OF ICELAND
SCHOOL OF HEALTH SCIENCES
FACULTY OF PHARMACEUTICAL SCIENCES

Leit að sjávarnáttúruefnum úr svömpum og samlífsörverum þeirra

Margarida Costa

Ritgerð til doktorsgráðu

Háskóli Íslands
Heilbrigðisvísindasvið
Lyfjafræðideild
Desember 2018

UNIVERSITY OF ICELAND
SCHOOL OF HEALTH SCIENCES

FACULTY OF PHARMACEUTICAL SCIENCES

Author´s address   Ana Margarida Pinto e Costa
Faculty of Pharmaceutical Sciences
School of Health Sciences
University of Iceland

Supervisor   Professor Margrét Thorsteinsdóttir
Faculty of Pharmaceutical Sciences
School of Health Sciences
University of Iceland

Co-supervisor   Professor Sesselja Ómarsdóttir
Faculty of Pharmaceutical Sciences
School of Health Sciences
University of Iceland

Doctoral committee   Professor Elín Soffia Ólafsdóttir
(other than   Faculty of Pharmaceutical Sciences
supervisors)   School of Health Sciences
University of Iceland

Dr. Marta Pérez
Natural Products Department
PharmaMar, Spain

Opponents   Professor Olivier Thomas
School of Chemistry, Marine Biodiscovery
National University of Ireland

Assistant Professor Benjamín Sveinbjörnsson
Faculty of Physical Sciences
School of Engineering and Natural Sciences
University of Iceland

Ágrip

Hafið hefur að geyma mikinn líffræðilegan fjölbreytileika er gríðarleg uppspretta lífvirkra efnasambanda með mikla möguleika á þróun nýrra lyfjasprota. Sjávarsvampar og samlífsörverur þeirra framleiða fjölbreytileg og einstök annarstigs efnasambönd. Markmið þessa verkefnis var að rannsaka efnainnihald og lífvirkni náttúruefna úr mismunandi sjávarasvömpum og samlífsörverum þeirra. Í því skyni var fimm svömpum safnað í hafinu í kringum Ísland, þremur svömpum úr Indó-Kyrrahafinu og tvær tegundir geislagerla (e.actinomycetes) safnað af svömpum, þeir ræktaðir upp og einangraðir. Hemjandi áhrif náttúruefnanna voru könnuð á krabbameinsfrumur, bakteríudrepandi áhrif í rækt og offituvirkni í sebrafiskalíkani.

Lífrænir úrdrættir úr fimm íslenskum sjávarsvömpum voru rannsakaðir. Óskautuðu úrdrættirnir innhéldu mikið af fituefnum. Efnagreiningaraðferð með háhraðavökvagreini tengdum massagreini (UPLC-QTOF-MS) var hámörkuð til að skima fyrir og fjarlægja (dereplication) þekkt náttúruefni til að auka skilvirkni við greiningu á skautuðum úrdráttum. Sjö þekktir núkleósíðar og núkleóbasar voru greindir í útdrættinum (e. dereplication) þegar leitað var eftir nýjum efnasamböndum. Þekktu efnasamböndin voru einangruð og efnabygging þeirra staðfest með ^{1}H-kjarnsegulgreiningu (NMR). Frekari rannsóknum á lífvirknileiddri einangrun og efnainnihaldi íslenskra sjávarsvampa var hins vegar hætt vegna þess að úrdrættirnir sem unnið var með sýndu enga lífvirkni í þeim prófunum sem framkvæmd voru.

Þrjár svamptegundir: *Acanthostrongylophora* sp., *Acanthodendrilla* sp. og *Acanthostrongylophora ingens* sem safnað var í Indó-Kyrrahafinu voru rannsakaðar. Nýtt haploscleridamín efni og köfnunarefnis-hliðstæðuefnasamband voru einangruð úr metanólúrdrætti *Acanthostrongylophora*. Tvö ný díterpen efnasambönd voru einangruð úr svampinum *Acanthodendrilla* og leiddi þessi uppgvötum í ljós að *Acanthodendrilla* var eina *Dendroceratida* ættkvíslin þar sem þessi efnasambönd höfðu ekki áður fundist. Fimm ný efnasambönd úr bisabólan-efnaflokknum voru einangruð og skilgreind úr svampnum *Acanthostrongylophora ingens*, ásamt eftirfarandi þekktum efnasamböndunum. Niðurstöður úr lífvirknimælingum sýndu að efnasambandið, 6-(1,5-dímetýl-1,4-hexadíenýl)-3-metýlbenzen-1,4-díol hafði

frumuhemjandi áhrif krabbameinsfrumur í rækt. Auk þess höfðu þessi bisabólan efnasambönd hamlandi áhrif í offituvirknilíkani í sebrafiskum.

Efnasambönd með tveimur flúorvirinín C hópum voru auðkennd í úrdráttum frá samlífsörverum svampa af geislagerlastofninum (e. Actinomycete) (DIL-12-02-135). Þessi efnasambönd voru auðkennd með massagreiningu og er þetta í fyrsta sinn sem þessi efnasambönd eru einagruð úr sjávarlífverum. Jafnframt voru tvö þekkt efni, mangrolide A og naphthoquinone, einangruð með aðstoð massagreiningaraðferðar úr öðrum geislagerlastofni (CP9-13-01-036). Niðurstöður sýndu að naphthoquinone hefur bæði krabbameinsfrumuhemjandi áhrif og sýklahemjandi áhrifa gegn *Staphylococcus aureus*.

Niðurstöður verkefnisins sýna að svampar og samlífsörverur þeirra eru rík uppspretta áhugaverðra og fjölbreyttra náttúruefna með mismunandi lífvirkni og því mikilvægt að halda áfram leitinni að nýjum og spennandi efnum úr lífverum í hafinu.

Lykilorð:

Sjávarnáttúruefni, sjávarsvampar, geislagerlar, annarstigs efnasambönd, lífvirkni

Abstract

The ocean represents a tremendous source of biologically active metabolites with great potential for the development of new pharmaceuticals. Marine sponges and their microbial associates are known as the most prolific source of structurally diverse and unique secondary metabolites. The present work aimed to explore the potential of different sponge and sponge-associated microorganisms as a source of natural compounds with possible pharmacological applications. Five sponge individuals collected in the Icelandic waters, three in the Indo-Pacific Ocean and two sponge-associated actinomycete strains were used for that purpose. Cytotoxic, anti-bacterial and anti-obesity activities were tested.

Organic extracts were prepared from the five sponges collected in Iceland. The apolar extracts were found to be rich in fatty acids. The UPLC-QTOF-MS method used for dereplication of the present natural compounds was successfully optimized in order to increase efficiency when analyzing polar extracts. Seven known nucleosides and a nucleobase were dereplicated. The compounds were isolated and their structure confirmed by ^{1}H-NMR. The Icelandic sponge's study was, however, discontinued due to the absence of promising extracts.

Three sponge specimens collected in the Indo-Pacific Ocean were studied: *Acanthostrongylophora* sp., *Acanthodendrilla* sp. and *Acanthostrongylophora ingens*. *Acanthostrongylophora* sp. methanolic extract resulted in the isolation of haploscleridamine and a new nitrogenated analog. *Acanthodendrilla* sp. was found to be the producer of two spongian diterpenes with novel structures. This discovery withdrew *Acanthodendrilla* of being the only *Dendroceratida* genus that had not been reported as a producer of this class of compounds. *Acanthostrongylophora ingens* revealed to be the producer of five new bisabolane related compounds, the previously reported 6-(1,5-dimethyl-1,4-hexadienyl)-3-methylbenzene-1,4-diol and 1-(2,4-dihydroxy-5-methylphenyl)ethan-1-one. The bioactivity studies showed that 6-(1,5-dimethyl-1,4-hexadienyl)-3-methylbenzene-1,4-diol have moderate cytotoxic activity against the tested cancer cell lines. Bisabolane-related compounds also demonstrated to have anti-obesity potential based on the zebrafish Red Nile assay.

The actinomycete strain DIL-12-02-135 mycelial cake was found to contain two group C fluvirucinins. Those compounds were obtained through mass spectrometry-guided isolation and represent the first isolation of this class of

compounds from marine sources. Another mass spectrometry-guided isolation carried out in the actinomycete strain CP9-13-01-036 yielded two known compounds: mangrolide A and a naphthoquinone. Naphtoquinone was shown to have both strong cytotoxic activity against the tested cell lines and anti-bacterial activity against *Staphylococcus aureus*.

The studied marine sponges and actinomycete strains resulted in several known and new compounds with valuable bioactivities. Marine sponges demonstrated, once again, to be a tremendous source of bioactive natural compounds.

Acknowledgments

I am very grateful for all the experience and knowledge acquired during this journey. I would like to thank, particularly, to my mentor Professor Margrét Thorsteinsdóttir for all the guidance, encouragement and advices during the past years. To my co-supervisor, Professor Sesselja Ómarsdóttir thanks for her continuous support and scientific input. Besides them, I would also like to thank my committee member Professor Elín Soffía Ólafsdóttir for her reviews, corrections and motivation.

A special acknowledgment goes to Marta Pérez, in PharmaMar. Thank you so much for the opportunity to be involved with that great company where marine natural products are the only focus, but more than that, thank you for all the scientific support. Your help was crucial for this work!

Still in PharmaMar, I would like to thank specially to Dr. Librada Cañedo for all the guidance during the work with microorganisms and to Dr. Rogélio Férnandez for all the NMR help. I would also like to thank everyone in the company that accepted me as one of them and that gave a bit of their time to listen to my doubts and answer my questions. Thank you so much Alfredo Rodríguez, Dr. Carlos Urda, Elena Gomez and Laura Coello for being great lab partners! Thanks to everyone else around that made those eight months so special!

I would like to thank all BluePharmTrain partners for the summer schools, workshops, conferences and meetings, from which we could network and have endless productive scientific discussions. The skills gained during those meetings were crucial for the conclusion of this Ph.D. A special acknowledgment goes to the coordinator of the project, Detmer Sipkema, who made a huge effort to connect the right people with incredibly different

backgrounds, together in this consortium. To the BluePharmTrain fellows: Agneya, Alex, Carla, Deepak, Eike, Erik, Georg, Johanna Gutleben, Johanna Silber, Maryam, Nele, Stephanie and Stephen, we were a special group. I have a profound admiration for each one of you, both as a person and as a scientist.

To all of my colleagues in Hagi, all the past and current, thank you for making this challenging period of my life more bright and colorful. Xiaxia, I will never be able to thank you enough for being the person that absolutely fulfilled my life in Iceland. You are the perfect lab partner and the perfect friend! Thanks for all the late night work together, the scientific discussions and complaints, the meals, travels and support when I was homeless! To all the other natural product´s geeks: Maonian, Sebastian and Sofia, thanks for all the science you carry around! To the kindest person that Hagi has ever seen: thanks Blanca for your friendship! I would also like to thank all the other Hagi colleagues and friends around: Agnieszka, Alexey, Chutimon, Helga, Ingólfur, Manisha, May, Mustafa, Natalia, Phennapha, Priyanka, Pui, Sunna, Svetlana, Tijana, Vivien and Zoltan. I would also like to thank Sigrún Sigurðardóttir for the continuous administrative support and to Auður Ágústsdóttir, who was always there to help. Thank you all!

I want to thank everyone in ArcticMass for giving me a different perspective of science. My sincere acknowledgments go to Finnur Eiriksson for his guidance and support. Thanks for the huge availability and help! To Unnur, thank you so much for the companionship during these years! It would have been completely different without your support and friendship! To Eydis, my sincere gratitude for being so welcoming. My first steps in the lab and in Iceland would have been more difficult without you. Thanks also to Martha and Yi!

To Ralph Urbatzka, in CIIMAR, Porto, Portugal, thank you so much for the help with the anti-obesity assays and also for getting me involved in other scientific projects.

To cousin Ana Osório, thanks for all the english revisions and corrections! Thanks also for all the video calls and advice.

To all the non-scientist friends I was able to make just because I started this adventure in Iceland, thank you so much for all the time spent together. My special gratitude to Bella, I´ve never felt so much at home like when I was living with you! To Adriana, Flor, Francis and Sara, thanks for being so special and making me feel the same!

To all the friends I left in Portugal that I constantly miss and wish I would see more often, thank you so much! Thanks for all the supportive words in the right moments and thanks for always believing in me. Thank you Bete, I am sure you are the one who suffers the most with my absence, but still you are always so positive! Thank you Bouça, Marisa, Sónia, Tiago and all the big and little ones you brought to our lives! Thank you Stef and Soraia for representing the real meaning of a long-distance relationship! To Aldo, Bruno, João Morais, Mafalda, Mariana, Raquel Castelo-Branco and Sandra, thank you so much for your crazy and insane friendship, just like scientists need to be! To Cristiana, thanks for the endless conversations when I go for a visit, just like if we had met the day before. To Ivone, thank you for being always so supportive and interested! To Sofia and Bruno, whom I met in Portugal and discovered their friendship in Iceland, thanks for always being around! To Pedro Leão, who will always be my eternal advisor, thank you for all the support!

I also want to leave my sincere gratitude to Fernando, who never lost his patience and has always been so supportive, even meeting me in the most stressful and busy period of my entire life.

Last, but not the least, I want to express my immense gratefulness to all my family members that have supported me from day number one. To aunt Manela for all her concerns and headaches. To aunt Zé for the immense support and talks at crucial moments. To my grandparents for their endless love and pride. To Cândida for all the details that always made me feel at home! To my mother and father for all the values they passed me and had revealed to be more important than ever! To my favorite person in this world: my best friend and young brother Nuno, thanks, mostly for being constantly teaching how to believe in my own capacities! You are the greatest!

To avó Palmirinha, the epitome of unconditional love. I am sure you would have been the proudest!

Contents

List of abbreviations

1D-NMR – One Dimensional Nuclear Magnetic Resonance

2D-NMR – Two Dimensional Nuclear Magnetic Resonance

ASW – Artificial Sea Water

ATCC - American Type Culture Collection

BuOH – *n*-butanol

CAD – Charged Aerosol Detector

COSY – Correlation Spectroscopy

DAD – Diode Array Detector

DEPT - Distortionless Enhancement by Polarization Transfer

DGGE - Denaturing Gradient Gel Electrophoresis

DHA - Docosahexaenoic Acid

DMSO - Dimethyl Sulfoxide

DNA – Deoxyribonucleic Acid

DPF – Days Post Fertilization

ECD – Electronic circular dichroism

ELSD - Evaporative Light Scattering Detector

EPA – Eicosapentaenoic Acid

ESI – Electrospray Ionization

ESIMS – Electrospray Ionization - Mass Spectrometry

EtOAc – Ethyl acetate

EtOH – Ethanol

FA – Formic Acid

FDA – Food and Drug Administration

FISH - Fluorescence in Situ Hybridization

FLD – Fluorescence Detector

Hex – Hexane

HMA – High Microbial Abundance

HMBC - Heteronuclear Multiple Bond Correlation

HPLC - High-Pressure Liquid Chromatography

HRESIMS – High Resolution Electrospray Ionization Mass Spectrometry

HRESITOFMS – High Resolution Electrospray Ionization Time-of-flight Mass Spectrometry

HSQC - Heteronuclear Single-Quantum Correlation

IgG1 - Immunoglobulin G1

iPrOH – Isopropanol

IR – Infrared

LC-MS - Liquid Chromatography coupled to Mass Spectrometry Detection

LC-MS/MS - Liquid Chromatography coupled to Tandem Mass Spectrometry Detection

LC-NMR - Liquid Chromatography coupled to Nuclear Magnetic Resonance Detection

LC-UV – Liquid Chromatography coupled to Ultraviolet Detection

LMA – Low Microbial Abundance

m/z - Mass-to-charge Ratio

MeCN – Acetonitrile

MeOH – Methanol

min - Minutes

MMA – Monomethyl auristatin E

MS – Mass Spectrometry

NCI – National Cancer Institute

NMR - Nuclear Magnetic Resonance

NOESY - Nuclear Overhauser Effect Spectroscopy

NP – Normal Phase

NP-VLC – Normal Phase Liquid Chromatography

PCR – Polymerase Chain Reaction

PLA2 - Phospholipase A2

ppm – part per million

QTOF – Quadrupole Time-of-flight

ROA – Raman Optical Activity

ROESY - Rotating frame Overhause Effect Spectroscopy

RP – Reverse Phase

RP-VLC – Reverse Phase Vacuum Liquid Chromatography

rRNA - Ribosomal Ribonucleic Acid

SEC – Size-Exclusion Chromatography

sp. – Species

SPE – Solid Phase Extraction

SRB – Sulforhodamine

TFA – Trifluoroacetic Acid

TLC – Thin Layer Chromatography

TOCSY - Total Correlation Spectroscopy

TOF – Time-of-flight

TSA – Tryptone Soya Agar

TSB – Tryptone Soya Broth

UPLC – Ultra Performance Liquid Chromatography

UV – Ultraviolet

VCD – Vibrational Circular Dichroism

VLC – Vacuum Liquid Chromatography

XRD – X-ray diffraction

List of figures

xix

List of tables

List of original papers

This thesis is based on the following original publications and manuscripts:

I. **Costa M.**, Liu, H.B., Eiriksson, F.F., Ómarsdóttir, S., Thorsteinsdóttir, M. New chromatographic method for an efficient dereplication of marine sponge nucleosides. (Publication submitted to Journal of Chromatography A).

II. **Costa M.**, Fernández, R., Pérez, M., Thorsteinsdóttir, M. Two new spongian diterpene analogues isolated from the marine sponge *Acanthodendrilla* sp.. Accepted for publication in Journal of Natural Product Research (DOI: 10.1080/14786419.2018.1548448)

III. **Costa M.**, Coello, L., Urbatzka, R., Pérez, M., Thorsteinsdóttir, M. New aromatic bisabolane derivatives from a marine sponge with lipid-reducing activity. (Manuscript will be submitted, as an invitation, to Marine Drugs in Marine Natural Products and Obesity Special Issue).

IV. **Costa, M.,** Zuñiga, P., Peñalver, A.M., Thorsteinsdóttir, M., Pérez, M., Cañedo, L.M., Cuevas, C. New fluvirucinin C1 and C2 produced by a marine-derived actinomycete. 2018 Natural product communications 12(5):679-682.

Additional book chapter:

I. Steinert, G., Stauffer, C.H., Aas-Valleriani, N. Borchert, E., Bhushan, A., Campbell, A., Mares, M.C., **Costa M.**, Gutleben, J., Knobloch, S., Lee, R.G., Munroe, S., Naik, D., Peters, E.E., Stokes, E., Wang, W., Einarsdóttir, E., Sipkema, D. BluePharmTrain – Biology and Biotechnology of Marine Sponges. In: Grand challenges in Marine Biotechnology, 2018, Springer International Publishing AG.

Declaration of contribution

The current Ph.D. project started in May 2014 as part of an Initial Training Network Marie Curie Action: BluePharmTrain.

The initial focus of the project was to find natural products in marine sponges collected in Iceland, from which resulted Paper I. That research work was planned and executed by Margarida Costa as was the results analysis. Hong-Bing Liu cooperated in the NMR analysis. The supervisors Margrét Thorsteinsdóttir and Sesselja Ómarsdóttir designed and guided the experiments. The scientific paper was written by Margarida Costa and read, reviewed and approved by all the authors.

A secondment of eight months in the industrial partner PharmaMar redirected the focus of the project to marine sponges and their associated microorganisms collected in the Indo-Pacific Ocean. Paper II resulted from that work. The research work was planned and executed by Margarida Costa as was the results analysis, with Rogélio Fernandéz guidance in the structural elucidation. The responsible researcher, Marta Pérez guided the experiments. The scientific paper was written by Margarida Costa and read, reviewed and approved by all the authors.

The study of microorganisms, also in PharmaMar, was planned and guided by Librada Cañedo. From that work resulted Paper IV. Margarida Costa executed the experiments and results analysis. Paz Zúñiga and Ana Peñalver, in the microbiology department, grown the strain studied. The scientific paper was written by Librada Cañedo and Margarida Costa and read, reviewed and approved by all the authors.

After the secondment in PharmaMar, several sponge samples from the Indo-Pacific Ocean were shipped to the University of Iceland. From the study of those sponges resulted Paper III. Margarida Costa planned and executed the isolation and structure elucidation of the compounds. The anti-obesity assays were performed in collaboration with Ralph Urbatzka. Marta Pérez and the supervisor Margrét Thorsteinsdóttir designed and guided the experiments. The scientific paper was written by Margarida Costa and read, reviewed and approved by all the authors.

In other publications, Margarida Costa contributed for the book chapter *BluePharmTrain – Biology and Biotechnology of Marine Sponges*, writing the

Isolation and purification of Sponge Secondary metabolites sub-chapter. This sub-chapter was written under Margrét Thorsteinsdóttir, Sesselja Ómarsdóttir and Marta Pérez guidance. The work was a collaboration of all BluePharmTrain fellows.

1 Introduction

1.1 History of Natural Products Drug Discovery

Since early times, mankind has felt the need for healing and treating injuries and diseases. At least 60,000 years back, traditional medicine emerged with the use of plants, animals and microorganisms as an empirical attempt to treat and prevent human diseases [1]. Many of those medicines, such as traditional Chinese medicine, Ayurveda, Kampo, traditional Korean medicine and Unani, have been used throughout the world for hundreds of years and evolved into regulated systems of medicine that are in use nowadays [2]. Today, chemical, pharmacological and clinical studies of ancient medicines represent the basis for the discovery of new drugs.

In the early 1800s, morphine was isolated from the opium plant and became the first isolated active compound being used for pharmacological purposes [3]. This represented a turning point for traditional medicine. During the 19th and 20th centuries, many active compounds were isolated from natural sources, in some cases based on traditional uses.

The 1980s brought the expansion of the chemical synthesis. Combinatorial chemistry emerged as an accelerator in the process of searching for new effective medicines. The idea of obtaining big libraries of new compounds in short periods of time and doing fast screenings for several biological activities revolutionized drug discovery. Also, the modern advances in hardware and software have allowed the development of a vast technology platform which combinatorial chemistry could take benefit of [4]. In the early 1990s, with the development of PCR technique and nucleic acid synthesizers, biosynthetic techniques became also an accelerating tool for combinatorial chemistry. Thousands of new compounds were discovered due to the combination of all these modern techniques and were screened in many biological assays. However, the delivery of new pharmaceuticals into the market was not proportional to the immense increment in new compounds. The kinase inhibitor sorafenib (Nexavar; Bayer Pharmaceuticals) was approved in December 2005 to be used in the treatment of advanced renal cell carcinoma [5] and was the only compound resultant from the combinatorial programs approved by Food and Drug Administration (FDA).

In fact, natural products have been selected, through natural evolution, to interact with specifically targeted macromolecules in a specific organism. This

resulted in more diversity and chemically complex structures, contributing strongly to the appearance of new molecules with drug-like properties [2].

Nowadays, it seems clear that the more efficient strategy for the development of new pharmaceuticals is going back to the basics. Researchers are, again, focusing drug discovery in the study of natural products, trying to meet the urgent need to find and develop new effective drugs.

1.1.1 The Ocean as an Unlimited Source of Natural Compounds

Covering more than 70% of the earth surface and with a mean depth over 3000 meters [6], oceans host an extraordinary vast chemical and biological diversity. From the 36 animal phyla taxonomically identified in nature, 34 can be found in the marine environment [7]. On some coral reefs, the density of species is believed to be much higher than the biodiversity observed in tropical rainforests [8]. This overwhelming marine habitat, with macro and microorganisms, continuously suffering a high selective pressure, due to the underwater physical, chemical and predatory conditions, forces them to develop highly specific and effective mechanisms of defense. This leads to the production of unusual and structurally complex secondary metabolites [8]. The majority of all known marine organisms have been investigated for their capacity to produce natural products and concluded to represent a valuable source of unknown compounds with great potential, not only as pharmaceuticals but also with other bioactivities precious for the human being such as nutritional supplements, cosmetics or agrochemicals [9-12]. As shown in Figure 1, pharmacology and toxicology represent the main topic whithin the publication of marine isolated natural compounds, but they are also published as part of many other fields like agriculture, engineering or environmental science.

Fundamentally, marine natural compounds often differ from the ones isolated from terrestrial sources. In contrast to terrestrial, marine organisms often produce halogenated secondary metabolites [13, 14]. From those halogenated marine metabolites, the majority contains bromine, which is especially abundant in the marine environment, whereas terrestrial organisms preferably synthesize chlorinated compounds [14]. The marine algal enzyme vanadium bromoperoxidase plays a crucial role oxidizing bromide for its incorporation into marine organic compounds [15].

2
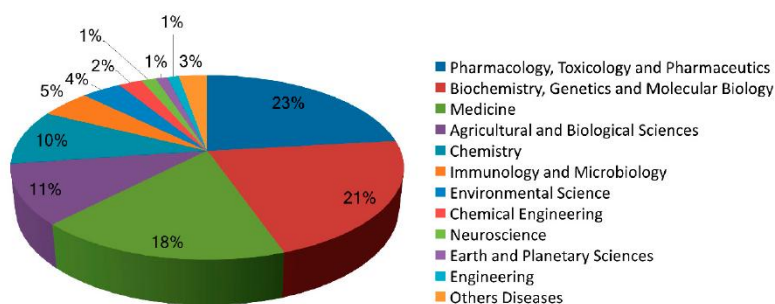
Figure 1 - Relevance of marine natural compounds published by subject area up to January 2017 [16].

In the 1950s, with the isolation of two bioactive nucleosides [17], the value of marine natural products was understood by scientists, marking the beginning of systematic screenings on marine organisms. Despite this late discovery, the expansion was tremendous. Blunt *et al.* publish every year a review compiling the late discovered marine natural compounds [9, 18, 19]. MarinLit is a marine natural compounds database, initially established by Blunt and Munro and later acquired by the Royal Society of Chemistry. This database currently contains approximately 30,000 entries [20]. Those indicators clearly place marine organisms on top of the richest sources of novel drug leads.

1.1.2 Marine Pharmaceuticals Pipeline

The pharmaceuticals pipeline is very long. From drug discovery to its market release, an enormous amount of time and money are spent. From dozens of thousands of new natural compounds discovered, only very few reach the stage of clinical trials in a process that lasts approximately 15 years as shown in Figure 2.

Currently, the marine pharmaceuticals clinical pipeline consists of seven FDA approved drugs, nine drugs in phase I of clinical trials, ten in phase II and six in phase III [21], as it is demonstrated in Table 1. Figure 3 illustrates the chemical structure of all isolated marine natural compounds that led to commercialized drugs. The first case of success regarding the clinical pipeline of marine pharmaceuticals can be traced to the 1950s. Bergmann and Feeney reported the isolation and structure elucidation of the two arabidose nucleosides spongothymidine and spongouridine from the Caribbean sponge *Tethya crypta* [22]. The antiviral properties of these two compounds were demonstrated [23] leading to the disprove of the ongoing theory stating that for

3

a nucleoside to have biological activity, the sugar moiety should be either a ribose or a deoxyribose. The synthesis of analogs of those two nucleosides led to the development of the compound Ara-A (Vidarabine), with enhanced antiviral activity against herpes viruses, and to an antitumor compound, Ara-C (Cytarabine) effective in acute lymphoid leukemia. Vidarabine was the first antiviral to be approved for the systematic treatment of herpes virus infection; however, it was discontinued because of new and more effective antiviral agents have appeared [24]. Cytarabine, on the other hand, is currently still a chemotherapy agent used mainly in the treatment of white blood cell cancers [25].
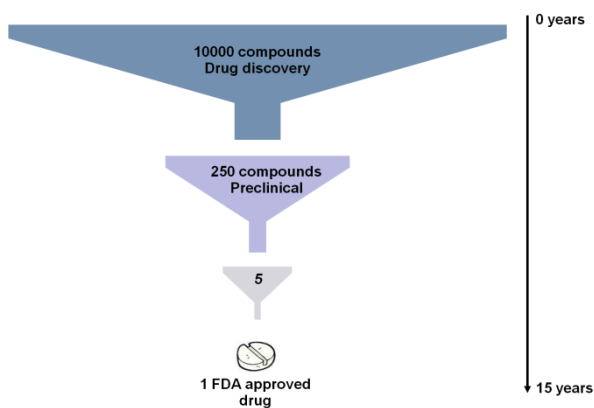
Figure 2 - Timeline and success rate of the process from the discovery of a compound until its approval as a drug.

Table 1 - Current marine pharmaceuticals pipeline [21].

Clinical status		Compound	Trademark (Company/Institution)	Marine organism	Chemical class	Disease / Disease area
FDA - approved	**2015**	Trabectedin (ET-743)	Yondelis® (PharmaMar)	Tunicate	Alkaloid	Soft tissue sarcoma and ovarian cancer
	2011	Brentuximab vedotin (SGN-35)	Adcetris® (Seattle Genetics)	Mollusk/ cyanobacterium	Antibody-Drug Conjugate	Anaplastic large T-cell systemic malignant lymphoma, Hodgkin's disease
	2010	Eribulin Mesylate (E7389)	Halaven® (Eisai Inc.)	Sponge	Macrolide	Metastatic breast cancer
	2004	Omega-3-acid ethyl esters	Lovaza® (GlaxoSmithKline)	Fish	Omega-3 fatty acids	Hypertriglyceridemia
		Ziconotide (ω-conotoxin MVIIA)	Prialt® (Jazz Pharmaceuticals)	Cone snail	Peptide	Severe chronic pain
	1976	Vidarabine (Ara-A)	Vira-A® (discontinued)	Sponge	Nucleoside	Herpes Simplex virus
	1969	Cytarabine (Ara-C)	Cytosar-U® (Pfizer)	Sponge	Nucleoside	Leukemia
Phase III		Plinabulin (NPI-2358)	NA (BeyondSpring Pharmaceuticals)	Fungus	Diketopipera-zine	Lung cancer, brain tumor
		Lurbinectedin (PM01183)	NA (PharmaMar)	Tunicate	Alkaloid	Ovarian, breast and lung cancers
		Depatuxizumab mafodotin (ABT-414)	NA (AbbVie)	Mollusk/ cyanobacterium	Antibody-Drug Conjugate	Glioblastoma, pediatric brain tumors
		Tetrodotoxin	Tectin® (WEX Pharmaceutical Inc.)	Pufferfish	Alkaloid	Chronic pain
		Polatuzumab vedotin	NA (Genentech/Roche)	Mollusk/ cyanobacterium	Antibody-Drug Conjugate	Lymphoma, leukemia
		Marizomib (Salinosporamide A; NPI-0052)	NA (Triphase)	Bacterium	Beta-lactone-gamma lactam	Lung and pancreatic cancers, melanoma, lymphoma, myeloma

Clinical status	Compound	Trademark (Company/Institution)	Marine organism	Chemical class	Disease / Disease area
	GTS-21 (DMXBA)	NA	Worm	Alkaloid	Schizophrenia, Alzheimer disease, attention deficit hyperactivity disorder, endotoxemia, sepsis, vagal activity
	AGS-16C3F	NA (Agensys & Astellas Pharma)	Mollusk/ cyanobacterium	Antibody Drug Conjugate	Renal cell carcinoma
	Plocabulin (PM060184)	NA (PharmaMar)	Sponge	Polyketide	Solid Tumors
	ABT-414 EGFRvIII - MMAF	NA (AbbVie)	Mollusk/ cyanobacterium	Antibody-Drug Conjugate	Breast cancer, melanoma
	Glembatumumab Vedotin (CDX-011)	NA (Celldex Therapeutics)	Mollusk/ cyanobacterium	Antibody-Drug Conjugate	Breast cancer, melanoma
Phase II	Agensys & Astellas Pharma Vedotin	HuMax®-TF-ADC (GenMab)	Mollusk/ cyanobacterium	Antibody-Drug Conjugate	Ovary, endometrial, cervix, bladder, prostate, esophagus and lung cancers, cancers of head and neck
	Enfortumab Vedotin ASG-22ME	NA (Seattle Genetics)	Mollusk/ cyanobacterium	Antibody-Drug Conjugate	Tumors, neoplasms, urothelial cancer
	GSK2857916	NA (GlaxoSmithKline)	Mollusk/ cyanobacterium	Antibody-Drug Conjugate	Multiple myelomas
	Bryostatin	NA (Neurotrope BioScience)	Bryozoan	Macrolide Lactone	Alzheimer disease
	Telisotuzumab vedotin (ABBV-399)	NA (Abbvie)	Mollusk/ cyanobacterium	Antibody-Drug Conjugate	Breast cancer, melanoma
Phase I	ABBV-085	NA (Abbvie)	Mollusk/ cyanobacterium	Antibody-Drug Conjugate	Solid tumors
	ASG-67E	NA (Astellas & Seattle Genetics)	Mollusk/ cyanobacterium	Antibody-Drug Conjugate	Refractory and relapsed lymphoid malignancies

Clinical status	Compound	Trademark (Company/Institution)	Marine organism	Chemical class	Disease / Disease area
	ASG-15ME	NA (Astellas & Seattle Genetics)	Mollusk/ cyanobacterium	Antibody-Drug Conjugate	Urothelial cancer
	CDX-014	NA (Celldex Therapeutics)	Mollusk/ cyanobacterium	Antibody-Drug Conjugate	Renal carcinoma
	ARX-788	NA (Ambrex & Zhejiang Medicine)	Mollusk/ cyanobacterium	Antibody-Drug Conjugate	Breast and gastric cancers
	SGN-CD48A	NA (Seattle Genetics)	Mollusk/ cyanobacterium	Antibody-Drug Conjugate	Myeloma
	XMT-1536	NA (Mersana Therapeutics)	Mollusk/ cyanobacterium	Antibody-Drug Conjugate	Solid tumors
	XMT-1522	NA (Mersana Therapeutics)	Mollusk/ cyanobacterium	Antibody-Drug Conjugate	Breast, lung and gastric cancers
	ALT-P7	NA (3SBio & Alteogen)	Mollusk/ cyanobacterium	Antibody-Drug Conjugate	Breast and gastric cancers

NA: Not available

Prialt® was initially isolated from the marine snail *Conus magus* as ω-conotoxin MVIIA or ziconotide. Prialt® is a potent analgesic and appeared with a novel mechanism of action that involves selective blockage of pre-synaptic neuronal N-type calcium channels in the spinal cord [26]. Prialt® got FDA approval in 2004 and it still remains today as the only selective N-type channel blocker approved for clinical use.

Lovaza® was approved in 2004 by FDA. It can be obtained from fish oils and consists in concentrated ω-3 polyunsaturated fatty acids, mainly eicosapentaenoic acid, 20:5(n - 3) (EPA), and docosahexaenoic acid, 22:6(n - 3) (DHA). Lovaza® is used to treat adults with severe hypertriglyceridemia [27].
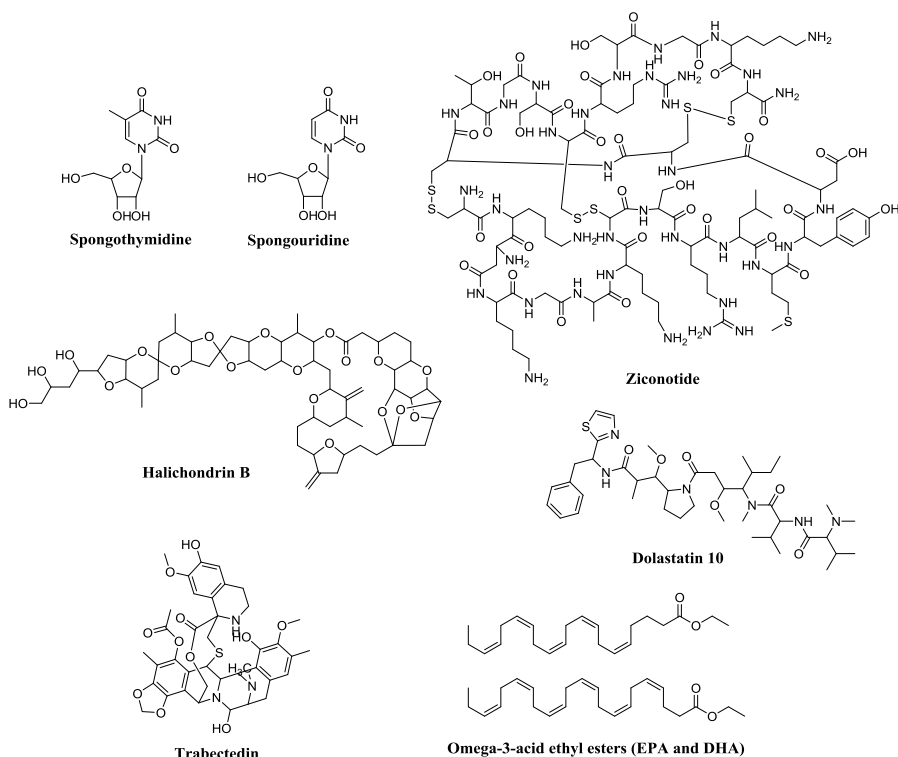
Figure 3 - Planar chemical structures of the marine natural compounds that led to commercialized drugs.

Halaven® appeared next, being approved by the FDA in 2010. It is a synthetic analog of halichondrin B, developed by Eisai Pharmaceuticals. Halichondrin B is a polyether macrolide with potent anticancer activity originally isolated from the marine sponge *Halichondria okadai* [28]. Halaven®´s interfere in the cell cycle, inhibiting microtubule growth and sequestering tubulin that causes G2-M cell cycle arrest and apoptosis [29]. The drug is approved for the treatment of metastatic breast cancer in patients who have progressed following prior chemotherapy [30].

Adcetris® is an antibody-drug conjugate and a synthetic analog of dolastatin 10, originally isolated from the sea hare *Dolabella auricularia* [31]. It conjugates the chimeric IgG1 antibody cAC10, the microtubule-disrupting agent monomethyl auristatin E (MMAE) and a protease-cleavable linker that covalently attaches MMAE to cAC10. MMAE binds to tubulin, disrupting the microtubule network and leading to cell cycle arrest and apoptosis [32]. Adcetris® was approved by FDA in 2011 for the treatment of anaplastic large T-cell systemic malignant lymphoma and Hodgkin's disease [33].

At last, in 2015 trabectedin was approved as Yondelis®. The alkaloid was originally extracted from the tunicate *Ecteinascidia turbinate* and introduced in the market by PharmaMar [34]. It is used for the treatment of soft tissue sarcoma and relapsed platinum-sensitive ovarian cancer [35].

Table 1 shows a detailed description of the current marine pharmaceuticals pipeline. A close look into the pipeline shows the high numbers of, not only approved marine drugs but also isolated compounds that are currently in clinical trials. The number of candidates to enter those clinical trials in a near future is expected to increase once marine natural compounds are in constant study and development and the need for new effective drugs becomes drastically urgent.

1.1.3 Statistics on Marine Natural Products

Approximately 30,000 structurally diverse marine metabolites have been isolated and characterized [20]. The number of new marine natural compounds increased dramatically to an average of, approximately, 1,600 per year over the last two decades, as illustrated in Figure 4a [36], with the greatest increase in the 1980s and remaining relatively constant since then. This is coincident with the development of instrumentation such as chromatographic techniques, NMR spectroscopy, and mass spectrometry as well as the invention of 2D-NMR [36]. The development of these techniques allowed a chemical characterization with a high degree of confidence and

with a little amount of material needed (below mg). This is reflected by the low percentage (1.4%) of corrections to previous publications across all marine natural products [37].

A biogeographic analysis revealed that marine compounds have been isolated from organisms collected from all over the globe. Japanese surrounding waters, including Okinawa, were the ones from which the higher number of natural compounds was isolated. This was followed by Chinese surrounding waters, as illustrated in Figure 4b [9].
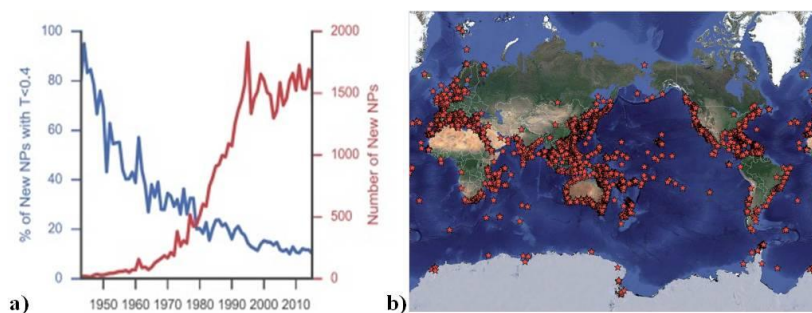
Figure 4 - Statistics on marine natural compounds. **a)** Percentage/Number of novel compounds published per year (adapted from Pye *et. al*, 2017 [36]). **b)** All collection sites leading to natural products isolation from 1965 to 2014 [9].

Regarding the source, the phyla *Porifera* appears to be the most prolific and *Cnidaria* is the one appearing next [38]. Additionally, macroalgae and microorganisms are also major sources of natural compounds [38]. In contrast to macro, microorganisms represent promising sources of natural compounds due to the sustainable and easy production of large quantities of metabolites by large-scale cultivation of the source organisms. A study performed in marine natural compounds isolated on the year of 2003 revealed that the relative incidence of any kind of bioactivity was greatest on green algae, followed by tunicates, echinoderms and sponges. However, in absolute numbers of isolated natural compounds, sponges are still the leaders [39].

1.2 Marine Sponges

Marine sponges had established a stable relationship with the environment, remaining, from an evolutionary point of view, as one of the oldest metazoan phylum existing today. A phylogenetic debate is currently open among the evolutionists about which was the first group, *Porifera* or *Ctenophora*, to

branch off the evolutionary tree as shown in Figure 5. Despite that *Porifera* has always been considered the simplest phylum, recent data supports the evidence that *Porifera* is more closely related to *Bilateria* and *Cnidaria* than *Ctenophora* [40]. Nevertheless, it is clearly accepted that at least 640 million years ago, sponges branched into a separated phylum - *Porifera* [41].

The human interest in sponges has been reported ages ago in ancient civilizations, such as in Crete-Minoan culture (1900 to 1750 BC) when sponges were used as decorations [42]. The use of bath sponges by Greeks and Romans was popular in the Mediterranean area and it spread out across Europe during the Middle-Ages and Renaissance [42]. Documents dating back to Hippocrates (460 to 370 BC) described the application of sponges on healing human injuries [43].
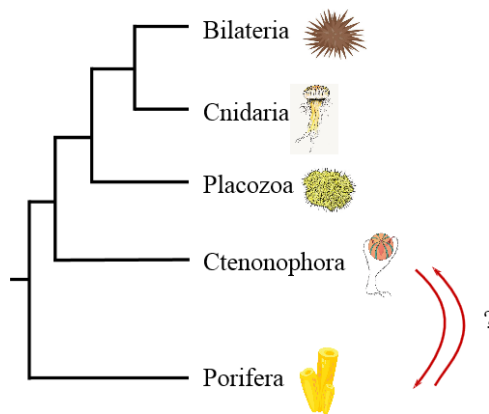
Figure 5 - Simplified scheme showing the phylogenetic position of sponges. The current query about the first phylum branching off is highlighted.

Sponges are exclusive aquatic animals, appearing in environments that vary from polar [44] to tropical [45] and play a crucial role in the maintenance of benthic ecosystems, in some cases occupying up to 80% of the available surfaces [46]. Sponges are known to grow in both fresh and marine waters. Adult marine sponges are largely sessile, living anchored to a non-mobile substrate or to other organisms [47].

Morphologically, sponges present a huge diversity of structures, sizes, shapes and colors. They are found, for instance, cushion-shaped, cup-shaped and branching. Sizes can range from several millimeters (crusts) to meters. Their consistency can be soft, compressible and fragile or rock hard [47].

Despite the wide variety of sponge morphologies, most of them are built upon the same simple body plan seen in Figure 6. Sponges are filter-feeders, pumping seawater through numerous pores – ostia - located on the external body wall. Instead of organs, muscles and sensory cells, sponges possess a structured body disposition based on totipotent cells, which are capable of differentiating and thus playing specific and independent functions within the sponge body [48]. Pinacoderm, the external cell layer, is formed by pinacocytes that are responsible for maintaining the structure and size of the sponge. Choanocytes, on the other side, are located in the inner layer and use their flagella to pump water through the ostia and the sponge aquiferous system, thereby filtering food particles such as bacteria and other microorganisms. Those are further transferred to the mesohyl, where amoebocytes carry out phagocytosis to ingest the food particles [49]. The mesohyl of many sponge species also hosts a dense, diverse and very specific microbial community that has found a way to avoid phagocytosis and in some cases is engaged in a close relationship with its host. Additional structures providing mechanical stability, called spicules, are also found within the mesohyl and form the "skeleton" of the sponge [46]. The general arrangement of this skeleton is a characteristic used for taxonomic identification. Spicules type, shape and sizes are also characteristics used to differentiate between sponge species.

The reproduction patterns of sponges can range from asexual by budding of body parts to sexual reproduction by fertilizing eggs. Some sponge species are hermaphroditic, producing both eggs and sperm, but at separate times to avoid self-fertilization. After release, the larvae swim for a short period to find a suitable substratum to settle until the adult phase [50].
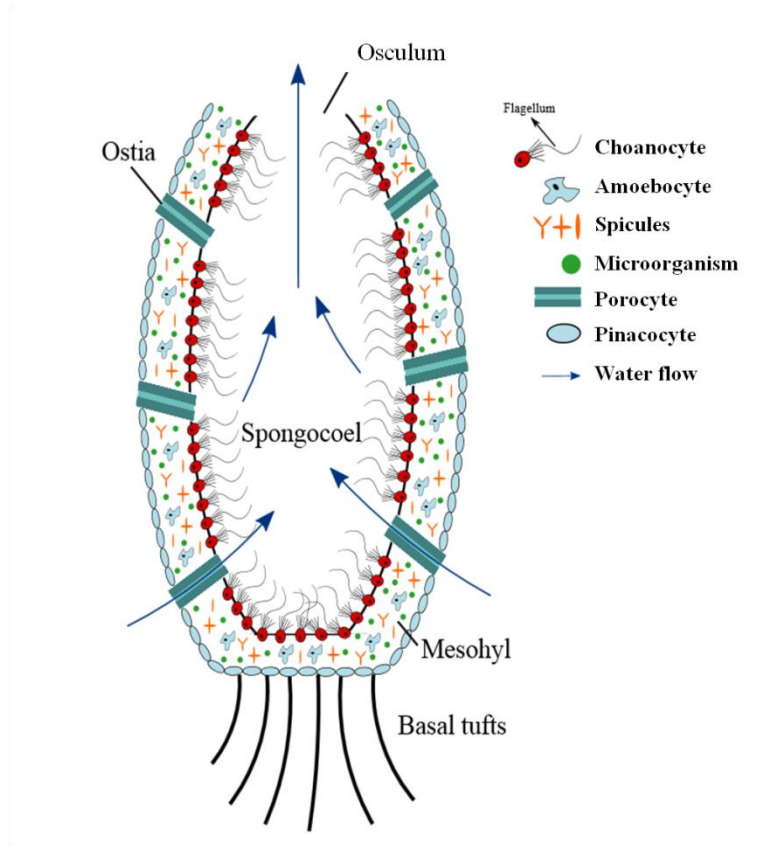
Figure 6 - Basic sponge body plan and main sponge cell types. Arrows show the water flow direction through ostia (in) and osculum (out). Microorganisms appear in mesohyl, together with other specialized cells and structures, like spicules.

Taxonomically, *Porifera* is a very diverse phylum containing three major classes: *Hexactinellida* (glass sponges), *Calcarea* (calcareous sponges), and *Demospongiae* (demosponges), with the last group containing the great majority of described species [51]. To the date, there are 9,082 sponges species registered in World Porifera Database, among almost 20,000 different taxon names [52]. However, every year, a large number of sponges are still being described and it is estimated that the number of accepted sponge species will rise to at least 12,000 by the end of the 21st century [51].

Hexactinellida and *Calcarea* are very small in numbers, consisting of 5 to 8% of the total sponge diversity each [53, 54]. *Calcarea* is an exclusively marine class and all species present a viviparous mode of reproduction [54]. Their taxonomy based on morphology is usually a big challenge for taxonomists as specimens are generally relatively small, colorless and live in

habitats with difficult access. They possess a skeleton entirely composed of calcareous spicules (calcium carbonate, $CaCO_3$), making *Calcarea* unique when compared to all other sponges species [54]. On the other hand, *Hexactinellida* is characterized by its siliceous spicules (silicon monoxide, SiO) of hexactinic, cubic symmetry, or derived shapes, and an absolute lack of calcareous minerals. *Hexactinellida* species are also exclusively marine and found in deep-water environments [54]. *Demospongiae* is the largest class of sponges and therefore, also the most diverse class. Sponges belonging to this class appear as encrusting, massive, lobate, tubular, branching, flabellate, cup-shaped or excavating sponges. Their skeleton is composed of spongin fibers and/or siliceous spicules. *Demospongiae* are mostly marine but several species may occur in freshwater habitats [55].

1.2.1 Marine Sponge-Associated Microbes

The interest in sponge-microbe associations appeared in the 1970s when it was reported in detail for the first time [56, 57]. Since then, it has been rising exponentially. Despite mutual symbiosis being commonly accepted, the exact nature of sponge-microbes association remains unclear. To the sponge, microbes can represent a nutritional source of nitrogen, carbohydrates and amino acids, either directly by intracellular digestion, or indirectly, by translocation of metabolites [58]. It is reported that microorganisms maintain the sponge rigidity [59] and that they are part of the host chemical defense against predators and biofouling by other micro- and macro-organisms [60, 61]. Microorganisms benefit from excreted ammonia from the sponge and take advantage of the rigid structure that the sponge represents [62]. Microbes can also represent pathogens or parasites to the sponge [49].

The associated microbial community can represent up to 40% of sponge tissue volume [56], appearing in orders of 10^8-10^{10} bacteria per gram of sponge wet weight. These values exceed bacterial concentrations in seawater by two to four magnitudes [62]. Microorganisms belonging to the three domains of life (*Bacteria*, *Archaea* and *Eukarya*) have been described as being associated with marine sponges [49].

The microbe's distribution within the sponge body follows a general pattern that suits their characteristics. The outer layers, that receive more light, are often populated with photosynthetic organisms, such as cyanobacteria or eukaryotic algae [63]. The mesohyl contains the greatest majority of both autotrophic and heterotrophic microorganisms which are mostly located extracellularly but can also appear inside of the cells [62].

Considering that the sponge microbiome is much more consistent over time than the microbiome in the surrounding seawater [64], the mesohyl seems to represent a stable habitat for the sponge-associated microbes.

Some sponge species, particularly demosponges, harbor extraordinarily dense and diverse microbial communities. These types of sponges are termed *high-microbial-abundance* (HMA) sponges or *bacteriosponges* and can host 10^8-10^{10} microbial cells per gram of sponge wet weight [62]. Other species have the mesohyl largely free of microorganisms and the abundance of microorganisms reflects that of the surrounding seawater: 10^5–10^6 microbial cells per gram of sponge wet weight [62]. These species are commonly called *low-microbial abundance* (LMA) sponges. HMA and LMA can coexist in the same habitat, but the reason for them to present these different microbial abundances is yet unknown. However, it seems that morphology is a determining factor: HMA sponges are frequently large and massive and generally have a firm touch, while LMA sponges are generally smaller and feel fragile [65].

The cultivation of sponge-associated microorganisms has been a challenge since its discovery in the 1970s. In the 1990s, it became accepted that only, approximately, 1% of the sponge microbiome was actually culturable [66]. That revealed the importance of finding new culture-independent approaches that would enable access to the remaining 99% present biodiversity. Until close to the end of the millennium very little progress was made in this field, however, it became clear that marine sponges are one of the richest producers of secondary metabolites with biological activity and that, at least some of them, were actually of microbial origin [67]. This made sponges an even more interesting target for researchers and led to a boom in marine sponge´s research in the following years.

The development of cultivation-independent techniques revolutionized sponge-microbial ecology. Early studies using 16S ribosomal ribonucleic (rRNA) or deoxyribonucleic (rDNA) acid analysis, fluorescent *in situ* hybridization (FISH), gradient gel electrophoresis (DGGE) or clone library construction led to the introduction of the concept of the rare microbial biosphere. In these rare microbial biospheres, a small number of abundant taxa dominate the microbial community, but the great diversity is composed of thousands of low abundance taxa [68].

One of the first studies using these novel molecular techniques aimed to compare sponge-derived sequence data from both culture-dependent and

independent studies [69]. From 190 sponge sequences, the authors were able to identify 14 sponge-specific clusters and they were the first workgroup to come up with the concept of a rare microbial community in sponges. They found that 70% of all sponge-derived sequences belonged to a single cluster and that those sequences were spread through several bacterial phyla: *Proteobacteria*, *Nitrospira*, *Bacteroidetes*, *Cyanobacteria*, *Actinobacteria*, *Acidobacteria* and *Chloroflexi* [69]. Later, several studies involving the same experimental approach supported the finding of sponge-specific microorganism lineages [62] and the sponge candidate phylum 'Poribacteria' was proposed [70]. Sponge-specific clusters are defined as sponge-derived groups of at least three 16S rRNA gene sequences which (i) are more similar to each other than to sequences from other non-sponge sources; (ii) are found in at least two host sponge species and/or the same host species from different geographic locations; and (iii) cluster together independently of the phylogeny method used in the study [69].

So far, 32 different bacterial phyla and candidate phyla have been identified in sponges [71]. Besides the proposed 'Poribacteria', *Proteobacteria* (*Alpha*-, *Beta*-, *Gamma*- and *Deltaproteobacteria*), *Chloroflexi*, *Acidobacteria*, *Actinobacteria*, *Cyanobacteria*, *Verrucomicrobia*, *Fusobacteria*, *Nitrospira*, *Firmicutes*, *Spirochaetes*, *Bacteroidetes*, *Gemmatimonadetes* are frequently found [49, 71, 72]. It is interesting to note that 'Poribacteria' have been found in sponges originated from very different geographic locations [70, 73].

Eukaryotic organisms, including dinoflagellates and diatoms, also occur in sponges, whereas diatoms are particularly common in polar sponges [74, 75]. Marine fungi isolated from sponges also present an incredible diversity [76-78] and their isolates are receiving increased research attention due to their promising biotechnological potential [77, 78].

The interest in sponge microbial communities was supported through the belated discoveries about the origin of secondary metabolites, originally thought to have been derived by the sponge itself [79]. Due to the various and often chemically mediated interactions occurring between microorganisms and sponges, it is reasonable to predict that the microbial communities contain particularly high amounts of bioactive secondary metabolite producing strains [80]. Polyketides and non-ribosomal peptides are two groups of compounds exclusively known as being produced by microorganisms [81], however, their structural similarities with some sponge isolated secondary metabolites, suggested a microbial origin of these

compounds. Initial studies were based on tissue dissociation analysis of individual cell populations. The bioactive compounds theopalauamide and swinholide A, for instance, were found in different bacterial cell populations of the marine sponge *Theonella swinhoei* [82]. With the recent advances in genome sequencing techniques, those became the methods of choice. Using single-cell genomics '*Candidatus Entotheonella*' sp. was identified as the producer of the cytotoxic compound calyculin A in the marine sponge *Discodermia calyx* [83].

1.2.2 Marine Sponge Natural Compounds

Chemical diversity usually comes together with biological diversity. Regarding the number of sponge species described, together with huge numbers of associated microbes, it is expected that a plethora of chemical entities isolated from them. In fact, today´s marine natural products discovery is centered in *Porifera* and a statistical study from Blunt and co-workers [18], illustrated in Figure 7, showed that from 1971 to 2015 *Porifera* was the most collected phylum for chemical-related studies. The high collection rates can be explained, not only by the fact that they are usually colorful and appear in peculiar shapes allowing an easy identification and differentiation from the other species, and also because sponges are easily accessible by scuba diving, and, more significant, they are available in substantial amount of biomass, allowing chemical isolations. Around 250 new natural compounds are isolated per year from Porifera [84], however, as seen before, sponges establish a close relationship with their associated microbes and the large chemical diversity found in sponge natural compounds can be explained by the fact that some of the molecules are a consequence of this association and a combination of both sponge and microorganism biosynthetic pathways.

Marine sponge-derived secondary metabolites have been shown to exhibit a diverse range of biological activities that include antifungal, cytotoxicity, anti-inflammatory and antibacterial [85]. The marine sponge isolated compounds can be categorized into four common structural groups: peptides, polyketides, alkaloids and terpenes [86].
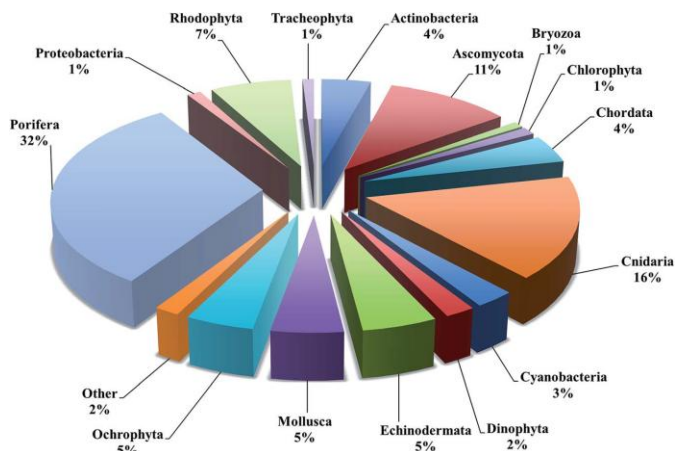
Figure 7 - Distribution by phylum of the collection of marine organisms resultant in the isolation of secondary metabolites, from 1971 to 2015 [18].

Marine sponge-derived peptides represent a significant study field, offering an incredibly high structural diversity when compared with other sources. The structural variations appear in both cyclic and linear forms, with unusual amino acids that are unique and specific to marine organisms [86].

The first sponge isolated peptide, discodermin A, was reported in 1985 by Matsunaga and co-workers from the marine sponge *Discodermia kiiensis* as having antibacterial properties [87]. Generally, discodermin peptides structures contain 13 to 14 amino acids, both common and uncommon, and cyclize through the lactonization of threonine, forming a macrocycle. Since the isolation of discodermin A, many sponge peptides have been reported, like halicylindramides, which have structures very similar to discodermins. Halicylindramides were isolated for the first time from *Halichondria cylindrata* and since then, have been reported as having antifungal [88, 89], cytotoxic [88] and human farnesoid X receptor (hFXR) antagonistic activities [90].

Jaspamide is another sponge peptide whose isolation represented a mark for sponge natural compounds. It was initially isolated from *Jaspis* sp. as an insecticidal and antifungal depsipeptide and represented the first of its class: cyclic depsipeptides with a propionate unit and two rare β-tyrosine amino acids. Orbiculamide A is also a sponge cyclic peptide containing three new unusual amino acids: 2-bromo-5-hydroxytryptophan, theonalanine and theoleucine. It was isolated from *Theonella* sp. and shows cytotoxic activity against P388 murine leukemia cells [91].

18
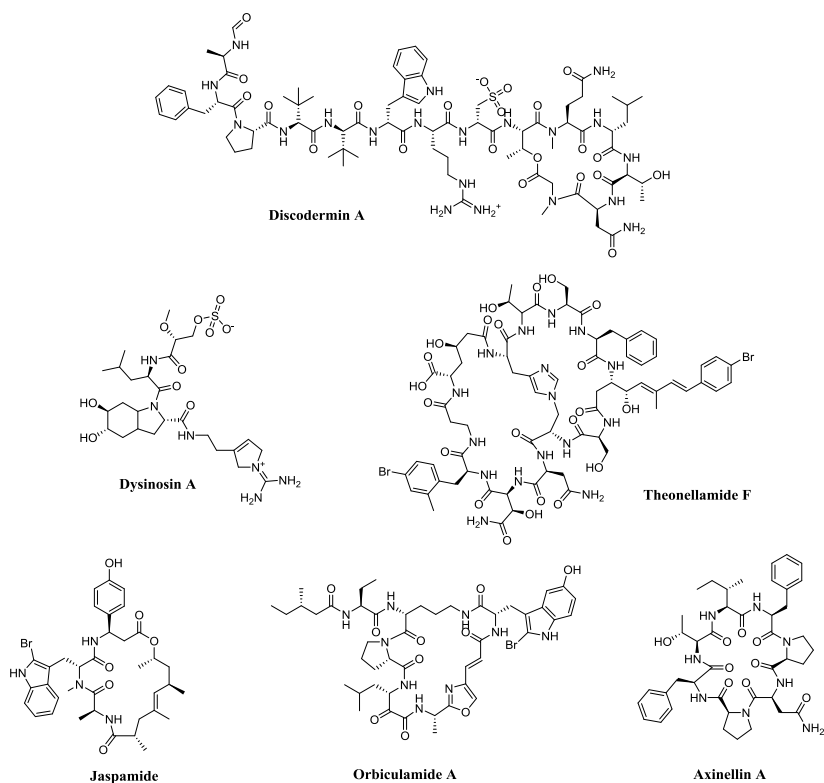
Figure 8 - Structures of several peptides isolated from marine sponges.

Dysinosin A was originally isolated from a *Dysideidae* sponge, with cytotoxic activity reported at the moment of isolation and elucidation [92]. The compound received some attention once it was structurally related with aeruginosins, previously isolated from the cyanobacterium *Microcystis aeruginosa* [93].

Many other bioactive peptides have also been described from marine sponges, such as dolastatins, theonellamides [94, 95], axinellins [96], among others.
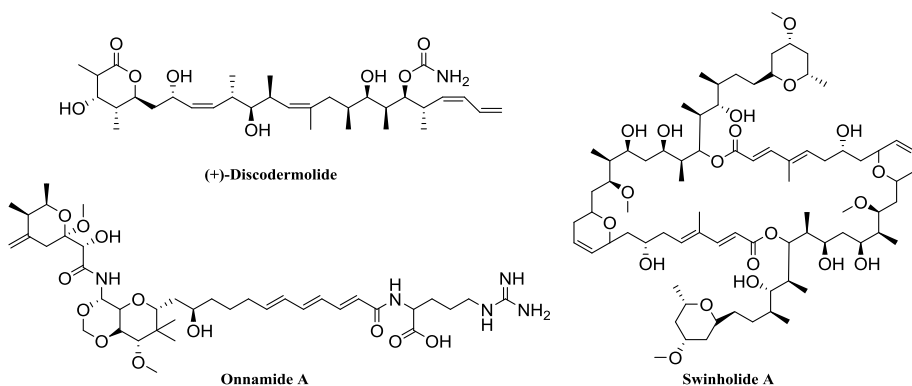
Figure 9 - Structures of several polyketides isolated from marine sponges.

Polyketides represent another large and diverse class of bioactive natural compounds as illustrated in Figure 9. Macrolides are polyketides that appear usually associated to antibacterial activities [97], however, they can also have others, as it is the case of the already mentioned Halichondrin B, originally isolated from *Halichondria okadai* with anticancer activity [28] and nowadays commercialized as Halaven®.

(+)-Discodermolide is a potent cytotoxic and immunosuppressive compound originally isolated from the deep-sea marine sponge *Discodermia dissoluta* [98]. This compound presents a distinctive linear backbone structure with a unique mechanism of action [99]. It was found by Gunasekera and co-workers [98] in 1998 and in 2004 Novartis initiated the Phase I clinical trials in patients with solid tumors. However, the trial was discontinued due to severe toxicity effects in lungs [100]. Even after failure on clinical trials, synthetic and semi-synthetic routes and mechanism of stabilization were still being studied [99, 101].

Polyketides are one of the most interesting classes of sponge secondary metabolites related to drug discovery. However, the origin of those compounds is controversial, once several polyketides have later been described to be produced by the sponge associated-microorganisms and not by the sponge itself. Swinholide A was originally isolated from the marine sponge *Theonella swinhoei* as a potent cytotoxic compound [102, 103], but later found in marine cyanobacterial samples [104]. Also, the origin of onnamide, another polyketide originally isolated from sponges, was later attributed to microorganisms instead of the host [105]. Parent sponge and associated-organism genome mapping allowed attributing the production of these compounds to the microorganisms [106].
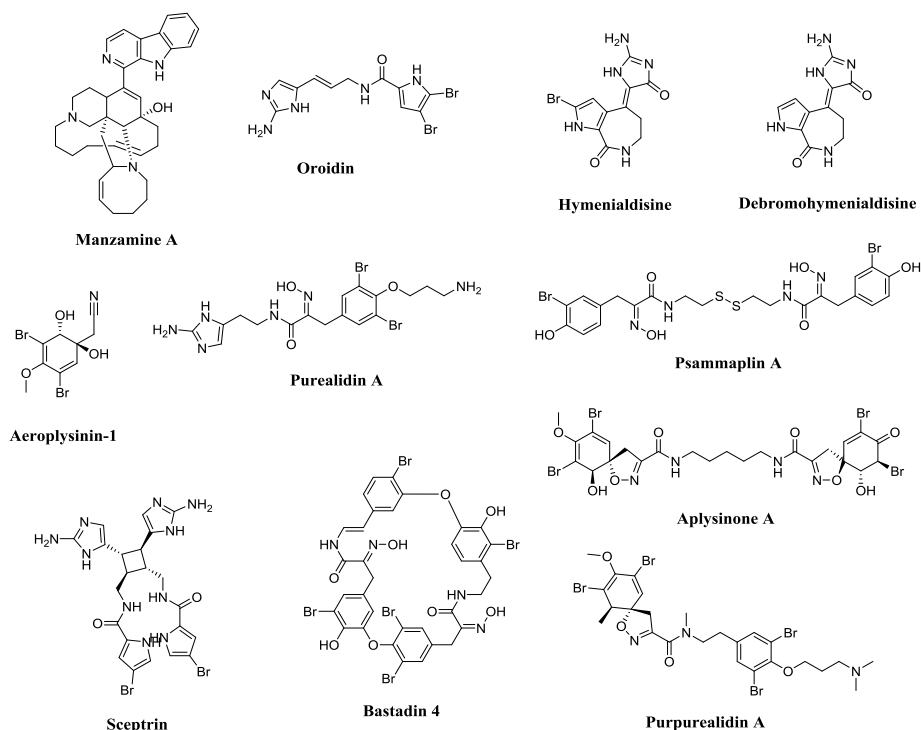
Figure 10 - Structures of several alkaloids isolated from marine sponges.

Alkaloids are of one of the most studied and exploited classes of natural products, both terrestrial and marine. Marine sponges are a rich source of unique and structurally diverse alkaloid compounds as shown in Figure 10. Manzamines are a big alkaloid family and the first isolated was manzamine A, from *Haliclona* sp. [107]. Manzamine A has a characteristic structure with a pentacyclic core of 6-, 6-, 5-, 13- and 8-membered rings. This class of compounds exhibits several different bioactivities, such as cytotoxicity or antibacterial [108].

Bromopyrrole alkaloids are exclusive from *Porifera* phylum. Oroidin, with its pyrrole-imidazole and bromopyrrole carboxamide moieties, was the first element of this class. It was isolated from *Agelas oroides* and since then many have been reported in the literature. Bromopyrrole alkaloids are mostly isolated from the families *Agelasidae*, *Axinellidae* and *Halichondridae* [109] and seem to play a predator deterrent ecological role [110]. This class of alkaloids has attracted much interest from the natural product researchers due to the diversity of biological activities, including insecticidal, antibacterial and cytotoxicity [111].

Several alkaloids showing small differences from the oroidin skeleton were identified. Hymenialdisine and debromohymenialdisine are cyclized forms of oroidin, both inhibitors of several protein kinases, giving them potent antitumor activity and a potential role in the treatment of cancer, diabetes and Alzheimer´s disease [112]. Dimerization can also happen in this type of alkaloids. Sceptrin is a sponge dimeric bromopyrrole alkaloid isolated from *Agelas sceptrum* with a broad range of bioactivities, as antimicrobial [113, 114], antimuscarinic [115] and antiviral [114].

Aeroplysinin-1 was the first described sponge bromotyrosine alkaloid. It was isolated from *Aplysina aerophoba* with antibacterial activity [116]. As the structure of aeroplysinin is very simple, structural diversity appears from small modifications as in degrees of bromination, oxidation, reduction and rearrangements. However, higher structural complexities can occur, as in the case of psammaplin A and aplysinone A. Psammaplin A was described in the 1980s from both *Psammaplysilla* sp. and *Thorectopsamma xana* [117, 118], with a disulfide bond linking two brominated tyrosine units. Aplysinone A, found in *Aplysina gerardogreeni*, is a spirocyclohexadienylisoxazoline-containing metabolite [119].

Purealidins, purpurealidins and bastadins are three other classes of bioactive bromotyrosine alkaloids. Several purealidins have been isolated from *Psammaplysilla purea* and cytotoxic activity is usually associated with them [120, 121]. The related purpurealidins, also isolated from the same species, present antibacterial activity [122]. Bastadins are commonly isolated from *Verongida* specimens and are heterodimers, characterized by the combination of two brominated tyrosine-tyramine amides. Many compounds belonging to this class have been isolated from sponges. Despite the first isolated bastadins failed to show any tested bioactivity [123], other had shown to be cytotoxic [124, 125].

The last big group of sponge metabolites is the terpenes group, which represent an incredibly diverse class (Figure 11). Terpenes are considered to be both primary and secondary metabolites and are composed of isoprene building blocks. The structural modifications of those units lead to the immense variability.
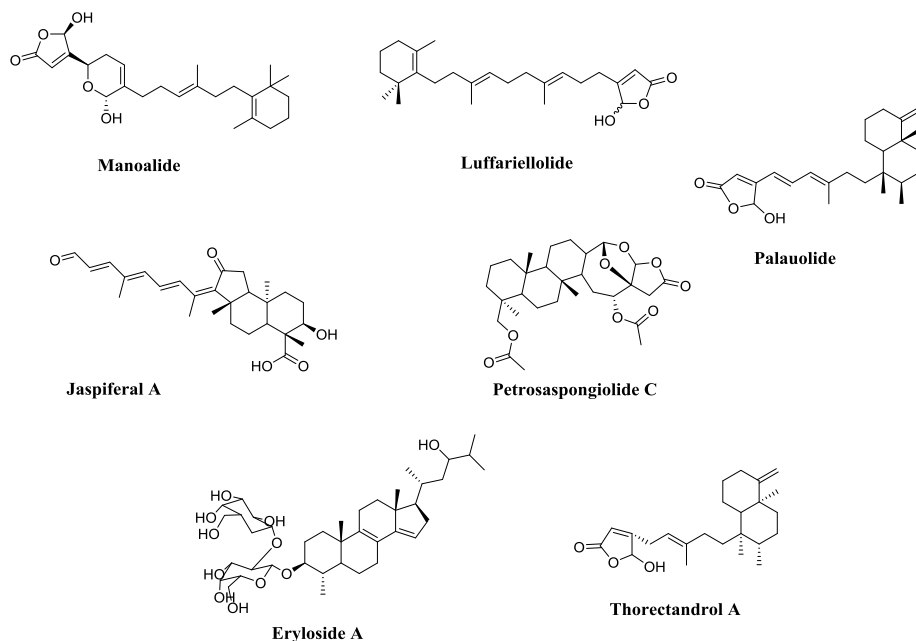
Figure 11 - Structures of several terpenes isolated from marine sponges.

Sesterterpenes (C_{25}) include manoalide, a compound first isolated from *Luffariella variabilis* with antibiotic activity against *Streptomyces pyogenes* and *Staphylococcus aureus* [126]. Later, marine sponges belonging to the genera *Luffariella*, *Hyrtios*, *Thorectandra*, *Cacospongia*, *Fasciospongia*, *Acanthodendrilla* and *Aplysinopsis*, were also found to be rich sources of sesterterpenoids related to manoalide [127]. Manoalide mechanism of action includes an irreversible bind to phospholipase A2 (PLA2) [128]. Luffariellolide, also isolated from *Luffariella*, has a slight structural difference from manoalide [129]. Luffariellolide is also active towards PLA2, but in contrast to manoalide, this one is slightly less potent and partially reversible [129]. More complex sesterpenes are also described as being produced by sponges, including palauolide, thorectandrols and petrosaspongiolides, all displaying cytotoxic activity [130-132].

Triterpenes (C_{15}) were the first marine terpenes to be found and the research on these compounds continues very actively until today due to their broad range of bioactivities and diverse structures. The isomalabaricane triterpenes and the steroidal saponins are the two big families of sponge triterpenes. Jaspiferal A, an isomalabaricane triterpene with a 3α-hydroxyl group, was isolated in 1996 from *Jaspis stellifera* and showed to have cytotoxic activity [133]. Malabaricanes are not unique to marine natural

compounds, they were also isolated from terrestrial sources [134]. Steroidal saponins are usually associated with other marine invertebrates; however, they have been described as produced by marine sponges. Eryloside A was isolated from *Erylus lendenfeld* as an antifungal and antitumor agent [135].

Despite sponges being an incredible source of diverse and numerous bioactive compounds with medicinal potential, the main limitation plaguing the development of more marine secondary metabolites as clinical agents is their supply. Many of the compounds are present in very small quantities and have complicated structures that make industrial syntheses very complicated, as well as time- and resources-consuming [136]. The development of biotechnological production of marine natural products using aquaculture such as in the production of bryostatin, through microorganisms fermentation such as partially used to produce trabectedin and also through the development of synthetic routes as used to obtain halichondrin B are becoming solutions for those plagues [137]. Thus, prospects of marine natural products as future medicine are still promising.

1.2.3 Organisms Studied During the Present Work

1.2.3.1 Marine Sponges

The compounds being produced by several sponge species: *Geodia macandrewi*, *Acanthodendrilla* sp., *Acanthostrongylophora* sp. and *Acanthostrongylophora ingens* were studied during this work. The sponge specimens were collected in different geographical locations and belong to diverse taxonomical groups, as illustrated in Figure 12.

Geodia is an abundant marine sponge genus with a wide geographic distribution. Specimens belonging to this genus are particularly abundant in continental slopes of the cold-temperate north Atlantic waters [138]. Those sponges can be found in dimensions that can go up to 80 cm in diameter and 38 kg. *Geodia* species possess characteristic round-shaped spicules called sterrasters which are part of the cortex. *Geodia* species are very rich in spicule diversity, which can be used to identify species [138]. *Geodia barretti* is the most well-studied species regarding natural products isolation [139], producing the 2,5-diketopiperazines barettin and 8,9-dihydrobarettin, two compounds with interesting non-toxic bioactivity as antifouling agents [140]. From *Geodia macandrewi*, the literature only reports the isolation of one secondary metabolite: geodiataurine, an N-acyl-taurine with no described bioactivities [141].
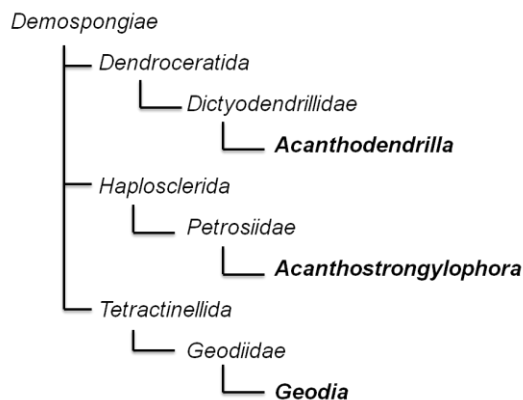
Figure 12 – Taxonomic relations between the sponge individuals used during this study.

Acanthodendrilla is a *Dendroceratida* genus reported for the first time in 1995. Only two species have been described within this group [142] and the number of compounds found in the literature is relatively low when compared with other genera [20]. Besides several alkaloids [143, 144], *Acanthodendrilla* produces many acantholides, sesterterpenes with *in vitro* cytotoxic activity and (+)-makassaric and (+)-subersic acids, two meroterpenoids inhibitors of protein kinase MK2 [144].

Acanthostrongylophora is another genus from which only two species are described: *Acanthostrongylophora ingens* and *Acanthostrongylophora ashmorica* [145]. This genus is the producer of two main classes of *β*-carboline alkaloids: manzamine and ingenines. As seen in section 1.2.2, manzamines are complex alkaloids characterized by the presence of a polycyclic system [146]. Ingenines are a class of pyridine *β*-carboline alkaloids, with several identified analogs, all active against cancer cell lines [147-149]. Considering the natural products described from these genera, it seems that they are yet underexplored and new chemical entities can be found.

1.2.3.2 Actinomycetes

During the present studies, two strains of sponge-isolated actinomycetes were also used for the isolation of secondary metabolites.

For decades, natural products isolated from microbes have been one of

the major resources for the discovery of novel drugs, being the *Actinomycetales* order (commonly called actinomycetes) producing most of the known microbial secondary metabolites [150]. As the marine environment is extremely different from the terrestrial one, it is known that actinomycetes adapted to the marine environment exhibit unique metabolic diversity and enzymatic potentialities [151].

The list of natural compounds produced by marine actinomycetes is immense and can be divided into several main chemical classes. Terpenes and terpenoids, polyketides and peptides represent the biggest classes, but others like quinones, macrolides or lactams have also been isolated from those organisms [152, 153]. Aliniketals are unusual bicyclic polyketides isolated from the marine actinomycete *Salinispora arenicola* and they were found to be inhibitors of ornithine decarboxylase biosynthesis. Inhibition of this enzyme´s production is a potential target for the chemoprevention of cancer [154]. The *Streptomyces* sp. 04DH110 strain was found to produce streptochlorin, a 3-substituted indole compound with significant anti-proliferative activity against human cultured cell lines [155]. Abyssomicin C is a polycyclic polyketide isolated from *Verrucosispora* sp., which possesses antibacterial activity against gram-positive bacteria, including clinical isolates of multiple resistant and vancomycin-resistant *Staphylococcus aureus* [156, 157]. Several of other secondary metabolites isolated from this rich class of microorganisms showed a wide variety of other bioactivities, such as anti-inflammatory, antimalarial, antiviral or anti-angiogenesis [153]. All these evidences place actinomycetes in a privileged position in what concerns to marine drug discovery.

1.3 Isolation and Purification of Sponge Secondary Metabolites

The medicinal chemist is usually focused on a series of known compounds with similar chemical and physical properties, which involves a limited number of separation techniques. Contrarily, the chemist focused on natural products is forced to be prepared to deal with a diverse spectrum of secondary metabolites. Those secondary metabolites can vary in several different properties like hydro- and lipophilicity, charge, solubility, and size.

The common way of studying natural products includes the preparation of organic and/or water crude extracts, fractionation of the extracts, separation and isolation of the individual components using chromatographic methods and structure elucidation using various spectroscopic (UV, IR, NMR) and

spectrometric methods (MS). Despite the massive development in those techniques during the last few decades, the isolation and structure elucidation of compounds from natural sources is still a very challenging and time-consuming task [158] as is represented in Figure 13.
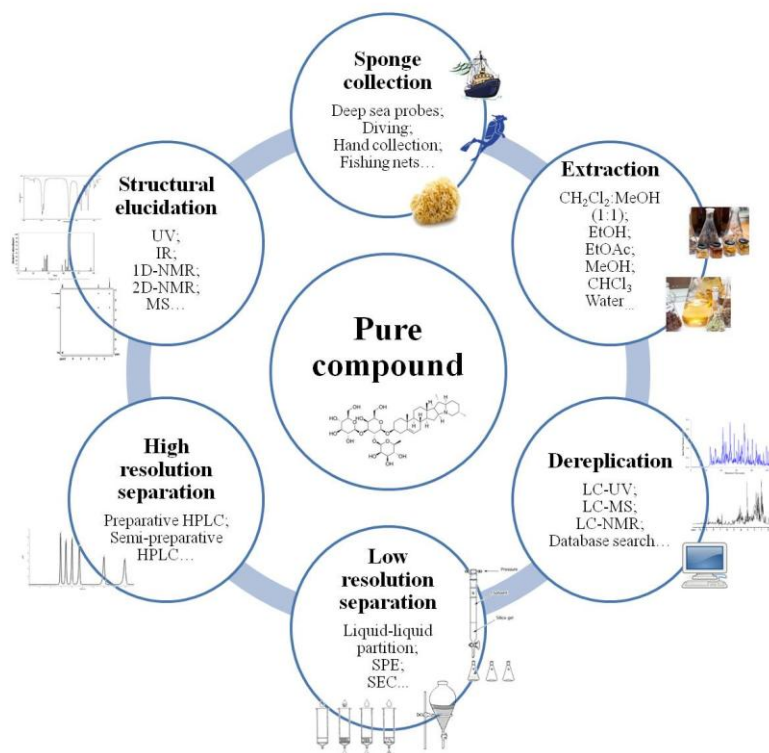
Figure 13 - Process of isolation and elucidation of a sponge secondary metabolite.

1.3.1 Extraction

The sponge material should be extracted immediately after collection. If not, the biomass should be frozen and kept at, at least, -20ºC until processing. The extraction is the first step for the obtainment of pure secondary metabolites, both produced by the sponge or by associated-microbes, and generally, it involves the submersion of the sponge material into organic and/or aqueous solvents. The sponge material can be freshly submerged into the solvents or it can be freeze-dried first. However, in some cases, the remaining sea-water may allow the degradation of the compounds by intracellular enzymes that are also released during the extraction [159].

Maceration or pre-cutting into small pieces also facilitate the solvent penetration and a more efficient extraction.

The solvents used during extraction depend on the physicochemical characteristics of the compounds, sponge biomass and the class of compounds to be extracted (if there is an aim for a specific class). Ethanol, ethyl acetate, methanol or chloroform can be used as extraction solvents, but a mixture of dichloromethane:methanol is the most common, as it covers a broad range of polarities. Aqueous extractions can also be performed following the organic extraction. Usually, the solvents are evaporated to obtain a crude extract.

1.3.2 Dereplication

Due to the cosmopolitan occurrence of many bioactive compounds, most natural product extracts contain compounds that have already been characterized. This leads to a high rediscovery rate of generally active compounds. Thus, the detection of molecules that are identical or highly similar to known compounds is essential for the identification of novel bioactive structures and its guided isolation [160]. The dereplication of compounds at an early stage of the drug discovery process allows focusing on samples with potentially new active molecules, saving time, cost and resources.

A single analytical technique capable of profiling all secondary metabolites in the biological source does not exist today. The dereplication procedure strongly relies on hyphenated techniques coupled to high-pressure liquid chromatography (HPLC) such as LC-UV (Liquid chromatography with ultraviolet detection), LC-MS (Liquid chromatography with mass spectrometry detection) and LC-MS/MS (Liquid chromatography with tandem mass spectrometry detection). Liquid chromatography, coupled with nuclear magnetic resonance (LC-NMR) is a relatively new technology that has been successfully and practically achieved in the last two decades for the dereplication of sponge natural compounds [161].

The combination of LC-UV, LC-MS and NMR information can be helpful in the first step of dereplication, especially when this information is combined with taxonomical searches in natural product databases. This approach is, however, still limited by the unavailability of general LC-MS and LC-MS/MS databases.

1.3.3 Isolation

As the crude extracts are very complex, containing neutral, acidic, basic, lipophilic and hydrophilic compounds, an unspecific crude fractionation is usually carried out as a first separation step. Liquid-liquid partition, solid phase extraction (SPE), size exclusion chromatography (SEC), vacuum liquid chromatography (VLC) and column chromatography are frequently used, as they represent low-resolution separation techniques and allow an initial separation of the different compounds.

The final separation usually includes high-resolution separation techniques. Preparative and semi-preparative HPLC are the most common techniques at this stage. When connected to a diode array detector (DAD), the compounds can be followed based on the retention time and their ultraviolet spectrum. Additionally, an evaporative light scattering (ELSD), fluorescence (FLD) or a charged aerosol detector (CAD), may allow for the detection of the compounds that do not absorb UV light.

This way, the sponge chemical components are isolated one by one, by chromatography of the respective extracts. This work is, obviously, very time- and resource-consuming. It is a major effort to isolate all the compounds in a pure form using the available technology.

1.3.4 Structural Elucidation

In natural product drug discovery programs, the major bottleneck has always been structure elucidation [162]. This is still a complex part of the process that requires modern techniques and equipment and detailed expertise in analyzing the data obtained from them.

Commonly, the isolated compound is submitted to a range of different analytical techniques that will lead to the structural elucidation. Those include spectroscopic methods like UV, infrared (IR), and NMR as well as MS methods. An integrated analysis of the data from all the different techniques should allow the detailed molecular structure to be predicted [163], however, MS and NMR are, for several reasons, the ones to which structural elucidation process relies the most on.

1.3.4.1 Mass Spectrometry

Mass spectrometers have been used as powerful tools both for dereplication and structural elucidation, giving information about fragmentation pattern and accurate molecular weight measurements of the compounds [164]. This technique provides an idea about the molecular formula, which is a very important step in the elucidation process. A great advantage of the use of MS is that it is generally a very sensitive technique, capable of detecting compounds in nano- or picogram quantities.

A typically simplified mass spectrometer is represented in Figure 14 and it consists of an ion source generating ions, a mass analyzer separating those ions based on their mass-to-charge ratio (m/z), and a detector measuring the separated ions [165].
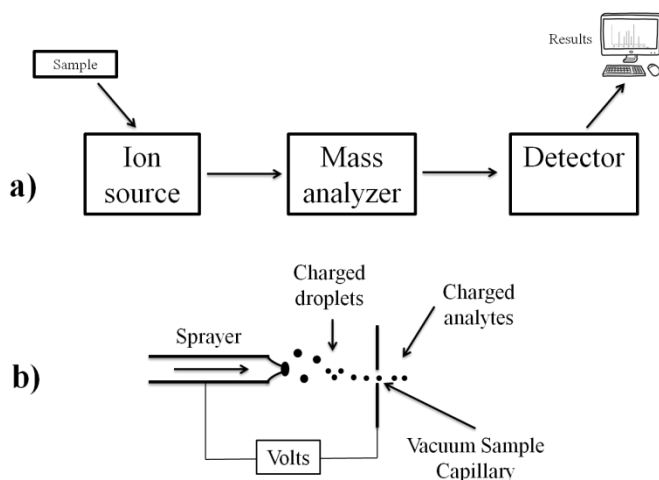
Figure 14 - Schematic diagrams of mass spectrometry. **(a)** A generic MS system consisting of an ion source, mass analyzer and mass detector. **(b)** A schematic diagram of electrospray ionization (ESI). Adapted from Shipovskov and Reimann (2007) [165].

Traditionally, purified samples were subjected to high-energy ionization under ultra-high vacuum conditions (e.g. electron ionization, EI). Electrospray ionization (ESI) appeared as a crucial milestone in natural products drug discovery. Opposed to earlier ionization techniques, which were applicable only to thermally stable, low molecular weight volatile compounds, any ion (ranging from inorganic salts to large macromolecules) can be analyzed by ESI-MS [166]. ESI-MS can also be directly coupled to liquid chromatography. The sample is sprayed into the ion source as a solution. As shown in Figure

14b, the solvent is evaporated under atmospheric pressure in the presence of an electric field, generating charged ions that will be further separated by the mass analyzer [165]. The mass analyzer appears as a unique chromatographic detector, giving valuable information about the several components present in the complex sponge extracts [166].

A big variety of mass analyzers have been developed. The separation of ions according to their *m/z* can be based on different principles, however, all mass analyzers use static or dynamic electric and magnetic fields, combined or not. Each mass analyzer has its advantages and limitations [166]. The quadrupole analyzer uses the stability of the trajectories in oscillating electric fields to separate ions according to their *m/z* ratios. It is constituted by four cylindrical metal rods, parallel to each other in a square formation. An oscillating radio frequency and direct current electric field are applied to the four rods, forcing the ions to travel through the space between the rods and oscillate in a similar manner. However, only ions of a specific *m/z* ratio will be able to maintain the same trajectory within the quadrupole.

Time-of-flight (TOF) represents another MS analyzer. It separates the ions, after their initial acceleration by an electric field, according to their velocities when they drift in a free-field region, the flight tube [166]. The longer the flight tube, the more accurate is the mass measurement.

1.3.4.2 *Nuclear Magnetic Resonance*

Despite the importance of MS and other spectroscopic techniques, NMR is the most powerful technique for structural elucidation as it provides detailed information about the structural components and the way they are organized, the dynamics and the 3D disposition of the molecule [167]. 1D experiments (^{1}H, DEPT, ^{13}C, ^{15}N, ^{19}F, ^{31}P and others) give information about the atoms present in the molecule, allowing a first indication of the molecular structure. 2D experiments (HSQC, COSY, TOCSY, HMBC, NOESY, ROESY and others) provide more detailed information and show correlations between the different atoms. In comparison with MS, NMR is a less sensitive technique; however, it provides much more detailed structural information. The technique also allows a total recovery of the sample. Both techniques, NMR and MS, are necessary for structural determination.

1.3.4.3 Stereochemistry

The last step for complete structural elucidation is the determination of the molecule 3D disposition, its stereochemistry. Due to the high complexity of this step, sometimes it becomes the most time consuming and because of that, many sponge natural compounds are reported only with a planar structure. Complex compounds require very often computational approaches, that many times, coupled to experimental NMR data allow decoding the 3D molecule disposition [168].

Techniques and approaches to determine the stereochemistry of sponge natural products, include direct methods, as X-ray diffraction (XRD), electronic and vibrational circular dichroism (ECD and VCD), and Raman optical activity (ROA), as well as indirect methods using a reference or a derivative agent with known stereochemistry, e.g. circular dichroism with empirical rules and NMR utilizing anisotropic effects of chiral derivatized agents. Well-defined conformations, as in the case of small cyclic compounds, can be easily accomplished from proton-proton *J*-coupling and/or NOE intensities.

2 Aims

The comprehensive aim of this work was to isolate and structurally elucidate secondary metabolites produced by selected specimens of marine sponges and sponge-associated actinomycetes as well as test drug discovery relevant bioactivities. The study-specific objectives were:

•   To develop efficient methods for the isolation of the secondary metabolites.

•   To elucidate the isolated compound's structure using spectroscopic and spectrometric techniques.

•   To evaluate the cytotoxic, anti-bacterial and anti-obesity activities of isolated compounds.

3 Materials and methods

3.1 General Experimental Procedures

All aqueous solutions were prepared with ultrapure water generated by a Milli-Q water purification system (18.2 MΩ, Millipore). All chemicals and laboratory supplies used were purchased from Sigma-Aldrich unless otherwise stated. Organic solvents were HPLC grade or a higher degree of purity and were purchased from Sigma-Aldrich unless another company is mentioned. Deuterated solvents were purchased from Merck (Darmstadt, Germany).

3.2 Biological Samples

3.2.1 Icelandic Sponges

Icelandic sponges were collected by hand while scuba diving or by deep-sea probes during sea excursions with the Icelandic Coast Guard and the Icelandic Marine Institute. Collection locations are shown in Figure 15 and Table 2, they were chosen as part of a major project aiming at marine invertebrate bioprospecting in the Icelandic waters [169]. Samples were frozen at -20ºC as fast as possible after collection. The sponges were kept under those conditions until extraction.

Sponge samples with clear morphology were immediately identified by the taxonomist Dr. Hans Tore Rapp, University of Bergen (Norway). A voucher specimen of each one of the studied individuals is deposited at the Faculty of Pharmaceutical Sciences, University of Iceland (Reykjavík, Iceland) under the code specified in Table 2 as "Entry".

Table 2 - Icelandic sponges collected in the Icelandic waters.

No.	Entry	Identification	Collection site (Lat, Long)	Mode of collection	Weight
1	JS-A9-2011 #1	Unidentified	65.4610, -27.3615	Deep sea probe	972.0 g
2	JS-A9-2011 #6	Unidentified	65.2550, -28.0068	Deep sea probe	660.0 g
3	A5-2010-93	*Geodia macandrewi*	63.5755,-25.1455	Deep sea probe	748.0 g
4	210111 #3	*Weberella bursa*	64.8431, -13.7008	Scuba diving	300.0 g
5	030915 #3	Unidentified	65.2038, -13.8024	Scuba diving	1572.0 g
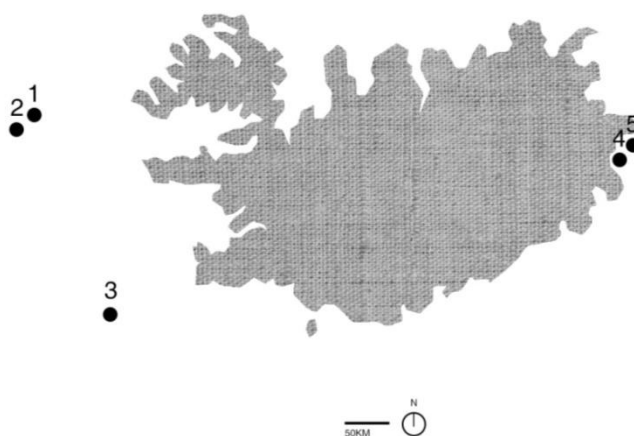
Figure 15 - Sampling locations of the Icelandic sponge specimens. **1)** JS-A9-2011 #1. **2)** JS-A9-2011 #6. **3)** A5-2010-93. **4)** 210111 #3. **5)** 030915 #3
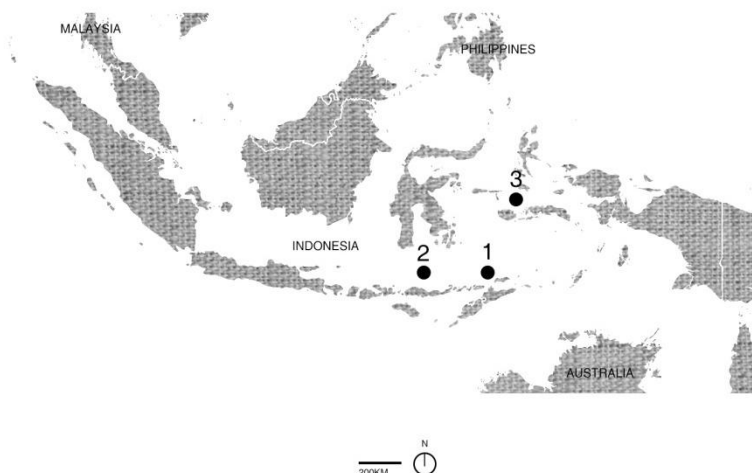
3.2.2 Sponges from the Indo-Pacific Ocean

The sponge samples from the Indo-Pacific Ocean were collected by hand while scuba diving. Those samples are part of PharmaMar collection and were selected based on previous indication of novel compounds (Table 3 and Figure 16). The Spanish biopharmaceutical company PharmaMar is the largest commercial organization investigating the marine environment for bioactive metabolites with antitumor activities, owning the largest collection (>130,000 extracts) of marine invertebrate samples in the world used for drug discovery [170]. The organisms were morphologically identified by PharmaMar´s collaborators. A voucher specimen of each one of the studied individuals is deposited at PharmaMar facilities, (Madrid, Spain) under the code specified in Table 3 as "Entry".

Table 3 - Sponge samples collected in the Indo-Pacific Ocean.

No.	Entry	Identification	Collection site	Weight
1	ORMA 124984	*Acanthostrongylophora* sp.	Wetar	82.0 g
2	ORMA 101324	*Acanthodendrilla* sp.	Pulau-Pulau	86.0 g
3	ORMA 135834	*Acanthostrongylophora ingens*	Boano	320.0 g

Figure 16 – Indo-Pacific Ocean sampling locations. **1)** Wetar. **2)** Pulau-Pulau. **3)** Boano.

3.2.3 Actinomycetes Isolated from Sponge Samples

The marine strains DIL-12-02-135 and CP9-01-036 were isolated from two individual sponge samples collected in the Indo-Pacific Ocean during PharmaMar´s ongoing screenings. Briefly, the strains were isolated from two grams of homogenized sponge in 10 mL artificial seawater (ASW) which was spread into solid BEN isolation medium supplemented with B group vitamins and 0.8 mM nalidixic acid. After a month of incubation time, the grown colonies were re-picked and re-isolated onto modified ATCC 172 medium. The strains were identified as *Actinobacteria* based on their morphological characteristics after isolation.

Fermentation occurred in scale-up steps, starting in few mL until reaching 2 L. The seed culture was grown on MIBM medium and fermentation occurred on fermentation medium. The culture was grown at 28°C with constant 220 rotations per minute (rpm). After 12 days of cultivation, the culture was centrifuged to separate the mycelial cake and other solids from the clarified broth. All media composition is resumed in Table 4.

Table 4 - Composition of the media used to isolate/cultivate *Actinobacteria*.

		DIL-12-02-135	CP9-01-036
BEN isolation medium	L-asparagine (g/L)	2.5	2.5
	Glycerol (g/L)	20.0	20.0
	NaCl (g/L)	---	5.34
	KCl (g/L)	5.35	0.15
	Na_2SO_4 (g/L)	7.50	7.50
	$Mg_2SO_4.7H_2O$ (g/L)	0.10	0.10
	$MgCl_2.6H_2O$ (g/L)	2.40	2.40
	Silice (g/L)	---	2.00
	Taurine (g/L)	0.50	---
	$FeSO_4.7H_2O$ (g/L)	0.10	0.10
	$CaCO_3$ (g/L)	0.10	0.10
	Agar (g/L)	20.0	20.0
ATCC 172 medium	Dextrose (g/L)	5.00	5.00
	Soluble starch (g/L)	10.0	10.0
	Yeast extract (g/L)	2.50	2.50
	Tryptone (g/L)	2.50	2.50
	Artificial marine salts (g/L)	10.0	10.0
	$CaCO_3$ (g/L)	2.00	2.00
	Agar (g/L)	15.0	15.0
MIBM medium	Dextrose (%)	0.10	0.10
	Soluble starch (%)	2.40	2.40
	Soy peptone (%)	0.30	0.30
	Yeast extract (%)	0.50	0.50
	Tryptone (%)	0.50	0.50
	Soya Flour (%)	0.50	0.50
	NaCl (%)	0.54	0.54
	KCl (%)	0.02	0.02
	$MgCl_2$ (%)	0.24	0.24
	Na_2SO_4 (%)	0.75	0.75
	$CaCO_3$ (%)	0.40	0.40
Fermentation medium	Soy peptone (%)	0.10	---
	Soy flour (%)	1.20	1.00
	Dextrose (%)	0.25	---
	Malt extract (%)	0.10	---
	Mannitol (%)	---	5.00
	Dextrin (%)	4.00	1.40
	ASW (%)	2.00	0.60
	$CaCO_3$ (%)	0.80	1.40
	$CaCl_2.6H_2O$ (%)	---	1.60

3.3 Spicules Analysis

Spicules were extracted using acid digestion. Small pieces (~0.5 cm^2 slide) of sponge were cut and placed in 1.5 mL Eppendorf tube. 400 µL of nitric acid (HNO_3) (ACS 70%) were added to the fragments and placed at a 95ºC water bath for around 10 minutes. Once cool, samples were microcentrifuged for 30 seconds at 13,000 rpm (Heraeus Pico 17, Thermofisher Scientific) and HNO_3 was discarded. The spicules were washed twice with 1 mL pure Milli-Q H_2O and finally dissolved in 300 µL H_2O. Preparations were mounted immediately and spicules observed under an optical light microscope (BHT-2, Olympus, Japan). Pictures were acquired using an Olympus CAMEDIA C-5050 zoom camera.

3.4 Organic Extractions

3.4.1 Sponge Samples

Before extraction, the frozen sponge samples were taken out of the freezer and thawed at room temperature. They were then cut into small pieces of, approximately, 1cm^3 and lyophilized (Snijders Scientific, Tilburg, Holland) during several days until complete dryness. Sponges collected in the Indo-Pacific Ocean were extracted without going through the freeze-drying process. Processed sponge samples were consecutively extracted while being soaked in CH_2Cl_2:MeOH (1:1 v/v) at room temperature. Extractions were conducted over variable periods of time, from few hours to a day, depending on the sponge sample, and repeated three times. The resultant material was filtered using a Whatman® grade 1 filtration paper, combined and concentrated to dryness under vacuum to yield a crude extract. Crude extracts were all stored at -20°C.

3.4.2 Actinomycetes

Mycelial cakes and/or clarified broths were homogenized with a mixture of ethyl acetate:isopropanol (EtOAc:iPrOH) (6:4 v/v). The resultant mixtures were stirred vigorously and then filtered through a pad of Celite® R-566. Organic phases were further concentrated under vacuum to obtain a crude extract. Crude extracts were all stored at -20 °C.

3.5 Compounds Separation and Isolation

3.5.1 Modified Kupchan Solvent Partition Method

The crude extracts resultant from Icelandic sponges were fractionated using a standard modified Kupchan solvent partition procedure [171, 172], as outlined in Figure 17. The crude extract was dissolved in MeOH:H_2O (9:1 v/v) and partitioned against *n*-hexane (Hex) to yield fraction A. The water content of the aqueous-methanolic phase was adjusted to 20% (v/v), by adding an additional 10% H_2O, and partitioned against chloroform ($CHCl_3$) (fraction B), then adjusted to 40% (v/v) and partitioned again against $CHCl_3$ (fraction C). MeOH was then evaporated and the remaining H_2O partitioned against BuOH (fractions E and D, respectively). Resultant fractions were all stored at -20 °C.
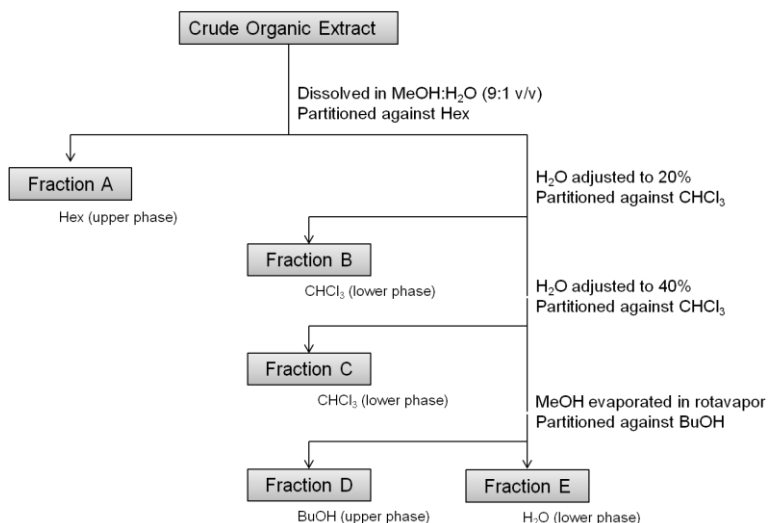
Figure 17 - Flow diagram of the Kupchan liquid/liquid partition modified method.

3.5.2 Thin Layer Chromatography (TLC)

Silica gel on TLC aluminum foils was cut according to the number of lanes needed and extracts spotted using Hirschmann® microcapillary pipettes. TLC plates were placed in a TLC developing tank, in which the various solvent systems had saturated the chambers. TLC plates were left to run until the solvent front had risen ¾ of the plate. After evaporation of mobile phase, the plate was visualized under both UV light (254 nm and 366 nm, Camag UV Cabinet, ThermoFisher Scientific) and daylight. TLC plates were further sprayed with anisaldehyde solution.

3.5.2.1 Anisaldehyde Staining

Anisaldehyde was used as a standard staining for visualization of the TLC plates. The solution was prepared by adding 5 mL H_2SO_4, 1.5 mL CH_3COOH and 3.7 mL *p*-anisaldehyde to 135 mL of absolute ethanol (EtOH). This solution was vigorously stirred and stored in a recipient protected from the light. TLC plates were sprayed with freshly prepared anisaldehyde solution and then heat-dried until clear visualization of the spots.

3.5.3 Vacuum Liquid Chromatography (VLC)

3.5.3.1 *Reverse-phase Vacuum Liquid Chromatography*

Reverse-phase vacuum liquid chromatography (RP-VLC) was performed in a fritted glass funnel dry packed with reverse-silica sorbent (RP-18, Merck KGaA, Darmstadt, Germany). Extracts to separate were dissolved in a polar solvent/mixture of solvents and applied in the upper portion of the sorbent. Those extracts were then separated using appropriate step-gradients of solvent mixtures, starting with the most polar mixture and gradually decreasing polarity, pulling the column dry between each fraction collected. The size of the column, together with the volume of solvents used for elution, was dependent on the initial mass of extract to separate.

3.5.3.2 *Normal-phase Vacuum Liquid Chromatography*

Normal-phase vacuum liquid chromatography (NP-VLCs) was performed in a fritted glass funnel dry packed with silica gel (0.035-0.070 60A, Merck KGaA, Darmstadt, Germany). Extracts for separation were dissolved in an apolar solvent/mixture of solvents and applied in the upper portion of the sorbent. Those extracts were then separated using appropriate step-gradients of solvent mixtures, starting with the less polar solvent and gradually increasing polarity, pulling the column dry between each fraction collected. The size of the column, together with the volume of solvents used for elution, was dependent on the initial mass of extract to separate.

3.5.4 Preparative and Semi-preparative HPLC

Preparative HPLC was performed in a Dionex UltiMate 3000 HPLC system, connected to UV detector (ThermoFisher Scientific, Waltham, MA USA). A Phenomenex Luna C18 (5µm, 250 x 21.20 mm) column was used for preparative separations. The conditions of separations were dependent on the physicochemical properties of the extract being separated. The chromatograms were monitored at both 254 and 215 nm. Data acquisition, analysis, and reporting were performed using Chromeleon 7 software (ThermoFisher Scientific).

Semi-preparative HPLC was performed using three different LC systems: a Dionex UltiMate 3000 HPLC system, connected to a UV detector (ThermoFisher Scientific); a Waters 2695 Alliance HPLC system connected to a 2487 UV detector (Waters, Milford, MA, USA) and an Agilent 1100 HPLC also connected to a UV detector (Agilent, Santa Clara, CA, USA). Columns and separation conditions were also dependent on the physicochemical

properties of the extract being separated. The chromatograms were followed at both 254 and 215 nm. Data acquisition, analysis, and reporting were performed using Chromeleon 7 software (ThermoFisher Scientific), ChemStation (Agilent) and Empower 3 (Waters), on each one of the semi-preparative systems, respectively.

3.6 Mass Spectrometry Analysis

HRESIMS spectra were recorded using a Waters Synapt G1 UPLC-QTOF-MS spectrometer, both in positive and negative ionization modes. An Agilent 6230 TOF LC/MS system was used for the same effect and ESI-MS spectra were recorded using an Agilent 1100 Series LC/MS spectrometer.

3.6.1 Metabolites Screening

The initial dereplication approach was carried out on an ACQUITY BEH C18 1.7 μm, 2.1 × 150 mm column (Waters), maintained at 60 ºC. A 98:2 to 0:100 (v/v) H_2O/MeCN (0.1% FA) gradient in 10 minutes, 0.45 mL/min was used to separate the compounds present in the extracts.

3.6.2 Optimized Conditions for Polar Fractions

The separation described in 3.6.1 was optimized to suit polar fractions. For extracts with high polarities, the separation was carried out on an ACQUITY UPLC BEH Amide 1.7 μm, 2.1 mm x 100 mm, column (Waters), maintained at 35 ºC. A 10:90 to 15:85% (v/v) H_2O/MeCN (0.2% CH_3COOH, 10 mM CH_3COONH_3) gradient in 8 minutes at 0.6 mL/min flow rate.

3.7 Nuclear Magnetic Resonance Spectroscopy Analysis

Nuclear Magnetic Resonance (NMR) data were obtained on a Bruker Avance spectrometer at 400/100 (^{1}H/^{13}C), at room temperature using a 5 mm BB-1H/D probe head (broadband). A Varian "Unity 500" at 500/125 MHz (^{1}H/^{13}C) and a Varian "Unity 400" at 400/100 MHz (^{1}H/^{13}C) spectrometers were also used. 2D experiments were performed according to standard pulse sequences. The samples were dissolved in appropriate deuterated solvents: chloroform-d_1; dichloromethane-d_2; DMSO-d_6; methanol-d_4. Solvent signals (for example, $δ_H$ 3.3 and $δ_C$ 49.0 for CD_3OD) were considered as an internal reference signal for calibration. The observed chemical shift values ($δ$) were given in ppm and coupling constants (J) in Hz. Data were processed using MestReNova NMR 12.0 software (Mestrelab Research, Santiago de Compostela, Spain).

3.8 Ultra-violet (UV) Analysis

A Dionex UltiMate 3000 HPLC system, connected to a PDA (Photodiode array) detector (ThermoFisher Scientific) was used to obtain UV spectra. Data acquisition, analysis and reports generation were performed using Chromeleon 7 software (ThermoFisher Scientific). An Agilent 8453 UV/vis spectrometer was also used for the same purpose.

3.9 Infra-red (IR) Analysis

A Nicolet iZ10 FT-IR spectrometer (ThermoFisher Scientific) was used to obtain IR spectra. Data acquisition, analysis and reports generation were performed using ValPro software (ThermoFisher Scientific). A Perkin-Elmer Spectrum 100 FT-IR spectrometer was also used for the same purpose.

3.10   Isolation Procedures

3.10.1 Nucleosides from *Geodia macandrewi*

Geodia macandrewi (A5-2010-93) frozen sponge sample (748.0 g) was cut into small pieces and lyophilized (388.0 g). The lyophilized material was repeatedly extracted with CH_2Cl_2:MeOH (1:1 v/v, 3x3L) at room temperature. The material was filtered and concentrated under vacuum to yield 9.4 g of crude extract. The crude extract was fractionated using the modified Kupchan solvent partition procedure described on 3.5.1. The butanolic fraction (1.65 g) was further separated by preparative HPLC on a Phenomenex Luna C18 (250 x 21.20 mm, 5µm) column, 99:1 to 76:24 (v/v) H_2O/MeOH (1M NaCl) gradient for 47 minutes at 10 mL/min to yield salted compounds **1** at 55 minutes, **2** at 23 minutes, **3** at 40 minutes, **4** at 24 minutes, **5** at 34 minutes, **6** at 18 minutes, **7** at 29 minutes and **8** at 36 minutes. Finally, compounds were desalted by dissolution in DMSO to obtain pure **2´-deoxyadenosine** (4.8 mg), **thymine** (1.1 mg), **thymidine** (4.7 mg), **2´-deoxyuridine** (4.6 mg), **2´-deoxyinosine** (3.5 mg), **2´-deoxycytidine** (1.0 mg), **adenosine** (6.4 mg) and **2´-deoxyguanosine** (7.5 mg).

3.10.2 Alkaloids from *Acanthostrongylophora* sp.

Acanthostrongylophora sp. (ORMA 124985) frozen sponge sample (72.0 g) was cut into small pieces and repeatedly extracted with CH_2Cl_2:MeOH (1:1 v/v, 3x300mL) at room temperature. The obtained material was concentrated under vacuum to yield 2.8 g of crude extract. The crude extract was subjected to RP-VLC over RP-18 silica gel with a step gradient from H_2O to

CH$_2$Cl$_2$, which resulted in five fractions. Fraction 3 (350.0 mg) eluted with pure MeOH and was further separated by semi-preparative HPLC (Symmetry C18 5µm (10.0 x 150 mm) column, gradient 95:5 to 70:30 (v/v) H$_2$O/MeCN (0.4% TFA) in 20 min, 3 mL/min) yielding seven HPLC fractions. HPLC fraction 1 eluted at 10 minutes (109.2 mg) and was again separated by semi-preparative HPLC: Varian Pursuit XRS 5µm (10.0 x 150 mm) column, isocratic 86:14 (v/v) H$_2$O/MeCN (0.1% TFA), 3.5 mL/min. Pure compounds eluted at minute 15 (**haploscleridamine (9)**, 12.2 mg) and minute 18 (compound **10**, 9.4 mg).

3.10.3 Spongian Diterpenes from *Acanthodendrilla* sp.

Frozen *Acanthodendrilla* sp. biomass (86.0 g) was cut into small pieces and repeatedly extracted with CH$_2$Cl$_2$:MeOH (1:1 v/v, 3x450mL) at room temperature. The obtained material was combined and dried under vacuum to yield 4.4 g of crude extract. The crude extract was then separated using preparative HPLC (Gemini-NX C18 5µm (250 x 21.2 mm) 78:22 to 22:78 (v/v) H$_2$O/MeCN in 45 minutes, 10 mL/min) to yield nine fractions. Fraction 6 (14.2 mg) eluted at 30 minutes and fraction 9 (10.6 mg) at 37 minutes. Each one of the fractions was further individually separated by semi-preparative HPLC (Xbridge C18 5µm, 150 x 10 mm, 3.5 mL/min). Compound **11** (0.9 mg) eluted at minute 29 of a 40:60 (v/v) H$_2$O/MeCN (0.1% TFA) isocratic run and compound **12** (1.6 mg) eluted at minute 26 of a 35:65 (v/v) H$_2$O/MeCN (0.1% TFA) isocratic run.

3.10.4 Bisabolane-derivatives from *Acanthostrongylophora ingens*

Frozen *Acanthostrongylophora ingens* biomass (320.0 g) was repeatedly extracted with CH$_2$Cl$_2$:MeOH (1:1 v/v, 3x500mL) at room temperature. The extracts were combined and concentrated under vacuum to yield 25.9 g of crude extract. This crude extract was subsequently dissolved in H$_2$O:Hex (1:1 v/v) and partitioned between H$_2$O (300 mL), Hex (3x500 mL), EtOAc (3x300 mL) and BuOH (2x250 mL). The Hex extract (6.1 g) was subjected to RP-VLC over RP-18 silica gel with a step gradient from H$_2$O:MeOH (3:1 v/v) to CH$_2$Cl$_2$. Fraction 1 eluted with H$_2$O:MeOH (3:1 v/v) and fraction 3 with pure MeOH. Fraction 1 (95.6 mg) was subjected to semi-preparative HPLC (Phenomenex Gemini-NX C18 5 µm (10.0 × 250 mm), 60:40 to 50:50 H$_2$O/MeCN (v/v) gradient in 15 min, 3 mL/min) to yield compound **13** (6.4 mg) at 10 min. Fraction 3 (1640.7 mg) was initially separated by preparative HPLC (Phenomenex Luna C18 5 µm (21.20 x 250 mm), 25:75 to 0:100

H$_2$O/MeCN (v/v) gradient in 30 min, 6 mL/min), yielding HPLC fraction 2 at minute 14 (444.2 mg). This fraction was separated in another round of preparative HPLC (Phenomenex Luna C18 5 µm (21.20 x 250 mm) 50:50 to 40:60 H$_2$O/MeCN (v/v) gradient in 25 min, 10 mL/min), yielding compound **14** (98.6 mg) at minute 21 and HPLC fraction 4 at minute 24 (146.6 mg). HPLC fraction 4 was submitted to a last semi-preparative HPLC separation (Phenomenex Gemini-NX C18 5µm (10.0 x 250 mm), 50:50 to 30:70 H$_2$O/MeCN (v/v) gradient in 35 min, 2.3 mL/min) to yield compounds **15** (13.1 mg) at minute 11, **16** (4.9 mg) at minute 21 and **17** (9.4 mg) at minute 34.

The EtOAc extract resultant from the liquid/liquid partition was also subjected to reversed phase VLC over RP-18 silica gel with a step gradient from H$_2$O:MeOH (3:1 v/v) to CH$_2$Cl$_2$. Fraction 2 (1021.7 mg) eluted with H$_2$O:MeOH (1:3 v/v) and was further separated by preparative HPLC (Phenomenex Luna C18 5 µm (21.20 x 250 mm) 50:50 to 20:80 H$_2$O/MeCN (v/v) gradient in 30 min, 8 mL/min), to yield compounds **18** (46.5 mg) at minute 28 and **19** (23.3 mg) at minute 19.

3.10.5 Fluvirucinin Derivatives from DIL-12-02-135

After 12 days of cultivation, the *Actinobacteria* culture was centrifuged to separate the mycelial cake and other solids (464.0 g) from the clarified broth. Mycelial cake was homogenized with a mixture of iPrOH:EtOAc (9:14 v/v). The mixture was vigorously stirred and filtered through a pad of Celite®. The organic phase was concentrated under vacuum to obtain 4.6 g of cell extract. Organic extract (4.6 g) was separated by RP-VLC with a stepwise H$_2$O-MeOH-CH$_2$Cl$_2$ gradient. Fractions 5 (774.5 mg) and 6 (837.9 mg) eluted with MeOH and were further separated using NP chromatography. A gradient elution of Hex-EtOAc-MeOH was applied on the Silica gel VLC system. **Fluvirucinin C$_1$ (20)** was found in silica gel fractions 3 (11.6 mg) and 4 (34.9 mg), which eluted with Hex:EtOAc (1:1 v/v) and 100% EtOAc respectively. **Fluvirucinin C$_2$ (21)** was detected in silica gel fractions 5 (23.6 mg) and 6 (9.1 mg) which eluted with EtOAc:MeOH (9:1 v/v) and EtOAc:MeOH (8:2 v/v) respectively. All fractions were further submitted to semi-preparative HPLC for a final purification of **20** and **21**. HPLC separations were carried on a XBridge C18 5 µm (10x150 mm) column, 50:50 to 20:80 (v/v) H$_2$O/MeCN (0.05% FA) gradient in 30 minutes, 3.5 mL/min to obtain pure **20** (1.5 mg eluted at minute 17) and 70:30 to 35:75 (v/v) H$_2$O/MeCN (0.05% FA) gradient in 20 minutes to yield **21** (1.0 mg eluted at minute 12).

3.10.6 Macrolide and Quinone from CP9-13-01-036

After 12 days of cultivation, the *Actinobacteria* culture was centrifuged to separate the mycelial cake and other solids from the clarified broth. Clarified broth (4.8 L) was homogenized with a mixture of iPrOH:EtOAc (9:14 v/v). The mixture was vigorously stirred and filtered through a pad of Celite®. The organic phase was concentrated under vacuum to obtain the cell extract (543.3 mg) and further separated using NP-VLC with a stepwise Hex:EtOAc (7:3 v/v)-EtOAc-MeOH gradient. Fractions 2 (18.3 mg) and 3 (61.5 mg) eluted with Hex:EtOAc (1:1 v/v) and 100% EtOAc, respectively. Those fractions were combined and suffered a following separation by semi-preparative HPLC. HPLC separation experiments were carried out on an XBridge C18 5µm (10x150 mm) column, 75:25 to 40:60 (v/v) H_2O/MeCN (0.05% FA) gradient in 25 minutes, 3.5 mL/min, to obtain pure **22** (1.9 mg eluted at minute 23).

Fractions 8 (17.4 mg) and 9 (11.2 mg) eluted with EtOAc:MeOH (3:1 v/v) and 100% MeOH, respectively, and were further combined and separated using semi-preparative HPLC. HPLC separation experiments were carried on a Symmetry C18 7µm (7.8x150 mm) 72:28 to 63:37 (v/v) H_2O/MeCN (0.05% FA) gradient in 20 minutes, 2.3 mL/min, to obtain pure **23** (1.4 mg eluted at minute 12).

3.11 Isolated Compounds Physical Characteristics and Spectroscopic Data

2´-Deoxyadenosine (1): White crystals; ^{1}H-NMR (400 MHz, DMSO-d_6): see **Table 7**; HRESIMS: *m/z* 252.1139 [M+H]$^+$ (calculated 252.1097), 274.1006 [M+Na]$^+$ (calculated 274.0916), 136.0664 [M-$C_5H_8O_3$+H]$^+$ (calculated 136.0623).

Thymine (2): White crystals; ^{1}H-NMR (400 MHz, DMSO-d_6): see **Table 7**; HRESIMS: *m/z* 127.0530 [M+H]$^+$ (calculated 127.0507), 253.0970 [2M+H]$^+$ (calculated 253.0937), 275.0793 [2M+Na]$^+$ (calculated 275.0756).

Thymidine (3): White crystals; ^{1}H-NMR (400 MHz, DMSO-d_6) see **Table 7**; HRESIMS: m/z 241.0881 [M-H]$^-$ (calculated 241.0824), 483.1743 [2M-H]$^-$ (calculated 483.1727).

2´-Deoxyuridine (4): White crystals; ^{1}H-NMR (400 MHz, DMSO-d_6): see **Table 7**; HRESIMS: *m/z* 227.0664 [M-H]$^-$ (calculated 227.0668), 455.1452 [2M-H]$^-$ (calculated 455.1414).

2´-Deoxyinosine (5): White crystals; ^{1}H-NMR (400 MHz, DMSO-d_6): see

Table 7; HRESIMS: m/z 251.0833 [M-H]$^-$ (calculated 251.0780), 503.1624 [2M-H]$^-$ (calculated 503.1639), 135.0346 [M-C$_5$H$_8$O$_3$-H]$^-$ (calculated 135.0307).

2´-Deoxycytidine (6): White crystals; ^{1}H-NMR (400 MHz, DMSO-d_6): see **Table 7**; HRESIMS: m/z 228.1005 [M+H]$^+$ (calculated 228.0984), 455.1949 [2M+H]$^+$ (calculated 445.1890), 477.1778 [2M+Na]$^+$ (calculated 477.1710), 112.0551 [M-C$_5$H$_8$O$_3$+H]$^+$ (calculated 112.0512).

Adenosine (7): White crystals; ^{1}H-NMR (400 MHz, DMSO-d_6): see **Table 7**; HRESIMS: m/z 268.1084 [M+H]$^+$ (calculated 268.1046), 252.1070 [M-OH+H]$^+$ (calculated 252.1097), 136.0642 [M-C$_5$H$_8$O$_3$+H]$^+$ (calculated 136.0623).

2´-Deoxyguanosine (8): White crystals; ^{1}H-NMR (400 MHz, DMSO-d_6): see **Table 7**; HRESIMS: m/z 266.0925 [M-H]$^-$ (calculated 266.0889), 533.1874 [2M-H]$^-$ (calculated 533.1857), 150.0451 [M-C$_5$H$_8$O$_3$-H]$^-$ (calculated 150.0416).

Haploscleridamine (9): Amorphous white solid; $[α]^{25}_D$ +4.1 (c 0.11, MeOH); IR (MeOH) $υ_{max}$ 2855 (br), 1673, 1436, 1366, 1204, 1136, 1002, 838, 800, 746, 723 cm^{-1}; UV/Vis (MeOH) $λ_{max}$ 272, 279, 289 nm. ^{1}H-NMR (400 MHz, CH$_3$OD): δ ppm 3.13 (m, 1H, H-4), 3.49 (m, 2H, H-3, H-10), 5.11 (dd, J = 9.0, 4.9 Hz, 1H, H-1), 7.09 (td J = 7.5, 7.5, 1.0 Hz, 1H, H-12), 7.20 (ddd, J = 8.2, 7.0, 1.2 Hz, 1H, H-6), 7.36 (d, J = 8.1 Hz, 1H, H-7), 7.39 (d, J = 8.1 Hz), 1H, H-8), 7.52 (d, J = 7.9 Hz, 1H, H-5), 8.93 (d, J = 1.2 Hz, 1H, H-13),; ESIMS: m/z 253.3[M+H]$^+$.

Compound 10: Amorphous white solid; $[α]^{25}_D$ +2.3 (c 0.14, MeOH); IR (MeOH) $υ_{max}$ 2853 (br), 2926, 1676, 1440, 1135, 1026, 839, 799, 723 cm^{-1}; UV/Vis (MeOH) $λ_{max}$ 221, 279, 289 nm. ^{1}H-NMR (400 MHz, d_6-DMSO) and ^{13}C-NMR (100 MHz, $d6$-DMSO): see **Table 8**; ESIMS: m/z 216.1 [M+H]$^+$.

3β-Acetoxy-15-hydroxyspongia-12-en (11): Amorphous white solid; $[α]^{25}_D$ +10.6 (c 0.03, CH$_3$OH); IR (neat) $υ_{max}$ 3413 (br), 2927, 2853, 1683, 1443, 1368, 1247, 1138, 725 cm^{-1}; UV/Vis (CH$_3$OH) $λ_{max}$ 199 nm. ^{1}H-NMR (500 MHz, CD$_3$OD) and ^{13}C NMR (100 MHz, CD$_3$OD): see **Table 9**; ESIMS m/z 345.4 [M-H$_2$O]$^+$, 385.3 [M+Na]$^+$ and 747.5 [2M+Na]$^+$. HRESITOFMS: m/z 345.2451 [M-H$_2$O]$^+$ (calculated for C$_{22}$H$_{33}$O$_3$, 345.2430), 362.2690 [M]$^+$ (calculated for C$_{22}$H$_{34}$O$_4$, 362.2457) 385.2381 [M+Na]$^+$ (calculated for C$_{22}$H$_{34}$O$_4$Na, 385.2355) 729.4733 [2M+Na-H$_2$O]$^+$ (calculated for C$_{44}$H$_{66}$O$_7$Na, 729.4706) 747.4845 [2M+Na]$^+$ (calculated for C$_{44}$H$_{68}$O$_8$Na, 747.4812).

3-Methylspongia-3,12-dien-16-one (12): Amorphous white solid; ^{1}H-NMR

(500 MHz, CD$_3$OD) and ^{13}C NMR (100 MHz, CD$_3$OD): see **Table 9**; ESIMS *m/z* 301.3 [M+H]$^+$, 323.3 [M+Na]$^+$, 602.5 [2M+H]$^+$ and 623.5 [2M+Na]$^+$. HRESITOFMS: *m/z* 301.2176 [M+H]$^+$ (calculated for C$_{20}$H$_{29}$O$_2$, 301.2168), 623.4072 [2M+Na]$^+$ (calculated for C$_{40}$H$_{56}$O$_4$Na, 623.4076).

1-(2,4-Dihydroxy-5-methyphenyl)ethan-1-one (13): Dark brown oil; [α]^{25}$_D$ +3.8 (c 0.0439, CH$_3$OH); IR (neat) υ$_{max}$, 3314 (br), 2971, 2853, 1652, 1406, 1038 cm^{-1}. UV/Vis (MeOH) λ$_{max}$ 194, 210, 232, 265, 360 nm. ^{1}H-NMR (400 MHz, CDCl$_3$) δ ppm 2.27 (s, 1H, H-7), 2.56 (s, 3H, H$_3$-14), 4.68 (br s, 1H, OH-1), 6.77 (s, 1H, H-5), 7.10 (s, 1H, H-2), 11.84 (br s, 1H, COO<u>H</u>-1); ^{13}C-NMR (100 MHz, CDCl$_3$) δ ppm 16.7 (C-7), 26.6 (C-14), 114.9 (C-2), 117.6 (C-3), 120.0 (C-5), 135.7 (C-6), 146.1 (C-1), 156.7 (C-4), 203.4 (<u>C</u>OOH-1); HRESIMS: *m/z* 165.0552 [M-H]$^-$ (calculated for C$_9$H$_9$O$_3$, 165.0552).

6-(1,5-Dimethyl-1,4-hexadienyl)-3-methylbenzene-1,4-diol (14): Dark brown oil; [α]^{25}$_D$ +17.9 (c 0.177, CH$_3$OH); IR (neat) υ$_{max}$ 3413 (br), 2970, 2913, 1416, 1187 cm^{-1}; UV/Vis (MeOH) λ$_{max}$ 229, 299 nm. ^{1}H-NMR (400 MHz, CDCl$_3$) and ^{13}C-NMR (100 MHz, CDCl$_3$): see **Table 10**; HRESIMS: *m/z* 231.1496 [M-H]$^-$ (calculated for C$_{15}$H$_{19}$O$_2$, 231.1385).

6-(3-Hydroxy-6-methyl-1,5-heptadien-2-yl)-3-methylbenzene-1,4-diol (15): Yellow amorphous solid; [α]^{25}$_D$ +0.72 (c 0.484, CH$_3$OH); IR (MeOH) υ$_{max}$ 3314 (br), 2943, 2831, 1033 cm^{-1}; UV/Vis (MeOH) λ$_{max}$ 195, 299 nm. ^{1}H-NMR (400 MHz, CDCl$_3$) and ^{13}C-NMR (100 MHz, CDCl$_3$): see **Table 10**; HRESIMS: *m/z* 247.1344 [M-H]$^-$ (calculated for C$_{15}$H$_{19}$O$_3$, 247.1334) 149.0575 [M-C$_6$H$_{11}$O]$^-$ (calculated for C$_9$H$_9$O$_2$, 149.0602).

4-Hydroxy-3,7-dimethyl-7-(3-methylbut-2-en-1-yl)benzofuran-17-one (16): Yellow amorphous solid; [α]^{25}$_D$ +2.2 (c 0.115, CH$_3$OH); IR (MeOH) υ$_{max}$ 3313 (br), 2944, 2832, 1656, 1451, 1035 cm^{-1}; UV/Vis (MeOH) λ$_{max}$ 196, 294 nm. ^{1}H-NMR (400 MHz, CDCl$_3$) and ^{13}C-NMR (100 MHz, CDCl$_3$): see **Table 10**; HRESIMS: *m/z* 245.1126 [M-H]$^-$ (calculated for C$_{15}$H$_{17}$O$_3$, 245.1177).

3,16-Dimethyl-7-(3-methylbut-2-en-1-yl)benzofuran-4-ol (17): Yellow amorphous solid; [α]^{25}$_D$ +2.2 (c 0.257, CH$_3$OH); IR (neat) υ$_{max}$ 3266 (br), 2915, 1437, 1168, 805, 434 cm^{-1}; UV/Vis (MeOH) λ$_{max}$ 203, 257, 297 nm. ^{1}H-NMR (400 MHz, CDCl$_3$) and ^{13}C-NMR (100 MHz, CDCl$_3$): see **Table 11**; HRESIMS: *m/z* 229.1234 [M-H]$^-$ (calculated for C$_{15}$H$_{17}$O$_2$, 229.1229).

6-(2-Methoxy-6-methylhept-5-en-2-yl)-3-methylbenzene-1,4-diol (18): Dark brown oil; [α]^{25}$_D$ +5.0 (c 0.0337, CH$_3$OH); IR (MeOH) υ$_{max}$ 3339 (br), 2926, 1453, 1374, 1183, 1051 cm^{-1}; UV/Vis (MeOH) λ$_{max}$ 196, 297 nm. ^{1}H-NMR (400 MHz, CDCl$_3$) and ^{13}C-NMR (100 MHz, CDCl$_3$): see **Table 11**;

HRESIMS: m/z 263.1610 [M-H]$^-$ (calculated for $C_{16}H_{23}O_3$, 263.1647).

3,7,11,11-Tetramethyl-1,9-dihydro-2-benzoxirenoxocin-6-ol (19): Green crystals; $[\alpha]^{25}_D$ -10.4 (c 0.0322, CH$_3$OH); IR (neat) υ_{max} 3388 (br), 2926, 1412, 1178, 994, 829, 597 cm^{-1}; UV/Vis (MeOH) λ_{max} 194, 217, 330 nm. ^{1}H-NMR (400 MHz, CDCl$_3$) and ^{13}C-NMR (100 MHz, CDCl$_3$): see **Table 11**; HRESIMS: m/z 245.1126 [M-H]$^-$ (calculated for $C_{15}H_{17}O_3$, 245.1177).

Fluvirucinin C$_1$ (20): Amorphous white solid; $[\alpha]^{25}_D$ +67.0 (c 0.05, MeOH/CHCl$_3$ 1:1). IR (KBr): υ_{max} 3300 (br), 3090, 2950, 1708, 1635, 1540, 1475 cm^{-1}. ^{1}H-NMR (500 MHz, CDCl$_3$/CD$_3$OD) and ^{13}C-NMR (100 MHz, CDCl$_3$/CD$_3$OD): see **Table 12**. ESIMS m/z 310.4 [M+H]$^+$, 332.3 [M+Na]$^+$, and 641.8 [2M+Na]$^+$. HRESIMS: m/z 310.2751 [M+H]$^+$ (calculated for $C_{19}H_{36}NO_2$, 310.2741), 332.2599 [M+Na]$^+$ (calculated for $C_{19}H_{35}NO_2Na$, 332.2568). 641.5283 [2M+Na]$^+$ (calculated for $C_{38}H_{70}N_2O_4Na$, 641.5249).

Fluvirucinin C$_2$ (21): Amorphous white solid; $[\alpha]^{25}_D$ +18.8 (c 0.10, MeOH/CHCl$_3$ 1:1). IR (KBr): υ_{max} 3320 (br), 3100, 2975, 1720, 1635, 1560, 1490, 1050 cm^{-1}. ^{1}H-NMR (500 MHz, CDCl$_3$) and ^{13}C-NMR (100 MHz, CDCl$_3$): see **Table 12**. ESIMS m/z 348.4 [M+Na]$^+$, 308.3 [M-H$_2$O+H]$^+$ and 673.5 [2M+Na]$^+$. HRESIMS: m/z 326.2771 [M+H]$^+$ (calculated for $C_{19}H_{36}NO_3$, 326.2690), 308.2602 [M-H$_2$O+H]$^+$ (calculated for $C_{19}H_{34}NO_2$, 332.2584), 348.2521 [M+Na]$^+$ (calculated $C_{19}H_{35}NO_3Na$, 348.2509), 673.5141 [2M+Na]$^+$ (calculated for $C_{38}H_{70}N_2O_6Na$, 673.5119).

2-Hydroxyethyl-3-methyl-1,4-naphthoquinone (22): Amorphous white solid; ^{1}H-NMR (500 MHz, CDCl$_3$): δ ppm 2.25 (s, 3H, 3′-H$_3$), 2.96 (t, J = 7.1 Hz, 2H, 1′-H$_2$), 3.85 (t, J = 6.5 Hz, 2H, 2′-H$_2$), 7.71 (m, 2H, 6-H, 7-H), 8.07 (m, 2H, 5-H, 8-H); ^{13}C NMR (100 MHz, CDCl$_3$): δ ppm 185.7 (C-1), 185.2 (C-4), 145.3 (C-3), 144.0 (C-2), 133.7 (C-6), 133.6 (C-7), 132.3 (C-8a), 132.1 (C-4a), 126.5 (C-5), 126.5 (C-8) 61.7 (C-2′), 30.8 (C-1′), 13.1 (C-3′). ESIMS m/z 217.1 [M+H]$^+$, 199.1 [M+-H$_2$O+H]$^+$.

Mangrolide A (23): Amorphous white solid; ^{1}H-NMR (500 MHz, CDCl$_3$) and ^{13}C-NMR (100 MHz, CDCl$_3$): see **Table 13**. ESIMS m/z 780.5 [M+H]$^+$.

3.12   Bioactivities

3.12.1 Cytotoxicity Activity

Cytotoxic activity assessment of pure compounds and extracts was performed towards A-549 human lung carcinoma cells, MDA-MB-231 human breast adenocarcinoma cells, HT-29 human colorectal carcinoma cells and

PSN1 human pancreatic adenocarcinoma cells. Briefly, cells were plated in 96-well plates at 5×10^3 cells/well and placed on an 37ºC incubator for 24 hours. After the incubation time, cells were treated with the respective pure compounds. One untreated plate was fixed and stained and used as a reference. Treated cells were further incubated for 48 hours and quantified using the sulforhodamine B (SRB) protein stain method [173]. 150 ppm SRB (w/v) and 380 ppm CH_3COOH (v/v) were added to each well and left at room temperature for 20 minutes. SRB was removed and the plates washed 5 times with 1% CH_3COOH before air drying. Bound SRB was solubilized with 200 mL 10 mM unbuffered Tris-base solution and plates were left on a plate shaker for 10 minutes. Absorbance was read in a 96-well plate reader at 492 nm subtracting the background measurement at 620 nm.

Pure compounds were tested at concentrations ranging from 2.6 to 10000 μg/mL. Cell survival was expressed as a percentage of control cell growth/cell death (i.e. cytostatic vs. cytotoxic compounds) using the National Cancer Institute (NCI) algorithm [174].

3.12.2 Anti-microbial Activity

Anti-microbial activity assessment of the pure compounds was performed using the paper disk diffusion method [175] against three bacteria, *Escherichia coli* (ATCC 8739), *Pseudomonas aeruginosa* (ATCC 9027), *Staphylococcus aureus* (ATCC 6538) and one fungus, *Candida albicans* (ATCC 10231). In brief, seed cultures of the target strains were prepared by incubating the organism for 24 hours at 28 °C in tryptone soya broth (TSB). Aliquots of the overnight cultures were used to inoculate tryptone soya agar (TSA) before solidification. Sterile filter disks (6 mm diameter) were infused with 10 μL of tested compound dissolved in MeOH at the desired concentration and added to the plates. The plates were incubated at 28 °C for 24 h. After the incubation time, the diameter of growth inhibition zones was measured around each disk. Pure compounds were tested at 1 μg/μL against the bacterial strains and at 1, 2 and 3 μg/μL against the fungal strain. Nalidixic acid, gentamicin, vancomycin and amphotericin B at 1 μg/μL were used as positive controls for *E. coli*, *P. aeruginosa*, *S. aureus* and *C. albicans*, respectively.

3.12.3 Anti-obesity Activity

The anti-obesity activity of the isolated compounds was performed using the zebrafish Nile red assay [176, 177]. In brief, zebrafish embryos were raised

from 1 day post fertilization (DPF) in egg water (60 µg/mL marine sea salts) with 200 µM 1-phenyl-2-thiourea to inhibit pigmentation. From 3 to 5 DPF, 6–8 zebrafish larvae/well in a 24-well plate were exposed to compounds at concentrations ranging from 312.5 nM to 10 µM. A solvent (0.1% DMSO) and positive controls (50 µM resveratrol) were included in the assay. Lipids were stained overnight with 10 ng/mL Nile red. For imaging, the larvae were anesthetized with tricaine (MS-222, 0.03%) for 5 minutes and fluorescence analyzed with a fluorescence microscope (Olympus BX43, Hamburg, Germany). Fluorescence intensity was quantified in individual zebrafish larvae using the software ImageJ [178].

4 Results

4.1 Icelandic Sponges

4.1.1 Biological Samples Extraction and Analysis

The five sponges used in this study and their diverse morphology are shown in Figure 18. Specimens were extracted and fractionated according to the procedure described in material and methods section 3.4.1. Dry weight of each one of the obtained crude extracts and respective Kupchan fractions was recorded and is summarized in Table 5.

JS-A9-2011 #1   JS-A9-2011 #6   A5-2010-93

210111 #3   030915 #1
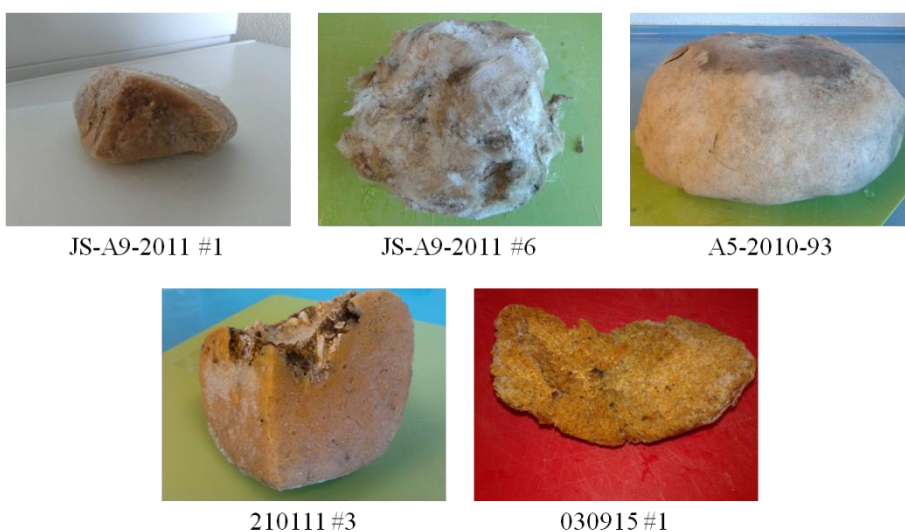
Figure 18 – Pictures of frozen sponges collected in the Icelandic waters and used in the study.

As a standard dereplication approach, all extracts were analyzed using QTOF-UPLC-MS. The obtained chromatograms/spectra were then compared using available databases. ^{1}H-NMR analysis of all extracts was performed to integrate the dereplication process. The first combined analysis of the selected sponges showed a clear indication that these sponges are rich in fatty acids, low molecular weight known compounds and primary metabolites. Fatty acids are commonly extracted in very complex mixtures and are very

difficult to separate from each other due to their high hydrophobic properties. Frequently, after the isolation process, fatty acids turn out to be non-active compounds.

Table 5 - Resume of yields obtained for each Icelandic sponge extraction/fractionation.

| | Dried sponge | Crude extract | Liquid/liquid partition fractions | | | | |
			A	B	C	D	E
JS-A9-2011 #1	280.0 g	12.13 g	1.079 g	1.844 g	0.1670 g	1.638 g	2.867 g
JS-A9-2011 #6	212.0 g	10.00 g	0.485 g	2.233 g	0.2680 g	0.1310 g	4.631 g
A5-2010-93	388.0 g	14.57 g	2.079 g	1.844 g	0.1680 g	1.638 g	2.867 g
210111 #3	64.00 g	15.36 g	3.564 g	2.033 g	0.5540 g	2.380 g	0.6500 g
030915 #3	2067 g	74.00 g	43.43 g	0.01200 g	0.4990 g	5.538 g	1.625 g

The UPLC-QTOF-MS method was chosen for the analysis of the sponge extracts because our research group had previous experience using this method for marine extracts analyses [179-181]. This method involves the use of an ACQUITY BEH C18 column covering both high and low polarity, to be able to efficiently separate the secondary metabolites present in the extracts. This resulted in a clear mass spectrum which allowed an attempt on the dereplication of each one of the peaks in the chromatogram. However, it was not possible to separate highly polar compounds using the standard UPLC-QTOF-MS method. Sponge Kupchan fractions D and E were often not retained by the column and not separated with the chromatographic conditions that were used.

Fraction D of sponge A5-2010-93 was one of the extracts showing the chromatographic profile previously described, as it can be seen in Figure 21a. A dereplication attempt showed that the pile of compounds that was not separating in the column and being eluted in the first three minutes, contained mainly marine nucleosides. Known marine nucleosides are very often not filtered by the dereplication process and end up being isolated [182, 183]. In an attempt to avoid that in future analysis and to improve the efficiency while looking for new natural compounds, this fraction was selected to optimize a chromatographic method to be used for dereplication of this type of compounds. The taxonomy of A5-2010-93 sponge sample was also studied.

4.1.2 Geodia macandrewi Identification

The sponge specimen A5-2010-93 (0.748 g) was collected in the southwest of Iceland at 226 meters dept using a deep sea probe. The sponge presented a whitish and massive body, with a globular lobately shape. The outside consistency was hard and rough to the touch and the inside was pulpy, as shown by the pictures in Figure 19. This morphology allowed a clear identification of the sponge as a *Geodia macandrewi* specimen (Taxonomist Professor Han Tore Rapp, University of Bergen, Norway). In an attempt of confirming this assumption, the sponge spicules were extracted using acid-digestion and observed on the electron microscope.

Figure 19 - External morphology of the sponge identified as *Geodia macandrewi*. **a)** Specimen after collection. **b)** Frozen sponge. **c)** Cut of the frozen sponge.

High abundance of straight pointed oxea-like spicules (around 150 µm length) was the first obvious observation in the slides. Dichotrienes and Anatrienes also appeared in high abundance (Figure 20b and b´). Protocladi with diameters up to 50 µm as well as sphereoasters and oxyasters up to 20 µm were also found as part of this sponge (Figure 20c-f). Finally, rounded-shaped sterrasters were found, which were rare (Figure 20f´). The morphological identification as *Geodia macandrewi* was confirmed according to Cárdenas *et al.*, 2013 [138].
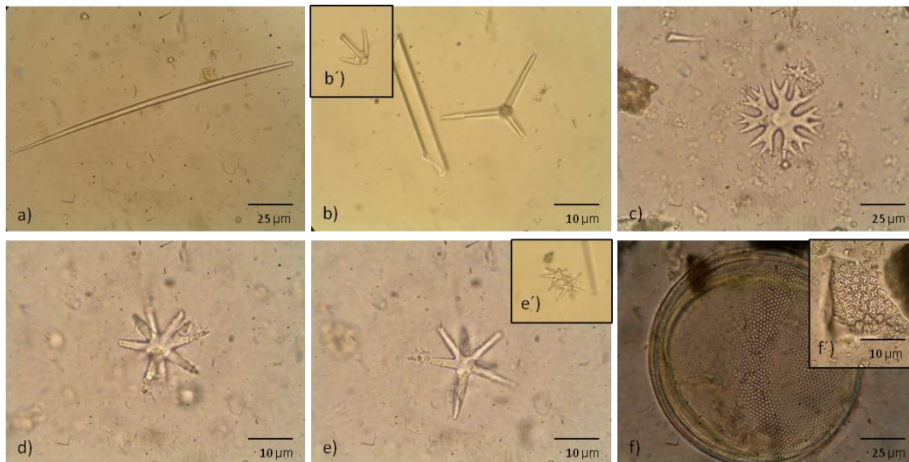
Figure 20 - Spicules of Geodia macandrewi Bowerbank, 1858. Megascleres: **a)** Pointed oxeas. **b)** Dichotriene. **b´)** Anatriene. **c)** Protocladi. **d)** Sphereoasters. **e)** and **e´)** oxyasters. **f)** Sterraster. **f´)** Close-up on the warty rosettes of a sterraster.

4.1.3 UPLC-QTOF-MS Analysis

Due to their similar chemical structures and high polarity, nucleosides are difficult to separate. An individual identification of each in the base peak intensity chromatogram was not possible using the UPLC method described in 3.6.1, as seen in the chromatogram represented in Figure 21a. To improve their separation, a BEH amide column was used. The separation performance was improved supplementing the mobile phases with 0.2% CH_3COOH and 10 mM CH_3COONH_4. *Geodia macandrewi* fraction D was analyzed at the optimized chromatographic conditions. The results are shown in the base peak intensity chromatogram presented in Figure 21b. The optimized conditions offer the possibility of a better individual visualization of the metabolites present in the extract and an individual dereplication of marine nucleosides in the mixture. A targeted approach was applied for nucleosides identification.
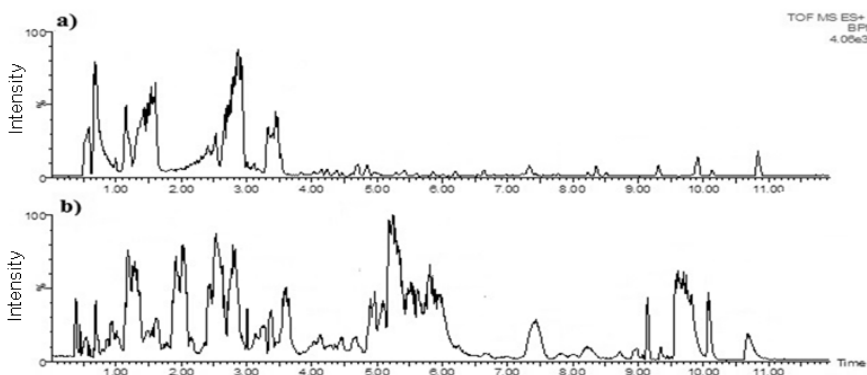
Figure 21 - UPLC-QTOF-MS base peak intensity chromatograms of *Geodia macandrewi* fraction D (BuOH fraction). **a)** Separation acquired using an ACQUITY BEH C18 1.7 µm (2.1 × 150 mm) column and a 98:2 to 0:100 H_2O/MeCN (0.1% FA). **b)** Separation acquired using an ACQUITY UPLC BEH Amide 1.7 µm (2.1 mm x 100 mm) column and a 10:90 to 15:85 H_2O/MeCN (0.2% CH_3COOH + 10 mM CH_3COONH_4) gradient.

Results found for the targeted identification of each one of the nucleosides in *Geodia macandrewi* fraction D using UPLC-QTOF-MS under optimized conditions are resumed on Figure 22. Both positive ((+)ESI) and negative ((-)ESI) ionization modes were used for analysis of the targeted nucleosides in the extract. (-)ESI was found to be more sensitive than (+)ESI for 2´-deoxyuridine, 2´-deoxyinosine, 2´-deoxyguanosine and thymidine. 2´-Deoxycytidine, thymine, 2´-deoxyadenosine and adenosine did not ionize in (-)ESI mode, but were ionized in (+)ESI mode. Zhao *et al.* (2013) [184] developed a method to analyze the fungal species *Cordyceps* nucleosides. Their results showed increased sensitivity in (+)ESI mode compared to (-)ESI for these compounds and they were able to detect thymidine in positive ionization mode. This is not in accordance with the results presented, which showed better sensitivity for most of the compounds in (-)ESI mode. Thymidine was also only detected in (-)ESI. These differences may be related to the complexity of the analyzed extracts. Sponge extracts are very complex and, consequently, the detection of targeted compounds may be suppressed or suffer from interference of other compounds present in the extract.
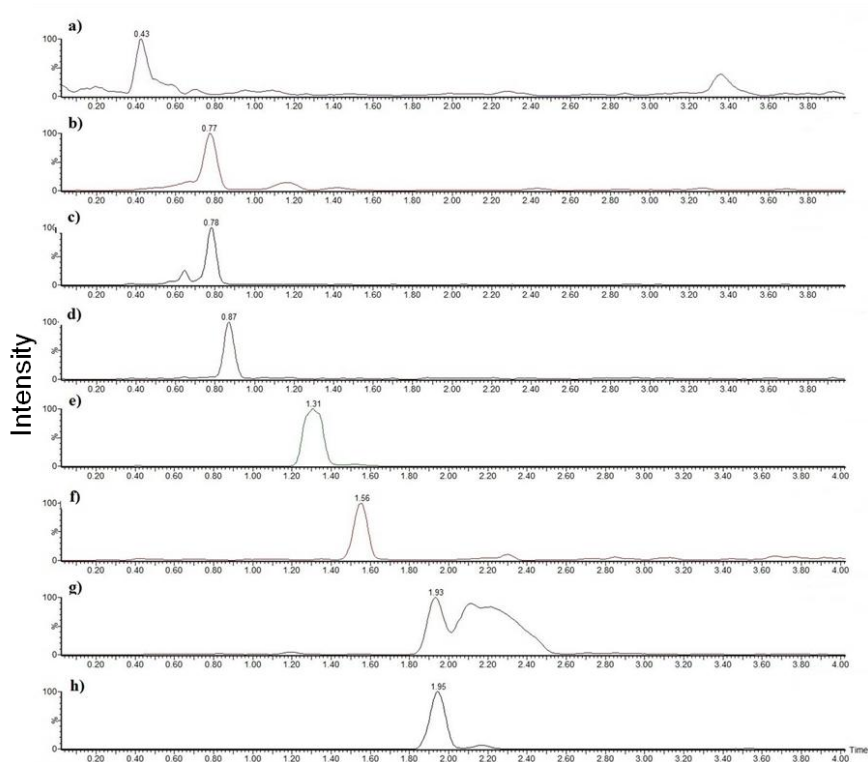
Figure 22 - Extracted ion chromatograms for the targeted nucleosides and nucleobase found in *Geodia macandrewi* fraction D (ACQUITY UPLC BEH Amide 1.7 µm (2.1 mm x 100 mm) column and a 10:90 to 15:85 H_2O/MeCN (0.2% CH_3COOH + 10 mM CH_3COONH_4) gradient). **a)** 2´-Deoxyadenosine. **b)** Thymine. **c)** Thymidine. **d)** 2´-Deoxyuridine. **e)** 2´-Deoxyinosine. **f)** 2´-Deoxycytidine. **g)** Adenosine. **h)** 2´-Deoxyguanosine. 2´-Deoxyadenosine, thymine, 2´-deoxycytidine and adenosine were detected in (+)ESI. The other compounds were detected in (-)ESI.

Table 6 - UPLC-QTOF-MS measurements for *Geodia macandrewi* targeted nucleosides and nucleobase.

Compound No	Retention time (min)	Compound	ESI mode	Proposed ions	Elemental composition	Theoretical value m/z	Experimental m/z	Error ppm
1	0.43	2´-Deoxyadenosine	+	$[M+H]^+$	$C_{10}H_{14}N_5O_3$	252.1097	252.1139	16.7784
				$[M+Na]^+$	$C_{10}H_{13}N_5O_3Na$	274.0916	274.1006	32.8357
				$[M-C_5H_8O_3+H]^+$	$C_5H_6N_5$	136.0623	136.0664	30.1333
2	0.77	Thymine	+	$[M+H]^+$	$C_5H_7N_2O_2$	127.0507	127.0530	18.1030
				$[2M+H]^+$	$C_{10}H_{13}N_4O_4$	253.0937	253.0970	13.0386
				$[2M+Na]^+$	$C_{10}H_{12}N_4O_4Na$	275.0756	275.0793	13.4508
3	0.78	Thymidine	-	$[M-H]^-$	$C_{10}H_{13}N_2O_5$	241.0824	241.0881	23.6434
				$[2M-H]^-$	$C_{20}H_{27}N_4O_{10}$	483.1727	483.1743	3.3114
4	0.87	2´-Deoxyuridine	-	$[M-H]^-$	$C_9H_{11}N_2O_5$	227.0668	227.0664	-1.7616
				$[2M-H]^-$	$C_{18}H_{23}N_4O_{10}$	455.1414	455.1452	8.3490
5	1.31	2´-Deoxyinosine	-	$[M-H]^-$	$C_{10}H_{11}N_4O_4$	251.0780	251.0833	30.2695
				$[2M-H]^-$	$C_{20}H_{23}N_8O_8$	503.1639	503.1624	-2.9811
				$[M-C_5H_8O_3-H]^-$	$C_5H_3N_4O$	135.0307	135.0346	28.8823
6	1.56	2´-Deoxycytidine	+	$[M+H]^+$	$C_9H_{14}N_3O_4$	228.0984	228.1005	9.2065
				$[2M+H]^+$	$C_{18}H_{27}N_6O_8$	445.1890	455.1949	12.9616
				$[2M+Na]^+$	$C_{18}H_{26}N_6O_8Na$	477.1710	477.1778	14.2507
				$[M-C_5H_8O_3+H]^+$	$C_4H_6N_3O$	112.0512	112.0551	34.8055
7	1.93	Adenosine	+	$[M+H]^+$	$C_{10}H_{13}N_5O_4$	268.1046	268.1084	14.1733
				$[M-OH+H]^+$	$C_{10}H_{14}N_5O_3$	252.1097	252.1070	-10.7096
				$[M-C_5H_8O_4+H]^+$	$C_5H_6N_5$	136.0623	136.0642	13.9642
8	1.95	2´-Deoxyguanosine	-	$[M-H]^-$	$C_{10}H_{12}N_5O_4$	266.0889	266.0925	13.5293
				$[2M-H]^-$	$C_{20}H_{23}N_{10}O_8$	533.1857	533.1874	3.1884
				$[M-C_5H_8O_3-H]^-$	$C_5H_4N_5O$	150.0416	150.0451	23.3269

Nucleosides and nucleobases were identified based on their exact masses. An example for compound **6** is shown in Figure 23, the exact masses extracted from the (+)ESI mass spectrum were *m/z* 477.1778, *m/z* 455.1949, *m/z* 228.1005 and *m/z* 112.0551. Those measurements resulted from the ions $[2M+Na]^+$, $[2M+H]^+$, $[M+H]^+$ and $[M-C_5H_8O_3+H]^+$, respectively, which were consistent with the elemental compositions $C_{18}H_{26}N_6O_8Na$, $C_{18}H_{27}N_6O_8$, $C_9H_{14}N_3O_4$ and $C_4H_6N_3O$. This allowed the identification of that specific chromatographic peak as 2´-deoxycytidine. The same principle was applied to all the other targeted nucleosides and nucleobase. The obtained results are summarized in Table 6. The molecular ion, $[M+H]^+$, was clearly identified for all compounds. For all the nucleosides analyzed in (+)ESI, the nucleobase appears as the most intense peak. However, for thymine and the nucleosides analyzed in (-)ESI, the highest intensity peak observed is the molecular ion, $[M+H]^+$. Dimeric and sodium adduct ions were also commonly seen in the obtained spectra.
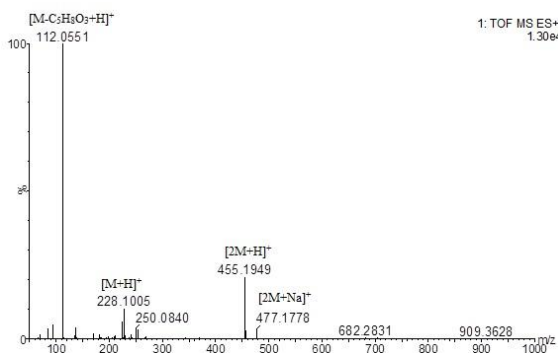
Figure 23 - (+)ESIMS spectrum obtained for 2´-deoxycytidine dereplicated in *Geodia macandrewi* fraction D (BuOH faction).

A compilation of the experimentally extracted exact masses and the correspondent theoretical value is shown in Table 6. The differences between those two values are also reported in Table 6. This difference seems to be significantly higher than others previously reported in the literature, which reported natural nucleosides with exact masses differing from theoretical masses not more than 4 ppm [184, 185]. This study shows differences that can go up to 35 ppm. That the elemental isotopic composition is variable

according to several geographical and biological parameters is well established [186]. Other studies have reported differences between theoretical and experimental exact masses within the same range, 35 ppm, or even higher of other compounds isolated from marine sponges [187-190]. This allows attributing those differences to natural variations.

To confirm the identity of the targeted compounds and their efficient dereplication, a separation and isolation by preparative HPLC and NMR analysis were performed.

4.1.4 Nucleosides Isolation and Identification by ^{1}H-NMR

Geodia macandrewi fraction D was then submitted to repeated preparative HPLC separation for purification of identified nucleosides and nucleobase. A resumed scheme of their isolation is represented in Figure 24. The nucleosides were purified using a preparative Phenomenex Luna C18 5µm column. The mobile phase used had a very high aqueous content due to the compound´s high polarity. The mobile phases were supplemented with 1M NaCl, once it was found to induce a noticeable retardation and separation of the peaks, as it can be seen in the UV-chromatograms represented in Figure 25.
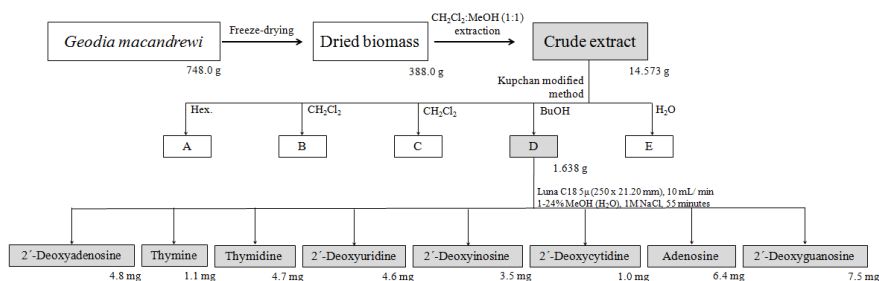
Figure 24 - Scheme of the workflow that led to the isolation of seven nucleosides and one nucleobase from the sponge *Geodia macandrewi*.
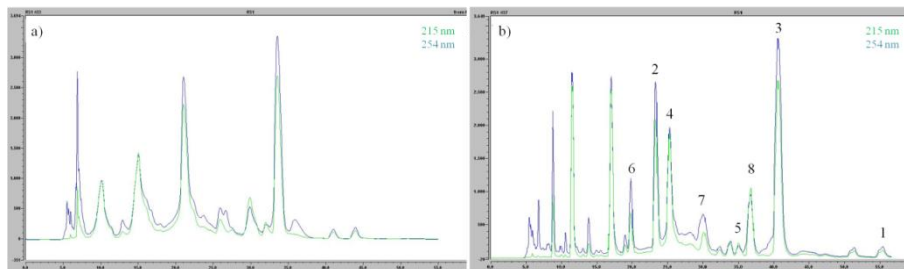
Figure 25 – *Geodia macandrewi* fraction D semi-preparative separation (Phenomenex Luna C18 5µm (250 x 21.20 mm) column, 99:1 to 76:24 (v/v) H₂O/MeOH gradient in 47 minutes, 10 mL/min). The separation was followed at 215 and 254 nm. **a)** Mobile phases not supplemented. **b)** Mobile phases supplemented with 1M NaCl. The numbers indicate the peaks correspondent to the targeted compounds.

The preparative HPLC separation led to 18 fractions. Those 18 fractions were analyzed by ^{1}H-NMR and eight of them were identified as the targeted pure compounds: 2´-deoxyadenosine (**1**), thymine (**2**), thymidine (**3**), 2´-deoxyuridine (**4**), 2´-deoxyinosine (**5**), deoxycytidine (**6**), adenosine (**7**) and 2´-deoxyguanosine (**8**). The structures are represented in Figure 26.

^{1}H-NMR obtained results are resumed in Table 7. Seven clear carbohydrate protons (δ_H 6.33, 4.40, 3.88, 3.60, 3.53, 2.71 and 2.25), together with two signals, that despite not being broad singlets were assigned as –OH (δ_H 5.38 and 5.27), were found in compound **1** proton spectrum, suggesting a deoxyribose for the sugar moiety. The remaining resonances δ_H 8.33 and 8.12 indicated the presence of an adenine as a nucleobase, which was confirmed by the NH₂-6 resonance (δ_H 7.28). ^{1}H-NMR data were then consistent to identify **1** as 2´-deoxyadenosine. Compound **7** proton spectrum was very similar to 2´-deoxyadenosine, only with an extra hydroxyl group in the sugar moiety, OH-2´ (δ_H 5.45), and a substitution of the methylene C-2´ (δ_H 2.71, 2.25) by a methine group (δ_H 4.60). This indicated a ribose as a sugar and confirmed **7** as adenosine. Signals δ_H 5.19 and 5.40 appearing as broad singlets also allowed confirming their entity as OH-3´ and OH-5´, respectively, endorsing deoxyribose as the sugar moiety present in **7** and **1**. By comparing the sugar signals, **3**, **4**, **5**, **6** and **8** were also found to contain a deoxyribose.

Table 7 - ^{1}H-NMR data (400 MHz) obtained for compounds **1-8**. Experiments were performed in DMSO-d_6.

Position	2´-Deoxyadenosine (δ_H, mult (J in Hz))	Thymine (δ_H, mult (J in Hz))	Thymidine (δ_H, mult (J in Hz))	2´-Deoxyuridine (δ_H, mult (J in Hz))	2´-Deoxyinosine (δ_H, mult (J in Hz))	2´-Deoxycytidine (δ_H, mult (J in Hz))	Adenosine (δ_H, mult (J in Hz))	2´-Deoxyguanosine (δ_H, mult (J in Hz))
1				5.62, d (8.0)		5.71, d (7.3)		10.60, br s
2	8.12, s	7.24, m	7.69, m	7.85, d (8.1)	8.05, s	7.78, d (7.2)	8.13, s	
3		10.90, br s						
5		10.90, br s	11.26, br s	11.41, br s				
8	8.33, s				8.30, s		8.33, br s	7.10, br s
1´	6.33, m		6.16, t (6.9)	6.14, t (6.8)	6.31, m	6.15, t (6.7)	5.87, d (6.2)	6.11, dd (7.83; 6.04)
2´	2.25, m 2.71, m		2.06, m	2.07, m	2.29, ddd (13.2, 6.2, 3.3) 2.63, m	1.91, m	4.60, m	2.19, ddd (13.1; 6.0; 3.0)
3´	4.40, m		4.23, m	4.22, d (3.5)	4.38, dd (5.7, 3.0)	4.19, m	4.14, m	4.33, p (6.0; 3.2)
4´	3.88, q (4.3)		3.75, q (3.8)	3.77, dd (6.7,3.7)	3.85, m	3.75, m	3.96, q (3.4)	3.80, td (4.6, 2.8)
5´	3.53, m 3.60, m		3.56, m	3.54, dt (11.6, 5.8)	3.59, m 3.51, m	3.54, m	3.53, m 3.67, d (12.0)	3.52, dtd, (16.7; 11.7; 5.0)
1-CH₃		1.72, s	1.77, s					
2-NH₂								6.44, br s
6-NH₂	7.28, br s					7.05, br s 7.12, br s	7.32, br s	
6-OH					12.35, br s			
2´-OH							5.45, br s	
3´-OH	5.38, d (4.0)		5.25, br s	5.26, d (4.1)	5.31, d (4.0)	5.18, br s	5.19, br s	5.24, d (3.9)
5´-OH	5.27, m		5.04, br s	5.04, t (5.1)	4.96, t (5.5)	4.97, br s	5.40, br s	4.93, t (5.5)
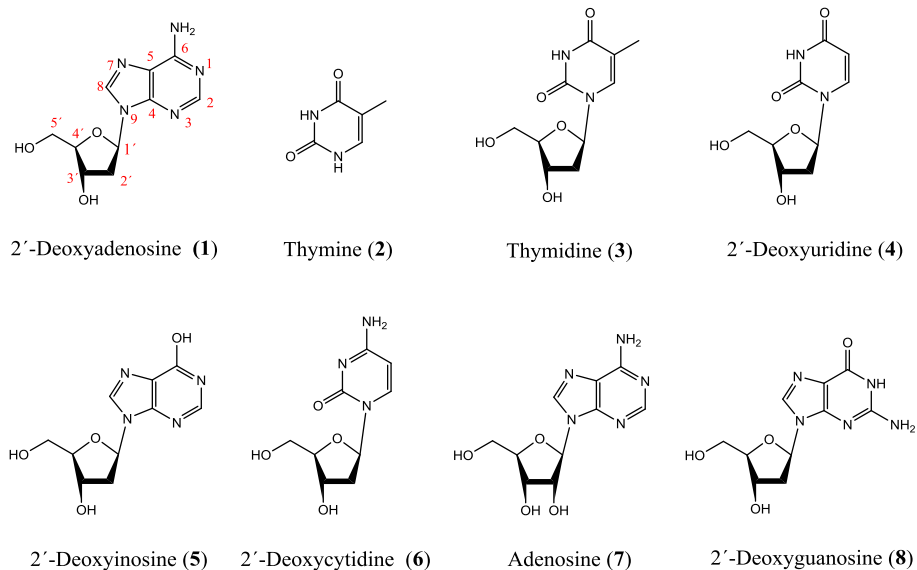
Figure 26 - Chemical structures of the nucleosides and nucleobase identified as being produced by *Geodia macandrewi* **(1-8)**.

Compound **5** proton spectrum was also very close to the one of **1**. The substitution of NH_2-6 (δ_H 7.28) in **1**, for OH-6 (δ_H 12.35) in **5**, suggested the presence of hypoxanthine as a nucleobase. **5** was, therefore, confirmed as 2´-deoxyinosine.

The methyl singlet Me-1 (δ_H 1.77) was indicative of the presence of thymine as the nucleobase of **3**. The presence of H-2 (δ_H 7.69), together with NH-5 resonance at δ_H 11.26 confirmed **3** as thymidine. Comparing its resonances with thymidine, **2** was identified as the nucleobase thymine. Also, based on proton resonance similarities, **4** was thought to be, structurally, very close to **3**. The substitution of the methyl signal by H-2 (δ_H 7.85) confirmed **4** as 2´-deoxyuridine.

A COSY cross-peak between H-1 (δ_H 5.71) and H-2 (δ_H 7.78) in **6**, seen in Figure 27, allowed the identification of the nucleobase as cytosine, confirming the identity of the nucleoside as 2´-deoxycytidine. Finally, the methine singlet H-8 (δ_H 7.10), together with the NH_2-2 (δ_H 6.44), undoubtedly indicated guanosine as the nucleobase of **8**, allowing a confirmation of its identity as 2´-deoxyguanosine.

Chemical structures of the nucleosides and nucleobases proposed based on mass spectrometry analysis were then confirmed by ^{1}H-NMR studies. All HRESIMS and ^{1}H-NMR spectra can be found in Appendixes 1 to 16.
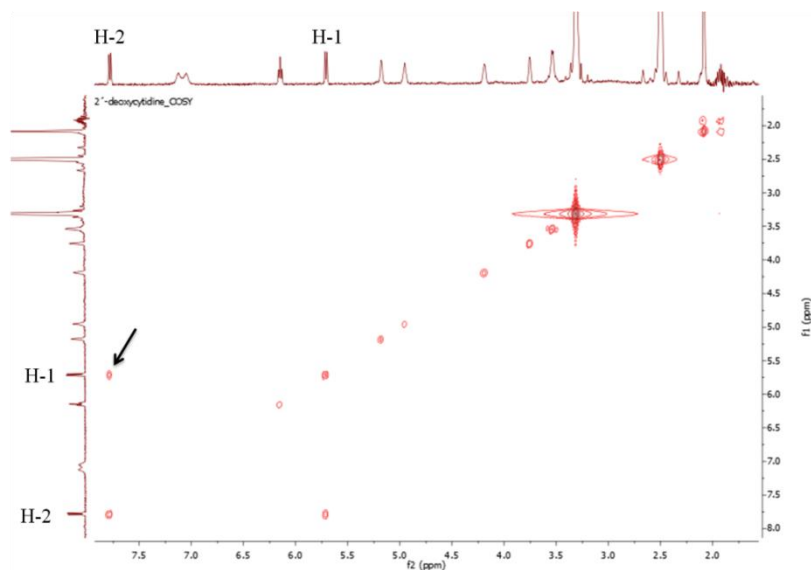
Figure 27 - *g*-COSY spectrum obtained for 2´-deoxycytidine (**6**). The arrow indicates the cross-signal H-1/H-2.

The possibility that these compounds could be the result of DNA degradation during the extraction procedure can be discarded because DNA is highly resistant to hydrolysis [191, 192]. Also, the nucleosides 2´-deoxyuridine and 2´-deoxyinosine do not occur naturally. Uracil appears exclusively in RNA and associates only with ribose and not with deoxyribose. 2´-deoxyuridine only appears in physiological conditions under high-stress mutagenic factors. Therefore, it was assumed that the isolated nucleosides are produced as secondary metabolites.

The newly developed method revealed to be extremely useful on the identification of nucleosides or structural-related compounds in marine sponge extracts. However, the search for new secondary metabolites was focused on sponge samples collected in warmer environments due to the presence of more promising chemical entities.

4.2 Sponges Collected in the Indo-Pacific Ocean

4.2.1 Alkaloids from *Acanthostrongylophora* sp.

The sponge sample labeled as ORMA 124985, collected by hand while scuba diving at Wetar (Indonesia), is shown in Figure 28. Regarding morphological features, it was identified as *Acanthostrongylophora* sp.. The sponge was immediately frozen and kept at those conditions until extraction.

Figure 28 - Picture of *Acanthostrongylophora* sp. fresh sponge sample, collected by hand while scuba diving in Wetar (Indonesia) and which led to the isolation of two alkaloids.

The procedure to purify two alkaloids was followed according to the workflow resumed in Figure 29. The sponge biomass was repeatedly extracted with CH_2Cl_2:MeOH (1:1 v/v) and the crude extract subsequently subjected to RP-VLC and semi-preparative HPLC. HPLC fraction 1 (109.2 mg) was initially indicated to contain the known compound haploscleridamine due to ^{1}H-NMR resonance similarities with published data and a MS spectrum peak at *m/z* 253.3. However, a closer look into the ^{1}H-NMR spectrum revealed the presence of an -NCH$_3$ singlet signal (δ_H 2.87), which did not belong to haploscleridamine. A careful analysis of the spectrum exposed some of the signals in duplicate. These findings, seen in Figure 30, led to the assumption that the faction should contain haploscleridamine, but was contaminated with another related compound.
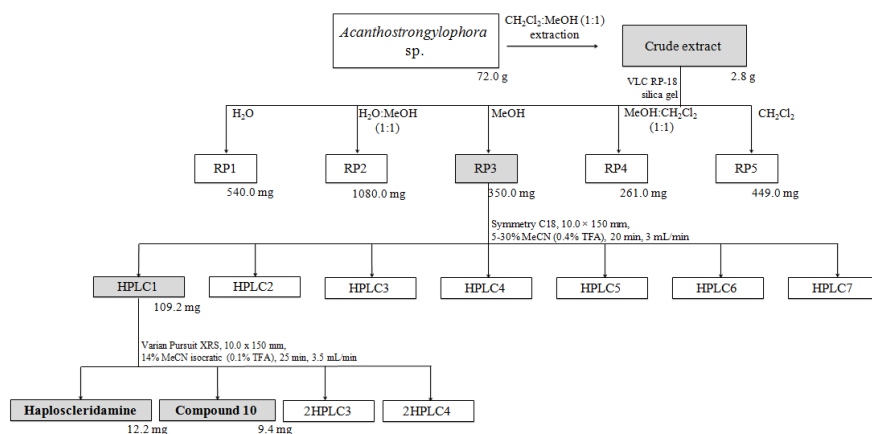
Figure 29 - Scheme of the workflow that led to the isolation of two alkaloids from the sponge *Acanthostrongylophora* sp..
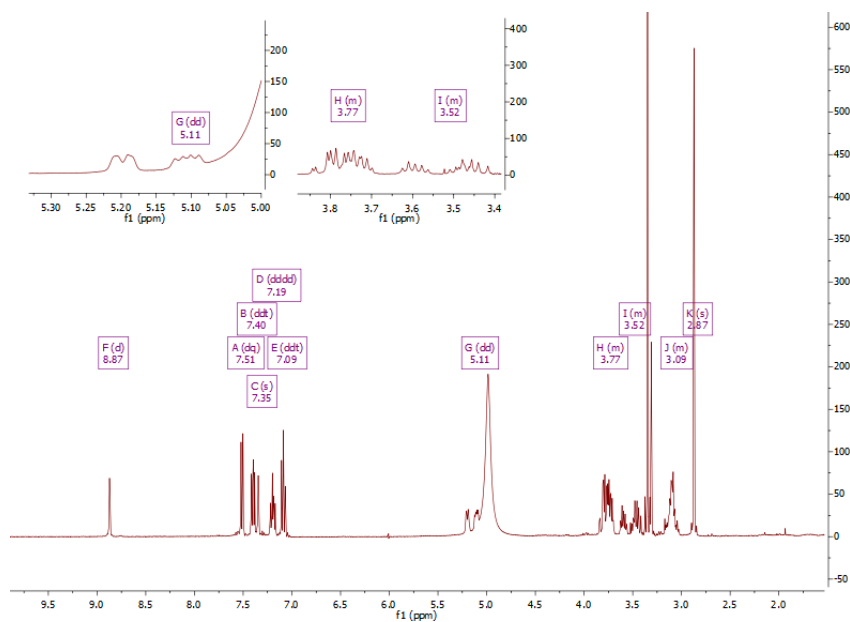
Figure 30 - ^{1}H-NMR spectrum obtained for *Acanthostrongylophora* sp. HPLC fraction 1 (400 MHz, CD$_3$OD). The regions containing double peaks are zoomed.
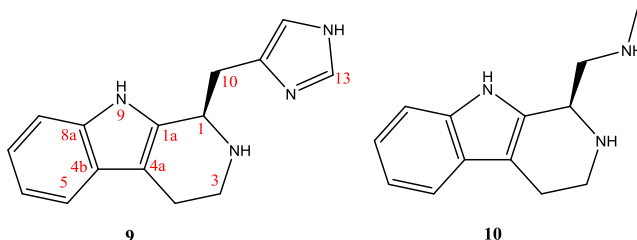
Figure 31 - Structures of haploscleridamine (**9**) and compound **10** isolated from *Acanthostrongylophora* sp..
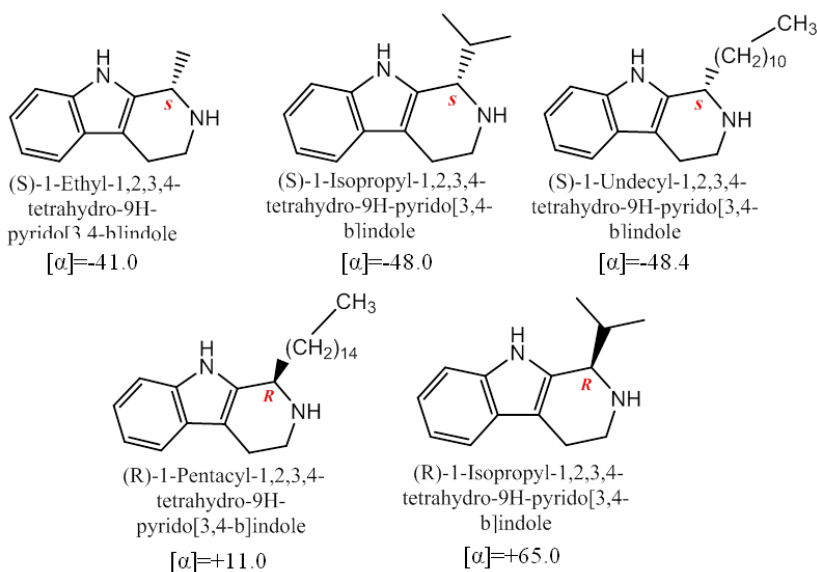
Figure 32 - Related compounds considered for the assignment of **9** and **10** stereochemistry and their respective optical values.

Compound **9** was isolated as an amorphous white powder. It was identified as haploscleridamine based on available spectral data described in Appendixes 17 to 20 [193]. However, the literature only describes this compound planar structure. The absolute stereochemistry of **9** was determined by comparison of its optical rotation with that of known related compounds. It was found that the related isomers with *S* configuration, showed negative values for optical rotation. *R* isomers, on the other hand, presented positive values for optical rotation, as it is seen in Figure 32 [194-197]. The obtained optical rotation for **9** was +4.1, indicating the presence of the *R* isomer. Therefore, compound **9** was elucidated as shown in Figure 31: (*R*)-haploscleridamine.

68

Table 8 - ^{1}H and ^{13}C-NMR data (400 and 100 MHz, respectively) obtained for compound **10**. Experiments performed in DMSO-d_6.

		Compound 10
Position	δ_C, type	δ_H, mult (*J* in Hz)
1	48.8, CH	5.09, br s
1a	125.7, C	
2-NH		1.75, br s
3	40.4, CH$_2$*	3.48, dt (12.5, 6.6)
		3.60, m
4	18.2, CH$_2$	2.95, m
4a	107.6, C	
4b	125.7, C	
5	118.3, CH	7.50, d (7.8)
6	119.3, CH	7.05, td (7.4, 7.0)
7	122.4, CH	7.16, ddd (8.1, 6.9, 1.2)
8	111.6, CH	7.41, d (8.2)
8a	136.3, C	
9-NH		11.24, br s
10	49.2, CH$_2$	3.65, m
12-NH		9.05, br s
10-NCH$_3$	33.5, CH$_3$	2.74, s

*Signal observed in *g*-HSQC.

Compound **10** was isolated as an amorphous white powder. 1D-NMR data is resumed in Table 8. Its ^{13}C-NMR spectrum confirmed the presence of thirteen carbon signals, which were assigned by HSQC spectrum analysis, to one methyl (δ_C 33.5), three methylenes (δ_C 49.2, 40.4, 18.2), five methines (δ_C 122.4, 119.3, 118.3, 111.6, 48.8) and four non-protonated carbons (δ_C 136.3, 125.7, 125.7, 107.6). The methylene δ_C 40.4 was only detected by HSQC. In accordance, the ^{1}H-NMR spectrum exhibited one nitrogen-methyl singlet (δ_H 2.74), three methylenes (δ_H 3.65, 3.60, 3.48, 2.95), from which one was splitting and had been assigned appealing to HSQC, and five methines (δ_H 7.50, 7.41, 7.16, 7.05, 5.09), being the last one the only non-aromatic. Based on ^{1}H and ^{13}C data and having present that this compound was structurally very similar with **9**, a pyridoindole core was proposed for **10**. The presence of the indole group was supported by the COSY correlations H-5/H-6, H-6/H-7 and H-7/H-8, as represented in Figure 33. Those, together with the HMBC cross-peaks H-5/C-8a, H-6/C-4b and H-7/C-8a and the correlations of 9-NH with H-1a, H-4a, H-4b and H-8a confirmed the indole group. C-3 deshielded carbon shift (δ_C 40.4) predicted a nitrogen-bonding, which combined with COSY cross-peak H-3/H-4 and HMBC correlations H-3/H-1, H-4/H-1a and H-4/H-4a, allowed the full elucidation of the pyridoindole. The nitrogen-methyl (δ_H 2.74) was linked to C-10 based on an HMBC cross-peak relating those two. The two sub-structures were connected together based on the COSY correlation H-1/H-10. The ESIMS molecular ion peak

m/z 216.1 confirmed the molecular formula as $C_{13}H_{17}N_3$ and the seven degrees of unsaturation. Spectral data obtained for **10** can be found in Appendixes 21 to 28.
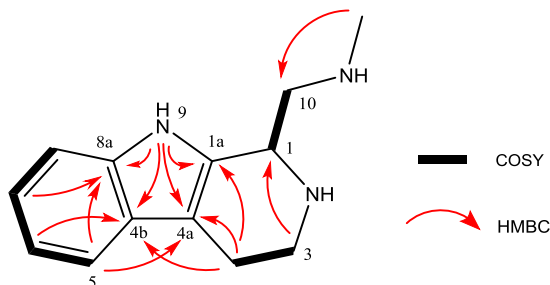
Figure 33 - Key ^{1}H-^{1}H COSY and HMBC correlations of compound **10**.

As for **9**, the stereochemistry of compound **10** was determined based on a comparison of its optical rotation with the known related compounds listed in Figure 32. The optical rotation obtained for **10** was +2.3, indicating, as for **9**, the presence of the *R* isomer. Compound **10** was then elucidated as the xestoamine analog shown in Figure 31. This represents a novel structure and the first report of this compound.

A large number of structurally diverse *β*-carbolinic alkaloids have been isolated from natural sources. These compounds have been found in plants [198], bacteria [199], fungi [200] and in marine invertebrates, mainly marine sponges [201]. The short chain alkyl substitution at C-1 seems to be widespread among the literature; however, this is the first report of compound **10** structure. Together with xestoamine, they represent the only described methylethanamine *β*-carbolinic alkaloids isolated from marine sponges.

4.2.2 Spongian Diterpene Analogs from *Acanthodendrilla* sp.

The sponge sample labeled as ORMA 101324, collected by hand while scuba diving at Pulau-Pulau, is shown in Figure 34. The sponge was identified as *Acanthodendrilla* sp. regarding morphological features. The frozen biomass was extracted with CH_2Cl_2:MeOH (1:1 v/v) and the resultant organic extract was further separated using preparative HPLC, followed by semi-preparative HPLC to yield compounds **11** (0.9 mg) and **12** (1.6 mg). The workflow of the isolation procedure is resumed in Figure 35.

Figure 34 - Picture of *Acanthodendrilla* sp. fresh sponge sample, collected by hand while scuba diving in Pulau-Pulau and which led to the isolation of spongian diterpene analogs.
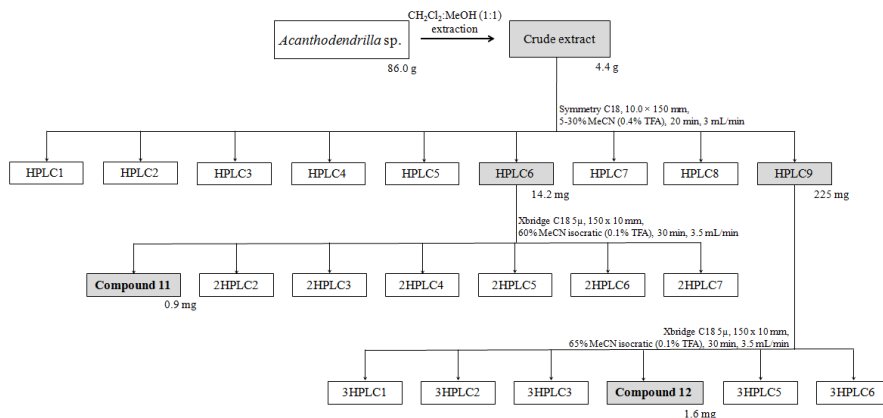
Figure 35 - Scheme of the workflow that led to the isolation of two spongian diterpenes from *Acanthodendrilla* sp..
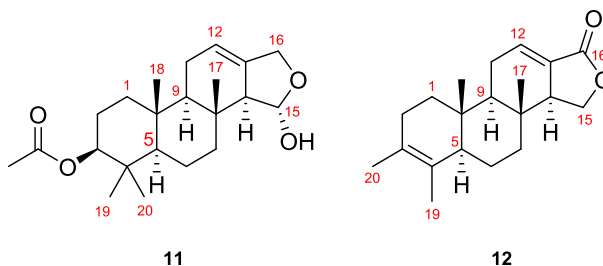
Figure 36 - Structures of the spongian diterpenes 3β-acetoxy -15-hydroxyspongia-12-en (**11**) and 3-methylspongia-3,12-dien-16-one (**12**) isolated from *Acanthodendrilla* sp..

Compound **11** was obtained as an amorphous white powder. Its molecular formula was established as $C_{22}H_{34}O_4$ based on (+)HRESTOFMS, indicating six degrees of unsaturation. 1D-NMR data are presented in Table 9. ^{13}C-NMR data confirmed the presence of 22 signals that, together with the HSQC data, were assigned to five sp^3 methyl carbons ($δ_C$ 28.5, 21.1, 17.1, 15.9, 15.2), six methylenes ($δ_C$ 69.2, 42.1, 39.0, 24.5, 23.9, 19.2), six methines ($δ_C$ 117.5, 100.3, 82.3, 62.8, 57.1, 55.9) and five non-protonated carbons ($δ_C$ 172.8, 137.8, 38.9, 38.2, 34.6). The listed resonances revealed one oxygenated ($δ_C$ 100.3) methine and one ester non-protonated carbon ($δ_C$ 172.8). Accordingly, the ^{1}H-NMR spectrum exhibited five methyl singlets ($δ_H$

2.03, 0.99, 0.91, 0.90, 0.82), six methylenes, which were splitting and so, assigned resorting to HSQC ($δ_H$ 4.41 and 4.11, 2.08 and 1.99, 1.92 and 1.38, 1.72 and 1.09, 1.64 and 1.63, 1.61 and 1.53) and six methines ($δ_H$ 5.50, 5.17, 4.47, 2.16, 1.27, 1.02). Among them, an olefinic ($δ_H$ 5.50), a vicinal ester ($δ_H$ 4.47) and hemiacetal ($δ_H$ 5.17) methine protons were noted. Based on COSY and HMBC spectral data, as shown in Figure 37, a spongian diterpene basic structure was proposed for this compound. The HMBC correlation H-3 ($δ_H$ 4.47) to the carbonyl group $δ_C$ 172.8 indicated the presence of a substitution, which was assigned to an acetoxy moiety based on the HMBC correlation of this carbonyl group to the methyl $δ_H$ 2.03. The position of the four remaining methyl groups which were all singlets, was also confirmed based on HMBC correlations: Me-17 to C-7 and C-8, Me-18 to C-9 and C-5 and Me-19 and Me-20 to C-3, C-4 and C-5. This confirmed the spongian skeleton as the basic structure of **11**. Additionally, the double bound anticipated on C-12 by the deshielded proton and carbon signals ($δ_C$ 117.5, $δ_H$ 5.50) was assigned based on the HMBC cross-correlations H-16 to C-13 and C-12. Finally, HMBC correlations H-16/C-12 and H-16/C-13 and H-15 to C-8, along with the proton ($δ_H$ 5.17, 4.11 and 4.41) and carbon ($δ_C$ 100.3, 69.2) chemical shifts for these centers, allowed ring D to be identified as a five-membered cyclic hemiacetal.
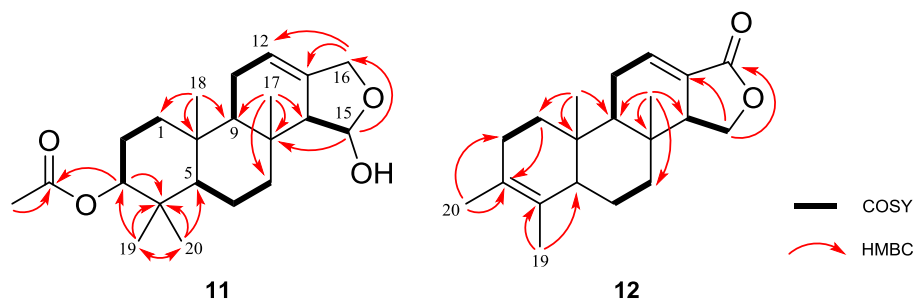
Figure 37 - Key ^{1}H-^{1}H-COSY and HMBC correlations found for compounds **11** and **12**.

The relative configuration of the asymmetric carbon centers in **11** was assigned based on combined coupling constants and ROESY analysis, as seen in Figure 38. Cross-peaks between H-6β, Me-17 and Me-18 and H-3 and H-7α suggested a trans-fused ring junction. The absence of a ROESY correlation between Me-18 and H-5 confirmed this configuration. The cross-peaks between H-6β, Me-18 and Me-17 were used to assign both Me-17 and

Me-18 groups as β-orientated relatively to the molecule. The correlation Me-17/H-15 allowed the assignment of H-15 as β-oriented, and consequently, OH-15 as α-oriented. A small coupling constant between H-14 and H-15 ($J = $ 4.8 Hz) confirmed their opposite locations relative to the molecule. Additional ROESY cross-peaks at H-3/H-5, H-5/H-9, H-9/H-14 and H-14/H-7α indicated that those protons were also α-oriented, while AcO–3 was assigned as β-oriented. Compound **11** was then elucidated as the spongian diterpene shown in Figure 36: 3β-acetoxy-15-hydroxyspongia-12-en. Spectral data obtained for **11** can be found in Appendixes 29 to 38.
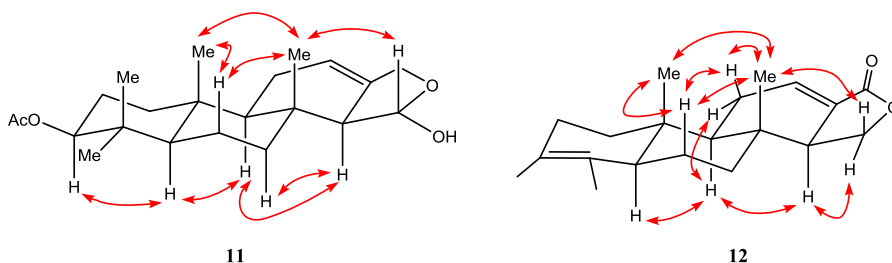
Figure 38 - Key NOESY correlations found for compounds **11** and **12**.

Compound **12** was obtained as an amorphous white powder. Its molecular formula was established as $C_{20}H_{28}O_2$, based on (+)-HRES-TOFMS, which indicated seven degrees of unsaturation. 1D-NMR data are resumed in Table 9. Its analysis showed that some common signals of the spongian diterpene nuclei found on **11** were also present on **12**. This included the B ring signals, Me-17 group and C-12(13) double bond. However, differences in the chemical shifts of the rest of the other signals suggested significant structural changes compared to **11**. C-3 ($δ_C$ 125.3) and C-4 ($δ_C$ 127.6) resonances pointed to olefinic carbons, suggesting the presence of a double bond between them. C-4 linkage to Me-19 and C-3 linkage to Me-20 were confirmed by HMBC correlations, as seen in Figure 37. Finally, the γ-lactone, which was suggested by the C-16 resonance ($δ_C$ 172.5), was confirmed based on the crucial HMBC correlations of H-15 to C-16, C-14 and C-13.

Similarly to **11**, ROESY analysis illustrated in Figure 38, was the key to assign the relative configurations of the asymmetric carbon centers present in **12**. A trans-fused ring junction was also proposed due to the cross-peaks between H-6β, H-11β, Me-17 and Me-18 and H-5, H-9 and H11α. Again, the absence of a ROESY correlation between Me-18 and H-5 confirmed this configuration. The cross-peaks H-11β/Me-17, Me-17/Me-18, H-6β/Me-18 and

Me-17/H-6β were used to assign both Me-17 and Me-18 groups as β-orientated to the molecule. Additional ROESY cross-peaks at H-5/H-9 and H-9/H-14 indicated that these protons were *α*-oriented. Therefore, compound **12** was identified as the spongian diterpene shown in Figure 36: 3-methylspongia-3,12-dien-16-one. Spectral data obtained for **12** can be found in Appendixes 39 to 46.

Table 9 - ^{1}H-NMR and ^{13}C-NMR data (500 and 100 MHz, respectively) obtained for compounds **11** and **12**. Experiments performed in CD_3OD.

Position	Compound 11		Compound 12	
	δ_C, type	δ_H, mult (*J* in Hz)	δ_C, type	δ_H, mult (*J* in Hz)
1	39.0, CH_2	α 1.09, m	37.1, CH_2	α 1.20, m
		β 1.72, m		β 1.16, m
2	24.5, CH_2	α 1.63, m	30.3, CH_2	α 1.95, m
		β 1.64, m		β 2.04, m
3	82.3, CH	4.47, dd (11.0, 5.1)	125.3, C	
4	38.9, C		127.6, C	
5	57.1, CH	1.02, m	51.1, CH	1.92, m
6	19.2, CH_2	α 1.53, qd (13.2, 3.1)	21.8, CH_2	α 1.38, m
		β 1.61, m		β 1.86, m
7	42.1, CH_2	α 1.38, td (13.3, 4.5)	41.0, CH_2	α 1.36, m
		β 1.92, dt (13.3, 3.6)		β 1.76, m
8	34.6, C		35.3, C	
9	55.9, CH	1.27, m	52.9, CH	1.42, dd (11.5, 5.3)
10	38.2, C		36.8, C	
11	23.9, CH_2	α 1.99, br d (12.0)	25.6, CH_2	α 2.21, dddd (20.2, 11.6, 5.0, 3.3)
		β 2.08, br d (17.9)		β 2.50, dq (20.3, 4.1)
12	117.5, CH	5.50, br s	138.2, CH	6.86, q (3.5)
13	137.8, C		128.8, C	
14	62.8, CH	2.16, m	52.4, CH	2.93, (tt, 9.2, 4.4)
15	100.3, CH	5.17, d (4.8)	68.9, CH_2	α 4.44, t (9.3)
				β 4.14, t (9.1)
16	69.2, CH_2	α 4.41, dt (11.7, 2.4)	172.5, C*	
		β 4.11, dt (11.5, 1.7)		
17	15.2, CH_3	0.82, s	14.7, CH_3	0.88, s
18	15.9, CH_3	0.99, s	12.7, CH_3	0.85, s
19	17.1, CH_3	0.91, s	15.7, CH_3	1.62, s
20	28.5, CH_3	0.90, s	19.4, CH_3	1.60, s
O<u>C</u>OCH₃	172.8, C			
OCO<u>C</u>H₃	21.1, CH_3	2.03, s		

*Signal observed in *g*-HMBC

11 and **12** belong to a known and well-studied class of marine natural compounds: spongian diterpenes. However, they have structures with novel features within the field of marine natural compounds. A C-16 carbonyl moiety is common in the literature, as seen for spongia-16-one and spongia-15,16-one [202]. The C-12(13) double bond has been reported before [203]

and 3-acetoxy-spongians can also be found reported in the literature [204, 205]. The rearrangement of the spongian skeleton resulting in a 3-methyl-3-en spongian-analog as seen in **12** is being reported for the first time. A trans-fused ring junction is consistent with the stereochemistry usually found for this class of compounds [202, 206]. Despite five-membered cyclic hemiacetals usually existing as two interconverting anomers, the D-ring of **11** appeared as a single isomer. This occurrence seems to be common for sponge isolated natural hemiacetals [206, 208]. Also, while ring A oxidations are common for *Dicyteroceratida*, they have never been previously reported for a sponge belonging to *Dendroceratida*.

Spongian diterpenes relevance in sponge chemotaxonomy has been discussed in the literature [209]. To date, *Acanthodendrilla* was the only *Dendroceratida* genus that had not been reported as a producer of this class of compounds. These results filled this gap. The reported data provide further opportunities for chemotaxonomic studies based on spongian diterpene profiling.

4.2.3 Bisabolane Derivatives from *Acanthostrongylophora ingens*

The sponge sample labeled as ORMA 135834 and seen in Figure 40 was collected by hand while scuba diving at Boano (Indonesia). It was identified as *Acanthostrongylophora ingens* regarding morphological features. The frozen biomass was extracted with CH_2Cl_2:MeOH (1:1 v/v) and the resultant organic extract was further partitioned between Hex, EtOAc, BuOH and H_2O. The Hex extract, after RP-VLC and several semi-preparative HPLC separations led to the isolation of compounds **13** (6.4 mg), **14** (98.6 mg) **15** (13.1 mg), **16** (4.9 mg) and **17** (9.4 mg). The EtOAc extract, after RP-VLC and semi-preparative HPLC led to the isolation of compounds **18** (46.5 mg) and **19** (23.3 mg). A simplified workflow of the isolation of those compounds is illustrated in Figure 39.
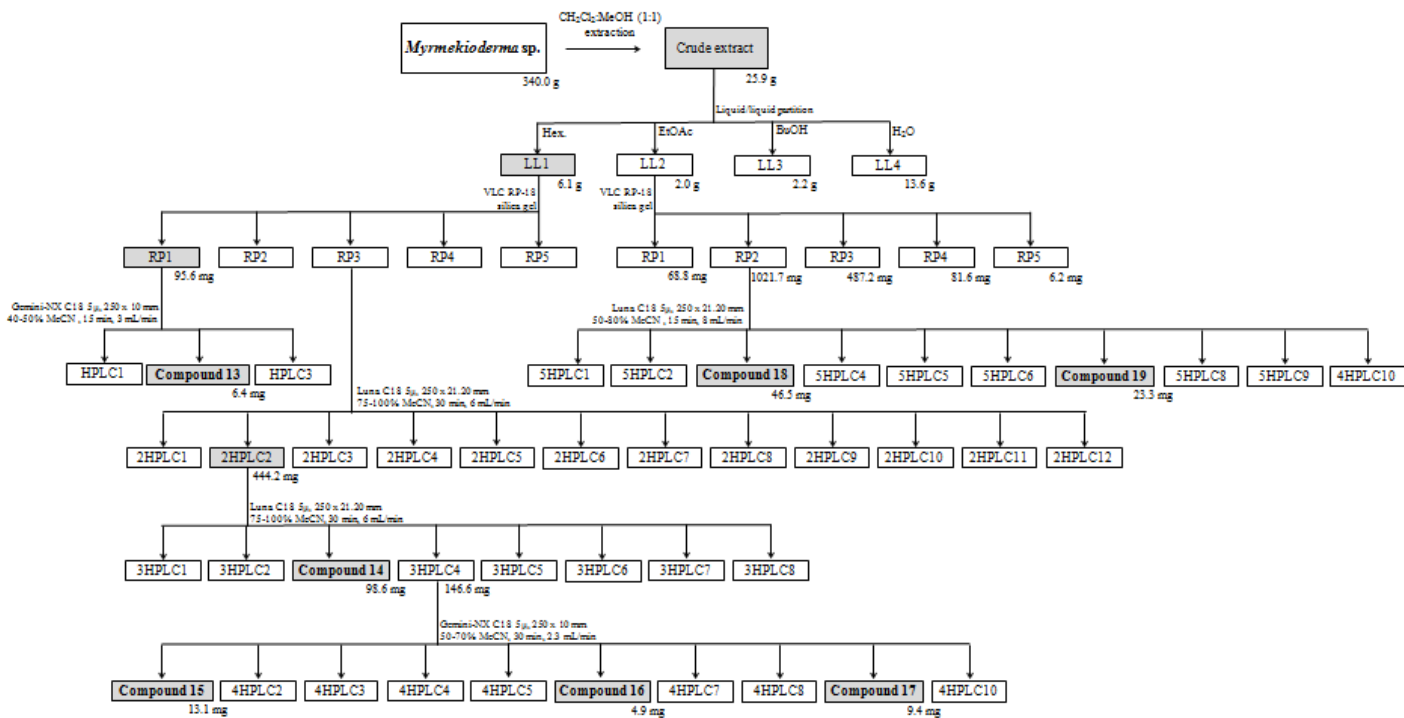
Figure 39 - Scheme of the workflow that led to the isolation of seven bisabolane derivatives from *Acanthostrongylophora ingens*.

Table 10 - ^{1}H and ^{13}C-NMR data (400 and 100 MHz, respectively) obtained for compounds **14-16**. Experiments performed in $CDCl_3$.

Position	δ_C, type	Compound 14 δ_H, mult (J in Hz)	δ_C, type	Compound 15 δ_H, mult (J in Hz)	δ_C, type	Compound 16 δ_H, mult (J in Hz)
1	145.4, C		147.5, C		146.4, C	
2	117.2, CH	6.69, s	118.8, CH	6.68, s	112.5, CH	6.87, s
3	124.3, C		125.4, C		123.9, C	
4	147.4, C		147.0, C		150.4, C	
5	114.7, CH	6.48, s	117.2, CH	6.50, s	110.0, CH	6.64, s
6	125.8, C		124.2, C		130.4, C	
7	131.0, C		148.0, C		48.1, C	
8	130.0, CH	5.63, td (7.5, 1.4)	76.7, CH	4.40, dd (8.6, 5.4)	37.4, CH_2	2.42, dd (14.1, 7.9) 2.58, dd (14.1, 8.3)
9	28.6, CH_2	2.53, t (7.3)	34.3, CH_2	α 2.30, m β 2.15, m	117.2, CH	4.85, dddd (9.7, 5.5, 2.8, 1.4)
10	121.7, CH	5.05, tdt (7.1, 2.7, 1.3)	118.8, CH	5.06, m	136.5, C	
11	132.9, C		136.9, C		18.0, CH_3	1.56, s
12	25.8, CH_3	1.66, s	26.1, CH_3	1.71, s		
13	17.8, CH_3	1.49, s	18.1, CH_3	1.53, s	25.8, CH_3	1.60, s
14	15.9, CH_3	2.21, s	15.8, CH_3	2.20, s	16.2, CH_3	2.26, s
15	25.2, CH_3	1.94, dd (3.9, 1.3)	120.3, CH_2	α 5.43, d (1.3) β 5.24, d (1.6)	23.5, CH_3	1.44, s
16					180.8, C	
OH-1		4.80, br s		8.02, br s		
OH-4		4.59, br s		4.48, br s		4.65, br s
OH-8				3.27, br s		

Figure 40 - Picture of *Acanthostrongylophora ingens* fresh sponge sample, collected by hand while scuba diving in Boano (Indonesia) and which led to the isolation of several bisabolane derivatives.

Compound **13** was isolated as a dark brown oil. It was identified as 1-(2,4-dihydroxy-5-methylphenyl)ethan-1-one, as shown in Figure 41, based on spectral data available in the literature [210]. Obtained 1D-NMR and mass spectrometry data can be found in Appendixes 47 to 51.
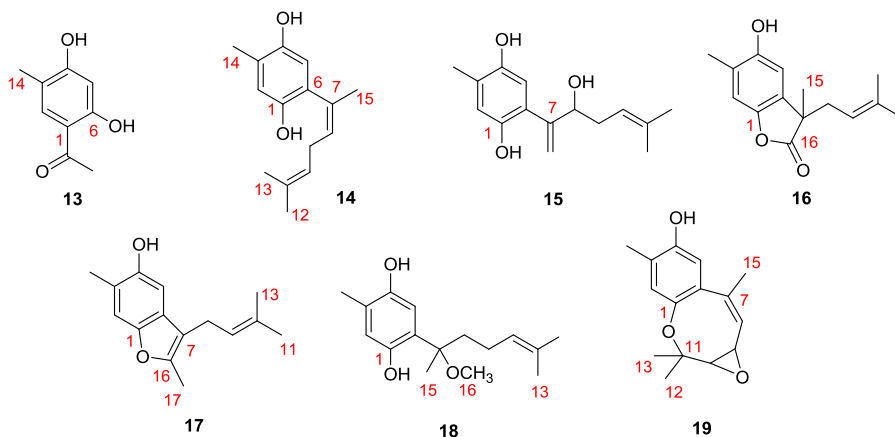
Figure 41 - Chemical structure of bisabolane-derivatives isolated from *Acanthostrongylophora ingens.*

Compound **14** was identified as 6-(1,5-dimethyl-1,4-hexadienyl)-3-methylbenzene-1,4-diol based on spectral data available in the literature, as resumed in Table 10 [211]. Obtained spectra can be found in Appendixes 52 to 57. A significant difference was found in C-15 shift (δ_C 25.2), which had been reported as steric shielded (δ_C 17.8) due to *E* configuration of the double bond [211]. This steric effect does not appear in **14**. The COSY cross-signal Me-15/H-8, together with a small coupling constant between them (J_{15-8}=1.3) supported the assignment of a *cis* configuration. The geometry of the double bound $\Delta^{7(8)}$ was therefore proposed to be *Z*-configured.
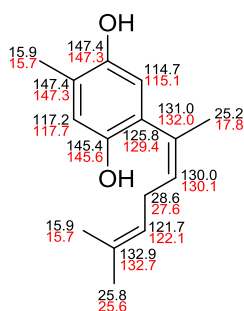
Figure 42 - Comparison of ^{13}C-NMR chemical shifts obtained for compound **14** (black) and the ones described in the literature (red) [211].

Compound **15** was isolated as a yellow amorphous solid. The molecular formula $C_{15}H_{20}O_3$ was established based on the (-)-HRESIMS molecular ion *m/z* 247.1344 [M-H]⁻, which imposed six degrees of unsaturation. Obtained 1D-NMR data are resumed in Table 10. The ^{13}C-NMR spectrum of **15** confirmed the presence of fifteen carbon signals which were assigned, by DEPT and HSQC spectra analysis, to two tertiary (δ_C 26.1, 18.1) and one secondary (δ_C 15.8) methyls, two methylenes (δ_C 120.3, 34.3) from which one was double bonded (δ_C 120.3), two aromatic (δ_C 118.8, 117.2), one double-bonded (δ_C 118.8) and one hydroxylated (δ_C 76.7) methines and six non-protonated carbons (δ_C 148.0, 147.5, 147.0, 136.9, 125.4, 124.2). From the listed non-protonated carbons, two were hydroxylated (δ_C 148.0, 147.5). In accordance, the ^{1}H-NMR spectrum exhibited three methyl singlets (δ_H 2.20, 1.71, 1.53), two splitting methylenes (δ_H 5.43 and 5.24, 2.30 and 2.15), the first two suggesting a double bond, and four methines (δH 6.68, 6.50, 5.06, 4.40). Based on COSY and HMBC spectral data, as shown in Figure 43, a sesquiterpene basic structure was proposed for this compound. ^{1}H and ^{13}C-NMR data, together with H-2 HMBC cross-correlations with C-1 and C-5

revealed the presence of a tetrasubstituted benzene ring. C1 and C4 deshielded carbon resonances (δ_C 147.5, 147.0) pointed to a benzene-1,4-diol. 3-methyl was assigned by the HMBC correlation Me-14/C-4 and C-6 substitution by the correlations H-5/C-7 and H_2-15/C-6. Further HMBC cross-peak H_2-15/C-8 allowed linking the hydroxyl group on C-8 to the side chain. Me-12 and Me-13 were assigned considering their respective HMBC correlations to C-11. Further HMBC signals, Me-12/H-10 and Me-12/Me-13 confirmed the assignment of those two methyls and the position of $\Delta^{10(11)}$ double bond. The two sub-structures were linked based on the COSY correlations H_2-9 to both H-8 and H-10. The stereochemistry of **15** could not be determined with the available resources. Thus, the structure of **15** was elucidated as the curcuhydroquinone derivative shown in Figure 41: 6-(3-hydroxy-6-methyl-1,5-heptadien-2-yl)-3-methylbenzene-1,4-diol. Obtained spectra can be found in Appendixes 58 to 67.
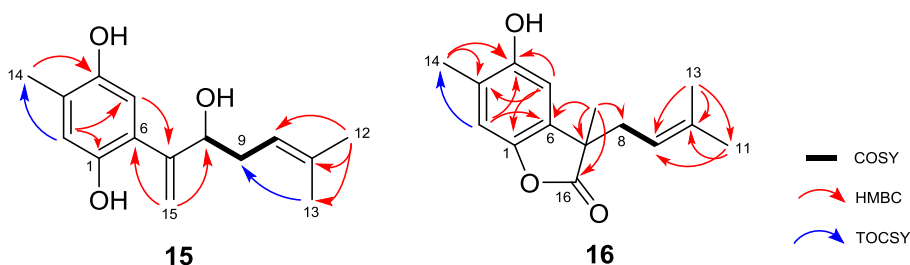
Figure 43 - Key ^{1}H-^{1}H COSY, TOCSY and HMBC correlations of **15** and **16**.

Compound **16** was isolated as a yellow amorphous powder. The molecular formula $C_{15}H_{18}O_3$ was calculated based on the (-)-HRESIMS *m/z* 245.1126 [M-H]⁻ peak indicating the existence of seven degrees of unsaturation. ^{1}H and ^{13}C-NMR spectral data of **16**, resumed in Table 10, resembled those of **14** and **15**. ^{13}C-NMR spectrum confirmed the presence of fifteen carbon signals which were assigned, by DEPT and HSQC spectra analysis, to four methyls (δ_C 25.8, 23.5, 18.0, 16.2), one methylene (δ_C 37.4), two aromatic (δ_C 112.5, 110.0) and one olefinic (δ_C 117.2) methines and seven non-protonated carbons (δ_C 180.8, 150.4, 146.4, 136.5, 130.4, 123.9, 48.1), from which two were hydroxylated (δ_C 150.4, 146.4) and one ester (δ_C 180.8). In accordance, the ^{1}H-NMR spectrum showed four methyl singlets (δ_H 2.26, 1.60, 1.56, 1.44), one splitting methylene (δ_H 2.58, 2.42), two aromatic (δ_H 6.87, 6.64) and one olefinic (δ_H 4.85) methines. The same tetrasubstituted benzene ring found in **14** and **15** was suggested for **16** by similarities of [1]H

and ^{13}C-NMR data and confirmed by the HMBC correlations H-2 to C-4 and C-6 and H-5 to C-1, C-3 and C4, as seen in Figure 43. Further HMBC correlations Me-14/C-3 and Me-14/C-4, together with the TOCSY crossing signal Me-14/H-2, corroborate the assignment of this methyl group. The most remarkable features of **16** were the carbonyl resonance (δ_C 180.8) and a non-protonated alkane carbon (δ_C 37.4). The allocation of those was accomplished based on the HMBC correlations of Me-15 with C-6, C-7, C-8 and C-16, confirming a furanone sub-structure. A methyl-butene moiety was also elucidated by the HMBC correlations of Me-11 and Me-13 with both C-9 and C-10. The COSY correlation H_2-8/H-9 allowed linking these two sub-structures. Spectral data for **16** can be found in Appendixes 68 to 77. The stereochemistry of **16** could not be determined with the available resources. Thus, the structure of compound **16** was elucidated as the curcuphenol derivative shown in Figure 41: 4-hydroxy-3,7-dimethyl-7-(3-methylbut-2-en-1-yl)benzofuran-17-one.

Compound **17** was isolated as a yellow amorphous powder. The (-)-HRESIMS *m/z* 229.1234 [M-H]⁻ molecular ion peak indicated the molecular formula $C_{15}H_{18}O_2$ and demanded seven degrees of unsaturation. Again, ^{1}H- and ^{13}C-NMR data of **17,** resumed in Table 11, resembled those of **14-16**. The phenol together with methylpentene sub-structures was elucidated by the similarity of reported resonances found for the previous compounds. COSY, TOCSY and HMBC correlations confirmed the premised sub-structure. A furan moiety, as seen in **16** was also found as part of **17**. A methylfuran then proposed based on the HMBC correlations of Me-17 with C-7 and C-16. The *m/z* 16 difference between **17** and **16**, confirmed the loss of the carbonyl group. The remaining part of **17** was elucidated based on resonances similarities, allowing the identification of this compound as the curcuphenol derivative shown in Figure 41: 3,16-dimethyl-7-(3-methylbut-2-en-1-yl)benzofuran-4-ol. Spectral data of **17** can be found in Appendixes 78 to 87.

Table 11 - [^1]H and [^13]C-NMR data (400 and 100 MHz, respectively) obtained for compounds **17-19**. Experiments with **17** and **19** were performed in CDCl$_3$ and with **18** in CD$_3$OD.

Position	Compound 17 δ$_C$, type	δ$_H$, mult (*J* in Hz)	Compound 18 δ$_C$, type	δ$_H$, mult (*J* in Hz)	Compound 19 δ$_C$, type	δ$_H$, mult (*J* in Hz)
1	149.0, C		149.5, C		146.7, C	
2	112.2, CH	7.12, s	118.9, CH	6.63, s	116.9, CH	6.70, s
3	120.0, C		124.5, C		125.1, C	
4	149.6, C		146.7, C		148.1, C	
5	103.7, CH	6.77, s	114.2, CH	6.48, s	110.3, CH	6.62, s
6	129.3, C		126.0, C		132.1, C	
7	109.0, C		82.4, C		122.0, C	
8	25.8, CH$_2$	3.39, d (7.1)	39.8, CH$_2$	1.84, m	118.7, C	5.36, dd (3.8, 1.5)
9	119.7, CH	5.31, dddd (7.0, 5.6, 2.8, 1.4)	22.8, CH$_2$	α 2.00, m β 1.89, m	75.6, CH	4.51, ddt (8.2, 3.9, 1.6)
10	133.7, C		123.9, CH	5.04, t (6.6, 6.5)	63.8, CH	3.06, d (8.2)
11	25.8, CH$_3$	1.73, s	132.0, C		57.7, C	
12			17.7, CH$_3$	1.51, m	25.1, CH$_3$	1.33, s
13	18.0, CH$_3$	1.74, s	25.8, CH$_3$	1.65, s	19.4, CH$_3$	1.35, s
14	16.6, CH$_3$	2.32, s	15.6, CH$_3$	2.18, s	15.9, CH$_3$	2.19, s
15			22.4, CH$_3$	1.55, s	18.3, CH$_3$	2.01, t (1.5)
16	153.4, C		50.5, CH$_3$	3.21, s		
17	8.1, CH$_3$	2.10, s				
OH-1				8.28, br s		
OH-4		4.54, br s		8.28, br s		3.49, br s
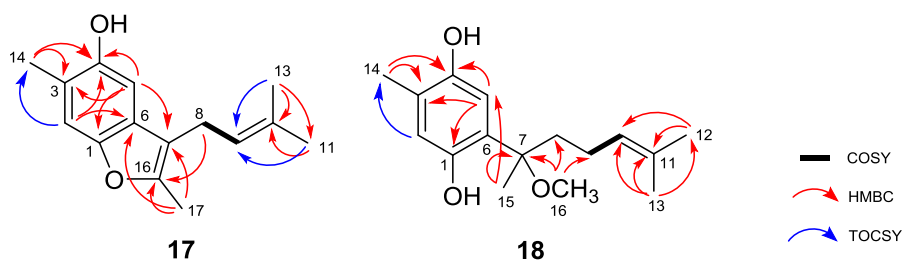
Figure 44 - Key ^{1}H-^{1}H COSY, TOCSY and HMBC correlations of **17** and **18**.

Compound **18** was isolated as a dark brown oil. The molecular formula $C_{16}H_{24}O_3$ was established based on (-)-HRESIMS *m/z* molecular ion peak 263.1610 [M-H]⁻, demanding five degrees of unsaturation. Both ^{1}H and ^{13}C-NMR, resumed in Table 11, indicated structural similarities with **13-17**. The same tetrasubstituted hydroquinone ring found in **13** and **14** was suggested for **18**, which was supported by HMBC spectral data, illustrated in Figure 44. HMBC correlations of H-5 to C1, C3 and C4 and Me-14 to C3 and C4 and TOCSY crossing signal H-2/Me-14 confirmed the proposed hydroquinone sub-structure. The HMBC correlations Me-15/C-7 and Me-16/C-7 were the keys for granting those methyl groups. The ^{13}C-NMR and DEPT data anticipated the presence of two methylenes (δ_C 39.8, 22.8), pointing for a side chain one carbon longer than the ones found until then. Me-12 and Me-13 were assigned resorting to their HMBC correlations with C-10 and C-11. The COSY correlation H-10/H-9 allowed finishing this second sub-structure, which was connected to the other one based on the HMBC correlation Me-16/H-9.
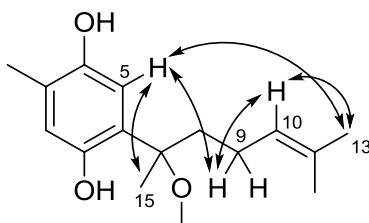
Figure 45 - Key NOESY correlations of **18**.

Finally, the configuration of the chiral center present in **18** was analyzed reviewing nuclear Overhauser effect spectroscopy (NOESY), as it is represented in Figure 45. The NOESY spectrum showed cross-peaks between H-5, H-9α, H-10, Me-13 and Me-15, indicating that those groups were all located on the same side of the molecule. Me-16 was then found to

be oriented to the opposite side and **18** was found to be *S* oriented. Based on biosynthetic considerations, the absolute stereochemistry of compound **18** was expected to be *S*. All known bisabolane related compounds exhibit 7*R* configuration, except for the sponge counterparts, which are 7*S* configured [193, 194]. Thus, the structure of **18** was elucidated as the curcuhydroquinone derivative shown in Figure 41: 6-(2-methoxy-6-methylhept-5-en-2-yl)-3-methylbenzene-1,4-diol. Spectral data of **18** can be found in Appendixes 88 to 97.

Compound **19** was isolated as a green crystal. The (-)-HRESIMS showed the molecular ion peak *m/z* 245.1126 [M-H]⁻, very similar to the reported for **16**. As for **16**, $C_{15}H_{18}O_3$ was the calculated molecular formula, indicating the existence of seven degrees of unsaturation. An analysis of 1D-NMR spectral data of **19**, resumed in Table 11, and its comparison with those of the elucidated related compounds revealed the presence of the phenolic part of the structure, however with considerable modifications on the side chain. The HMBC correlations Me-15 to C-6 and C-7 (Figure 46a), together with the deshielded resonance of C-7 ($δ_C$ 122.0) allowed assigning Me-15 and the $Δ^{7(8)}$ double bond. COSY correlations H-8/H-9 and H-9/H-10 assigned those three methine groups together and C-8 was linked to C-7 based on the HMBC cross-peak Me-15/C-8. C-9 and C-10 deshielded resonances ($δ_C$ 75.6, 63.8), together with the ^1H-^1H coupling constants between the involved protons which were consistent with the presence of a *cis* epoxide unit (J_{9-10} = 8.2 Hz). Finally, the HMBC correlations Me-12 with C-10, C-11 and C-13 and Me-13/C-11 allowed concluding the structure. An octa-membered ring was then elucidated as part of **19** structure and linked to the phenol group on C-1 and C-6.

This was supported by the MS fragmentation pattern showing the *m/z* fragments 230.1421, 165.0497, 122.0332, as it can be seen in Figure 47.
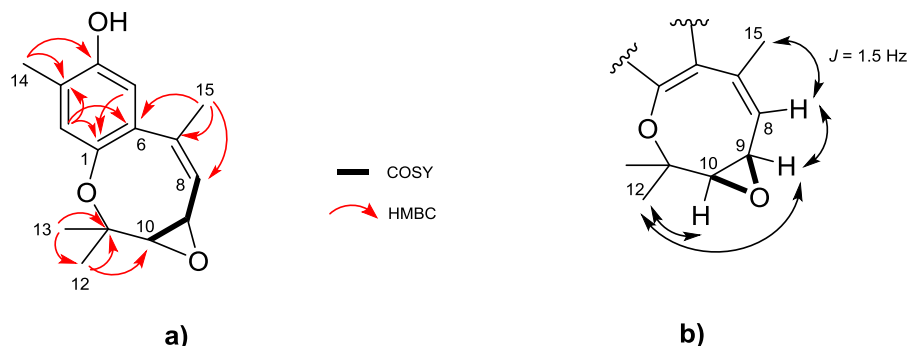
Figure 46 - Key correlations for the elucidation of **19**. **a)** ^{1}H-^{1}H COSY, HMBC and TOCSY. **b)** NOESY (partial structure).
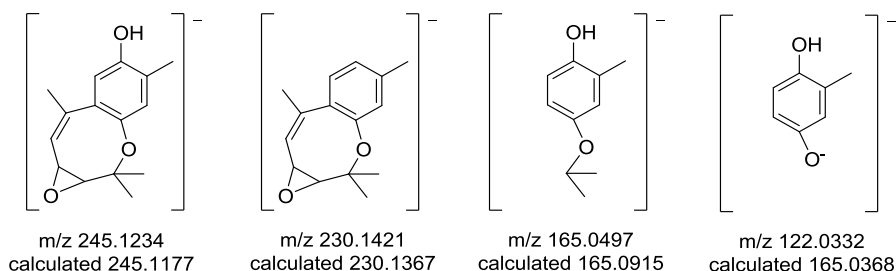
Figure 47 - Compound **19** MS fragmentation ions induced by (-)ESI.

The relative stereochemistry of **19** was resolved based on NOESY, as resumed in Figure 46b and coupling constant analysis. The geometry of the double bound $\Delta^{7(8)}$ was suggested to be *Z* based on the NOE correlation Me-15/H-8. This is supported by the small coupling constant between those two (J_{15-8} = 1.5 Hz) and by the correlation due to *w*-coupling appearing in the COSY spectrum. In addition, the NOESY spectrum showed the cross-peaks Me-12/H-9, Me-12/H-10 and H-9/H-8, locating them all on the same side of the molecule. Me-13 and the epoxy group were then located in the opposite side. Therefore, the structure of **19** was elucidated as the curcuphenol derivative shown in Figure 41: 3,7,11,11-tetramethyl-1,9-dihydro-2-benzoxirenoxocin-6-ol. Spectral data of **19** can be found in Appendixes 98 to 107.

Several bisabolane-type sesquiterpenoids have been reported from different marine organisms, such as the marine sponge *Halichondria* sp. [211], the gorgonians *Pseudopterogorgia* spp. [212] or the red algae *Laurencia scoparia* [213]. The isolation of bisabolane-related compounds

from microorganisms, such as the marine-derived fungus *Aspergillus* sp. [214] had been suggested as evidence that these compounds are produced by microbial-associated organisms and not directly by the host. In the present studies, it was not clear if the producer of the isolated five new bisabolane-related compounds is the sponge or possible associated-microorganisms. Once the metabolites were extracted indistinctly, the possibility of the real producer being an associated microbe exists.

Bisabolane-like compounds had been previously isolated from marine sponges [215, 216], however, this represents the first report of this class of compounds in *Acanthostrongylophora ingens*. Consequently, these compounds could be of significant interest in future biogenetic and taxonomic studies. Besides belonging to a known class of compounds, the five new isolated bisabolane-related metabolites show novel structural features. Both cyclic bisabolane and metabolites bearing oxo functionality are not common among this group of compounds, highlighting the importance of these discoveries. Also, besides being described in the literature as involved in the biosynthesis of the marine compounds peniphenones [217], **13** has only been reported from terrestrial sources [218]. These studies represent its first isolation from marine organisms.

Despite sponges being found in all seas, they reach the highest biodiversity in the tropical region. The Indo-Pacific Ocean is one of the largest marine ecosystems. Indo-Pacific sponges are a good representative of its great biodiversity [219, 220]. As stated before, chemical diversity usually comes together with biological diversity and considering the analyzed sponge samples, the search for structurally diverse new chemical entities was more productive in individuals collected in the Indo-Pacific Ocean than in Icelandic waters, resulting in higher novelty rates. Seeing that sponges in tropical areas suffer more pressure from predation as well as microbiological infections [221], the obtained results might be explained based on that. A lower selective pressure on the sponges growing in the Icelandic waters does seem to promote the production of natural compounds as a mechanism of defense in the same degree as the tropical water surrounding the sponges growing in the Indo-Pacific Ocean.

4.3 Microorganism Isolated from Sponges

4.3.1 Fluvirucinins from the Actinomycete DIL-12-02-135

The marine strain DIL-12-02-135 was isolated from a sponge sample collected in the Indo-Pacific Ocean, in Timor. The colonies of the microorganism showed to be encrusting, mate-pale yellowish with the oldest colonies showing a whitish peripheral sporulation, as seen in Figure 48. These morphological characteristics are typical of filamentous Actinomycete bacteria, allowing an identification of the strain as an *Actinobacteria*.

The strain was fermented in a step-wise scale-up procedure until reaching 5.0 L of culture medium. After inoculation, the culture was grown for 12 days. At the end of cultivation time, the entire culture volume was centrifuged and the mycelial cake and other solids (464.0 g) were separated from 4.8 L of clarified broth. The mycelial cake was extracted with EtOAc:iPrOH (6:4 v/v) to yield the cell crude extract. The organic cell extract was separated using RP-VLC. An ESIMS analysis of silica gel fractions 3, 4, 5 and 6 revealed the presence of 2 compounds with an *m/z* 16 difference between them, as shown in Figure 50. According to MS profile, it was not possible to obtain a reasonable dereplication. Therefore, the two compounds were further isolated after several semi-preparative HPLC separations under MS-guiding. The simplified workflow leading to the isolation of **20** and **21** is resumed in Figure 49.

Figure 48 - DIL-12-02-135 strain growing on modified ATCC 172 solid medium (172M) at 28 ºC after isolation from a sponge sample.
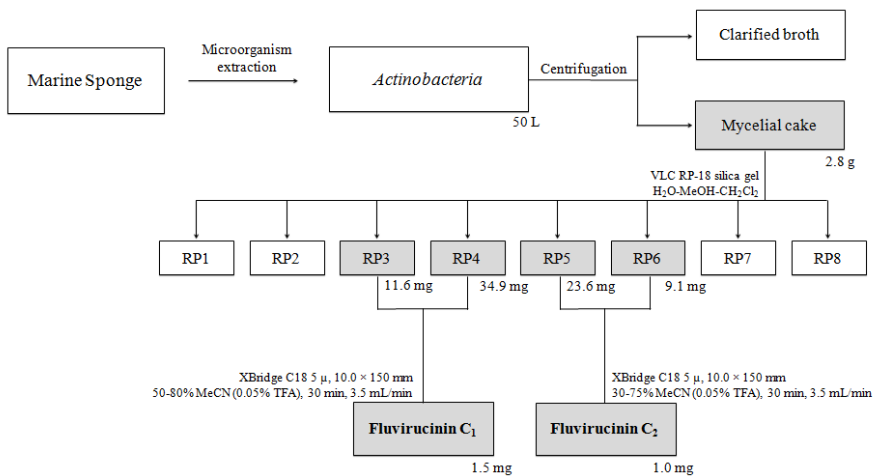
Figure 49 - Scheme of the simplified workflow that led to the isolation of two fluvirucinins from the marine actinomycete strain DIL-12-02-135.
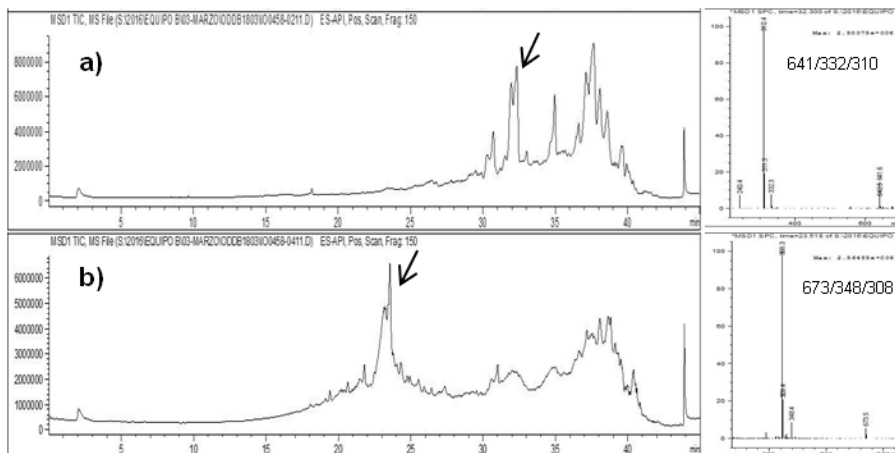
Figure 50 - DAD-chromatograms of Silica gel fractions **a)** 2 and **b)** 4. Peaks of interest are highlighted with an arrow and respective MS spectrum is shown on the right side.
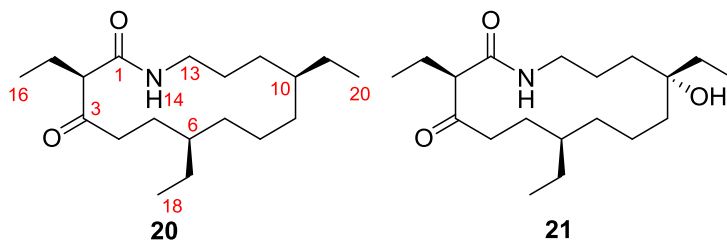
Figure 51 - Chemical structures of fluvirucinins isolated from DIL-12-02-135.

Compound **20** was obtained as an amorphous white solid. The (+)-HRESIMS molecular ion peak *m/z* 310.2751 allowed establishing the molecular formula as $C_{19}H_{35}NO_2$, indicating three degrees of unsaturation. The obtained 1D-NMR data are resumed in Table 12. The ^{13}C-NMR spectrum displayed 19 signals, which were assigned, together with HSQC, to three methyls (δ_C 11.9, 11.9, 11.4), 11 methylenes (δ_C 39.4, 38.9, 31.7, 30.6, 27.7, 27.6, 26.8, 25.4, 25.1, 22.5, 20.0), three methines (δ_C 63.4, 38.2, 37.3), and two non-protonated carbons that consisted of a ketone (δ_C 169.4) and an amide carbonyl (δ_C 208.9). In accordance, ^{1}H-NMR data exhibited three triplet methyls (δ_H 0.82, 0.80, 0.78), 11 methylenes, some of them splitting and assigned resorting to HSQC (δ_H 3.17, 2.55 and 2.40, 1.77, 1.55 and 1.45, 1.45 and 1.33, 1.28 and 1.02, 1.25 and 1.07, 1.25 and 1.01, 1.20, 1.19, 1.06 and 1.01) and three methines (δ_H 3.19, 1.20, 1.18). A combined analysis of COSY and TOCSY spectra allowed establishing four partial fragments: C-2 to C-16, C-4 to C-7 to C-18, C-9 to C-20 and C-11 to C-13, as seen in Figure 52. HMBC spectral data fully supported the elucidation of those four fragments. The additional HMBC cross-peaks correlating H_2-15 and H-2 to C-3 and C-1, H_2-4 to C-3 and H_2-13 to C-1 were crucial for the assignment of the ketone group at C-3 and the amide carbonyl at C-1. Further HMBC signals relating H_2-19/C-9, H_2-19/C-11, H_2-7/C-8 and H_2-7/C-9 allowed the full structure of a 2-, 6-, 10- tri-ethyl 14-membered ring macrolactam to be established. Hence, the planar structure of **20** was determined as the new member of the fluvirucin aglycone shown in Figure 51 and named fluvirucinin C_1. Spectral data for **20** can be found in Appendixes 108 to 114.
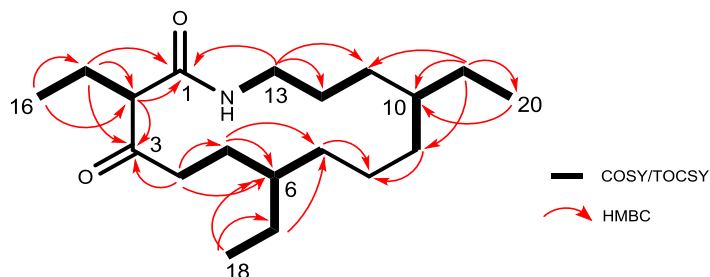
Figure 52 - Key ^{1}H-^{1}H COSY, HMBC and TOCSY correlations for the elucidation of **20**.

Table 12 - ^{1}H and ^{13}C-NMR data (500 and 100 MHz, respectively) obtained for compounds **20** and **21**. Experiments with **20** were performed in CDCl$_3$/CD$_3$OD and with **21** in CDCl$_3$.

Position	Compound 20		Compound 21	
	δ_C, type	δ_H, mult (J in Hz)	δ_C, type	δ_H, mult (J in Hz)
1	169.4, C		168.8, C	
2	63.4, CH	3.19, t (8.0)	63.6, CH	3.24, m
3	208.9, C		208.9, C	
4	38.9, CH$_2$	2.55, m	37.6, CH$_2$	2.54, m
		2.40, m		
5	25.1, CH$_2$	1.55, m	25.1, CH$_2$	1.70, m
		1.45, m		1.56, m
6	38.2, CH	1.20, m	38.3, CH	1.30, m
7	30.6, CH$_2$	1.25, m	32.4, CH$_2$	1.31, m
		1.01, m		1.07, m
8	20.0, CH$_2$	1.06, m	20.2, CH$_2$	1.17, m
		1.01, m		1.06, m
9	31.7, CH$_2$	1.28, m	37.6, CH$_2$	1.35, m
		1.02. m		
10	37.3, CH	1.18, m	74.4, C	
11	26.8, CH$_2$	1.25, m	34.2, CH$_2$	1.45, m
		1.07, m		1.37, m
12	25.4, CH$_2$	1.33, m	24.3, CH$_2$	1.44, m
		1.45, m		
13	39.4, CH$_2$	3.17, m	39.5, CH$_2$	3.31, m
				3.23, m
14 -NH		6.63, br. s		6.11, br. s
15	22.5, CH$_2$	1.77, m	22.8, CH$_2$	1.87, m
16	11.9, CH$_3$	0.82, t (7.5)	12.0, CH$_3$	0.91, t (7.4)
17	27.7, CH$_2$	1.19, m	28.0, CH$_2$	1.24, m
18	11.9, CH$_3$	0.80, t (7.0)	11.9, CH$_3$	0.87, t (7.1)
19	27.6, CH$_2$	1.20, m	32.9, CH$_2$	1.42, m
20	11.4, CH$_3$	0.78, t (7.4)	7.1, CH$_3$	0.89, t (7.4)

Compound **21** was isolated as an amorphous white solid. The molecular formula $C_{19}H_{35}NO_3$ was deduced from (+)-HRESIMS *m/z* 326.2771 molecular ion peak, indicating 3 degrees of unsaturation. The *m/z* 16 difference of **21** when compared with **20**, predicted the presence of a related compound with an extra hydroxyl group present in its structure. The ^{13}C-NMR spectrum of **21,** resumed in Table 12 displayed 19 signals, which were assigned, together with HSQC, to three methyls (δ_C 7.1, 11.9, 12.0), 11 methylenes (δ_C 39.5, 37.6, 37.6, 34.2, 32.9, 32.4, 28.0, 25.1, 24.3, 22.8, 20.2), two methines (δ_C 63.8, 38.3), and three quaternary carbons (δ_C 208.9, 168.8, 74.4). Accordingly, ^{1}H-NMR displayed three triplet methyls (δ_H 0.91, 0.87, 0.87), 11 methylenes, some of them splitting and then assigned together through HSQC and H2MBC (δ_H 3.31 and 3.23, 2.54, 1.87, 1.70 and 1.56, 1.45 and 1.37, 1.44, 1.35, 1.42, 1.31 and 1.07, 1.24, 1.17 and 1.06) and two methines (δ_H 3.24, 1.30). Both ^{1}H and ^{13}C-NMR data of **21** pointed for the presence of the same core skeleton (C-1 to C-20) found in **20**. However, methine C-10 (δ_C 37.3) in **20** seemed to be replaced by an oxygenated quaternary carbon (δ_C 74.4, C-10) in **21**. The position of the hydroxyl group at C-10 was confirmed by the HMBC correlations H_3-20/C-10 and H_2-19/C-10. **21** was therefore found to be a new member of the fluvirucin aglycone family shown in Figure 51 and named fluvirucinin C_2. Spectral data of **21** can be found in Appendixes 115 to 122.

The available spectroscopic data did not allow a determination of the relative configuration of the asymmetric carbon centers C-2, C-6 and C-10 of both compounds. However, based on highly similar 1D-NMR data of related compounds [222-225], a relative stereochemistry similar to those reported before in the literature for A and B series of fluvirucins was proposed.

Fluvirucins are a family of macrolactam glycoside compounds characterized by a C-2, 6 and 10 tri-methyl and/or ethyl 14-membered macrolactam ring linked to an amino sugar on C-3 or 9. Fluvirucin A_2 is the only exception, having the ethyl group on C-2 hydroxylated [226]. This class of compounds is typically produced by terrestrial actinomycete strains [224, 227] and had never been reported before from marine sources. Also, fluvirucinins, the common aglycone of fluvirucins, have previously been obtained by synthesis [228-230] but never from natural sources. The isolation of fluvirucinins C_1 and C_2 as naturally derived secondary metabolites from a marine-derived microorganism is being reported for the first time.

4.3.2 Macrolide and Quinone from the Actinomycete CP9-13-01-036

The marine strain CP9-13-01-036 was isolated from a sponge sample, also collected in the Indo-Pacific Ocean. The morphology of this strain appeared very similar to the one found for DIL-12-02-135: encrusting mate-pale yellowish colonies and the oldest ones appearing with a whitish peripheral sporulation, as shown in Figure 53. Based on these morphological characteristics, the strain was identified as a filamentous actinomycete bacterium.

Figure 53 - CP9-13-01-036 strain growing on modified ATCC 172 solid medium (172M) at 28 ºC after isolation from a sponge sample.

The strain was fermented in a step-wise scale-up procedure until reaching 5.0 L of culture medium. After inoculation, the culture was grown for 12 days. At the end of cultivation time, the entire culture volume was centrifuged and the mycelial cake and other solids were separated from 4.8 L of clarified broth. The clarified broth was extracted with EtOAc:iPrOH (14:9 v/v). The organic crude extract was separated using RP-VLC and a final semi-preparative HPLC separation to yield compound **22** (1.9 mg). The simplified isolation procedure is shown in Figure 54.

Compound **22** was isolated as an amorphous powder. It was identified as 2-hydroxyethyl-3-methyl-1,4-naphthoquinone based on spectral data available in the literature [231]. Spectral data for **22** can be found in Appendixes 123 to 124.
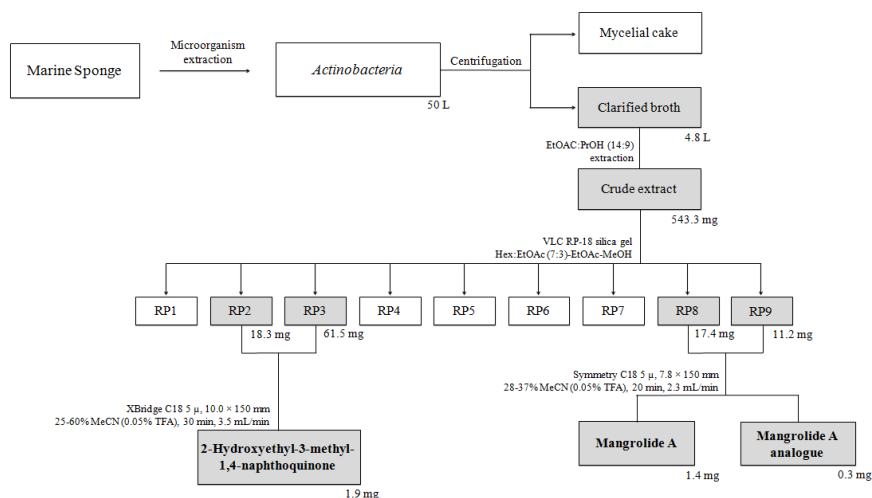
Figure 54 - Scheme of the simplified workflow that led to the isolation of two mangrolides and a naphtoquinone from the marine actinomycete strain CP9-13-01-036.

An ESIMS analysis of silica gel fractions 8 (17.4 mg) and 9 (11.2 mg) revealed the presence of two compounds with *m/z* 16 difference between them. Based on MS profile, it was not possible to obtain a reasonable dereplication. Therefore, the two compounds were followed after several semi-preparative separations under mass spectrometry guiding.
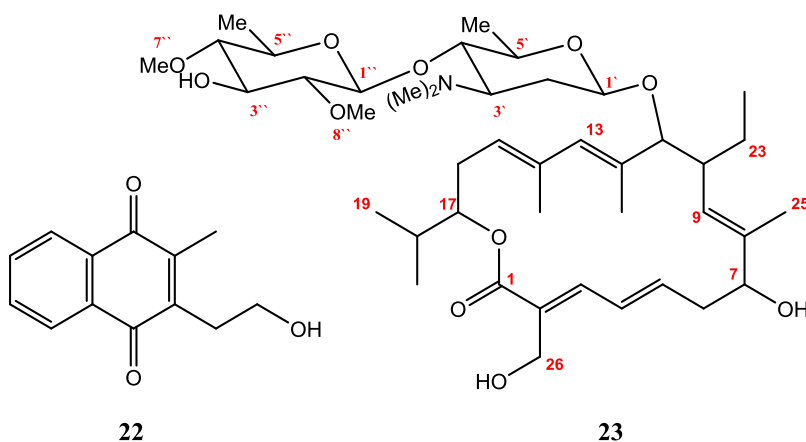
Figure 55 - Chemical structure of 2-hydroxyethyl-3-methyl-1,4-naphthoquinone (**21**) mangrolide A (**23**) isolated from CP9-13-01-036.

94

Compound **23** was obtained as an amorphous white solid. 1D-NMR data is resumed on Table 13. Its ^{13}C-NMR spectrum revealed the presence of 42 carbon signals which were assigned, together with HSQC, to 12 methyls (δ_C 60.8, 60.7, 40.7, 40.7, 19.4, 17.8, 17.8, 17.5, 16.9, 14.7, 13.0, 10.6), four methylenes (δ_C 56.6, 36.1, 28.5, 25.5), 21 methines (δ_C 142.5, 140.5, 133.4, 127.7, 124.2, 122.8, 102.5, 102.4, 93.2, 84.6, 83.8, 78.7, 76.0, 75.7, 72.3, 71.4, 70.6, 70.6, 68.3, 41.3, 30.3) and five non-protonated carbons (δ_C 168.5, 135.6, 135.5, 134.5, 127.4). From the listed non-protonated carbons, two were hydroxylated (δ_C 148.0, 147.5). In accordance, the ^{1}H-NMR spectrum exhibited 12 methyls (δ_H 3.53, 3.50, 3.04, 3.04, 1.73, 1.58, 1.58, 1.25, 1.25, 0.93, 0.90, 0.81), four splitting methylenes and so, assigned resorting to HSQC spectrum analysis (δ_H 4.32 and 4.27, 2.62 and 2.43, 2.39 and 2.33, 1.97 and 1.23) and 21 methines (δ_H 7.14, 6.46, 5.71, 5.76, 5.34, 5.01, 4.69, 4.38, 4.30, 4.20, 3.69, 3.54, 3.45, 3.40, 3.30, 3.25, 2.94, 2.87, 2.76, 2.66, 2.03). An integrated analysis of both 1D spectra led to a first assumption of the presence of a polyketide structure with five double bonds and two sugar moieties.

The COSY spectrum allowed relating the olefinic protons H-3 (δ_H 7.14), H-4 (δ_H 6.46) and H-5 (δ_H 5.76) in a conjugated double bond system, as it is illustrated in Figure 56. H-5 was also related by COSY with the methylene H$_2$-6 (δ_H 6.46) and this one with the hydroxylated H-7 (δ_H 4.20). A second substructure elucidation was initiated based on HMBC spectrum analysis: the triplet methyl Me-24 (δ_H 0.81) was linked with H$_2$-23 and this one with H-10. The COSY cross-peaks H-9/H-10 and H-10/H-11 allowed to relate those methines and H-9 resonance (δ_H 5.01) anticipated a double bond. The HMBC correlation H-7/C-8 allowed connecting this system with the previous one. The Me-25/H-9 cross-peak appeared in the COSY spectrum due to *w*-coupling and was the key to link this multiplet methyl to the structure. A third sub-structure was constructed based on the HMBC correlations H-13/C-11, H-13/C-15, Me-21/C-13, H$_2$-16/C-14. H$_2$-6/H-17 COSY cross-peak allowed relating those two. The remaining groups of the macrolide were linked based on HMBC cross-signals: H-13/Me-22, H-18/H-17, H-17/Me-19 and H-18/Me-20.

95

Table 13 - ^{1}H-NMR and ^{13}C-NMR data (500 and 100 MHz, respectively) obtained for compound **23**. Experiments were performed in CDCl$_3$/CD$_3$OD.

Position	δ_C, type	δ_H, mult (J in Hz)
		Compound 23
1	168.5, C	
2	127.4, C	
3	142.5, CH	7.14, d (11.4)
4	127.7, CH	6.46, t (13.5)
5	140.5, CH	5.76, td (10.3, 5.1)
6	36.1, CH$_2$	2.62, m
		2.43, m
7	72.3, CH	4.20, s
8	135.6, C	
9	122.8, CH	5.01, dt (10.4, 1.6)
10	41.3, CH	2.66, m
11	93.2, CH	3.69, d (9.7)
12	134.5, C	
13	133.4, CH	5.71, s
14	135.5, C	
15	124.2, CH	5.34, t (8.2)
16	28.5, CH$_2$	2.39, m
		2.33, m
17	78.7, CH	4.69, dt (8.8, 4.5)
18	30.3, CH	2.03, m
19	17.5, CH$_3$	0.93, d (6.8)
20	19.4, CH$_3$	0.90, d (6.7)
21	16.9, CH$_3$	1.58, m
22	13.0, CH$_3$	1.73, d (1.3)
23	25.5, CH$_2$	1.97, m
		1.23, m
24	10.6, CH$_3$	0.81, t (7.4)
25	14.7, CH$_3$	1.58, m
26	56.6, CH$_2$	4.32, d (7.8)
		4.27, d (12.6)
1´	102.4, CH	4.30, d (7.7)
2´	68.3, CH	3.45, dd (10.5, 7.5)
3´	70.6, CH	2.94, t (10.3)
4´	76.0, CH	3.54, m
5´	72.3, CH	3.30, dd (8.9, 6.2)
6´	17.8, CH$_3$	1.25, d (6.2)
7´	40.7, CH$_3$	3.04, s
8´	40.7, CH$_3$	3.04, s
1´´	102.5, CH	4.38, d (7.7)
2´´	83.8, CH	2.87, dd (9.2, 7.7)
3´´	75.7, CH	3.40, t (9.1)
4´´	84.6, CH	2.76, t (9.2)
5´´	71.4, CH	3.25, dd (9.4, 6.2)
6´´	17.8, CH$_3$	1.25, d (6.2)
7´´	60.7, CH$_3$	3.53, s
8´´	60.8, CH$_3$	3.50, s
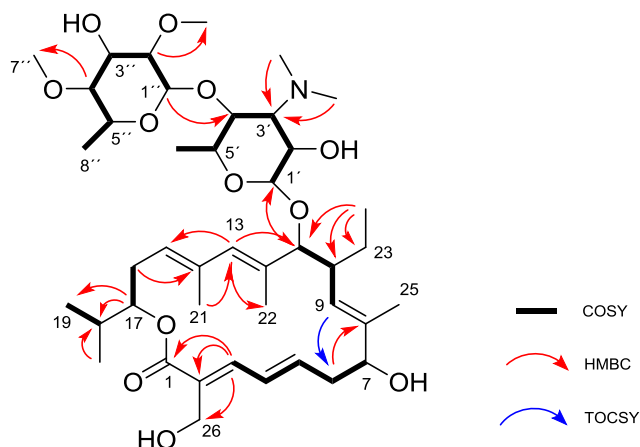
Figure 56 - Key ^{1}H-^{1}H COSY, HMBC and TOCSY correlations for the elucidation of mangrolide A (**23)**.

The elucidation of the two sugars was immediate. The first sugar was assigned to a mycaminose based on the chain COSY correlations of the anomeric H-1´ to the oxymethine H-2´, to the amine methine H-3´, to the oxymethine H-4´, to the oxymethine H-5´ and finally, from that one to Me-6´. The second sugar was assembled based on the same principle: COSY cross-correlations: H-1´´-H-2´´-H-3´´-H-4´´-H-5´´-Me-6´´. The shielded carbon shifts found for C-2´´(δ_H 83.8) and C-4´´ (δ_H 84.6) were indicative of the presence of two oxymethyls, resulting in a 6-deoxy-2,4-dimethyl-glucose. The two sugars were connected by a glycosidic bond as elucidated by the HMBC correlation H-1´´/C-4´. Another HMBC correlation H-11/C-1´ was the key to locate both sugars in the macrolide structure. The (+)-ESIMS *m/z* 780.5 molecular ion peak confirmed the proposed compound with the molecular formula $C_{42}H_{69}NO_{12}$ and nine degrees of unsaturation. The planar structure of **23** was established as shown in Figure 55, however, against the first indications of being new, **23** is described in the literature as mangrolide A [232]. Spectral data for **23** can be found in Appendixes 125 to 131.

The compound showing *m/z* 796.4 [M+H]$^+$ was also isolated, but the available mass (0.3 mg) did not allow its structure elucidation.

Macrolides are characteristic secondary metabolites isolated from actinomycetes, erythromycin being the most successful one [233]. Mangrolide A had been reported before, also isolated from an *Actinobacteria* strain [234]. Jamison *et. al* reported the isolation of three mangrolide analogs, being mangrolide A also the dominant compound in the extract. Mangrolides B and C were methylated and ethylated forms of mangrolide A, however,

isolated at very low yield. The structure of mangrolide C could not also be confirmed by NMR studies [234]. A hydroxylated analog haven´t been reported before, however, it was not possible to fully structure elucidate during the time of these studies.

2-hydroxyethyl-3-methyl-1,4-naphthoquinone had been previously isolated from terrestrial soil *Myxobacterium* [231] and *Actinobacterium* [235]. However, this represents its first isolation from a marine source.

The secondary metabolites isolated from the two studied actinomycete strains re-enforce the immeasurable value of microorganisms in the production of natural compounds. Their biosynthetic pathways have been selected, through evolution, to produce compounds which give them advantages in their environment [236]. Actinomycetes are considered to be the most potent source for the production of secondary metabolites [237, 238]. Also, the use of marine microorganism's secondary metabolites overcomes the supply-issue raised when sponge biomass is directly collected from the ocean. Microorganisms can be produced in large scale under controlled laboratory conditions. However, the process of secondary metabolites isolation from microorganisms has proven to be more demanding than from the sponges themselves. The complex composition of isolation and fermentation media is reflected in the crude extract, forcing to an extremely careful dereplication process, more resources and time-consuming isolation until the achievement of a pure secondary metabolite.

4.4 Bioactivities

Pure isolated compounds were all tested for their cytotoxic activity against four cell lines: A-549 human lung carcinoma cells, MDA-MB-231 human breast adenocarcinoma cells, HT-29 human colorectal carcinoma cells and PSN1 human pancreatic adenocarcinoma cells using the protein binding dye SRB method. The other tested bioassays: anti-bacterial and anti-obesity were performed based on its relevance and availability of the assay at the time of isolation.

Table 14 - Summary of growth inhibitory effects (µM) measured for all isolated compounds.

	A-549 Lung carcinoma	MDA-MB-231 Breast adenocarcinoma	HT-29 Colorectal carcinoma	PSN1 Pancreatic adenocarcinoma
2´-Deoxyadenosine (**1**)	> 39.7	> 39.7	> 39.7	> 39.7
Thymine (**2**)	> 79.4	> 79.4	> 79.4	> 79.4
Thymidine (**3**)	> 41.1	> 41.1	> 41.1	> 41.1
2´-Deoxyuridine (**4**)	> 43.9	> 43.9	> 43.9	> 43.9
2´-Deoxyinosine (**5**)	> 39.7	> 39.7	> 39.7	> 39.7
2´-Deoxycytidine (**6**)	> 44.1	> 44.1	> 44.1	> 44.1
Adenosine (**7**)	> 37.4	> 37.4	> 37.4	> 37.4
2´-Deoxyguanosine (**8**)	> 37.4	> 37.4	> 37.4	> 37.4
Haploscleridamine (**9**)	> 46.0	> 46.0	> 46.0	> 46.0
Compound **10**	> 39.6	> 39.6	> 39.6	> 39.6
Spongian compound **11**	> 27.5	> 27.5	> 27.5	> 27.5
Spongian compound **12**	> 33.3	> 33.3	> 33.3	> 33.3
Compound **13**	60.2	60.2	60.2	60.2
Bisabolane compound **14**	29.7	19.4	6.9	---
Bisabolane compound **15**	> 40.3	> 40.3	> 40.3	> 40.3
Bisabolane compound **16**	> 40.6	> 40.6	> 40.6	> 40.6
Bisabolane compound **17**	> 43.4	> 43.4	> 43.4	> 43.4
Bisabolane compound **18**	> 37.8	> 37.8	> 37.8	> 37.8
Bisabolane compound **19**	> 40.6	> 40.6	> 40.6	> 40.6
Fluvirucinin C_1 (**20**)	> 32.3	> 32.3	> 32.3	> 32.3
Fluvirucinin C_2 (**21**)	> 32.3	> 32.3	> 32.3	> 32.3
Naphthoquinone (**22**)	0.786	0.356	0.601	0.823
Mangrolide A (**23**)	> 12.8	> 12.8	> 12.8	> 12.8

Results are given as the lowest concentration causing 50% of cell growth inhibition (GI_{50}) after a continuous exposure to the compounds during 48h.

Obtained GI_{50} for cell growth inhibitory bioassay are resumed in Table 14. The great majority of the compounds revealed not to be active against A-549, MDA-MB-231, HT-29 and PSN1 cancer cell lines, not showing cell growth inhibition at the highest tested concentration (10 mg/mL). However, not surprisingly, compound **22** showed strong growth inhibitory activity against the four tested cell lines with GI_{50} = 786 nM, 356 nM, 601 nM and 823 nM for A-549, MDA-MB-231, HT-29 and PSN1, respectively. Despite compound **22** had never been described as an anticancer agent, quinone compounds form a large class of anticancer approved drugs with a mechanism of action based on their redox potential [239].
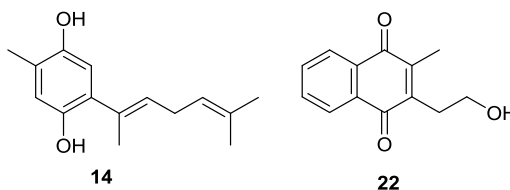
Figure 57 - Structure of the compounds with measured *in vitro* cytotoxicity activity.

Compound **14** showed moderate growth inhibition on HT-29 colorectal carcinoma cells with a GI_{50} of 6.9 μM. Phenoxy radicals play a crucial role in the development of activities in a biological system and therefore, phenolic compounds are another well-studied class of antitumor compounds [240]. Compound **15**, despite being structurally very similar to compound **14**, did not show cytotoxic activity at the tested concentrations (GI_{50} > 40.3 μM), highlighting also, in this particular case, the important role of the side chain in the bioactivity.

Table 15 - Summary of antimicrobial activity measured for compounds **20-23**.

	E. coli ATCC 8739	*P. aeruginosa* ATCC 9027	*S. aureus* ATCC 6538	*C. albicans* ATCC 10231
Fluvirucinin C_1 (**20**)	NA	NA	NA	NA
Fluvirucinin C_2 (**21**)	---	---	---	NA
Naphthoquinone **22**	NA	NA	60% inhibition	NA
Mangrolide A (**23**)	NA	NA	NA	NA
Nalidixic acid	100% inhibition	---	---	---
Gentamicin	---	100% inhibition	---	---
Vancomicin	---	---	100% inhibition	---
Amphotericin B	---	---	---	100% inhibition

Results are given as a percentage of inhibition relative to the respective control antibiotic after a continuous exposure to the compounds during 24h. NA: Not active.

Compounds isolated from microorganisms were tested for their antimicrobial activity using the disk diffusion antibiotic sensitivity test against *Escherichia coli* (ATCC 8739), *Pseudomonas aeruginosa* (ATCC 9027), *Staphylococcus aureus* (ATCC 6538) and *Candida albicans* (ATCC 10231). Macrolactams are a known class of anti-fungal compounds and glycosylated fluvirucins have been previously described as possessing this activity [222, 241]. Fluvirucins, the glycosylated form of fluvirucinins, were described as potent selective antifungal agents [222]. However, in contrast to what would be expectable, none of the isolated fluvirucinins were shown to be active against the tested microbial strains. A comparison of the obtained activities with those described for fluvirucins suggests that the sugar moiety is essential for the antifungal *in vitro* activity.
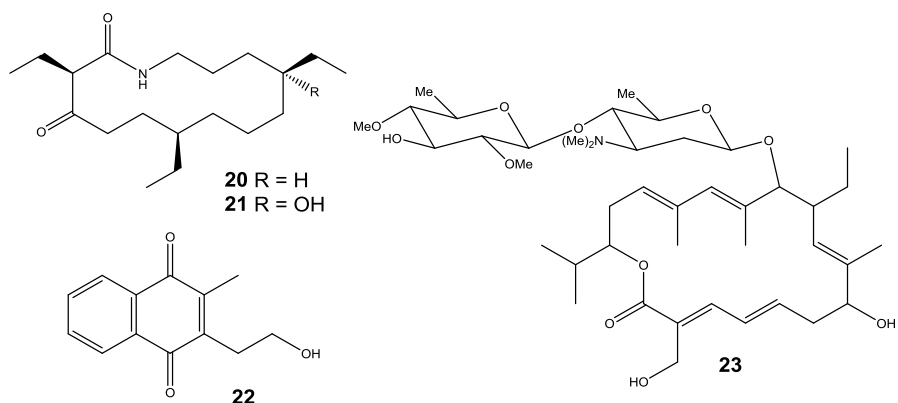
Figure 58 - Structure of the compounds tested for antimicrobial activity.

Macrolides are an old and well-established class of antimicrobial agents that have long played an important role in the treatment of infectious diseases [242]. Mangrolide A, specifically, had been described as a selective potent antibiotic against a number of clinically important Gram-negative bacteria: *Burkholderia cenocepacia*, *Acinetobacter baumannii, Escherichia coli* and *Staphylococcus aureus* [243]. However, the antimicrobial results obtained for **23** do not confirm its described bioactivity, the glycosylated macrocyclic mangrolide A (**23**) was not found to be active against any of the tested bacterial strains, including the Gram-negative ones (Table 15).

Compound **22** showed positive results when tested against the Gram-positive bacteria *Staphylococcus aureus*. Its activity is comparable to those standard antibiotics currently in therapeutics, with the advantage of being also active against fungi, yeast [231] and other Gram-positive and Gram-negative bacterial strains [231, 235]. Along with anticancer activity, quinones are also typical antimicrobial compounds.
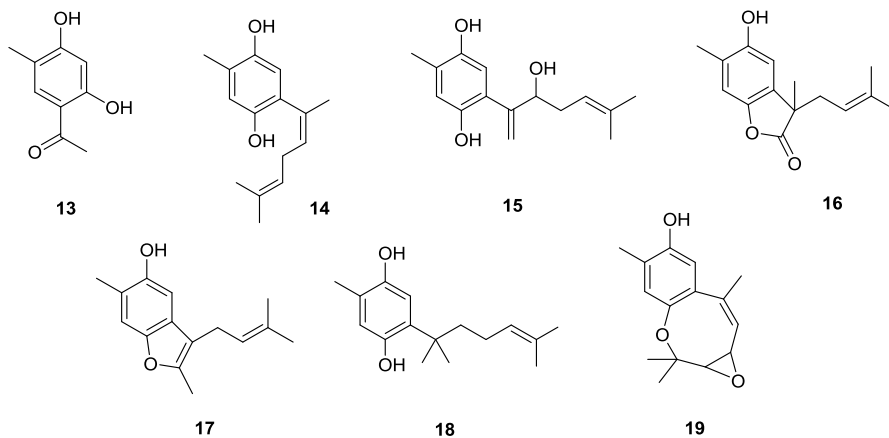
Figure 59 - Structure of the compounds tested for anti-obesity activity.

Table 16 - Summary of anti-obesity activity measured for compounds **13-19**.

Compound	EC$_{50}$ [µM]
Compound **13**	NA
Compound **14**	1.78
Compound **15**	7.89
Compound **16**	12.61
Compound **17**	0.84
Compound **18**	NA
Compound **19**	1.22

Results are given as the half maximum inhibitory concentration (IC$_{50}$). Data are obtained from 6-8 replicates per concentration. NA: Not active

Obesity is increasing at epidemic rates and the development of new drugs is urgently needed. Several marine natural compounds had already proven to have anti-obesity activity [177, 244] and also many phenolic natural compounds have demonstrated anti-obesity properties [245]. In this context, **13-19** were tested for anti-obesity activity based on their lipid reducing capacity in zebrafish Nile red assay.
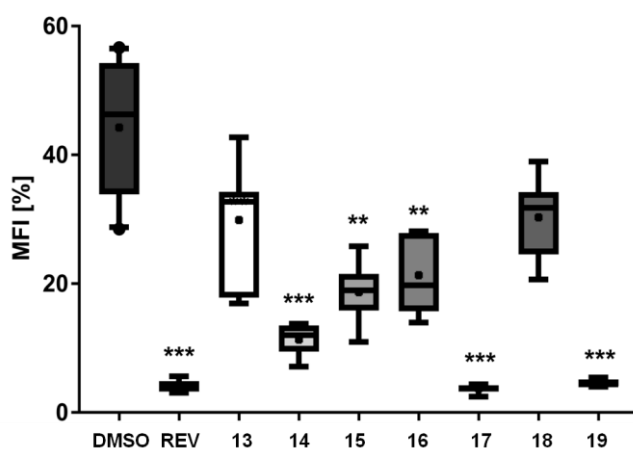
Figure 60 - Anti-obesity activity of compounds **13-19** in zebrafish larvae Nile red assay.1% DMSO and 50 µM resveratrol (REV) were used as negative and positive controls, respectively. 6-8 individual larvae were used per treatment.** $p < 0.01$, *** $p < 0.001$.
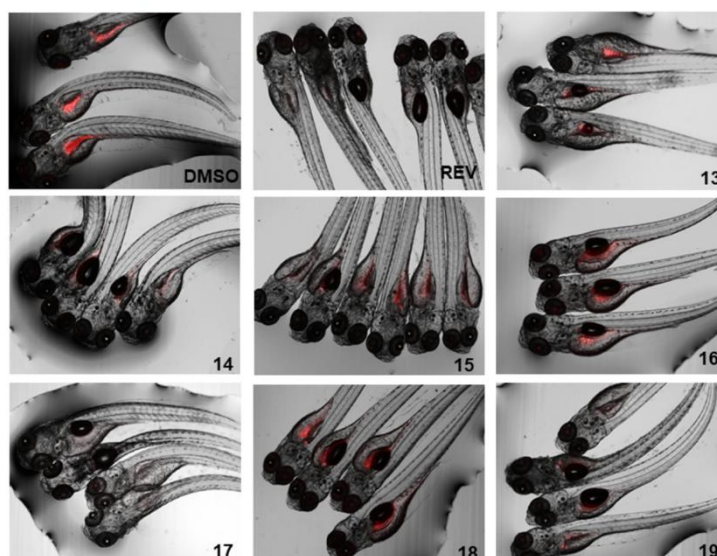
Figure 61 - Representative images of the zebrafish Nile red assay. Images show the overlay of the fluorescence and phase contrast. 0.1% DMSO was used as a solvent control and 50 µM resveratrol (REV) as the positive control.

A resume of the obtained IC_{50} is shown in Table 16 and the results can be visualized in Figures 60 and 61. The results showed that **14**, **17** and **19** have potent anti-obesity activity (IC_{50} = 1.78, 0.84 and 1.22 µM, respectively), reducing significantly the zebrafish total amount of lipids. Compounds **15** and **16** also presented anti-obesity activity (IC_{50} = 7.89, 12.61 µM, respectively), showing a moderate reduction in zebrafish total amount of lipids. It is interesting to observe that **13** did not show activity, suggesting an anti-obesity potential for bisabolane-type compounds. Further, the structural differences found when compounds **14** or **15** are compared to compound **18,** as seen in Figure 59, are able to cause the inactivation of the compound, but cyclising the side chain, as seen in **19**, does not.

5 Summary and Conclusions
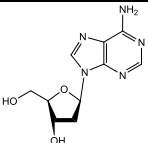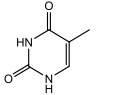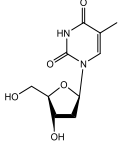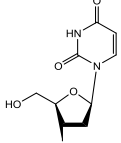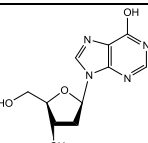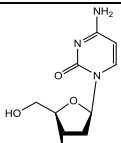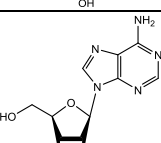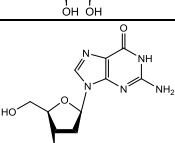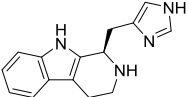
The present study aimed to investigate the secondary metabolites produced by marine sponges and sponge-associated microorganisms from different sampling locations and to evaluate their relevant and potential biological activities. A total of 23 sponge natural compounds comprising diverse structural groups were isolated, 10 of which have structures never reported before in the literature. The structures of the new compounds were unambiguously established based on NMR spectroscopic (1D and 2D) and mass spectrometric data. The identities of the known compounds were established by comparison with previously published data. The chemical diversity found in the present studies highlights the great biosynthetic capacities of both sponges and their associated microbes. The biological activities screened for the isolated compounds were cytotoxicity, anti-microbial and anti-obesity activities.
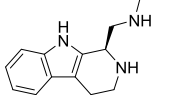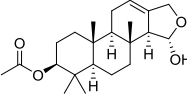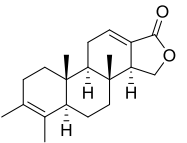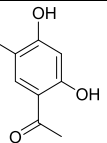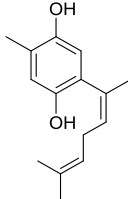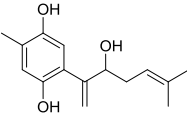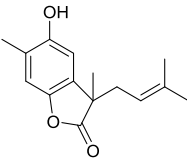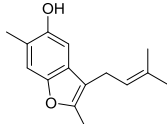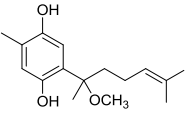
The compounds resulted from this study were tested against the human cancer cell lines A-549 human lung carcinoma cells, MDA-MB-231 human breast adenocarcinoma cells, HT-29 human colorectal carcinoma cells and PSN1 human pancreatic adenocarcinoma. Among them, 2-hydroxyethyl-3-methyl-1,4-naphthoquinone (**22**), the quinone isolated from the *Actinobacteria* CP9-13-01-036, and 6-(1,5-dimethyl-1,4-hexadienyl)-3-methylbenzene-1,4-diol (**14**), the bisabolane-related compound isolated from *Acanthostrongylophora ingens* displayed, respectively, strong and moderate *in vitro* growth inhibitory activity against the tested human cancer cell lines. Thus, these two compounds represent novel chemical scaffolds with potential for the development of new anticancer derivatives.
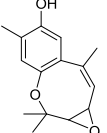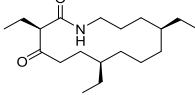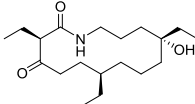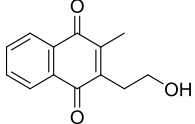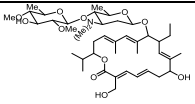
2-hydroxyethyl-3-methyl-1,4-naphthoquinone (**22**) revealed also to be a promising antibacterial agent against *Staphylococcus aureus* infections. Its activity is comparable to those standard antibiotics currently in therapeutics, with the advantage of being also active against fungi, yeast and other bacterial strains.

Five bisabolane-related compounds isolated from *Acanthostrongylophora ingens* showed inhibitory effects on zebrafish total amount of lipids (**14-17**,**19**). These results, indicating bisabolane class of compounds as anti-obesity agents, are of great importance regarding the fact that obesity represents one of the top health problems of humanity.

Table 17– Summary of compounds isolated from sponges or sponge-associated microbes, their sources, novelty and studied bioactivities.

No.	Source	Trivial name	Chemical structure	Novelty	Bioactivities
1	*Geodia macandrewi*	2´-Deoxyadenosine		Known	Not active
2	*Geodia macandrewi*	Thymine		Known	Not active
3	*Geodia macandrewi*	Thymidine		Known	Not active
4	*Geodia macandrewi*	2´-Deoxyuridine		Known	Not active
5	*Geodia macandrewi*	2´-Deoxyinosine		Known	Not active
6	*Geodia macandrewi*	2´-Deoxycytidine		Known	Not active
7	*Geodia macandrewi*	Adenosine		Known	Not active
8	*Geodia macandrewi*	2´-Deoxyguanosine		Known	Not active
9	*Acanthostron-gylophora* sp.	Haploscleridamine		Known	Not active

No.	Source	Trivial name	Chemical structure	Novelty	Bioactivities
10	*Acanthostron-gylophora* sp.	Haploscleridamine derivative **10**		New	Not active
11	*Acanthodendrilla* sp.	3β-Acetoxy -15-hydroxyspongia-12-en		New	Not active
12	*Acanthodendrilla* sp.	3-Methylspongia-3,12-dien-16-one		New	Not active
13	*Acanthostron-gylophora* ingens	1-(2,4-Dihydroxy-5-methyphenyl)ethan-1-one		Known	Not active
14	*Acanthostron-gylophora* ingens	6-(1,5-Dimethyl-1,4-hexadienyl)-3-methylbenzene-1,4-diol		Known	Cytotoxic Anti-obesity
15	*Acanthostron-gylophora* ingens	6-(3-Hydroxy-6-methyl-1,5-heptadien-2-yl)-3-methylbenzene-1,4-diol		New	Anti-obesity
16	*Acanthostron-gylophora* ingens	4-Hydroxy-3,7-dimethyl-7-(3-methylbut-2-en-1-yl)benzofuran-17-one		New	Anti-obesity
17	*Acanthostron-gylophora* ingens	3,16-Dimethyl-7-(3-methylbut-2-en-1-yl)benzofuran-4-ol		New	Anti-obesity
18	*Acanthostron-gylophora* ingens	6-(2-Methoxy-6-methylhept-5-en-2-yl)-3-methylbenzene-1,4-diol		New	Anti-obesity

No.	Source	Trivial name	Chemical structure	Novelty	Bioactivities
19	*Acanthostron-gylophora* ingens	3,7,11,11-Tetramethyl-1,9-dihydro-2-benzoxirenoxocin-6-ol		New	Anti-obesity
20	Actinomycete strain DIL-12-02-135	Fluvirucinin C_1		New	Not active
21	Actinomycete strain DIL-12-02-135	Fluvirucinin C_2		New	Not active
22	Actinomycete strain CP9-13-01-036	2-Hydroxyethyl-3-methyl-1,4-naphthoquinone		Known	Cytotoxic Antibacterial
23	Actinomycete strain CP9-13-01-036	Mangrolide A		Known	Not active

Despite the lack of activity found for the new haploscleridamine derivative (**10**), the two new spongian diterpenes derivatives (**11-12**), 1-(2,4-dihydroxy-5-methylphenyl)ethan-1-one (**13**), the bisabolane-related compound **18** and the two fluvirucinins (**20-21**), they should be considered in other biological activity assays, against different diseases.

The isolation of those compounds for the first time from selected macro- and microspecies contributed to a new insight, not only based on the identification of new sources of sponge and actinomycetes secondary metabolites with relevant biological properties, but also on to their chemotaxonomic value. The isolated 3β-acetoxy-15-hydroxyspongia-12-en (**11**) and 3-methylspongia-3,12-dien-16-one (**12**) are a good example. *Dendroceratida* class is known by producing spongian diterpenes and *Acanthodendrilla* was the only genus that had not been reported as a producer of this class of compounds. The present study provides valuable opportunities for further chemotaxonomic studies. The isolation of several other compounds from other sponge species and actinomycete strains during this study can also be classified as additional tools for the purpose of taxonomic identification.

Sponges collected in the Indo-Pacific Ocean led to the isolation of more known and new natural compounds than the one from Icelandic waters, being in accordance with the fact that the majority of marine drug candidates are originally isolated from tropical or subtropical seas. Microorganisms also revealed to be a valuable source of structurally diverse natural compounds, however, their isolation was a demanding and time-consuming procedure.

Marine sponges are identified as a tremendous and remarkable source of biologically active metabolites, extremely valuable for the development of new drugs. This study directly confirms this premise with the isolation of structurally diverse new and known compounds with anticancer, antimicrobial and anti-obesity agents.

References

[1] Solecki, R.S. Shanidar IV, a Neanderthal Flower Burial in Northern Iraq. *Science, 190*(4217), 880-881. (1975)

[2] Yuan, H., Ma, Q., Ye, L., & Piao, G. The Traditional Medicine and Modern Medicine from Natural Products. *Molecules, 21*(5). (2016)

[3] Hamilton, G.R. & Baskett, T.F. In the arms of morpheus: the development of morphine for postoperative pain relief. *Canadian Journal of Anesthesia, 47*(4), 367-374. (2000)

[4] Inc, N. A. Combinatorial chemistry *Nature Biotechnology, 18*, IT50-IT52. (2000)

[5] Wilhelm, S., Carter, C., Lynch, M., Lowinger, T., Dumas, J., Smith, R.A., Schwartz, B., Simantov, R. & Kelley, S. Discovery and development of sorafenib: a multikinase inhibitor for treating cancer. *Nature Reviews Drug Discovery, 5*(10), 835-844. (2006)

[6] Newman, D.J. & Cragg, G.M. Drugs and Drug Candidates from Marine Sources: An Assessment of the Current "State of Play". *Planta Medica, 82*(9-10), 775-789. (2016)

[7] Arrieta, J.M., Arnaud-Haond, S. & Duarte, C.M. What lies underneath: Conserving the oceans' genetic resources. *Proceedings of the National Academy of Sciences of the United States of America, 107*(43), 18318-18324. (2010)

[8] Haefner, B. Drugs from the deep: marine natural products as drug candidates. *Drug Discovery Today, 8*(12), 536-544. (2003)

[9] Blunt, J.W., Copp, B.R., Keyzers, R.A., Munro, M.H. & Prinsep, M.R. Marine natural products. *Natural Product Reports, 33*(3), 382-431. (2016)

[10] Yaakob, Z., Ali, E., Zainal, A., Mohamad, M. & Takriff, M.S. An overview: biomolecules from microalgae for animal feed and aquaculture. *Journal of Biological Research, 21*(1), 6. (2014)

[11] Ariede, M.B., Candido, T.M., Jacome, A.L.M., Velasco, M.V.R., de Carvalho, J.C.M. & Baby, A.R. Cosmetic attributes of algae - A review. *Algal Research, 25*, 483-487. (2017)

[12] Peng, J., Shen, X., El Sayed, K.A., Dunbar, D.C.H., Perry, T.L., Wilkins, S.P., Hamann, M.T., Bobzin, S., Huesing, J., Camp, R., Prinsen, M., Krupa, D. & Wideman, M.A. Marine Natural Products as Prototype Agrochemical Agents. *Journal of Agricultural and Food Chemistry, 51*(8), 2246-2252. (2003)

[13] Blunt, J.W., Copp, B.R., Munro, M.H., Northcote, P.T. & Prinsep, M.R. Marine natural products. *Natural Product Reports, 27*(2), 165-237. (2010)

[14] Pauletti, P.M., Cintra, L.S., Braguine, C.G., da Silva, A.A., Silva, M.L.A.E., Cunha, W.R. & Januario, A.H. Halogenated Indole Alkaloids from Marine Invertebrates. *Marine Drugs, 8*(5), 1526-1549. (2010)

[15] Butler, A. & Carter-Franklin, J.N. The role of vanadium bromoperoxidase in the biosynthesis of halogenated marine natural products. *Natural Product Reports, 21*(1), 180-188. (2004)

[16] Ruiz-Torres, V., Encinar, J.A., Herranz-Lopez, M., Perez-Sanchez, A., Galiano, V., Barrajon-Catalan, E. & Micol, V. An Updated Review on Marine Anticancer Compounds: The Use of Virtual Screening for the Discovery of Small-Molecule Cancer Drugs. *Molecules, 22*(7). (2017)

[17] Cragg, G.M. & Newman, D.J. Natural products: A continuing source of novel drug leads. *Biochimica et Biophysica Acta (BBA) - General Subjects, 1830*(6), 3670-3695. (2013)

[18] Blunt, J.W., Copp, B.R., Keyzers, R.A., Munro, M.H.G. & Prinsep, M.R. Marine natural products. *Natural Product Reports, 34*(3), 235-294. (2017)

[19] Blunt, J.W., Copp, B.R., Keyzers, R.A., Munro, M.H.G. & Prinsep, M.R. Marine natural products. *Natural Product Reports, 32*(2), 116-211. (2015)

[20] MarineLit. (2018) Retrieved November 3rd, 2018, from http://pubs.rsc.org/marinlit/

[21] Mayer, A. (2017) Marine Pharmaceuticals: the Clinical Pipeline. Retrieved November 3rd, 2018, from http://marinepharmacology.midwestern.edu/index.htm

[22] Bergmann, W. & Feeney, R. J. Contributions to the study of marine products. XXXII. The nucleosides of sponges. I.1. *The Journal of* Organic Chemistry, 16(6), 981-987. (1951)

[23] Privatdegarilhe, M. & De Rudder, J. Effect of 2 Arabinose Nucleosides on the Multiplication of Herpes Virus and Vaccine in Cell Culture. *Comptes rendus hebdomadaires des séances de l'Académie des sciences*, 259, 2725-2728. (1964)

[24] Sagar, S., Kaur, M. & Minneman, K.P. Antiviral Lead Compounds from Marine Sponges. Marine Drugs, 8(10), 2619-2638. (2010)

[25] Shepshelovich, D., Edel, Y., Goldvaser, H., Dujovny, T., Wolach, O. & Raanani, P. Pharmacodynamics of cytarabine induced leucopenia: a retrospective cohort study. *British Journal of Clinical Pharmacology*, 79(4), 685-691. (2015)

[26] McGivern, J.G. Ziconotide: a review of its pharmacology and use in the treatment of pain. *Neuropsychiatric Disease and Treatment, 3*(1), 69-85. (2007)

[27] Koski, R.R. Omega-3-acid Ethyl Esters (Lovaza) For Severe Hypertriglyceridemia. *Pharmacy and Therapeutics, 33*(5), 271-303. (2008)

[28] Hirata, Y. & Uemura, D. Halichondrins - Antitumor Polyether Macrolides from a Marine Sponge. *Pure and Applied Chemistry, 58*(5), 701-710. (1986)

[29] Doherty, M.K. & Morris, P.G. Eribulin for the treatment of metastatic breast cancer: an update on its safety and efficacy. *International Journal of Women's Health, 7*, 47-58. (2015)

[30] Eslamian, G., Wilson, C. & Young, R.J. Efficacy of eribulin in breast cancer: a short report on the emerging new data. *OncoTargets and therapy, 10*, 773-779. (2017)

[31] Bai, R., Petit, G.R. & Hamel, E. Dolastatin 10, a powerful cytostatic peptide derived from a marine animal: Inhibition of tubulin polymerization mediated through the vinca alkaloid binding domain. *Biochemical Pharmacology, 39*(12), 1941-1949. (1990)

[32] van de Donk, N.W.C.J. & Dhimolea, E. Brentuximab vedotin. *mAbs, 4*(4), 458-465. (2012)

[33] Shanbhag, S. & Ambinder, R.F. Hodgkin Lymphoma: A Review and Update on Recent Progress. *Cancer Journal for Clinicians, 68*(2), 116-132. (2018)

[34] Rinehart, K.L., Holt, T.G., Fregeau, N.L., Stroh, J.G., Keifer, P.A., Sun, F., Li, L.H. & Martin, D.G. Ecteinascidins 729, 743, 745, 759A, 759B, and 770: potent antitumor agents from the Caribbean tunicate *Ecteinascidia turbinata*. *The Journal of Organic Chemistry, 55*(15), 4512-4515. (1990)

[35] D'Incalci, M., Badri, N., Galmarini, C. M. & Allavena, P. Trabectedin, a drug acting on both cancer cells and the tumour microenvironment. *British Journal of Cancer, 111*(4), 646-650. (2014)

[36] Pye, C.R., Bertin, M.J., Lokey, R.S., Gerwick, W.H. & Linington, R.G. Retrospective analysis of natural products provides insights for future discovery trends. *Proceedings of the National Academy of Sciences of the United States of America, 114*(22), 5601-5606. (2017)

[37] Blunt, J.W., Copp, B.R., Keyzers, R.A., Munro, M.H. & Prinsep, M.R. Marine natural products. *Natural Product Reports, 29*(2), 144-222. (2012)

[38] Mehbub, M.F., Lei, J., Franco, C. & Zhang, W. Marine sponge derived natural products between 2001 and 2010: trends and opportunities for discovery of bioactives. *Marine Drugs, 12*(8), 4539-4577. (2014)

[39] Blunt, J.W., Copp, B.R., Munro, M.H., Northcote, P.T. & Prinsep, M.R. Marine natural products. *Natural Product Reports, 22*(1), 15-61. (2005)

[40] Telford, M.J., Moroz, L.L. & Halanych, K.M. Evolution: A sisterly dispute. *Nature, 529*(7586), 286-287. (2016)

[41] Yin, Z.J., Zhu, M.Y., Davidson, E.H., Bottjer, D.J., Zhao, F.C. & Tafforeau, P. Sponge grade body fossil with cellular resolution dating 60 Myr before the Cambrian. *Proceedings of the National Academy of Sciences of the United States of America, 112*(12), E1453-E1460. (2015)

[42] Pronzato, R. & Manconi, R. Mediterranean commercial sponges: over 5000 years of natural history and cultural heritage. *Marine Ecology - an Evolutionary Perspective, 29*(2), 146-166. (2008)

[43] Voultsiadou, E. Therapeutic properties and uses of marine invertebrates in the ancient Greek world and early Byzantium. *Journal of Ethnopharmacology, 130*(2), 237-247. (2010)

[44] Berne, S., Kalauz, M., Lapat, M., Savin, L., Janussen, D., Kersken, D., Ambrožič, A.J., Zemljič J.Š., Jaklič, D., Gunde-Cimerman, N., Lunder, M., Roškar, I., Eleršek, T., Turk, T. & Sepčić, K. Screening of the Antarctic marine sponges (Porifera) as a source of bioactive compounds. *Polar Biology, 39*(5), 947-959. (2016)

[45] Kim, C.K., Woo, J.K., Kim, S.H., Cho, E., Lee, Y.J., Lee, H.S., Sim, C.J., Oh, D.C., Oh, K.B. & Shin, J. Meroterpenoids from a Tropical *Dysidea* sp Sponge. *Journal of Natural Products, 78*(11), 2814-2821. (2015)

[46] Hentschel, U., Piel, J., Degnan, S.M. & Taylor, M.W. Genomic insights into the marine sponge microbiome. *Nature Reviews Microbiology, 10*(9), 641-U675. (2012)

[47] Laport, M.S., Santos, O.C.S. & Muricy, G. Marine Sponges: Potential Sources of New Antimicrobial Drugs. *Current Pharmaceutical Biotechnology, 10*(1), 86-105. (2009)

[48] Leys, S.P. & Hill, A. (2012). The Physiology and Molecular Biology of Sponge Tissues. In: Becerro, Uriz, Maldonado & Turon (Eds.), *Advances in Marine Biology* (Vol. 62, pp. 1-56): Academic Press.

[49] Taylor, M.W., Radax, R., Steger, D. & Wagner, M. Sponge-associated microorganisms: Evolution, ecology, and biotechnological potential. *Microbiology and Molecular Biology Reviews, 71*(2). (2007)

[50] Bergquist, P.R. (1970). Sponges. (Hutchinson: London, University of California Press, Berkeley & Los Angeles): 1-268.

[51] Van Soest, R. W. M., Boury-Esnault, N., Vacelet, J., Dohrmann, M., Erpenbeck, D., De Voogd, N.J., Santodomingo, N., Vanhoorne, B., Kelly, M. & Hooper, J.N.A. Global Diversity of Sponges (*Porifera*). *Plos One, 7*(4), e35105. (2012)

[52] WPD. (2017). World Porifera Database. Retrieved November 3rd, 2018

[53] Reiswig, H.M. (2002). Class *Hexactinellida* Schmidt, 1870. In Hooper, Van Soest & Willenz (Eds.), *Systema Porifera: A Guide to the Classification of Sponges* (pp. 15-51). Boston, MA: Springer US.

[54] Manuel, M., Borojevic, R., Boury-Esnault, N., & Vacelet, J. (2002). Class *Calcarea* Bowerbank, 1864. In Hooper, Van Soest & Willenz (Eds.), *Systema Porifera: A Guide to the Classification of Sponges* (pp. 15-51). Boston, MA: Springer US.

[55] Hooper, J.N.A. & Van Soest, R.W.M. (2002). Class *Demospongiae* Sollas, 1885. In Hooper, Van Soest & Willenz (Eds.), *Systema Porifera: A Guide to the Classification of Sponges* (pp. 15-51). Boston, MA: Springer US.

[56] Vacelet, J. & Donadey, C. Electron microscope study of the association between some sponges and bacteria. *Journal of Experimental Marine Biology and Ecology, 30*(3), 301-314. (1977)

[57] Wilkinson, C.R. Microbial associations in sponges. II. Numerical analysis of sponge and water bacterial populations. *Marine Biology, 49*(2), 169-176. (1978)

[58] Wilkinson, C.R. Nutrient translocation from green algal symbionts to the freshwater sponge *Ephydatia fluviatilis*. *Hydrobiologia, 75*(3), 241-250. (1980)

[59] Wilkinson, C.R., Nowak, M., Austin, B. & Colwell, R.R. Specificity of bacterial symbionts in Mediterranean and Great Barrier Reef sponges. *Microbial Ecology, 7*(1), 13-21. (1981)

[60] Lee, O.O. & Qian, P.Y. Chemical Control of Bacterial Epibiosis and Larval Settlement of *Hydroides elegans* in the Red Sponge *Mycale adherens*. *Biofouling, 19*, 171-180. (2003)

[61] Thakur, N.L., Anil, A.C. & Muller, W.E.G. Culturable epibacteria of the marine sponge *Ircinia fusca*: temporal variations and their possible role in the epibacterial defense of the host. *Aquatic Microbial Ecology, 37*(3), 295-304. (2004)

[62] Hentschel, U., Usher, K. M. & Taylor, M.W. Marine sponges as microbial fermenters. *FEMS Microbiology Ecology, 55*(2), 167-177. (2006)

[63] Webster, N. S. & Thomas, T. The Sponge Hologenome. *Mbio, 7*(2), e00135-00116. (2016)

[64] Erwin, P. M., Pita, L., López-Legentil, S. & Turon, X. Stability of Sponge-Associated Bacteria over Large Seasonal Shifts in Temperature and Irradiance. *Applied and Environmental Microbiology, 78*(20), 7358-7368. (2012)

[65] Gloeckner, V., Wehrl, M., Moitinho-Silva, L., Gernert, G., Schupp, P., Pawlik, J.R., Lindquist, N.L., Erpenbeck, D., Wörheide, G. & Hentschel, U. The HMA-LMA Dichotomy Revisited: an Electron Microscopical Survey of 56 Sponge Species. *The Biological Bulletin, 227*(1), 78-88. (2014)

[66] Amann, R.I., Ludwig, W. & Schleifer, K. H. Phylogenetic identification and *in situ* detection of individual microbial cells without cultivation. *Microbiological Reviews, 59*(1), 143-169. (1995)

[67] Althoff, K., Schütt, C., Steffen, R., Batel, R. & Müller, W.E.G. Evidence for a symbiosis between bacteria of the genus *Rhodobacter* and the marine sponge *Halichondria panicea*: harbor also for putatively toxic bacteria? *Marine Biology, 130*(3), 529-536. (1998)

[68] Pedrós-Alió, C. The Rare Bacterial Biosphere. *Annual Review of Marine Science, 4*(1), 449-466. (2012)

[69] Hentschel, U., Hopke, J., Horn, M., Friedrich, A.B., Wagner, M., Hacker, J. & Moore, B.S. Molecular Evidence for a Uniform Microbial Community in Sponges from Different Oceans. *Applied and Environmental Microbiology, 68*(9), 4431-4440. (2002)

[70] Fieseler, L., Horn, M., Wagner, M. & Hentschel, U. Discovery of the Novel Candidate Phylum "Poribacteria" in Marine Sponges. *Applied and Environmental Microbiology, 70*(6), 3724-3732. (2004)

[71] Schmitt, S., Tsai, P., Bell, J., Fromont, J., Ilan, M.,Lindquist, N., Perez, T., Rodrigo, A., Schupp, P.J., Vacelet, J., Webster, N., Hentschel, U. & Taylor, M.W. Assessing the complex sponge microbiota: core, variable and species-specific bacterial communities in marine sponges. *The Isme Journal, 6*, 564. (2011)

[72] Webster, N.S., Taylor, M.W., Behnam, F., Lücker, S., Rattei, T., Whalan, S., Horn, M. & Wagner, M. Deep sequencing reveals exceptional diversity and modes of transmission for bacterial sponge symbionts. *Environmental Microbiology, 12*(8), 2070-2082. (2010)

[73] Steinert, G., Gutleben, J., Atikana, A., Wijffels, R.H., Smidt, H. & Sipkema, D. Coexistence of poribacterial phylotypes among geographically widespread and phylogenetically divergent sponge hosts. *Environmental Microbiology Reports, 10*(1), 80-91. (2018)

[74] Amsler, C.D., Moeller, C.B., McClintock, J.B., Iken, K.B. & Baker, B.J. Chemical defenses against diatom fouling in Antarctic marine sponges. *Biofouling, 16*(1), 29-45. (2000)

[75] Bavestrello, G., Arillo, A., Calcinai, B., Cattaneo-Vietti, R., Cerrano, C., Gaino, E., Penna, A. & Sara, M. Parasitic diatoms inside antarctic sponges. *Biological Bulletin, 198*(1), 29-33. (2000)

[76] Rozas, E.E., Albano, R.M., Lôbo-Hajdu, G., Müller, W.E.G., Schröder, H.C. & Custódio, M.R. Isolation and cultivation of fungal strains from *in vitro* cell cultures of two marine sponges (Porifera: *Halichondrida* and *Haplosclerida*). *Brazilian Journal of Microbiology, 42*, 1560-1568. (2011)

[77] Wiese, J., Ohlendorf, B., Blümel, M., Schmaljohann, R. & Imhoff, J.F. Phylogenetic Identification of Fungi Isolated from the Marine Sponge *Tethya aurantium* and Identification of Their Secondary Metabolites. *Marine Drugs, 9*(4), 561-585. (2011)

[78] Höller, U., Wright, A.D., Matthee, G.F., Konig, G.M., Draeger, S., Aust, H.J. & Schulz, B. Fungi from marine sponges: diversity, biological activity and secondary metabolites. *Mycological Research, 104*(11), 1354-1365. (2000)

[79] Kerr, R.G. & Kerr, S.S. Marine natural products as therapeutic agents. *Expert Opinion on Therapeutic Patents, 9*(9), 1207-1222. (1999)

[80] Penesyan, A., Kjelleberg, S. & Egan, S. Development of Novel Drugs from Marine Surface Associated Microorganisms. *Marine Drugs, 8*(3), 438-459. (2010)

[81] Wang, H., Fewer, D.P., Holm, L., Rouhiainen, L. & Sivonen, K. Atlas of nonribosomal peptide and polyketide biosynthetic pathways reveals common occurrence of nonmodular enzymes. *Proceedings of the National Academy of Sciences of the United States of America, 111*(25), 9259-9264. (2014)

[82] Bewley, C.A. & Faulkner, D.J. *Lithistid* sponges: Star performers or hosts to the stars. *Angewandte Chemie-International Edition, 37*(16), 2163-2178. (1998)

[83] Wakimoto, T., Egami, Y., Nakashima, Y., Wakimoto, Y., Mori, T., Awakawa, T., Ito, T., Kenmoku, H., Asakawa, Y., Piel, J. & Abe, I. Calyculin biogenesis from a pyrophosphate protoxin produced by a sponge symbiont. *Nature Chemical Biology, 10*, 648. (2014)

[84] Leal, M.C., Puga, J., Serodio, J., Gomes, N.C.M. & Calado, R. Trends in the Discovery of New Marine Natural Products from Invertebrates over the Last Two Decades - Where and What Are We Bioprospecting? *Plos One, 7*(1). (2012)

[85] Agrawal, S., Adholeya, A. & Deshmukh, S. K. The Pharmacological Potential of Non-ribosomal Peptides from Marine Sponge and Tunicates. *Frontiers in Pharmacology, 7*, 333. (2016)

[86] Ebada, S. & Proksch, P. (2012). The Chemistry of Marine Sponges. In Fattorusso, E., Gerwick, W.H. & Taglialatela-Scafati, O. (Eds.), *Handbook of Marine Natural Products* (pp. 191-293). Dordrecht: Springer Netherlands.

[87] Matsunaga, S., Fusetani, N. & Konosu, S. Bioactive Marine Metabolites, IV. Isolation and the Amino Acid Composition of Discodermin A, an Antimicrobial Peptide, from the Marine Sponge *Discodermia kiiensis*. *Journal of Natural Products, 48*(2), 236-241. (1985)

[88] Li, H., Matsunaga, S. & Fusetani, N. Halicylindramides A-C, antifungal and cytotoxic depsipeptides from the marine sponge *Halichondria cylindrata*. *Journal of Medicinal Chemistry, 38*(2), 338-343. (1995)

[89] Li, H., Matsunaga, S., & Fusetani, N. Halicylindramides D and E, Antifungal Peptides from the Marine Sponge *Halichondria cylindrata*. *Journal of Natural Products, 59*(2), 163-166. (1996)

[90] Hahn, D., Kim, H., Yang, I., Chin, J., Hwang, H., Won, D.H., Lee, B., Nam, S., Ekins, Me., Choi, H. & Kang, H. The Halicylindramides, Farnesoid X Receptor Antagonizing Depsipeptides from a *Petrosia* sp. Marine Sponge Collected in Korea. *Journal of Natural Products, 79*(3), 499-506. (2016)

[91] Fusetani, N., Sugawara, T., Matsunaga, S. & Hirota, H. Orbiculamide A: a novel cytotoxic cyclic peptide from a marine sponge *Theonella* sp. *Journal of the American Chemical Society, 113*(20), 7811-7812. (1991)

[92] Carroll, A.R., Pierens, G.K., Fechner, G., de Almeida, P.L., Ngo, A., Simpson, M., Hyde, E., Hooper, J.N.A., Boström, S.L., Musil, D. & Quinn, R.J. Dysinosin A: A Novel Inhibitor of Factor VIIa and Thrombin from a New Genus and Species of Australian Sponge of the Family *Dysideidae*. *Journal of the American Chemical Society, 124*(45), 13340-13341. (2002)

[93] Ishida, K., Okita, Y., Matsuda, H., Okino, T. & Murakami, M. Aeruginosins, protease inhibitors from the cyanobacterium *Microcystis aeruginosa*. *Tetrahedron, 55*(36), 10971-10988. (1999)

[94] Espiritu, R.A., Cornelio, K., Kinoshita, M., Matsumori, N., Murata, M., Nishimura, S., Kakeya, H., Yoshida, M. & Matsunaga, S. Marine sponge cyclic peptide theonellamide A disrupts lipid bilayer integrity without forming distinct membrane pores. *Biochimica et Biophysica Acta (BBA) - Biomembranes, 1858*(6), 1373-1379. (2016)

[95] Matsunaga, S., Fusetani, N., Hashimoto, K. & Walchli, M. Theonellamide F. A novel antifungal bicyclic peptide from a marine sponge *Theonella* sp. *Journal of the American Chemical Society, 111*(7), 2582-2588. (1989)

[96] Randazzo, A., Dal Piaz, F., Orrù, S., Debitus, C., Roussakis, C., Pucci, P. & Gomez-Paloma, L. Axinellins A and B: New Proline-Containing Antiproliferative Cyclopeptides from the Vanuatu Sponge Axinella *carteri*. *European Journal of Organic Chemistry, 1998*(11), 2659-2665. (1998)

[97] Abu-Gharbieh, E., Vasina, V., Poluzzi, E., & De Ponti, F. Antibacterial macrolides: a drug class with a complex pharmacological profile. *Pharmacological Research, 50*(3), 211-222. (2004)

[98] Gunasekera, S.P., Gunasekera, M., Longley, R.E. & Schulte, G.K. Discodermolide: a new bioactive polyhydroxylated lactone from the marine sponge *Discodermia dissoluta*. *The Journal of Organic Chemistry, 55*(16), 4912-4915. (1990)

[99] Smith, A.B. & Freeze, B.S. (+)-Discodermolide: Total Synthesis, Construction of Novel Analogues, and Biological Evaluation. *Tetrahedron, 64*(2), 261-298. (2007)

[100] Mita, A., Lockhart, A.C., Chen, T.L., Bochinski, K., Curtright, J., Cooper, W., Hammond, L., Rothenberg, M., Rowinsky, E. & Sharma, S. A phase I pharmacokinetic (PK) trial of XAA296A (Discodermolide) administered every 3 wks to adult patients with advanced solid malignancies. *Journal of Clinical Oncology, 22*(14), 133s-133s. (2004)

[101] Jogalekar, A.S., Kriel, F.H., Shi, Q., Cornett, B., Cicero, D. & Snyder, J.P. The Discodermolide Hairpin Structure Flows from Conformationally Stable Modular Motifs. *Journal of Medicinal Chemistry, 53*(1), 155-165. (2010)

[102] Carmely, S. & Kashman, Y. Structure of swinholide-a, a new macrolide from the marine sponge *Theonella swinhoei*. *Tetrahedron Letters, 26*(4), 511-514. (1985)

[103] Kobayashi, M., Tanaka, J., Katori, T., Matsuura, M., & Kitagawa, I. Structure of swinholide A, a potent cytotoxic macrolide from the Okinawan marine sponge *Theonella Swinhoei*. *Tetrahedron Letters, 30*(22), 2963-2966. (1989)

[104] Andrianasolo, E.H., Gross, H., Goeger, D., Musafija-Girt, M., McPhail, K., Leal, R.M., Mooberry, S.L. & Gerwick, W.H. Isolation of Swinholide A and Related Glycosylated Derivatives from Two Field Collections of Marine Cyanobacteria. *Organic Letters, 7*(7), 1375-1378. (2005)

[105] Piel, J., Hui, D., Wen, G., Butzke, D., Platzer, M., Fusetani, N. & Matsunaga, S. Antitumor polyketide biosynthesis by an uncultivated bacterial symbiont of the marine sponge *Theonella swinhoei*. *Proceedings of the National Academy of Sciences of the United States of America, 101*(46), 16222-16227. (2004)

[106] Fisch, K.M., Gurgui, C., Heycke, N., van der Sar, S.A., Anderson, S.A., Webb, V.L., Taudien, S., Platzer, M., Rubio, B.K., Robinson, S.J., Crews, P. & Piel, J. Polyketide assembly lines of uncultivated sponge symbionts from structure-based gene targeting. *Nature Chemical Biology, 5*, 494. (2009)

[107] Sakai, R., Higa, T., Jefford, C.W. & Bernardinelli, G. Manzamine A, a novel antitumor alkaloid from a sponge. *Journal of the American Chemical Society, 108*(20), 6404-6405. (1986)

[108] Kim, C.K., Riswanto, R., Won, T.H., Kim, H., Elya, B., Sim, C.J., Oh, D.C., Oh, K.B. & Shin, J. Manzamine Alkaloids from an *Acanthostrongylophora* sp. Sponge. *Journal of Natural Products, 80*(5), 1575-1583. (2017)

[109] Braekman, J.C., Daloze, D., Stoller, C. & Van Soest, R.W.M. Chemotaxonomy of *Agelas* (Porifera: Demospongiae). *Biochemical Systematics and Ecology, 20*(5), 417-431. (1992)

[110] Lindel, T., Hoffmann, H., Hochgürtel, M. & Pawlik, J.R. Structure–Activity Relationship of Inhibition of Fish Feeding by Sponge-derived and Synthetic Pyrrole–Imidazole Alkaloids. *Journal of Chemical Ecology, 26*(6), 1477-1496. (2000)

[111] Edrada, R.A., Proksch, P., Wray, V., Witte, L., Müller, W.E.G. & Van Soest, R.W.M. Four New Bioactive Manzamine-Type Alkaloids from the Philippine Marine Sponge *Xestospongia ashmorica*. *Journal of Natural Products, 59*(11), 1056-1060. (1996)

[112] Martinez, A., Castro, A., Dorronsoro, I. & Alonso, M. Glycogen synthase kinase 3 (GSK-3) inhibitors as new promising drugs for diabetes, neurodegeneration, cancer, and inflammation. *Medicinal Research Reviews, 22*(4), 373-384. (2002)

[113] Walker, R.P., Faulkner, D.J., Van Engen, D. & Clardy, J. Sceptrin, an antimicrobial agent from the sponge *Agelas sceptrum*. *Journal of the American Chemical Society, 103*(22), 6772-6773. (1981)

[114] Keifer, P.A., Schwartz, R.E., Koker, M.E.S., Hughes, R.G., Rittschof, D. & Rinehart, K.L. Bioactive bromopyrrole metabolites from the Caribbean sponge *Agelas conifera*. *The Journal of Organic Chemistry, 56*(9), 2965-2975. (1991)

[115] Rosa, R., Silva, W., de Motta, G.E., Rodríguez, A.D., Morales, J.J & Ortiz, M. Anti-muscarinic activity of a family of C11N5 compounds isolated from *Agelas* sponges. *Experientia, 48*(9), 885-887. (1992)

[116] Fattorusso, E., Minale, L. & Sodano, G. Aeroplysinin-1, an antibacterial bromo-compound from the sponge *Verongia aerophoba*. *Journal of the Chemical Society, Perkin Transactions 1*(0), 16-18. (1972)

[117] Quiñoà, E. & Crews, P. Phenolic constituents of *Psammaplysilla*. *Tetrahedron Letters, 28*(28), 3229-3232. (1987)

[118] Rodriguez, A.D., Akee, R.K. & Scheuer, P.J. Two bromotyrosine-cysteine derived metabolites from a sponge. *Tetrahedron Letters, 28*(42), 4989-4992. (1987)

[119] Hernández-Guerrero, C.J., Zubía, E., Ortega, M.J. & Carballo, J.L. Cytotoxic dibromotyrosine-derived metabolites from the sponge *Aplysina gerardogreeni*. *Bioorganic & Medicinal Chemistry, 15*(15), 5275-5282. (2007)

[120] Kobayashi, J., Honma, K., Sasaki, T., & Tsuda, M. Purealidins J-R, New Bromotyrosine Alkaloids from the Okinawan Marine Sponge *Psammaplysilla purea*. *Chemical & Pharmaceutical Bulletin, 43*(3), 403-407. (1995)

[121] Ishibashi, M., Tsuda, M., Ohizumi, Y., Sasaki, T. & Kobayashi, J. Purealidin A, a new cytotoxic bromotyrosine-derived alkaloid from the Okinawan marine sponge *Psammaplysilla purea*. *Experientia, 47*(3), 299-300. (1991)

[122] Tilvi, S., Rodrigues, C., Naik, C.G., Parameswaran, P.S. & Wahidhulla, S. New bromotyrosine alkaloids from the marine sponge *Psammaplysilla purpurea*. *Tetrahedron, 60*(45), 10207-10215. (2004)

[123] Kazlauskas, R., Lidgard, R.O., Murphy, P.T. & Wells, R.J. Brominated tyrosine-derived metabolites from the sponge *Ianthella basta*. *Tetrahedron Letters, 21*(23), 2277-2280. (1980)

[124] Carney, J.R., Scheuer, P.J. & Kelly-Borges, M. A New Bastadin from the Sponge *Psammaplysilla purpurea*. *Journal of Natural Products, 56*(1), 153-157. (1993)

[125] Greve, H., Kehraus, S., Krick, A., Kelter, G., Maier, A., Fiebig, H.H., Wright, A.D. & König, G.M. Cytotoxic Bastadin 24 from the Australian Sponge *Ianthella quadrangulata*. *Journal of Natural Products, 71*(3), 309-312. (2008)

[126] de Silva, E.D. & Scheuer, P.J. Manoalide, an antibiotic sesterterpenoid from the marine sponge *luffariella variabilis* (polejaeff). *Tetrahedron Letters, 21*(17), 1611-1614. (1980)

[127] Ebada, S. S., Lin, W. & Proksch, P. Bioactive Sesterterpenes and Triterpenes from Marine Sponges: Occurrence and Pharmacological Significance. *Marine Drugs, 8*(2), 313-346. (2010)

[128] Lombardo, D. & Dennis, E. A. Cobra Venom Phospholipase-A2 Inhibition by Manoalide - a Novel Type of Phospholipase Inhibitor. *Journal of Biological Chemistry, 260*(12), 7234-7240. (1985)

[129] Albizati, K. F., Holman, T., Faulkner, D. J., Glaser, K. B., & Jacobs, R. S. Luffariellolide, an anti-inflammatory sesterterpene from the marine sponge *Luffariella* sp. *Experientia, 43*(8), 949-950. (1987)

[130] Chang, Y.C., Tseng, S.W., Liu, L.L., Chou, Y., Ho, Y.S., Lu, M.C. & Su, J.H. Cytotoxic Sesterterpenoids from a Sponge *Hippospongia* sp. *Marine Drugs, 10*(5), 987-997. (2012)

[131] Charan, R. D., McKee, T. C., & Boyd, M. R. Thorectandrols A and B, New Cytotoxic Sesterterpenes from the Marine Sponge *Thorectandra* Species. *Journal of Natural Products, 64*(5), 661-663. (2001)

[132] Gomez Paloma, L., Randazzo, A., Minale, L., Debitus, C. & Roussakis, C. New cytotoxic sesterterpenes from the New Caledonian marine sponge Petrosaspongia nigra (Bergquist). *Tetrahedron, 53*(30), 10451-10458. (1997)

[133] Kobayashi, J. i., Yuasa, K., Kobayashi, T., Sasaki, T., & Tsuda, M. Jaspiferals A - G, new cytotoxic isomalabaricane-type nortriterpenoids from Okinawan marine sponge *Jaspis stellifera*. *Tetrahedron, 52*(16), 5745-5750. (1996)

[134] Jakupovic, J., Eid, F., Bohlmann, F., & El-Dahmy, S. Malabaricane derivatives from *Pyrethrum santolinoides*. *Phytochemistry, 26*(5), 1536-1538. (1987)

[135] Carmely, S., Roll, M., Loya, Y. & Kashman, Y. The Structure of Eryloside A, a New Antitumor and Antifungal 4-Methylated Steroidal Glycoside from the Sponge *Erylus lendenfeldi*. *Journal of Natural Products, 52*(1), 167-170. (1989)

[136] Davidson, B.S. New dimensions in natural products research: cultured marine microorganisms. *Current Opinion in Biotechnology, 6*(3), 284-291. (1995)

[137] Montaser, R. & Luesch, H. Marine natural products: a new wave of drugs? *Future medicinal chemistry, 3*(12), 1475-1489. (2011)

[138] Cárdenas, P., Rapp, H.T., Klitgaard, A.B., Best, M., Thollesson, M. & Tendal, O.S. Taxonomy, biogeography and DNA barcodes of *Geodia* species (Porifera, Demospongiae, Tetractinellida) in the Atlantic boreo-arctic region, *Zoological Journal of the Linnean Society*, 169(2) 251-311. (2013)

[139] Soldatou, S. & Baker, B.J., Cold-water marine natural products, 2006 to 2016, *Natural product reports*, 34(6) 585-626. (2017)

[140] Lidgren, G., Bohlin, L. & Bergman, J., Studies of swedish marine organisms VII. A novel biologically active indole alkaloid from the sponge *Geodia baretti*, Tetrahedron Letters, 27(28) 3283-3284. (1986)

[141] Olsen, E.K., Soderholm, K.L., Isaksson, J., Andersen, J.H. & Hansen, E. Metabolomic Profiling Reveals the N-Acyl-Taurine Geodiataurine in Extracts from the Marine Sponge *Geodia macandrewii* (Bowerbank), *Journal of Natural Products*, 79(5) 1285-1291. (2016)

[142] Van Soest, R. *Acanthodendrilla australis* Bergquist, 1995, in, Van Soest, R.W.M; Boury-Esnault, N.; Hooper, J.N.A.; Rützler, K.; de Voogd, N.J.; Alvarez de Glasby, B.; Hajdu, E.; Pisera, A.B.; Manconi, R.; Schoenberg, C.; Klautau, M.; Picton, B.; Kelly, M.; Vacelet, J.; Dohrmann, M.; Díaz, M.-C.; Cárdenas, P.; Carballo, J. L., 2009.

[143] Sirimangkalakitti, N., Olatunji, O.J., Changwichit, K., Saesong, T., Chamni, S., Chanvorachote, P., Ingkaninan, K., Plubrukarn, A. & Suwanborirux, K. Bromotyrosine Alkaloids with Acetylcholinesterase Inhibitory Activity from the Thai Sponge *Acanthodendrilla* sp., *Natural Product Communications*, 10(11) 1945-1949. (2015)

[144] Sirimangkalakitti, N., Yokoya, M., Chamni, S., Chanvorachote, P., Plubrukrn, A., Saito, N. & Suwanborirux, K. Synthesis and Absolute Configuration of Acanthodendrilline, a New Cytotoxic Bromotyrosine Alkaloid from the Thai Marine Sponge *Acanthodendrilla* sp., *Chemical and Pharmaceutical Bulletin*, 64(3) 258-262. (2016)

[145] Van Soest, R. *Acanthostrongylophora Hooper*, 1984, in, Van Soest, R.W.M; Boury-Esnault, N.; Hooper, J.N.A.; Rützler, K.; de Voogd, N.J.; Alvarez, B.; Hajdu, E.; Pisera, A.B.; Manconi, R.; Schönberg, C.; Klautau, M.; Picton, B.; Kelly, M.; Vacelet, J.; Dohrmann, M.; Díaz, M.-C.; Cárdenas, P.; Carballo, J. L.; Ríos, P.; Downey, R. , 2018.

[146] Radwan, M., Hanora, A., Khalifa, S. & Abou-El-Ela, S.H. Manzamines, *Cell Cycle*, 11(9) 1765-1772. (2012)

[147] Ibrahim, S.R.M. & Mohamed, G.A. Ingenines C and D, new cytotoxic pyrimidine-*β*-carboline alkaloids from the Indonesian sponge *Acanthostrongylophora ingens*, *Phytochemistry Letters*, 18 168-171. (2016)

[148] Ibrahim, S.R.M. & Mohamed, G.A. Ingenine E, a new cytotoxic *β*-carboline alkaloid from the Indonesian sponge *Acanthostrongylophora ingens*, *Journal of Asian Natural Products Research*, 19(5) 504-509. (2017)

[149] Ibrahim, S.R.M., Mohamed, G., Al Haidari, R., El-Kholy, A. & Zayed, M. Ingenine F: A New Cytotoxic Tetrahydro Carboline Alkaloid from the Indonesian Marine Sponge *Acanthostrongylophora ingens*, *Pharmacognosy magazine*, 14(54) 231-234. (2018)

[150] Subramani, R. & Aalbersberg, W. Marine actinomycetes: An ongoing source of novel bioactive metabolites, *Microbiological Research*, 167(10) 571-580. (2012)

[151] Nakashima, N., Mitani, Y. & Tamura, T. Actinomycetes as host cells for production of recombinant proteins, *Microbial Cell Factories*, 4(1) 7. (2005)

[152] Jensen, P.R., Mincer, T.J., Williams, P.G. & Fenical, W. Marine actinomycete diversity and natural product discovery, *Antonie van Leeuwenhoek*, 87(1) 43-48. (2005)

[153] Manivasagan, P., Kang, K.H., Sivakumar, K., Li-Chan, E.C.Y., Oh, H.M. & Kim, S.K. Marine actinobacteria: An important source of bioactive natural products, *Environmental Toxicology and Pharmacology*, 38(1) 172-188. (2014)

[154] Williams, P.G., Asolkar, R.N., Kondratyuk, T., Pezzuto, J.M., Jensen, P.R. & Fenical, W. Saliniketals A and B, Bicyclic Polyketides from the Marine Actinomycete *Salinispora arenicola*, *Journal of Natural Products*, 70(1) 83-88. (2007)

[155] Shin, H.J., Jeong, H.S., Lee, H.S., Park, S.K., Kim, H.M. & Kwon, H.J. Isolation and structure determination of streptochlorin, an antiproliferative agent from a marine-derived *Streptomyces* sp. 04DH110, Journal of microbiology and biotechnology, 17(8) 1403-1406. (2007)

[156] Riedlinger, J., Reicke, A., Zahner, H., Krismer, B., Bull, A.T., Maldonado, L.A., Ward, A.C., Goodfellow, M., Bister, B., Bischoff, D., Sussmuth, R.D. & Fiedler, H.P. Abyssomicins, inhibitors of the para-aminobenzoic acid pathway produced by the marine *Verrucosispora* strain AB-18-032, *Journal of Antibiotics*, 57(4) 271-279. (2004)

[157] Rath, J.P., Kinast, S. & Maier, M.E. Synthesis of the Fully Functionalized Core Structure of the Antibiotic Abyssomicin C, Organic Letters, 7(14) 3089-3092. (2005)

[158] Bucar, F., Wube, A. & Schmid, M. Natural product isolation-how to get from biological material to pure compounds. *Natural Product Reports, 30*(4), 525-545. (2013)

[159] Quinn, R.J (1988). Chemistry of Aqueous Marine Extracts: Isolation Techniques. In P. J. Scheuer (Ed.), *Bioorganic Marine Chemistry* (pp. 1-41). Berlin, Heidelberg: Springer Berlin Heidelberg.

[160] Perez-Victoria, I., Martin, J. & Reyes, F. Combined LC/UV/MS and NMR Strategies for the Dereplication of Marine Natural Products. *Planta Medica, 82*(9-10), 857-871. (2016)

[161] Bobzin, S.C., Yang, S. & Kasten, T.P. LC-NMR: a new tool to expedite the dereplication and identification of natural products. *Journal of Industrial Microbiology and Biotechnology, 25*(6), 342-345. (2000)

[162] Jaspars, M. Computer assisted structure elucidation of natural products using two-dimensional NMR spectroscopy. *Natural Product Reports, 16*(2), 241-248. (1999)

[163] Li, K., Chung-Davidson, Y.W., Bussy, U. & Li, W.M. Recent Advances and Applications of Experimental Technologies in Marine Natural Product Research. *Marine Drugs, 13*(5), 2694-2713. (2015)

[164] Bouslimani, A., Sanchez, L.M., Garg, N. & Dorrestein, P.C. Mass spectrometry of natural products: current, emerging and future technologies. *Natural Product Reports, 31*(6), 718-729. (2014)

[165] Shipovskov, S. & Reimann, C.T. Electrospray ionization mass spectrometry in enzymology: uncovering the mechanisms of two-substrate reactions. *Analyst, 132*(5), 397-402. (2007)

[166] Stroobant, V. & Hoffmann, E. (2007). *Mass spectrometry: principles and applications. 2nd ed.*

[167] Breton, R. C. & Reynolds, W. F. Using NMR to identify and characterize natural products. *Natural Product Reports, 30*(4), 501-524. (2013)

[168] Riccio, R., Bifulco, G., Cimino, P., Bassarello, C. & Gomez-Paloma, L. (2003). Stereochemical analysis of natural products. Approaches relying on the combination of NMR spectroscopy and computational methods *Pure and Applied Chemistry* (Vol. 75, pp. 295).

[169] Omarsdottir, S., Einarsdottir, E., Ogmundsdottir, H.M., Freysdottir, J., Olafsdottir, E.S., Molinski, T.F. Svavarsson, J. Biodiversity of benthic invertebrates and bioprospecting in Icelandic waters. *Phytochemistry Reviews, 12*(3), 517-529. (2013)

[170] Giddings, L.A. & Newman, D.J. (2015). Bioactive Compounds from Marine Extremophiles (pp. 1-124). Springer International Publishing.

[171] Kupchan, S.M., Britton, R.W., Ziegler, M.F. & Sigel, C.W. Bruceantin, a new potent antileukemic simaroubolide from *Brucea antidysenterica*. *The Journal of Organic Chemistry, 38*(1), 178-179. (1973)

[172] VanWagenen, B.C., Larsen, R., Cardellina, J.H., Randazzo, D., Lidert, Z. C. & Swithenbank, C. Ulosantoin, a potent insecticide from the sponge *Ulosa ruetzleri*. *The Journal of Organic Chemistry, 58*(2), 335-337. (1993)

[173] Papazisis, K.T., Geromichalos, G.D., Dimitriadis, K.A. & Kortsaris, A.H. Optimization of the sulforhodamine B colorimetric assay. *Journal of Immunological Methods, 208*(2), 151-158. (1997)

[174] Boyd, M.R. & Paull, K.D. Some practical considerations and applications of the national cancer institute in vitro anticancer drug discovery screen. *Drug Development Research, 34*(2), 91-109. (1995)

[175] Bonev, B., Hooper, J. & Parisot, J. Principles of assessing bacterial susceptibility to antibiotics using the agar diffusion method. *Journal of Antimicrobial Chemotherapy, 61*(6), 1295-1301. (2008)

[176] Urbatzka, R., Freitas, S., Palmeira, A., Almeida, T., Moreira, J., Azevedo, C., Afonso, C., Correia-da-Silva, M., Sousa, E., Pinto, M. & Vasconcelos, V. Lipid reducing activity and toxicity profiles of a library of polyphenol derivatives. *European Journal of Medicinal Chemistry, 151*, 272-284. (2018)

[177] Noinart, J., Buttachon, S., Dethoup, T., Gales, L., Pereira, J.A., Urbatzka, R., Freitas, S., Lee, M., Silva, A.M.S., Pinto, M.M.M., Vasconcelos, V. & Kijjoa, A. A New Ergosterol Analog, a New Bis-Anthraquinone and Anti-Obesity Activity of Anthraquinones from the Marine Sponge-Associated Fungus *Talaromyces stipitatus* KUFA 0207. *Marine Drugs, 15*(5), 139. (2017)

[178] ImageJ. (2018). Retrieved November 3rd, 2018, from https://imagej.nih.gov/ij/index.html

[179] Einarsdottir, E., Liu, H. B., Freysdottir, J., Gotfredsen, C. H., & Omarsdottir, S. Immunomodulatory N-acyl Dopamine Glycosides from the Icelandic Marine Sponge *Myxilla incrustans* Collected at a Hydrothermal Vent Site. *Planta Medica, 82*(9-10), 903-909. (2016)

[180] Kale, V., Freysdottir, J., Paulsen, B. S., Friðjónsson, Ó. H., Óli Hreggviðsson, G. & Omarsdottir, S. Sulphated polysaccharide from the sea cucumber *Cucumaria frondosa* affect maturation of human dendritic cells and their activation of allogeneic CD4(+) T cells in vitro. *Bioactive Carbohydrates and Dietary Fibre, 2*(2), 108-117. (2013)

[181] Einarsdottir, E., Magnusdottir, M., Astarita, G., Köck, M., Ögmundsdottir, H., Thorsteinsdottir, M., Rapp, H., Omarsdottir, S. & Paglia, G. Metabolic Profiling as a Screening Tool for Cytotoxic Compounds: Identification of 3-Alkyl Pyridine Alkaloids from Sponges Collected at a Shallow Water Hydrothermal Vent Site North of Iceland. *Marine Drugs, 15*(2), 52. (2017)

[182] Menna, M., Aiello, A., D'Aniello, F., Fattorusso, E. Imperatore, C., Luciano, P. & Vitalone, R. Further Investigation of the Mediterranean Sponge *Axinella polypoides*: Isolation of a New Cyclonucleoside and a New Betaine. *Marine Drugs, 10*(11), 2509-2518. (2012)

[183] Capon, R. J. & Trotter, N. S. N-3,5'-cycloxanthosine, the first natural occurrence of a cyclonucleoside. *Journal of Natural Products, 68*(11), 1689-1691. (2005)

[184] Zhao, H. Q., Wang, X., Li, H. M., Yang, B., Yang, H. J. & Huang, L. Characterization of nucleosides and nucleobases in natural *Cordyceps* by HILIC-ESI/TOF/MS and HILIC-ESI/MS. *Molecules, 18*(8), 9755-9769. (2013)

[185] Chen, J. H., Shi, Q., Wang, Y. L., Li, Z. Y. & Wang, S. Dereplication of Known Nucleobase and Nucleoside Compounds in Natural Product Extracts by Capillary Electrophoresis-High Resolution Mass Spectrometry. *Molecules, 20*(4), 5423-5437. (2015)

[186] Kaur, P. & O'Connor, P. B. Quantitative Determination of Isotope Ratios from Experimental Isotopic Distributions. *Analytical Chemistry, 79*(3), 1198-1204. (2007)

[187] Agena, M., Tanaka, C., Hanif, N., Yasumoto-Hirose, M. & Tanaka, J. New cytotoxic spongian diterpenes from the sponge *Dysidea* cf. *arenaria*. *Tetrahedron, 65*(7), 1495-1499. (2009)

[188] Harrigan, G.G., Goetz, G.H., Luesch, H., Yang, S. & Likos, J. Dysideaprolines A-F and barbaleucamides A-B, novel polychlorinated compounds from a *Dysidea* species. *Journal of Natural Products, 64*(9), 1133-1138. (2001)

[189] Jadulco, R., Brauers, G., Edrada, R.A., Ebel, R., Wray, V., Sudarsono, S. & Proksch, P. New metabolites from sponge-derived fungi *Curvularia lunata* and *Cladosporium herbarum*. *Journal of Natural Products, 65*(5), 730-733. (2002)

[190] Ankisetty, S. & Slattery, M. Antibacterial Secondary Metabolites from the Cave Sponge *Xestospongia* sp. *Marine Drugs, 10*(5), 1037-1043. (2012)

[191] Murray, A. P., Araya, E., Maier, M. S. & Seldes, A. M. Nucleosides and nucleobases from *Ophiactis asperula*, *Ophiacantha vivipara* and *Gorgonocephalus chilensis*. *Biochemical Systematics and Ecology, 30*(3), 259-262. (2002)

[192] Wang, B., Dong, J., Zhou, X.F., Lee, K.J., Huang, R.M., Zhang, S. & Liu, Y. H. Nucleosides from the Marine Sponge *Haliclona* sp. *Journal of Biosciences, 64*(1-2), 143-148. (2009)

[193] Patil, A. D., Freyer, A. J., Carte, B., Taylor, P. B., Johnson, R. K. & Faulkner, D. J. Haploscleridamine, a novel tryptamine-derived alkaloid from a sponge of the order *haplosclerida*: an inhibitor of cathepsin K. *Journal of Natural Products, 65*(4), 628-629. (2002)

[194] Yamada, K., Takeda, M. & Iwakuma, T. Asymmetric reduction of cyclic imines with chiral sodium acyloxyborohydrides. *Journal of the Chemical Society, Perkin Transactions 1*(0), 265-270. (1983)

[195] Wanner, M.J., van der Haas, R.N.S., de Cuba, K.R., van Maarseveen, J.H. & Hiemstra, H. Catalytic Asymmetric Pictet–Spengler Reactions via Sulfenyliminium Ions. *Angewandte Chemie International Edition, 46*(39), 7485-7487. (2007)

[196] Espinoza-Moraga, M., Petta, T., Vasquez-Vasquez, M., Laurie, V.F., Moraes, L. A.B., & Santos, L.S. Bioreduction of β-carboline imines to amines employing *Saccharomyces bayanus. Tetrahedron: Asymmetry, 21*(16), 1988-1992. (2010)

[197] Shankaraiah, N., da Silva, W.A., Andrade, C.K.Z. & Santos, L.S. Enantioselective total synthesis of (S)-(−)-quinolactacin B. *Tetrahedron Letters, 49*(27), 4289-4291. (2008)

[198] Moloudizargari, M., Mikaili, P., Aghajanshakeri, S., Asghari, M.H. & Shayegh, J. Pharmacological and therapeutic effects of *Peganum harmala* and its main alkaloids. *Pharmacognosy Reviews, 7*(14), 199-212. (2013)

[199] Alamri, S.A. & Mohamed, Z.A. Selective inhibition of toxic cyanobacteria by β-carboline-containing bacterium *Bacillus flexus* isolated from Saudi freshwaters. *Saudi Journal of Biological Sciences, 20*(4), 357-363. (2013)

[200] Bratchkova, A., Ivanova, V., Gousterova, A. & Laatsch, H. β-Carboline Alkaloid Constituents from a *Thermoactinomyces* sp. Strain Isolated from Livingston Island, Antarctica. *Biotechnology & Biotechnological Equipment, 26*(3), 3005-3009. (2012)

[201] Sakai, E., Kato, H., Rotinsulu, H., Fitje, L., Remy, M., de Voogd, N., Yokosawa, H. & Tsukamoto, S. Variabines A and B: new β-carboline alkaloids from the marine sponge *Luffariella variabilis. Journal of Natural Medicines, 68*(1), 215-219. (2014)

[202] Kernan, M. R., Cambie, R. C., & Bergquist, P. R. Chemistry of Sponges, IX. New Diterpenes from the Marine Sponge *Dictyodendrilla cavernosa. Journal of Natural Products, 53*(3), 724-727. (1990)

[203] Cimino, G., Derosa, D., Destefan.S, & Minale, L. Isoagatholactone, a Diterpene of a New Structural Type from Sponge *Spongia officinalis. Tetrahedron, 30*(5), 645-649. (1974)

[204] Cambie, R.C., Craw, P.A., Stone, M.J. & Bergquist, P.R. Chemistry of Sponges, IV. Spongian Diterpenes from *Hyatella intestinalis. Journal of Natural Products, 51*(2), 293-297. (1988)

[205] Searle, P.A., & Molinski, T.F. Isolation of Spongosine and 2'-Deoxyspongosine from a Western-Australian Sponge of the Order *Hadromerida (Tethyidae). Journal of Natural Products, 57*(10), 1452-1454. (1994)

[206] Ahmadi, P., Haruyama, T., Kobayashi, N., de Voogd, N.J. & Tanaka, J. Spongian Diterpenes from the Sponge *Hyattella* aff. *intestinalis. Chemical and Pharmaceutical Bulletin, 65*(9), 874-877. (2017)

[207] Lai, Y.Y., Lu, M.C., Wang, L.H., Chen, J.J., Fang, L.S., Wu, Y.C. & Sung, P.J. New Scalarane Sesterterpenoids from the Formosan Sponge *Ircinia felix. Marine Drugs, 13*(7), 4296. (2015)

[208] von Salm, J.L., Witowski, C.G., Fleeman, R.M., McClintock, J.B., Amsler, C.D., Shaw, L.N. & Baker, B.J. Darwinolide, a New Diterpene Scaffold That Inhibits Methicillin-Resistant *Staphylococcus aureus* Biofilm from the Antarctic Sponge *Dendrilla membranosa. Organic Letters, 18*(11), 2596-2599. (2016)

[209] Keyzers, R.A., Northcote, P.T. & Davies-Coleman, M.T. Spongian diterpenoids from marine sponges. *Natural Products Report, 23*(2), 321-334. (2006)

[210] Schmidt, N.G., Pavkov-Keller, T., Richter, N., Wiltschi, B., Gruber, K. & Kroutil, W. Biocatalytic Friedel–Crafts Acylation and Fries Reaction. *Angewandte Chemie International Edition, 56*(26), 7615-7619. (2017)

[211] Capon, R., Ghisalberti, E. & Jefferies, P. New aromatic sesquiterpenes from a *Halichondria* sp. *Australian Journal of Chemistry, 35*(12), 2583-2587. (1982)

[212] Miller, S.L., Tinto, W.F., McLean, S., Reynolds, W.F. & Yu, M. Bisabolane Sesquiterpenes from Barbadian *Pseudopterogorgia* spp. *Journal of Natural Products, 58*(7), 1116-1119. (1995)

[213] Davyt, D., Fernandez, R., Suescun, L., Mombru, A.W., Saldana, J., Dominguez, L., Fujii, M. T. & Manta, E. Bisabolanes from the red alga *Laurencia scoparia*. *Journal of Natural Products, 69*(7), 1113-1116. (2006)

[214] Wei, M.Y., Wang, C.Y., Liu, Q.A., Shao, C.L., She, Z.G. & Lin, Y.C. Five Sesquiterpenoids from a Marine-Derived Fungus *Aspergillus* sp Isolated from a Gorgonian *Dichotella gemmacea*. *Marine Drugs, 8*(4), 941-949. (2010)

[215] Yegdaneh, A., Putchakarn, S., Yuenyongsawad, S., Ghannadi, A. & Plubrukarn, A. 3-Oxoabolene and 1-Oxocurcuphenol, Aromatic Bisabolanes from the Sponge *Myrmekioderma* sp. *Natural Product Communications, 8*(10), 1355-1357. (2013)

[216] Wright, A.E., Pomponi, S.A., McConnell, O.J., Kohmoto, S. & McCarthy, P.J. (+)-Curcuphenol and (+)-Curcudiol, Sesquiterpene Phenols from Shallow and Deep Water Collections of the Marine Sponge *Didiscus flavus*. *Journal of Natural Products, 50*(5), 976-978. (1987)

[217] Li, H., Jiang, J., Liu, Z., Lin, S., Xia, G., Xia, X., Ding, B., He, L., Lu, Y. & She, Z. Peniphenones A–D from the Mangrove Fungus *Penicillium dipodomyicola* HN4-3A as Inhibitors of *Mycobacterium tuberculosis* Phosphatase MptpB. *Journal of Natural Products, 77*(4), 800-806. (2014)

[218] Gao, J., Li, Y., Xie, S., Zhang, A., Shi, X. & Zhang, W. Application of compound 2,4-dyhydroxyl-5-methyl-acetophenone separated and prepared with fermentation broth of *Polyporus picipes*. F. Z. Shenqing. (2009)

[219] Wafar, M., Venkataraman, K., Ingole, B., Ajmal Khan, S., & LokaBharathi, P. State of Knowledge of Coastal and Marine Biodiversity of Indian Ocean Countries. *Plos One, 6*(1), e14613. (2011)

[220] Outlook Report on the State of the Marine Biodiversity in the Pacific Islands Region, SPREP Library (2010).

[221] Proksch, P., Edrada, R., & Ebel, R. Drugs from the seas – current status and microbiological implications. *Applied Microbiology and Biotechnology, 59*(2), 125-134. (2002)

[222] Hegde, V., Patel, M., Horan, A., Gullo, V., Marquez, J., Gunnarsson, I., Gentile, F., Loebenberg, D., King, A., Puar, M. & Pramanik, A. Macrolactams: a novel class of antifungal antibiotics produced by *Actinomadura* spp. SCC 1776 and SCC 1777. *Journal of Antibiotics, 45*(5), 624-632. (1992)

[223] Ayers, S., Zink, D.L., Mohn, K., Powell, J.S., Brown, C.M., Murphy, T., Grund, A., Genilloud, O., Salazar, O., Thompson, D. & Singh, S.B. Anthelmintic Macrolactams from *Nonomuraea turkmeniaca* MA7364. *Journal of Natural Products, 70*(8), 1371-1373. (2007)

[224] Ayers, S., Zink, D.L., Powell, J.S., Brown, C.M., Grund, A., Genilloud, O., Salazar, O., Thompson, D. & Singh, S.B. Anthelmintic Macrolactams from *Nonomuraea turkmeniaca* MA7381. *Journal of Antibiotics, 61*(2), 59-62. (2008)

[225] Naruse, N., Konishi, M., Oki, T., Yoshinobu, I. & Kakisawa, H. Fluvirucins A1, A2, A1, A2, A3, A4 and A5, new antibiotics active against influenza a virus III. The stereochemistry and absolute configuration of fluvirucin A1. *Journal of Antibiotics, 44*(7), 756-761. (1991)

[226] Naruse, N., Tsuno, T., Sawada, Y., Konishi, M. & Oki, T. Fluvirucins A1, A2, B1, B2, B3, B4 and B5, new antibiotics active against influenza A virus II. Structure determination. *Journal of Antibiotics, 44*(7), 741-755. (1991)

[227] Hegde, V.R., Patel, M.G., Gullo, V.P., Horan, A.C., King, A.H., Gentile, F., Wagman, G.H., Puar, M.S. & Loebenberg, D.A. Novel macrolactam-disaccharide antifungal antibiotic. Taxonomy, fermentation, isolation, physico-chemical properties, structure elucidation and biological activity. *Journal of Antibiotics, 46*(7), 1109-1115. (1993)

[228] Llàcer, E., Urpí, F., & Vilarrasa, J. Efficient Approach to Fluvirucins B2−B5, Sch 38518, and Sch 39185. First Synthesis of their Aglycon, via CM and RCM Reactions. *Organic Letters, 11*(15), 3198-3201. (2009)

[229] Xu, Z., Johannes, C.W., Salman, S.S. & Hoveyda, A.H. Enantioselective Total Synthesis of Antifungal Agent Sch 38516. *Journal of the American Chemical Society, 118*(44), 10926-10927. (1996)

[230] Xu, Z., Johannes, C.W., Houri, A.F., La, D.S., Cogan, D.A., Hofilena, G.E. & Hoveyda, A.H. Applications of Zr-Catalyzed Carbomagnesation and Mo-Catalyzed Macrocyclic Ring Closing Metathesis in Asymmetric Synthesis. Enantioselective Total Synthesis of Sch 38516 (Fluvirucin B1). *Journal of the American Chemical Society, 119*(43), 10302-10316. (1997)

[231] Jansen, R., Mohr, K.I., Bernecker, S., Stadler, M. & Müller, R. Indothiazinone, an Indolyl Thiazolyl Ketone from a Novel Myxobacterium Belonging to the *Sorangiineae*. *Journal of Natural Products, 77*(4), 1054-1060. (2014)

[232] Hattori, H., Roesslein, J., Caspers, P., Zerbe, K., Miyatake-Ondozabal, H., Ritz, D., Rueedi, G. & Gademann, K. Total Synthesis and Biological Evaluation of the Glycosylated Macrocyclic Antibiotic Mangrolide A. *Angewandte Chemie International Edition, 57*(34), 11020-11024. (2018)

[233] Mahajan, G.B. & Balachandran, L. Antibacterial agents from actinomycetes - a review. *Frontiers in Bioscience (Elite Ed), 4*, 240-253. (2012)

[234] Jamison, M. T. (2013). *Mangrolide A, a novel marine derived polyketide with selective antibiotic activity.* (PhD), The University of Texas Southwestern Medical Center at Dallas, Dallas, Texas.

[235] Fukami, A., Nakamura, T., Kawaguchi, K., Rho, M.C., Matsumoto, A., Takahashi, Y., Shiomi, K.. Hayashi, M., Komiyama, K. & Omura, S.. A new antimicrobial antibiotic from *Actinoplanes capillaceus* sp. K95-5561T. *Journal of Antibiotics (Tokyo), 53*(10), 1212-1214. (2000)

[236] Stone, M.J. & Williams, D.H. On the evolution of functional secondary metabolites (natural products). *Molecular Microbiology, 6*(1), 29-34. (1992)

[237] Bentley, S.D., Chater, K.F., Cerdeno-Tarraga, A.M., Challis, G.L., Thomson, N.R., James, K.D., Harris, D.E., Quail, M.A., Kieser, H., Harper, D., Bateman, A., Brown, S., Chandra, G., Chen, C.W., Collins, M., Cronin, A., Fraser, A., Goble, A., Hidalgo, J., Hornsby, T., Howarth, S., Huang, C.H., Kieser, T., Larke, L.,Murphy, L., Oliver, K., O'Neil, S., Rabbinowitsch, E., Rajandream, M.A., Rutherford, K., Rutter, S., Seeger, K., Saunders, D., Sharp, S., Squares, R., Squares, S., Taylor, K., Warren, T., Wietzorrek, A., Woodward, J., Barrell, B. G., Parkhill, J. & Hopwood, D.A. Complete genome sequence of the model actinomycete *Streptomyces coelicolor* A3(2). *Nature, 417*(6885), 141-147. (2002)

[238] Sosio, M., Bossi, E., Bianchi, A. & Donadio, S. Multiple peptide synthetase gene clusters in Actinomycetes. *Molecular & General Genetics, 264*(3), 213-221. (2000)

[239] O'Brien, P.J. Molecular mechanisms of quinone cytotoxicity. *Chemico-Biological Interactions, 80*(1), 1-41. (1991)

[240] Nandi, S., Vracko, M. & Bagchi, M.C. Anticancer activity of selected phenolic compounds: QSAR studies using ridge regression and neural networks. *Chemical Biology & Drug Design, 70*(5), 424-436. (2007)

[241] Hegde, V.R., Patel, M.G., Gullo, V.P., Ganguly, A.K., Sarre, O., Puar, M.S. & McPhail, A.T. Macrolactams: a new class of antifungal agents. *Journal of the American Chemical Society, 112*(17), 6403-6405. (1990)

[242] Mazzei, T., Mini, E., Novelli, A. & Periti, P. Chemistry and mode of action of macrolides. *Journal of Antimicrobial Chemotherapy, 31:* 1-9. (1993)

[243] Debrabander, J. (2015). USA Patent No. PCT/US2015/030621

[244] Xue, D.Q., Liu, H.L., Chen, S.H., Mollo, E., Gavagnin, M., Li, J., Li, X.W. & Guo, Y.W. 5-Alkylpyrrole-2-carboxaldehyde derivatives from the Chinese sponge *Mycale lissochela* and their PTP1B inhibitory activities. *Chinese Chemical Letters, 28*(6), 1190-1193. (2017)

[245] Yun, J.W. Possible anti-obesity therapeutics from nature – A review. *Phytochemistry, 71*(14), 1625-1641. (2010)

Appendixes
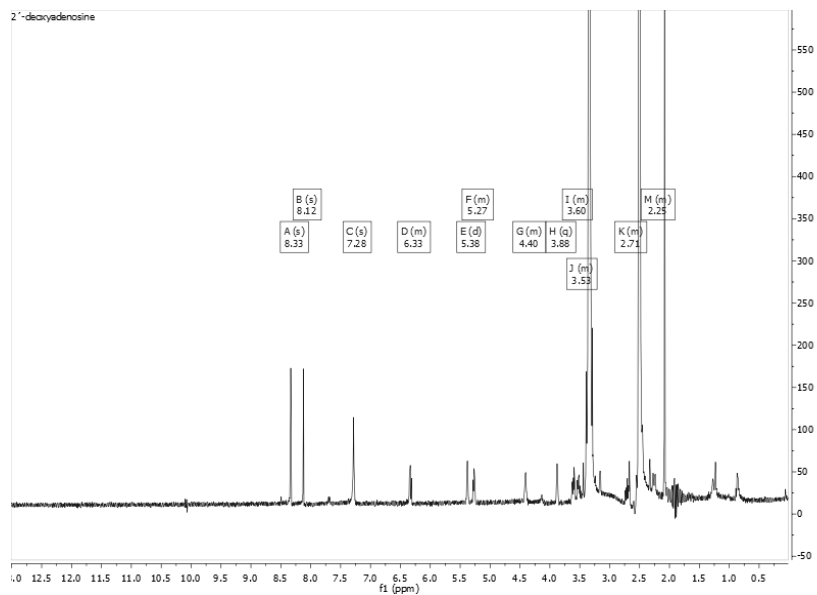
Appendix 1 - ^{1}H-NMR spectrum for 2´-deoxyadenosine (**1**) (400 MHz, DMSO-d_6).
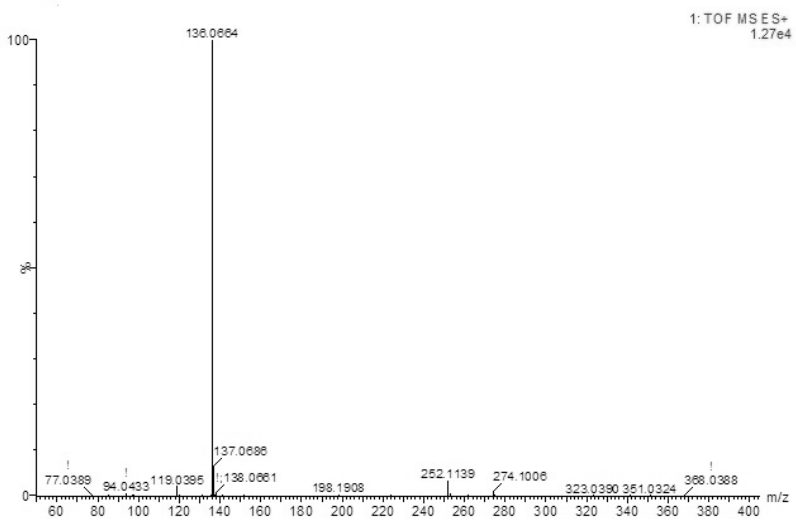
Appendix 2 - HRESIMS spectrum for 2´-deoxyadenosine (**1**).
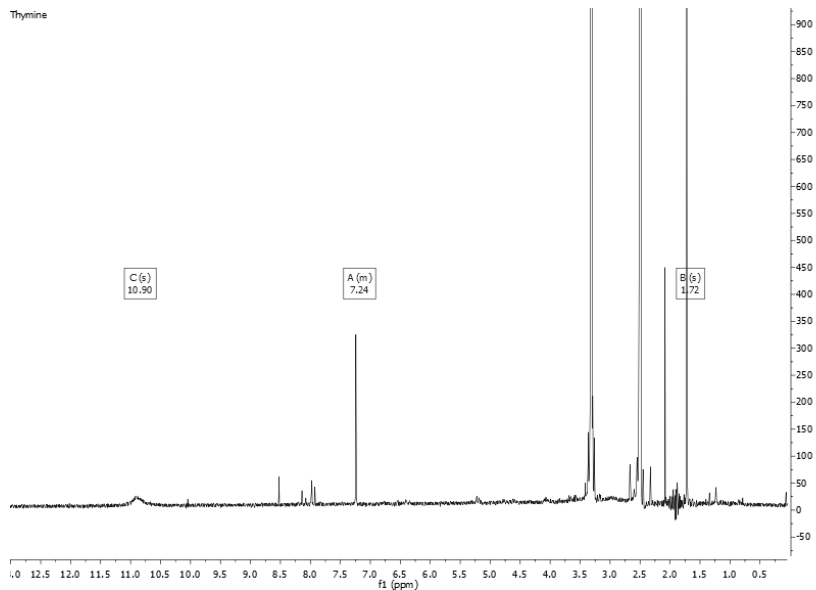
Appendix 3 - ¹H-NMR spectrum for thymine (**2**) (400 MHz, DMSO-*d₆*).
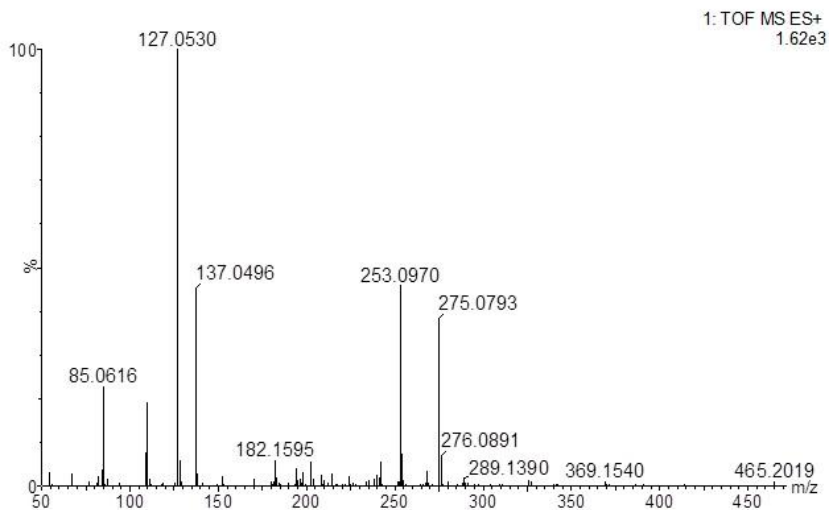
Appendix 4 - HRESIMS spectrum for thymine (**2**).
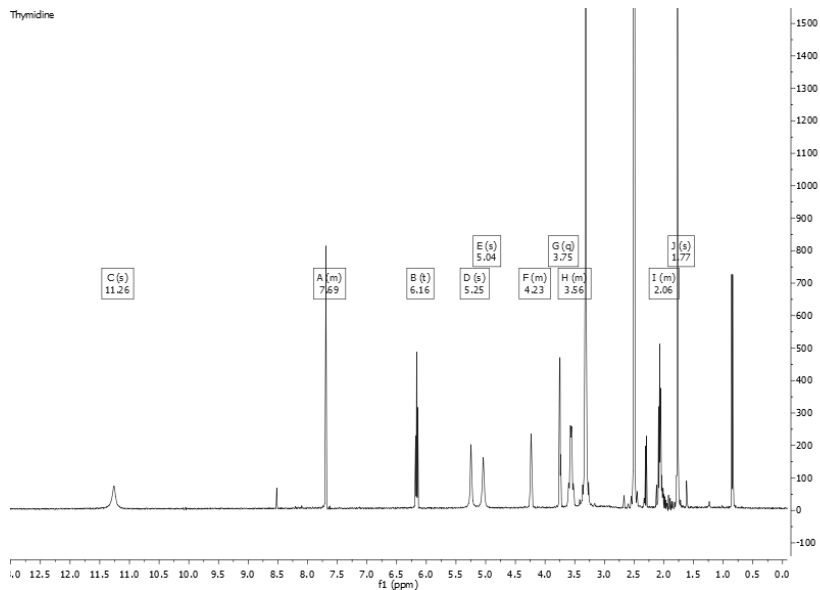
Appendix 5 - ¹H-NMR spectrum for thymidine (**3**) (400 MHz, DMSO-*d₆*).
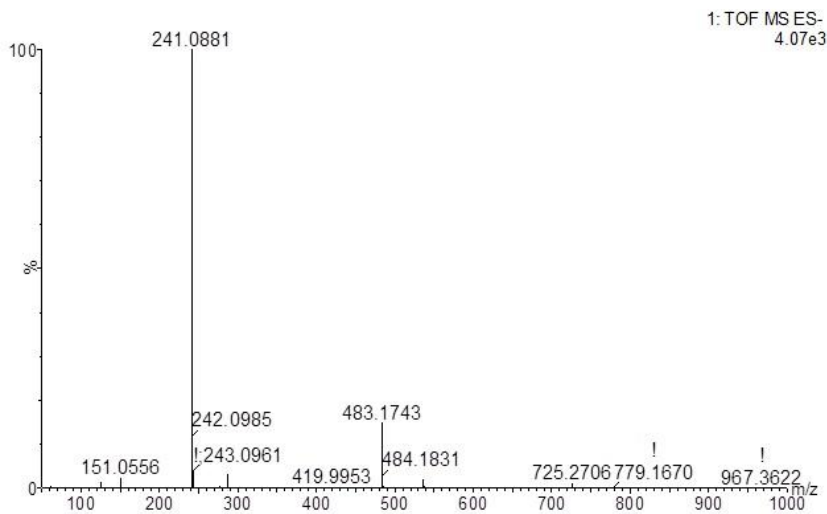
Appendix 6 - HRESIMS spectrum for thymidine (**3**).
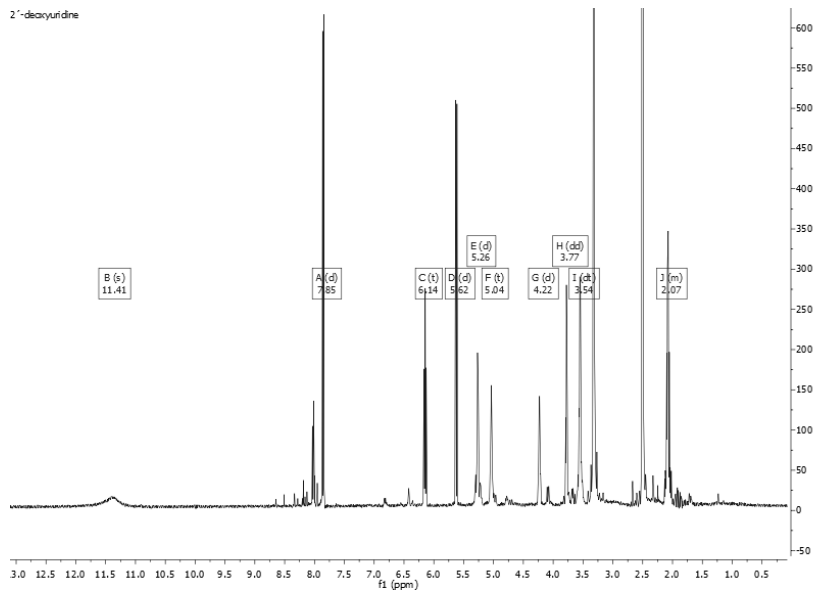
Appendix 7 - ^{1}H-NMR spectrum for 2´-deoxyuridine (**4**) (400 MHz, DMSO-d_6).
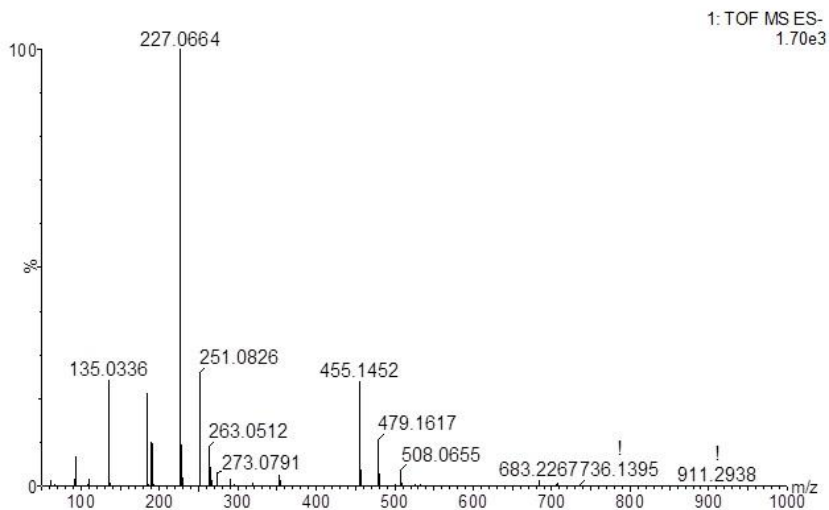
Appendix 8 - HRESIMS spectrum for 2´-deoxyuridine (**4**).
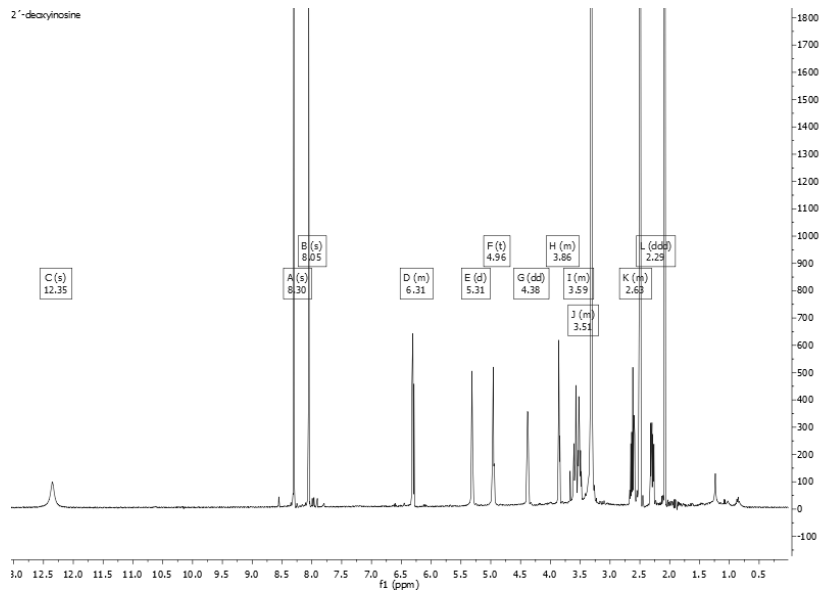
Appendix 9 - ^{1}H-NMR spectrum for 2´-deoxyinosine (5) (400 MHz, DMSO-d_6).
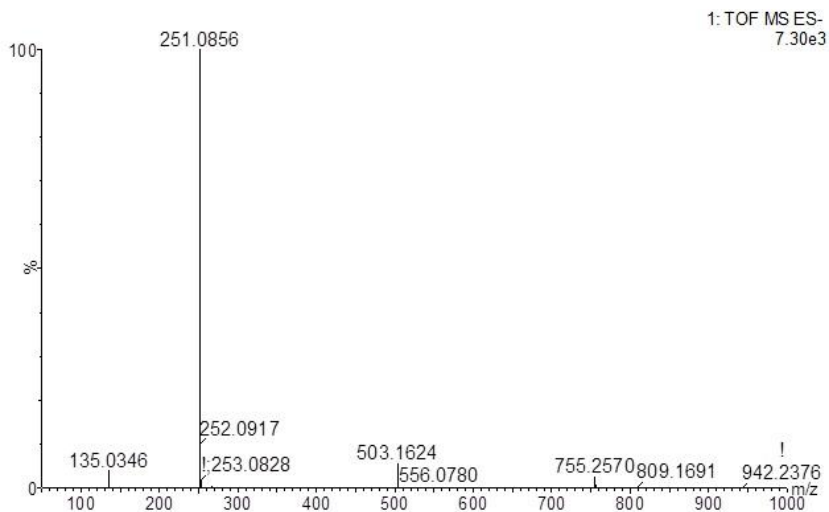
Appendix 10 - HRESIMS spectrum for 2´-deoxyinosine (**5**).

2´-deoxycytidine

| A (d) 7.78 | | J (s) 7.12 | K (s) 7.05 | | B (t) 6.15 | C (d) 5.71 | | D (s) 5.18 | E (s) 4.95 | | F (m) 4.19 | | G (m) 3.75 | H (m) 3.54 | | I (m) 1.91 |
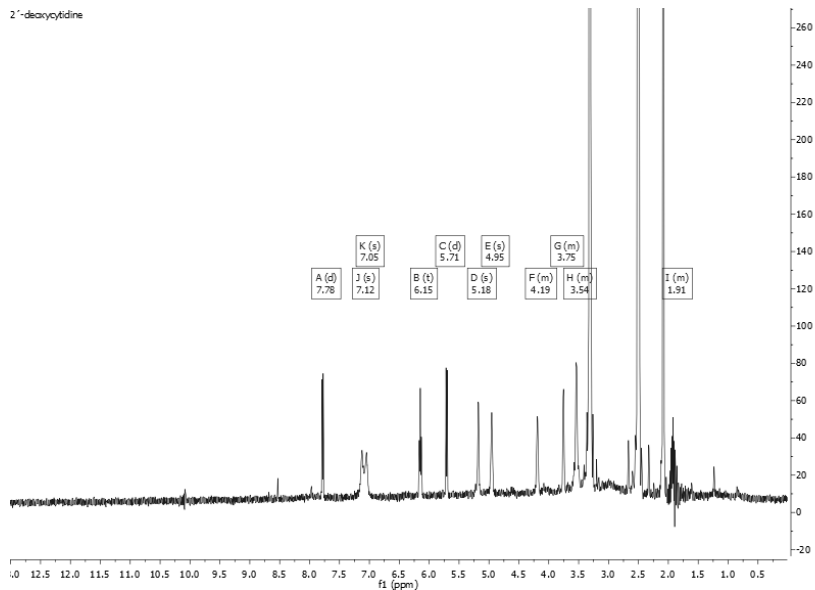
Appendix 11 - ^{1}H-NMR spectrum for 2´-deoxycytidine (**6**) (400 MHz, DMSO-d_6).

1: TOF MS ES+
1.30e4

112.0551

455.1949

228.1005
250.0840

477.1778

682.2831

909.3628
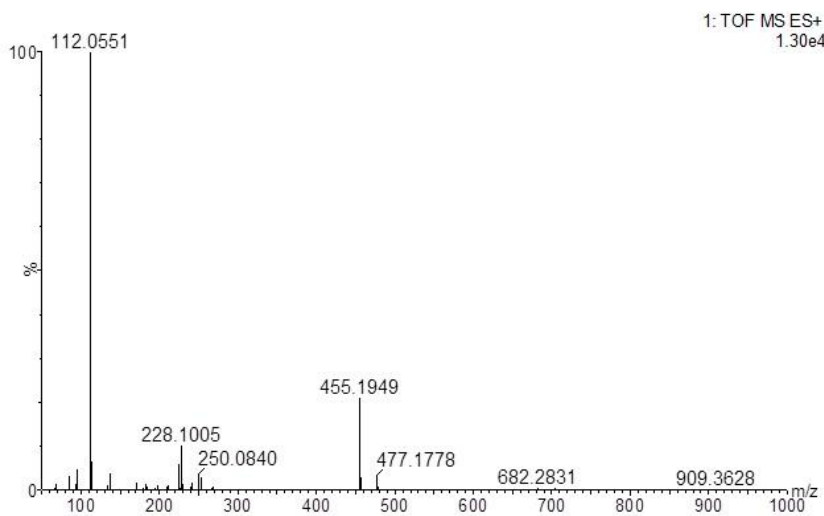
Appendix 12 - HRESIMS spectrum for 2´-deoxycytidine (**6**).
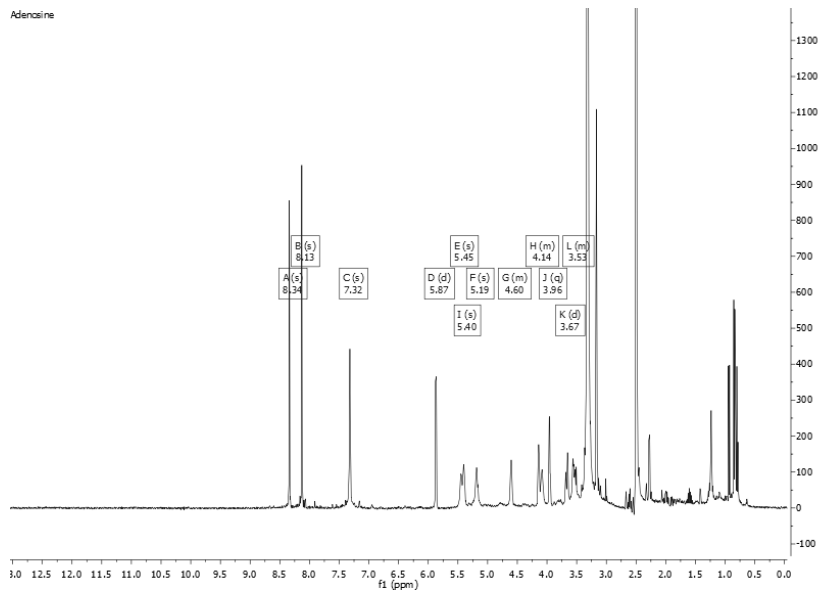
Appendix 13 - ^{1}H-NMR spectrum for adenosine (**7**) (400 MHz, DMSO-d_6).
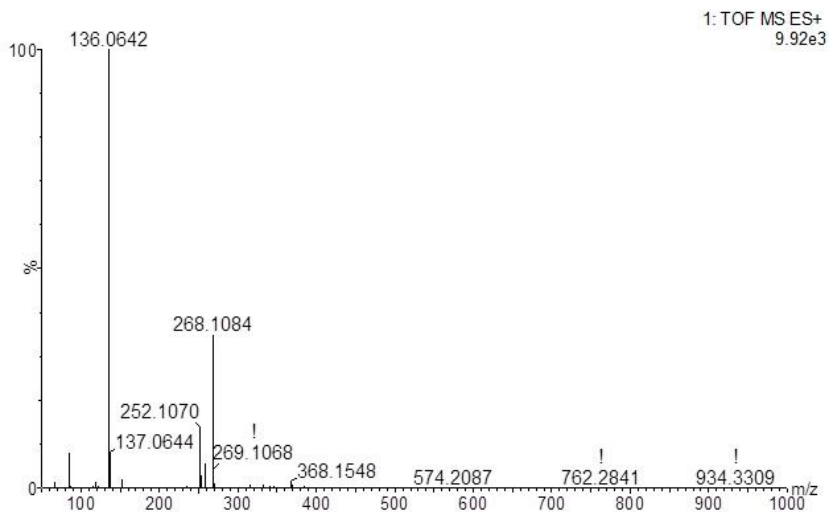
Appendix 14 - HRESIMS spectrum for adenosine (**7**).
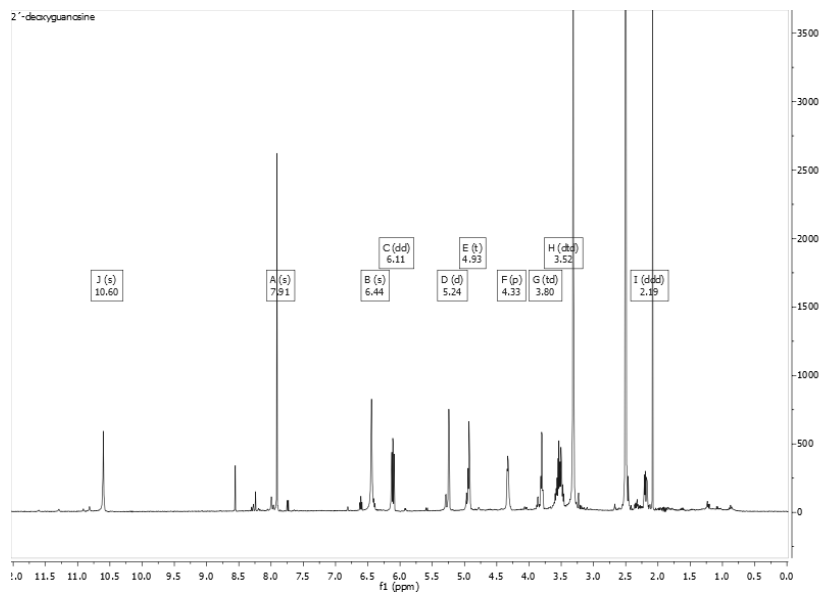
Appendix 15 - ^{1}H-NMR spectrum for 2´-deoxyguanosine (**8**) (400 MHz, DMSO-d_6).
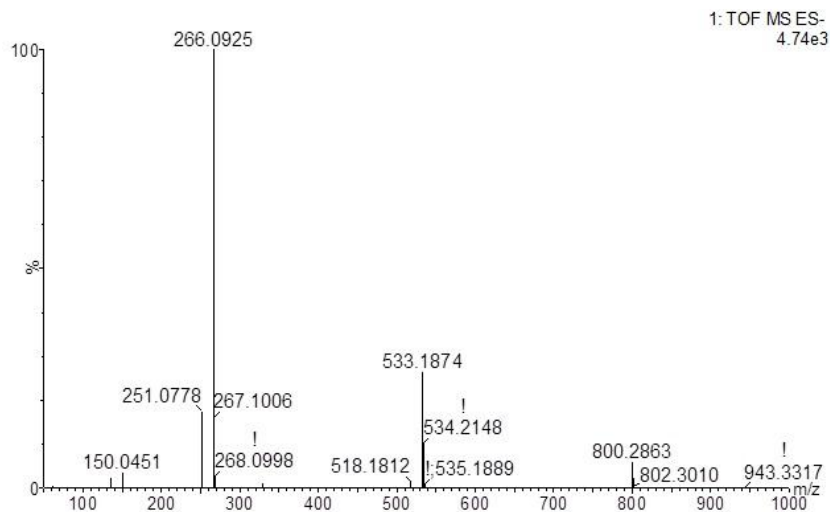
Appendix 16 - HRESIMS spectrum for 2´-deoxyguanosine (**8**).
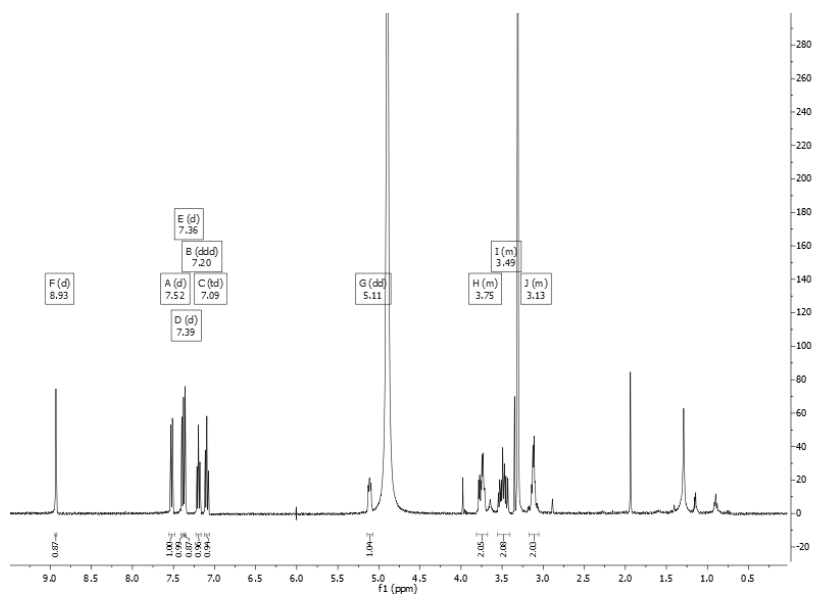
Appendix 17 - ^{1}H-NMR spectrum for haploscleridamine (**9**) (400 MHz, CH₃OD).
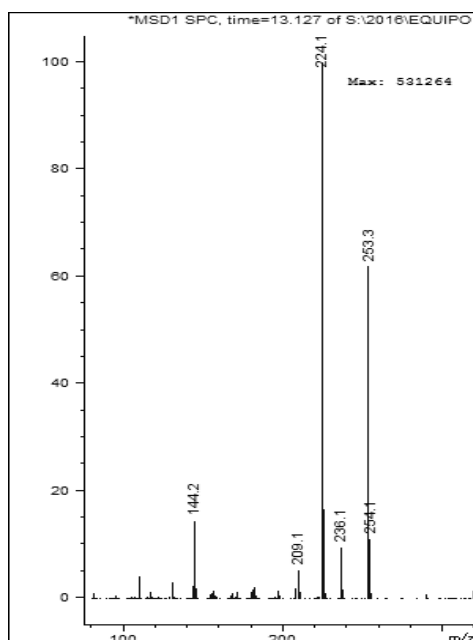
Appendix 18 - ESIMS spectrum for haploscleridamine (**9**).
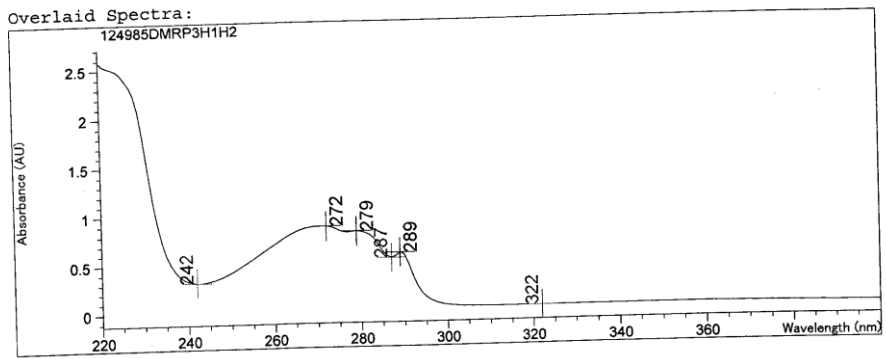
Appendix 19 - UV spectrum for haploscleridamine (**9**) (MeOH).
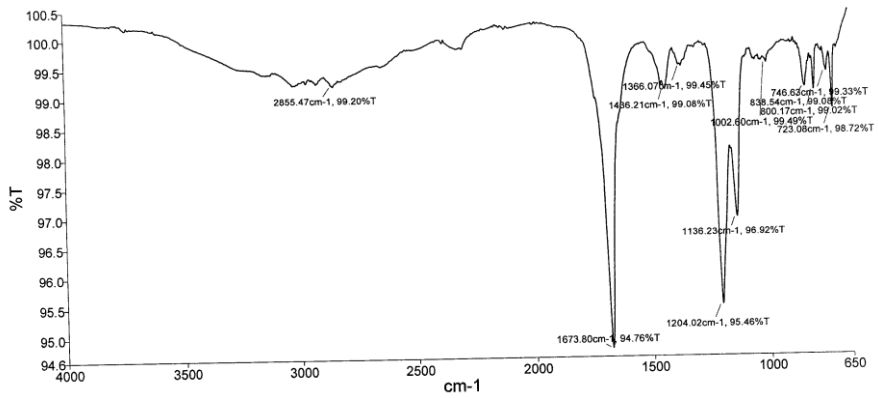
Appendix 20 - IR spectrum for haploscleridamine (**9**) (MeOH).
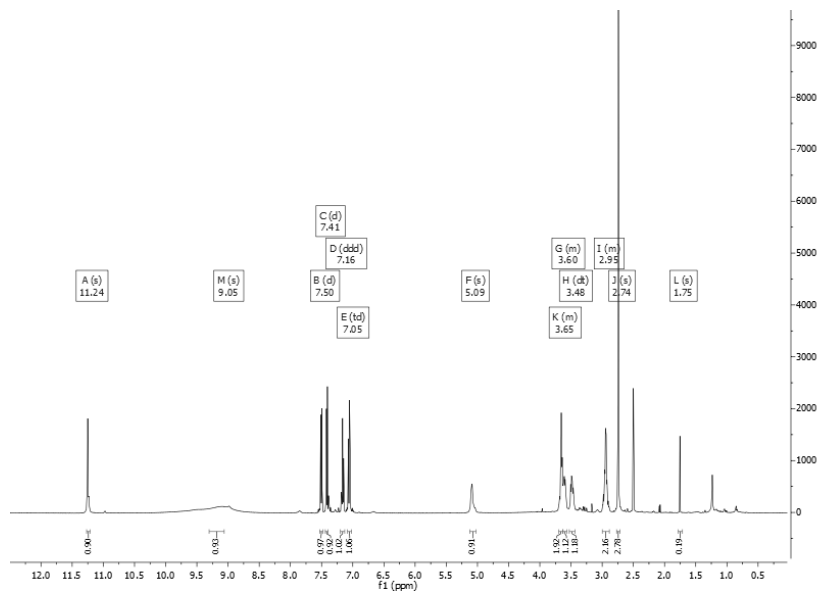
Appendix 21 - ^{1}H-NMR spectrum for compound **10** (400 MHz, DMSO-d_6).
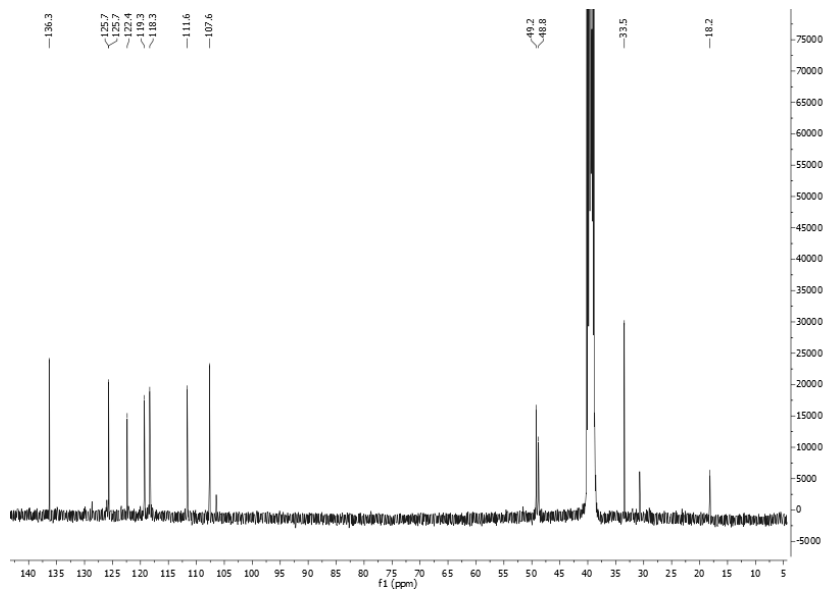
Appendix 22 - ^{13}C-NMR spectrum for compound **10** (100 MHz, DMSO-d_6).
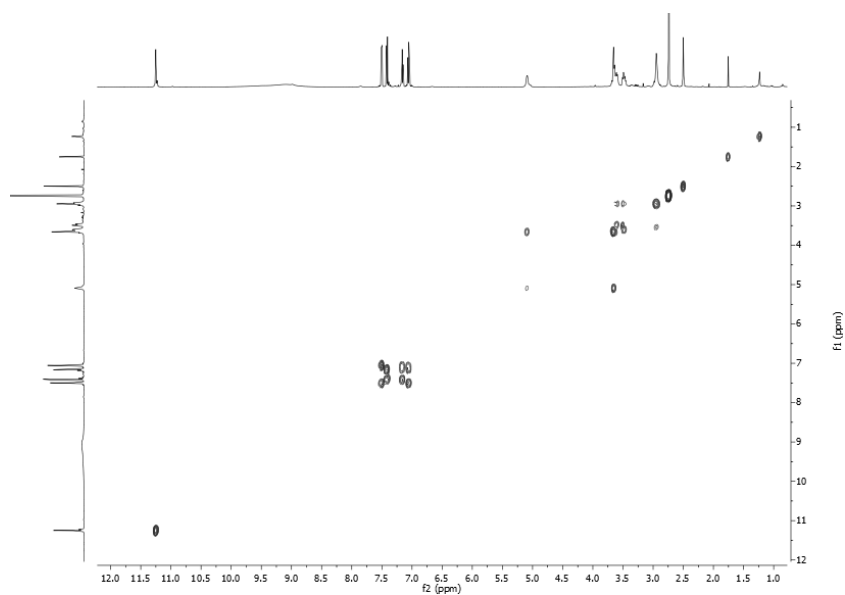
Appendix 23 - *g*-COSY spectrum for compound **10** (400 MHz, DMSO-*d₆*).
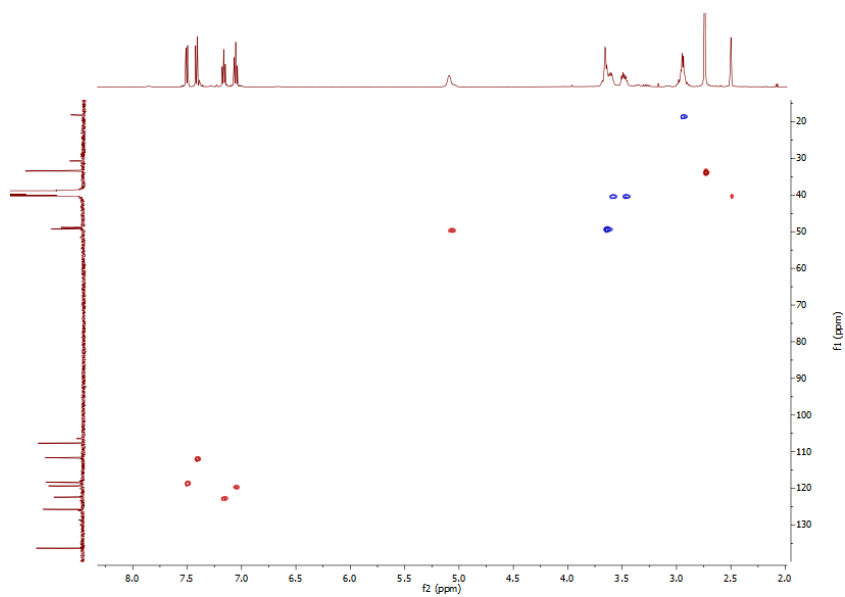
Appendix 24 - *g*-HSQC spectrum for compound **10** (400 MHz, DMSO-*d₆*).
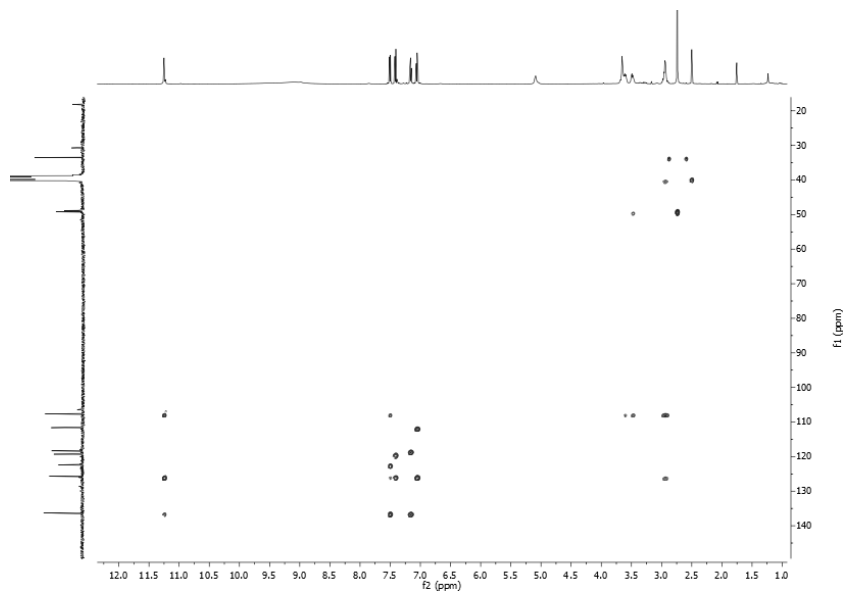
Appendix 25 - *g*-HMBC spectrum for compound **10** (400 MHz, DMSO-*d₆*).
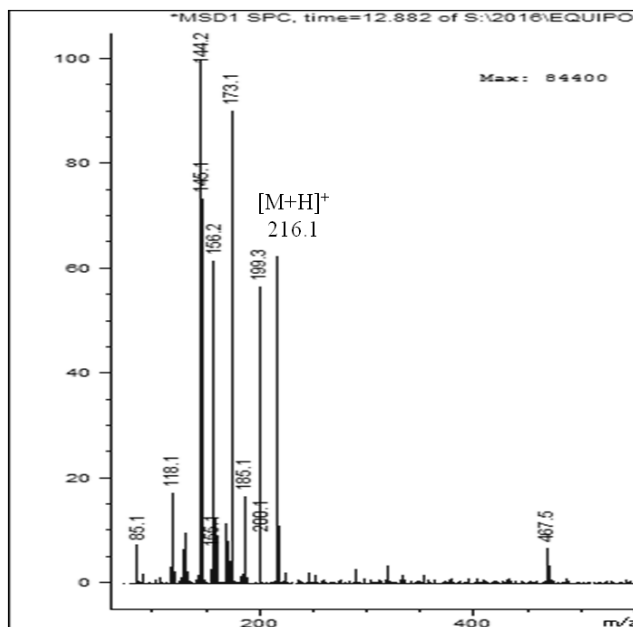
Appendix 26 - ESIMS spectrum for compound **10**.
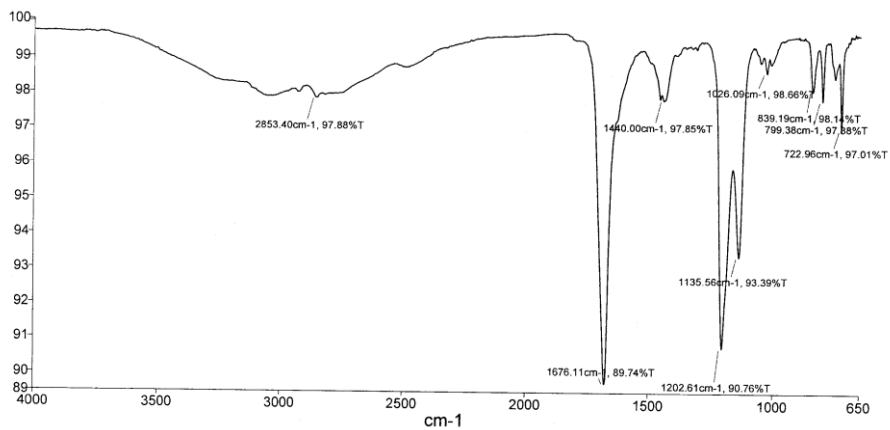
Appendix 27 - IR spectrum for compound **10** (MeOH).
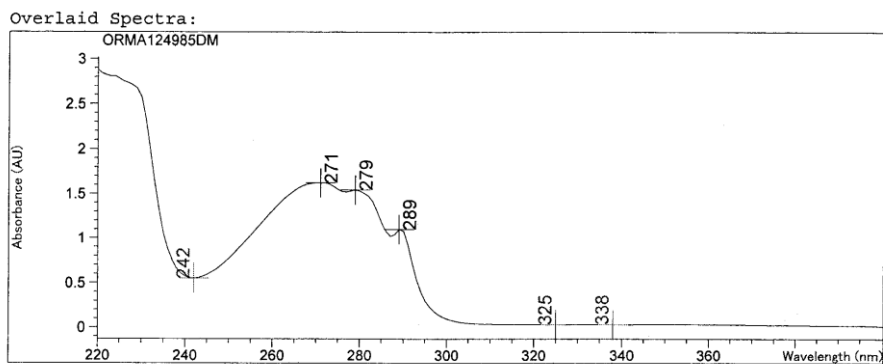
Appendix 28 - UV spectrum for compound **10** (MeOH).

141

Appendix 29 - ^{1}H-NMR spectrum for compound **11** (500 MHz, CD$_3$OD).

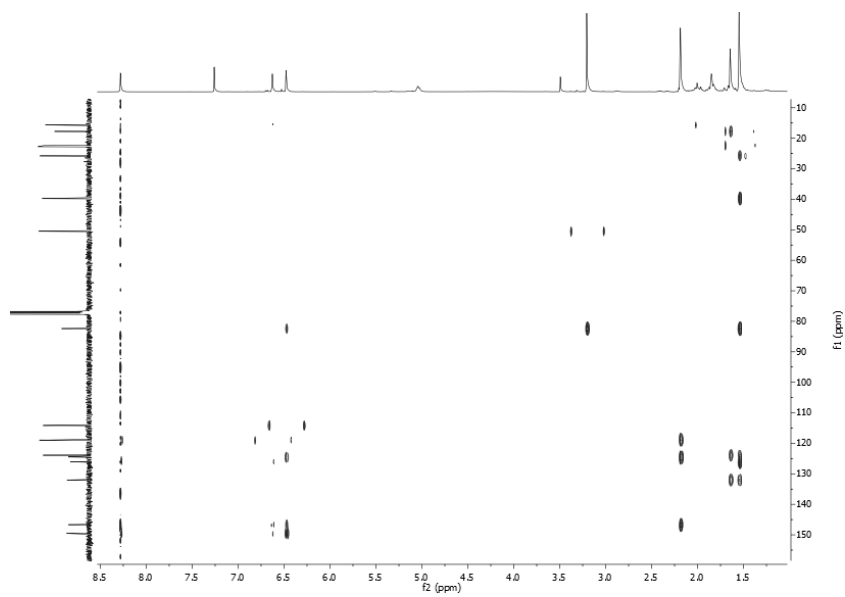**Appendix 30 -** ^{13}C-NMR spectrum for compound **11** (100 MHz, CD$_3$OD).

142
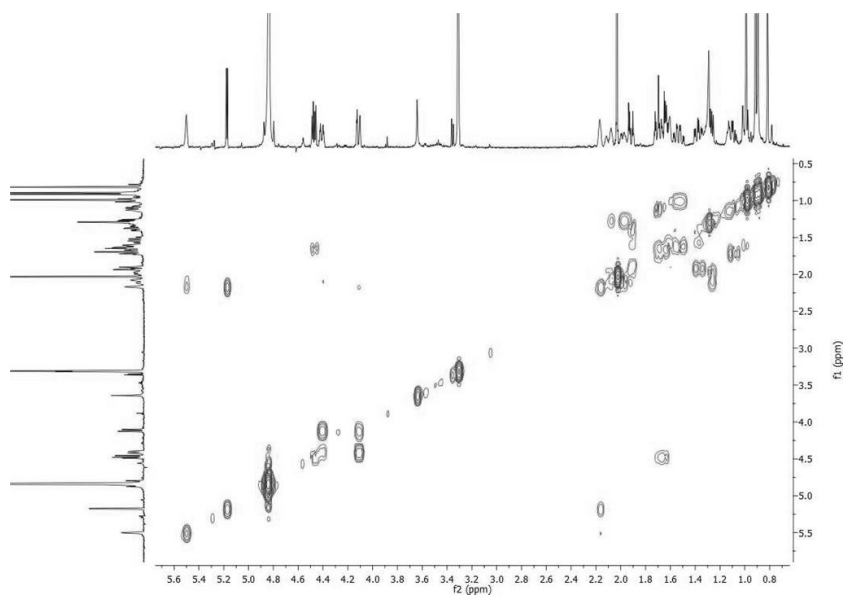
Appendix 31 - *g*-COSY spectrum for compound **11** (500 MHz, CD₃OD).
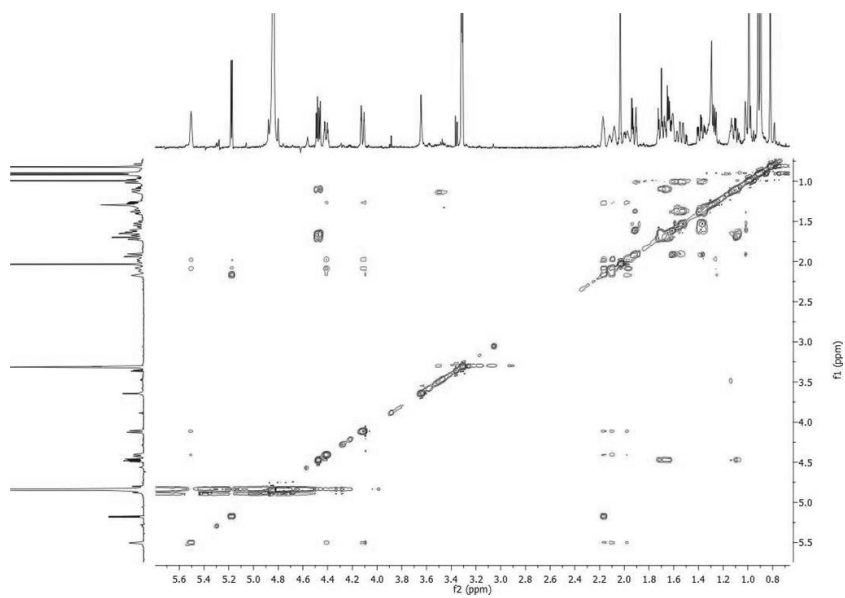
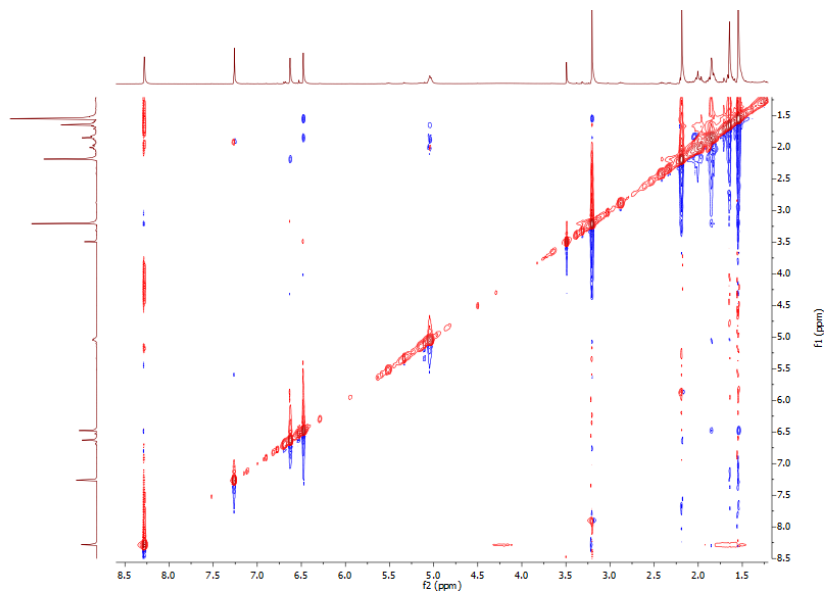**Appendix 32 -** TOCSY spectrum for compound **11** (500 MHz, CD₃OD).
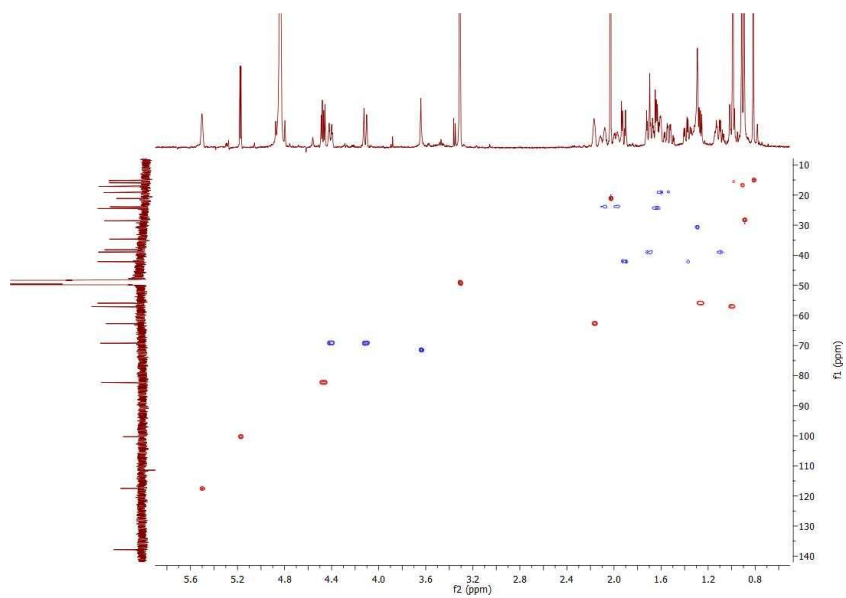
**Appendix 33 -** *g*-HSQC spectrum for compound **11** (500 MHz, CD₃OD).
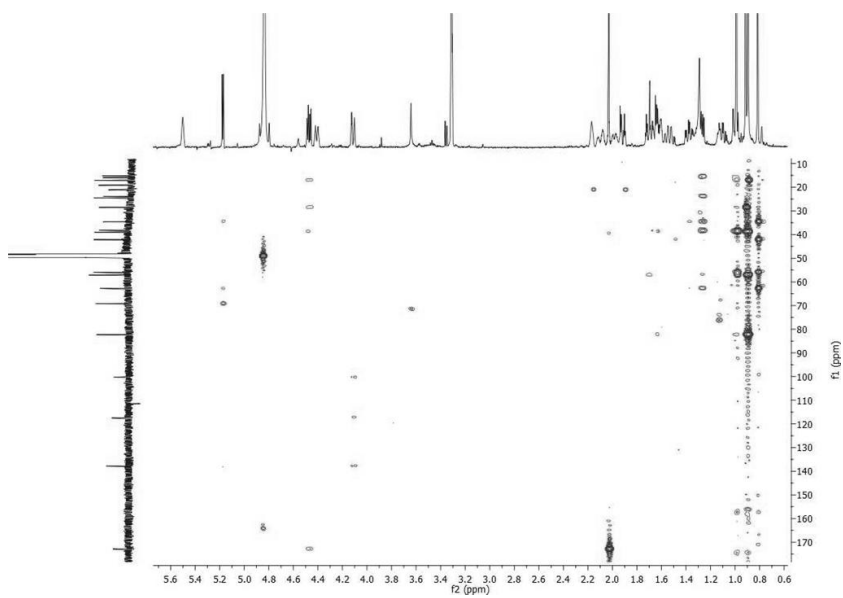
Appendix 34 - *g*-HMBC spectrum for compound **11** (500 MHz, CD₃OD).

144
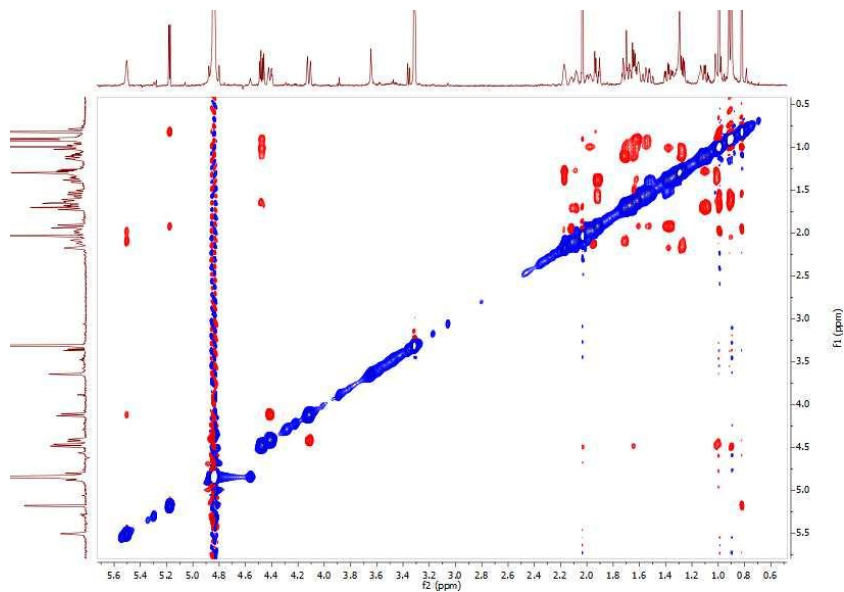
Appendix 35 - ROESY spectrum for compound **11** (500 MHz, CD₃OD).
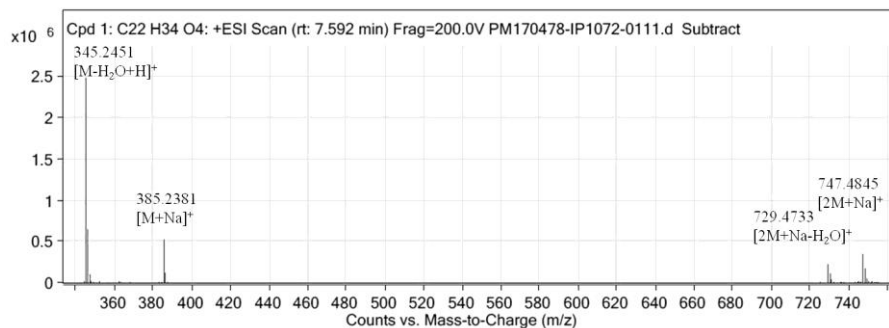
Appendix 36 - HRESTOFMS spectrum for compound **11**.
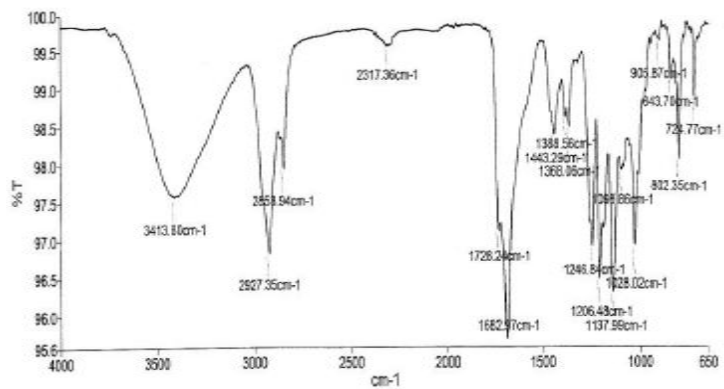
Appendix 37 - IR spectrum for compound **11** (MeOH).
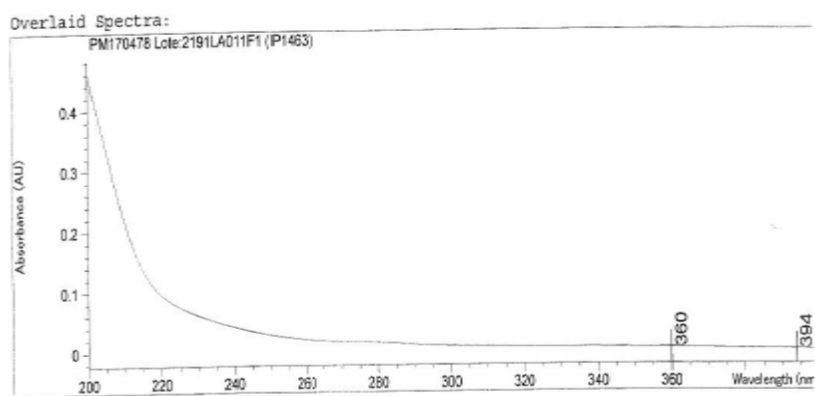
Appendix 38 - UV spectrum for compound **11** (MeOH).

146

Appendix 39 - ^{1}H-NMR spectrum for compound **12** (500 MHz, CD$_3$OD).

Appendix 40 - ^{13}C-NMR spectrum for compound **12** (100 MHz, CD$_3$OD).
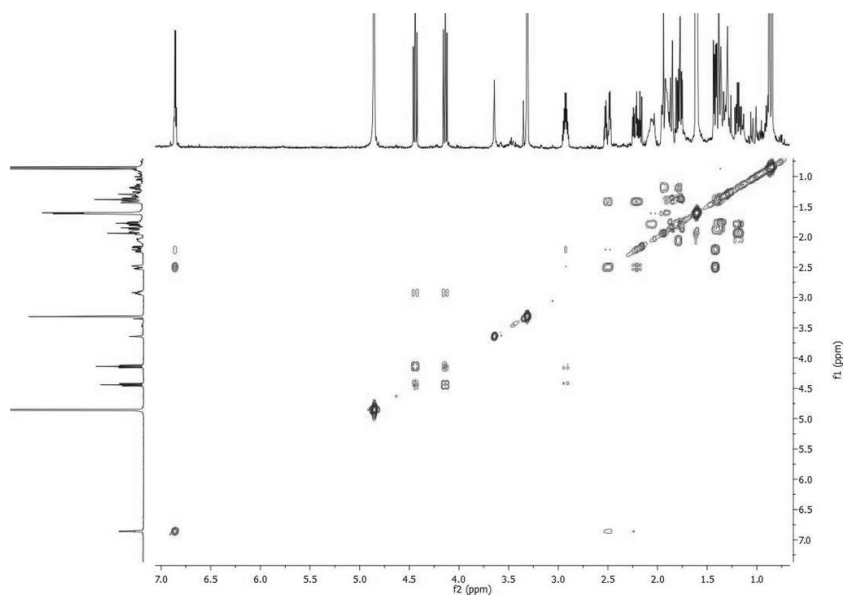
Appendix 41 - g-COSY spectrum for compound **12** (500 MHz, CD$_3$OD).
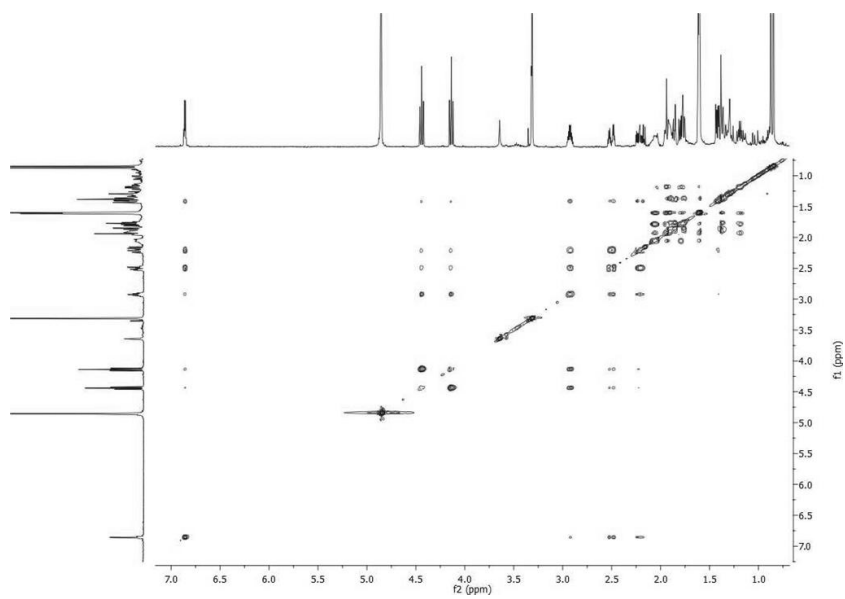
Appendix 42 - TOCSY spectrum for compound **12** (500 MHz, CD$_3$OD).
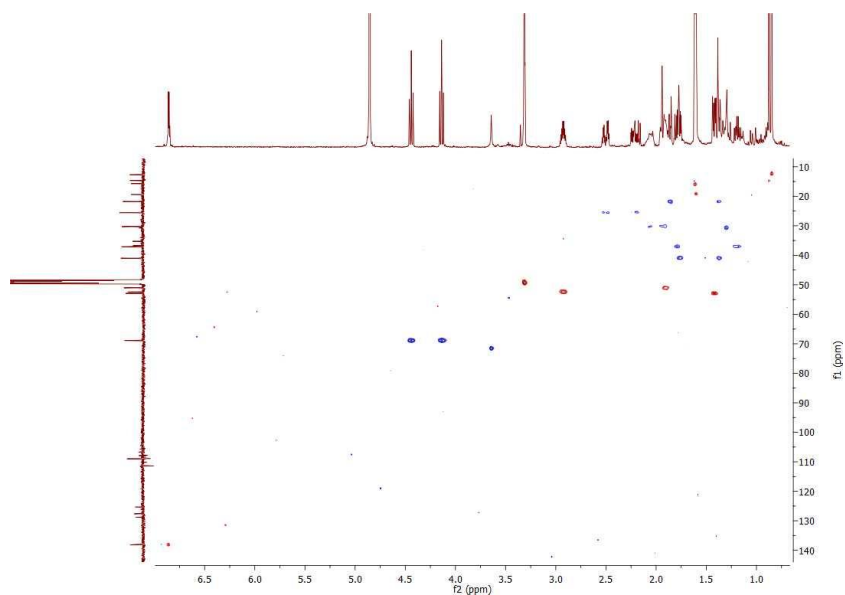
**Appendix 43** - *g*-HSQC spectrum for compound **12** (500 MHz, CD₃OD).
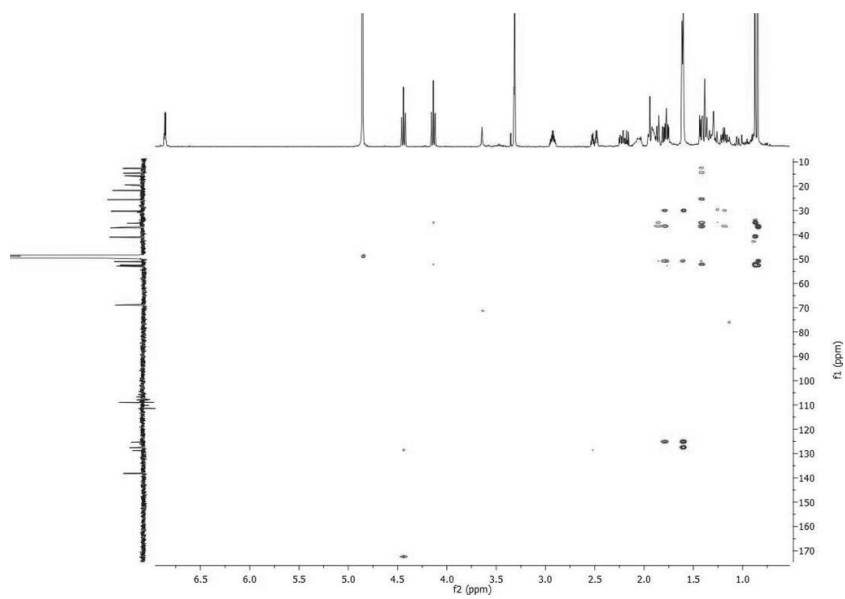
**Appendix 44 -** *g*-HMBC spectrum for compound **12** (500 MHz, CD₃OD).
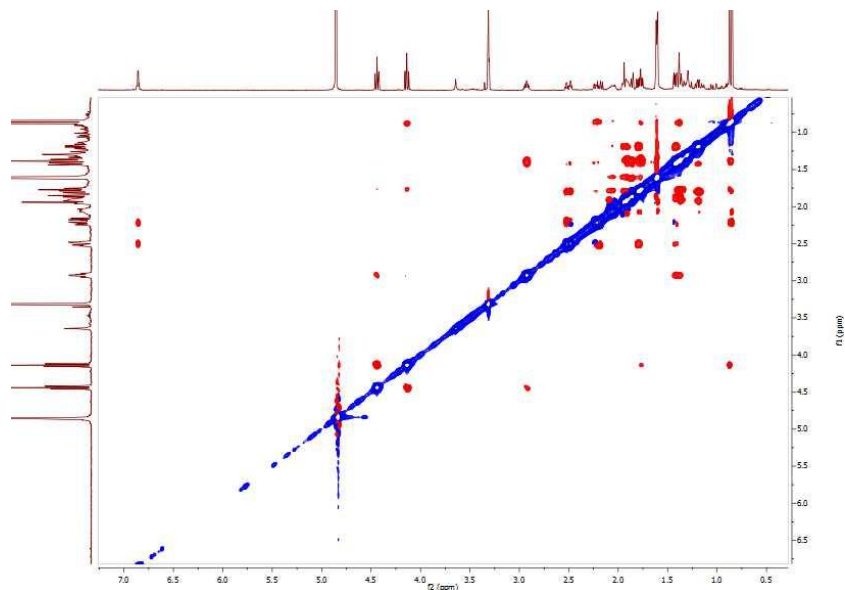
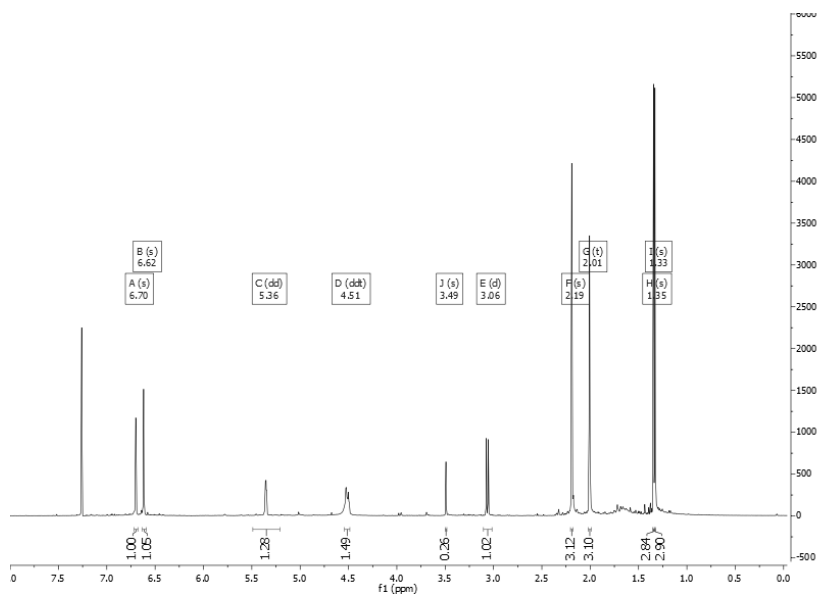**Appendix 45 -** ROESY spectrum for compound **12** (500 MHz, CD$_3$OD).
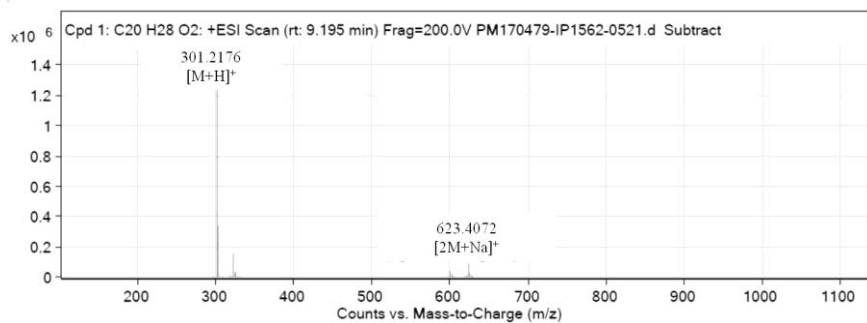
Appendix 46 - HRESTOFMS spectrum for compound **12**.

150
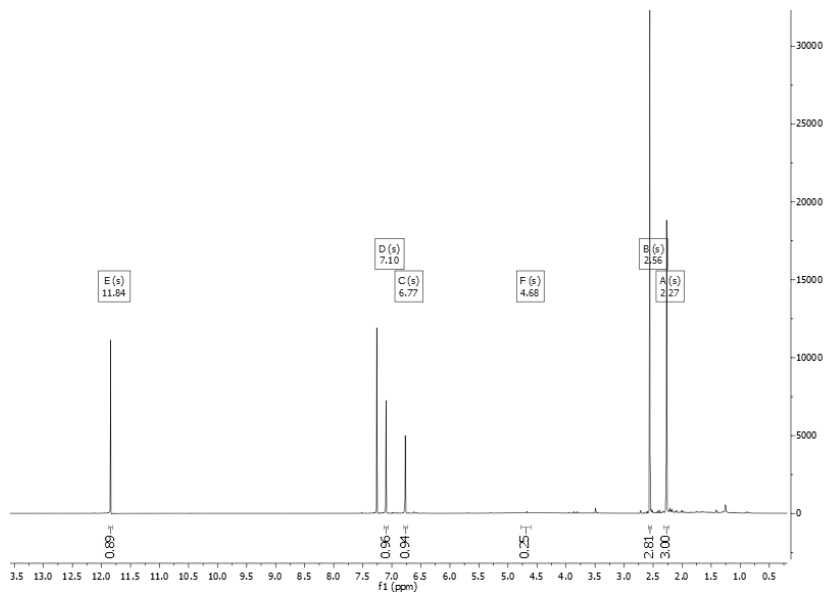
Appendix 47 - ^{1}H-NMR spectrum for compound **13** (400 MHz, CDCl$_3$).
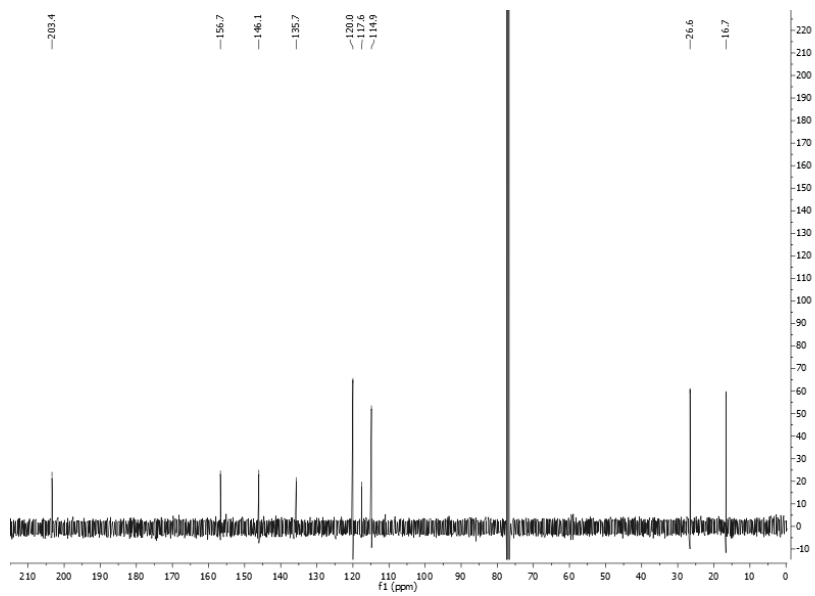
Appendix 48 - ^{13}C-NMR spectrum for compound **13** (100 MHz, CDCl$_3$).
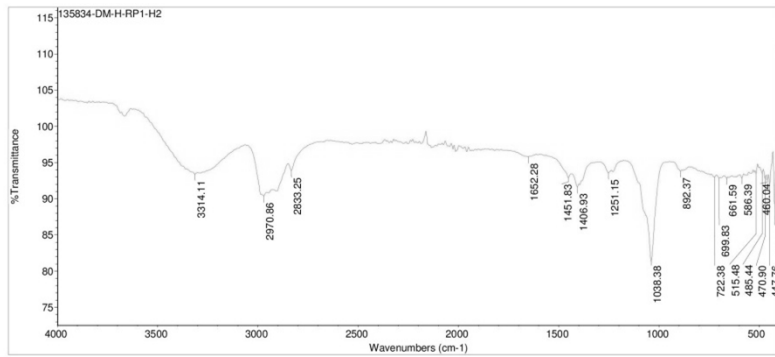
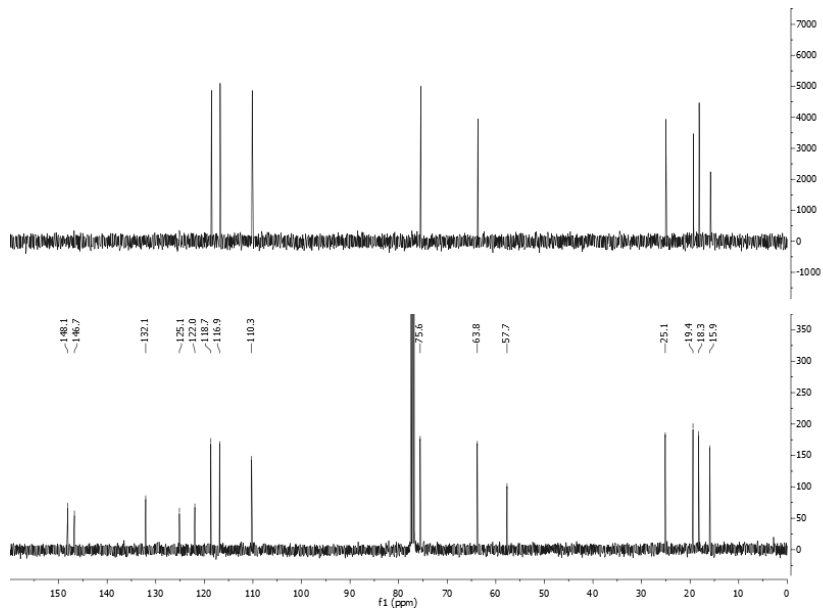**Appendix 49 -** IR spectrum for compound 13 (neat).
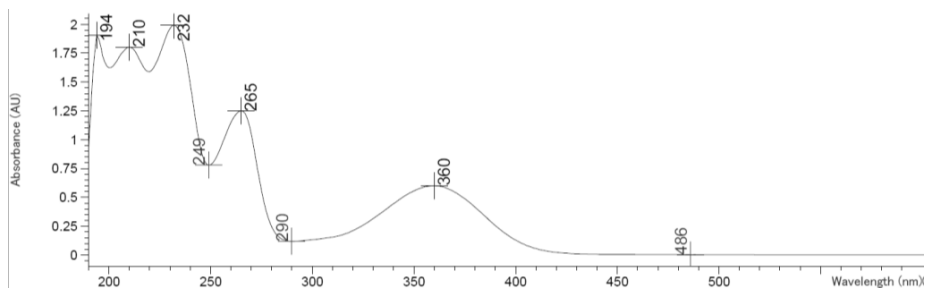
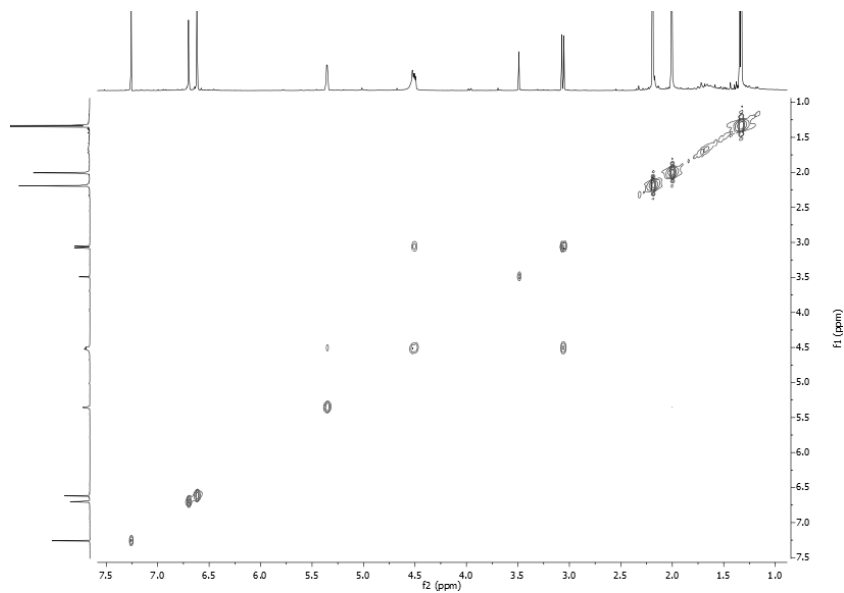

Appendix 50 - UV spectrum for compound **13** (MeOH).
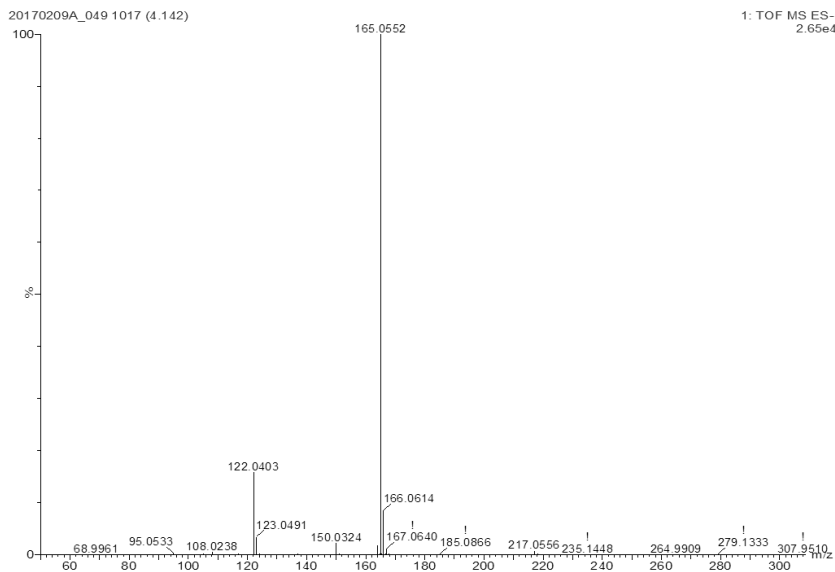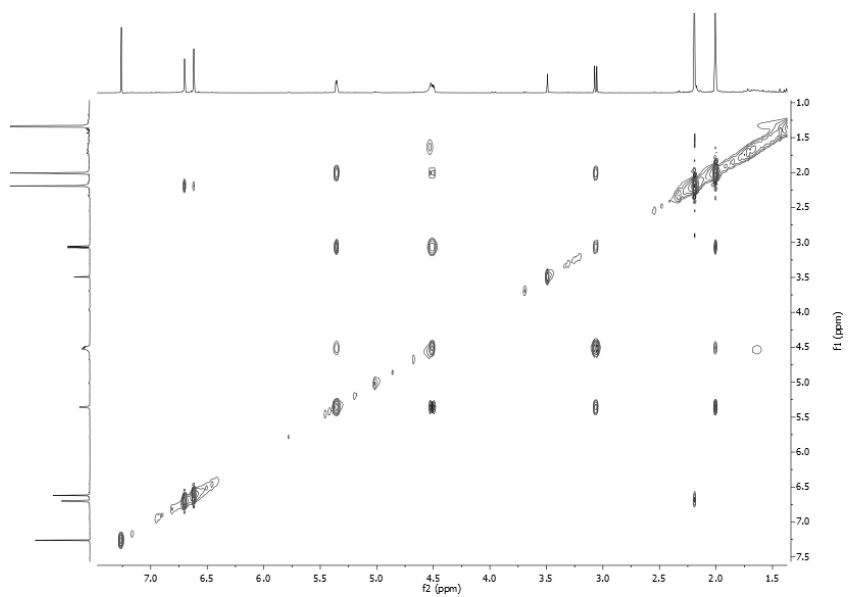

Appendix 51 - HRESIMS spectrum for compound **13**.

152
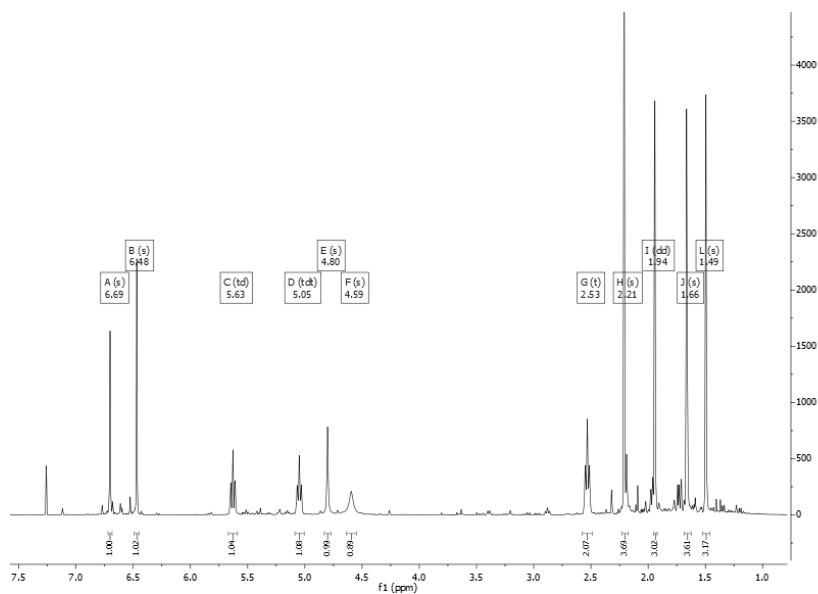
Appendix 52 – ^{1}H-NMR spectrum for compound **14** (400 MHz, (CDCl$_3$).
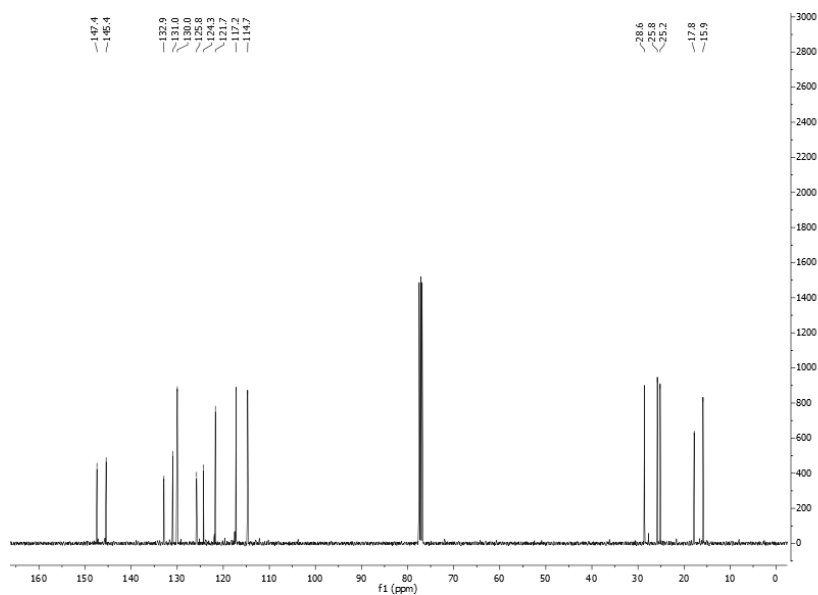
Appendix 53 - ^{13}C-NMR spectrum for compound **14** (100 MHz, CDCl^3).
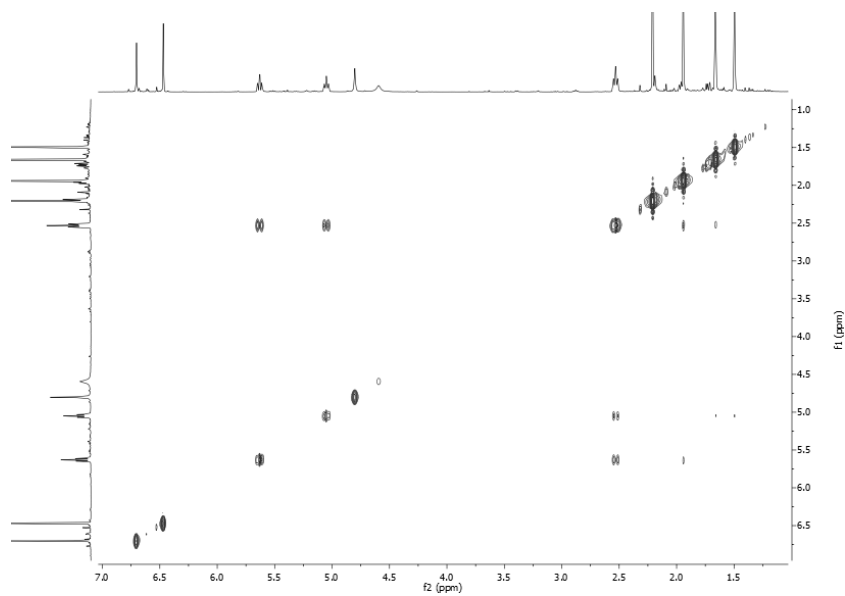
Appendix 54 - *g*-COSY spectrum for compound **14** (400 MHz, CDCl3).
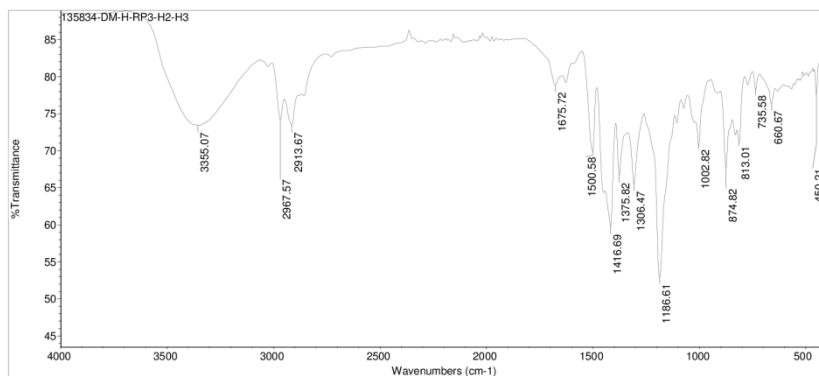
Appendix 55 - UV spectrum for compound **14** (neat).
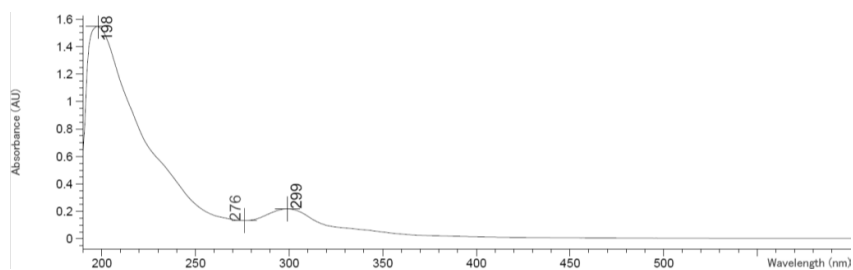
Appendix 56 - UV spectrum for compound **14** (MeOH).

154
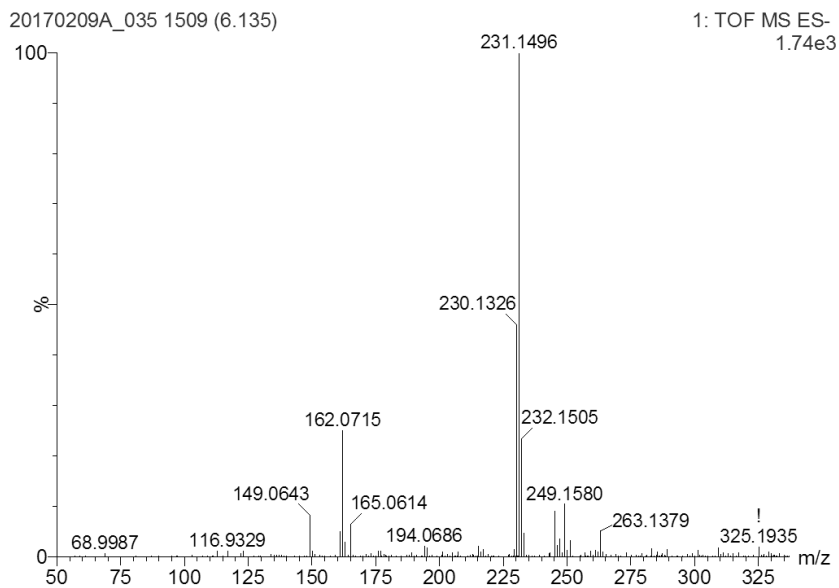
Appendix 57 - HRESIMS spectrum for compound **14**.
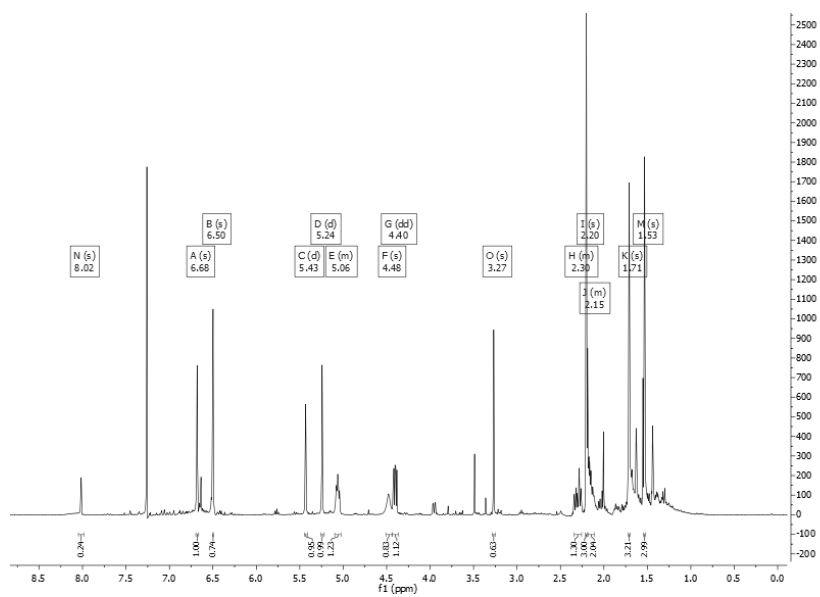
Appendix 58 - ^{1}H-NMR spectrum for compound **15** (400 MHz, CDCl$_3$).

155
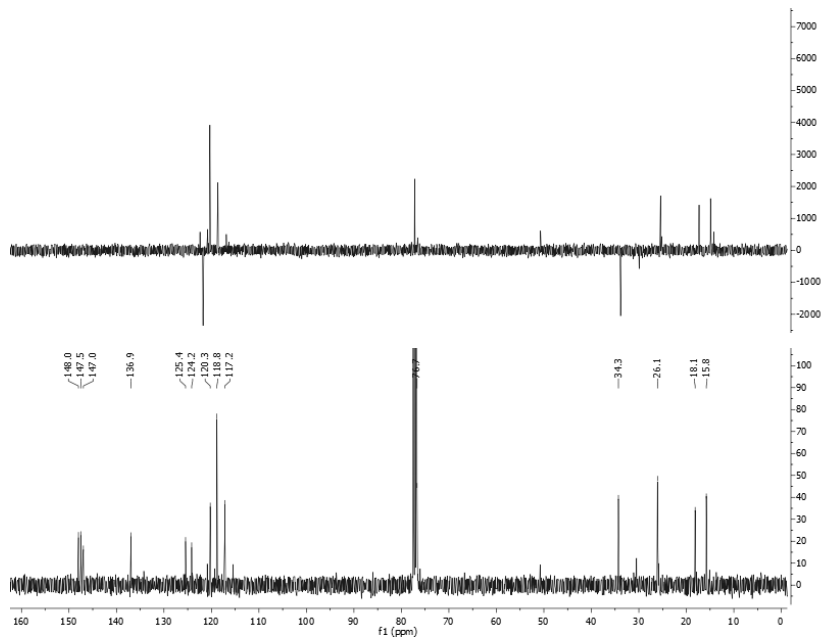
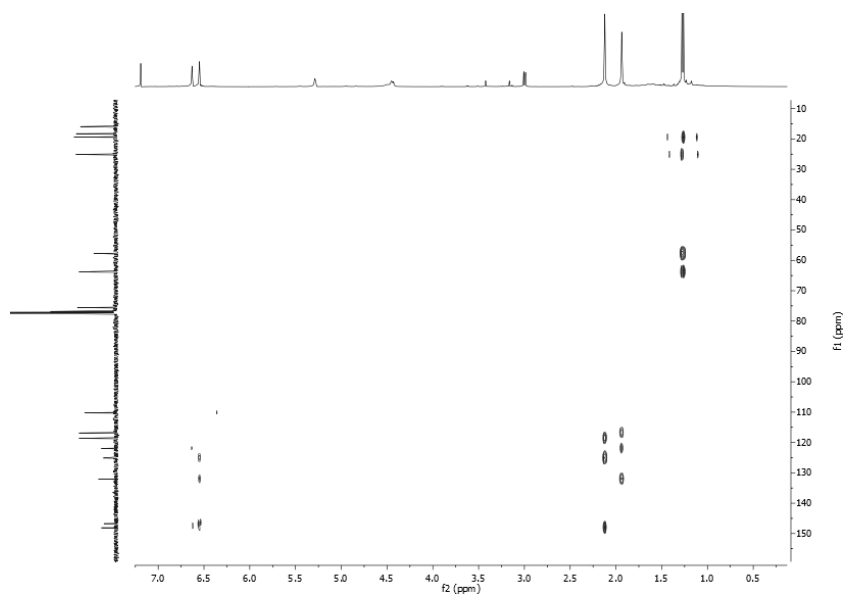**Appendix 59 -** DEPT and ^{13}C-NMR spectra for compound **15** (100 MHz, CDCl$_3$).
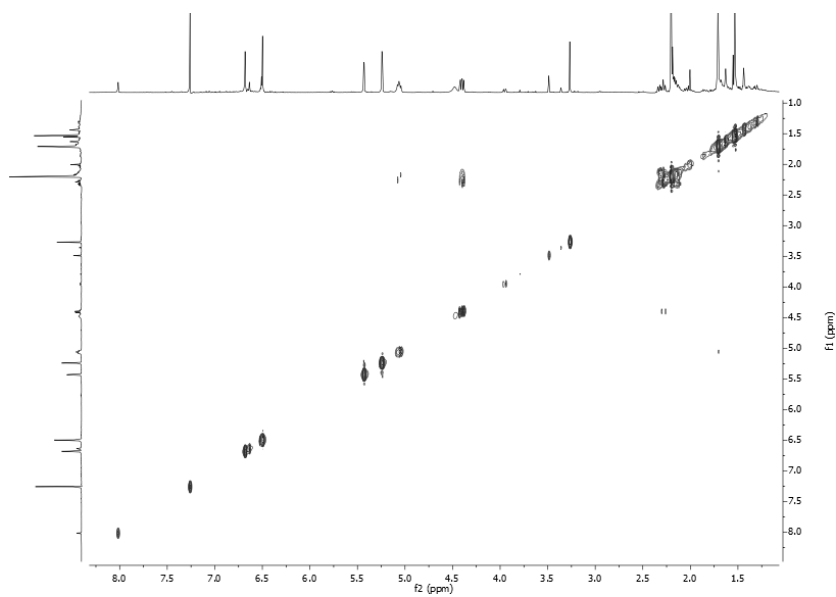
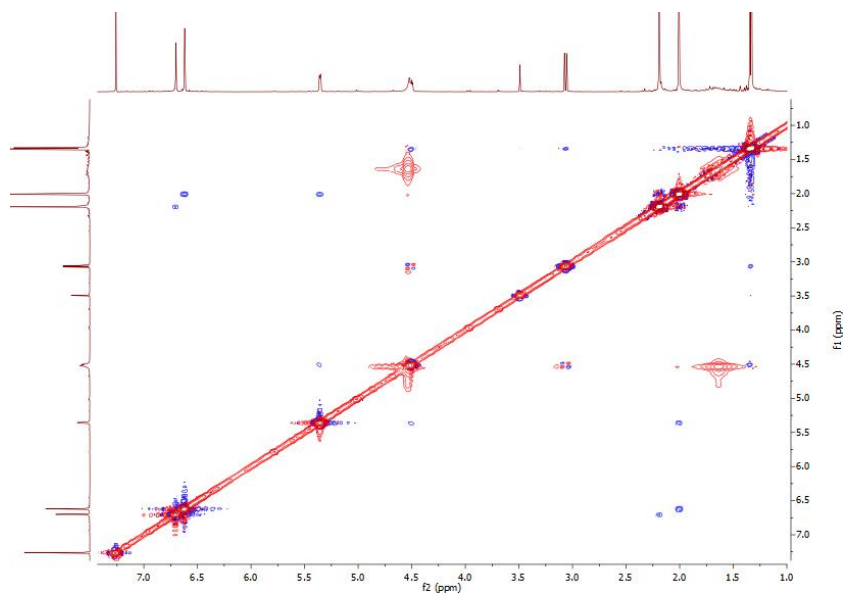**Appendix 60 -** *g*-COSY spectrum for compound **15** (400 MHz, CDCl$_3$).
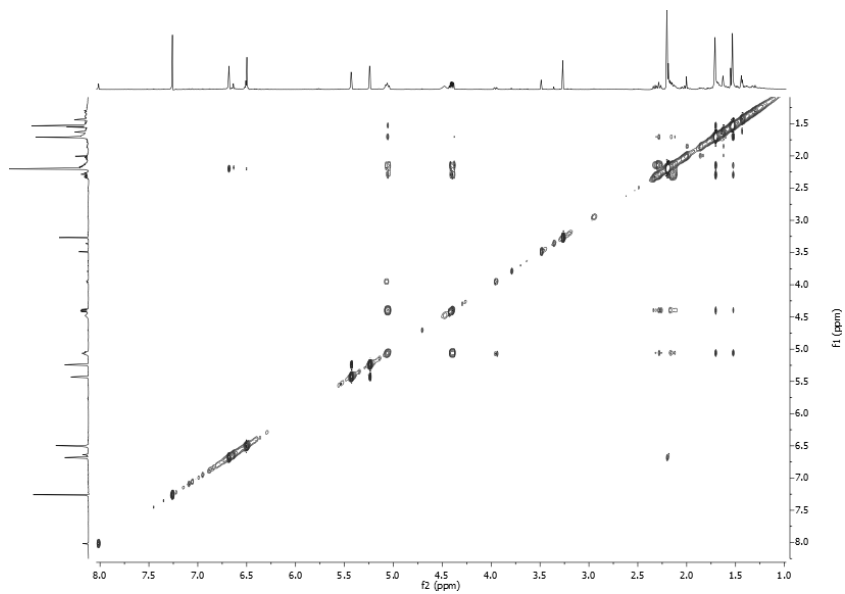
Appendix 61 - TOCSY spectrum for compound **15** (400 MHz, CDCl₃).
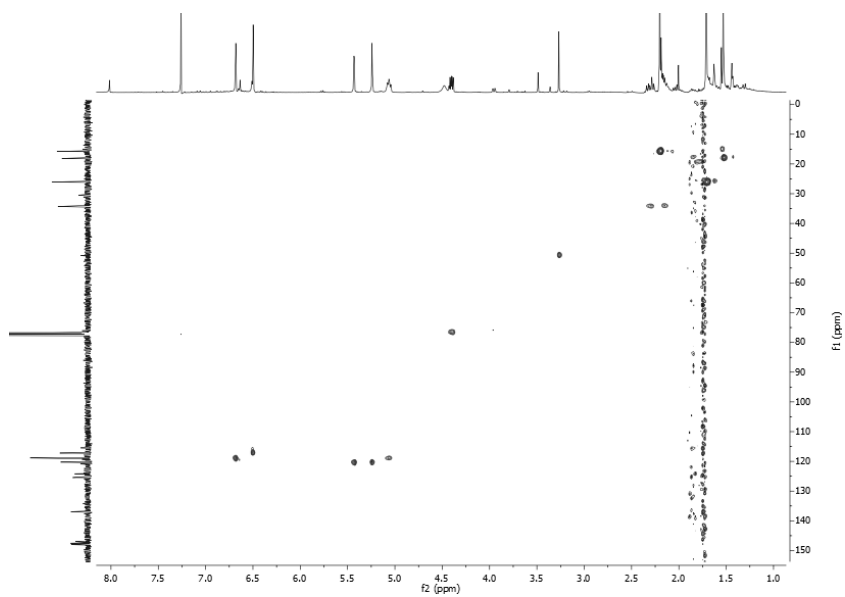
**Appendix 62 -** *g*-HSQC spectrum for compound **15** (400 MHz, CDCl₃).

157
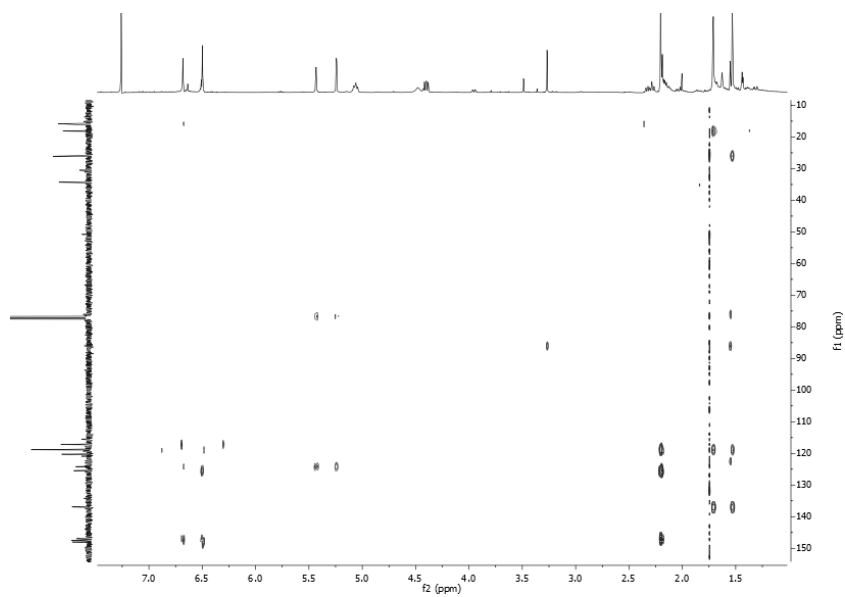
Appendix 63 - *g*-HMBC spectrum for compound **15** (400 MHz, CDCl₃).
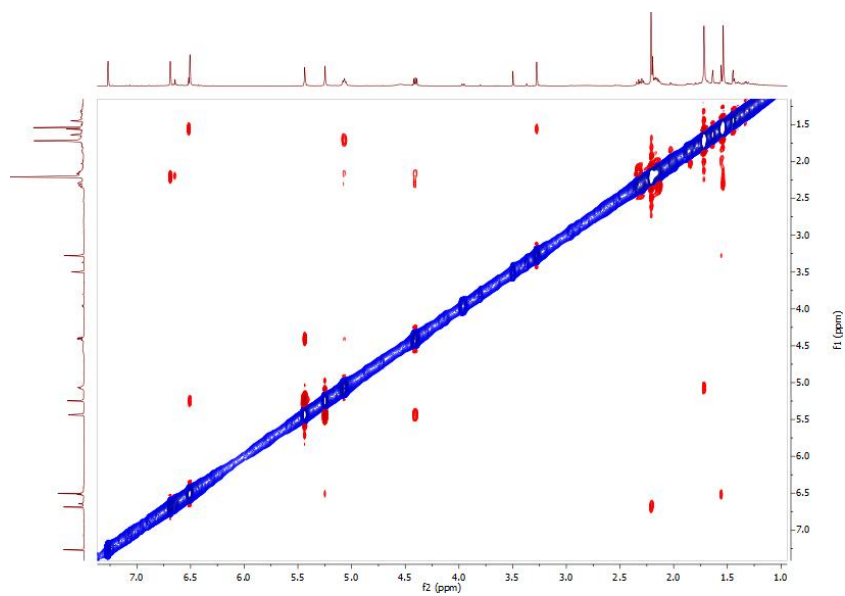
Appendix 64 - NOESY spectrum for compound **15** (400 MHz, CDCl₃).
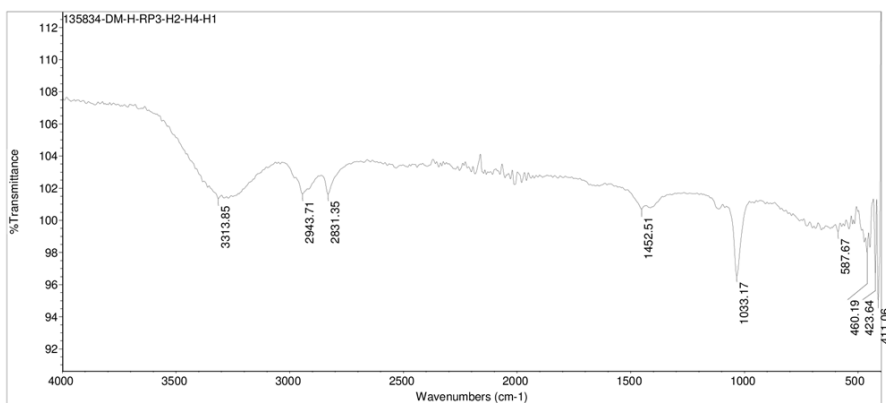
Appendix 65 - IR spectrum for compound **15** (MeOH).
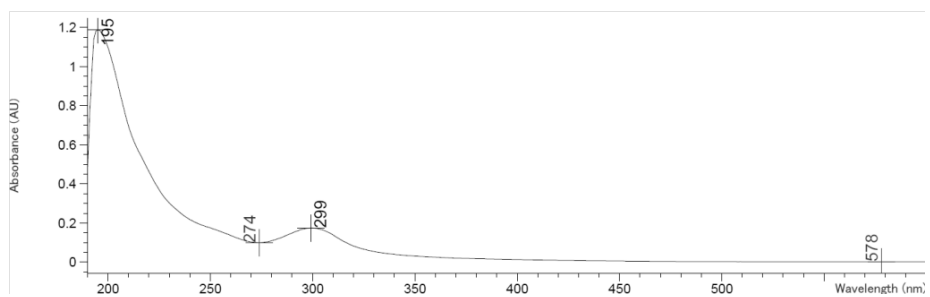
Appendix 66 - UV spectrum for compound **15** (MeOH).
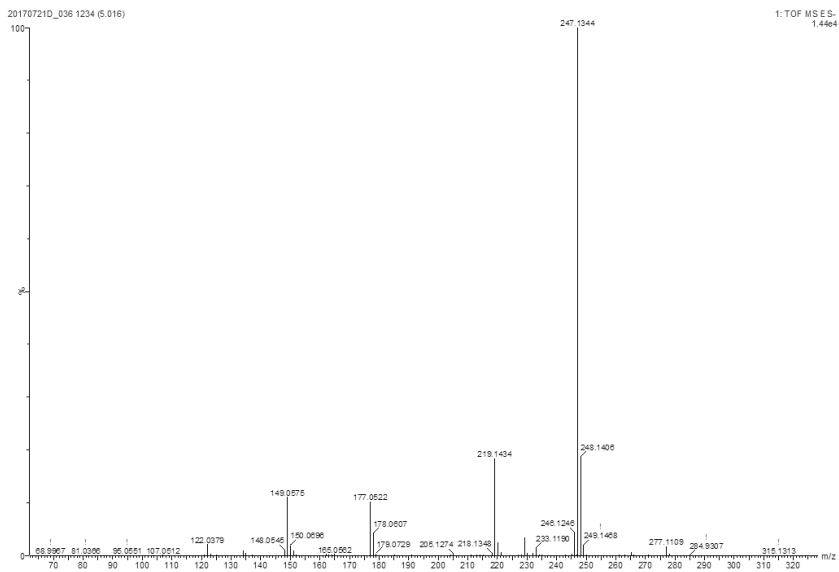
Appendix 67 - (-)-HRESIMS spectrum for compound **15**.
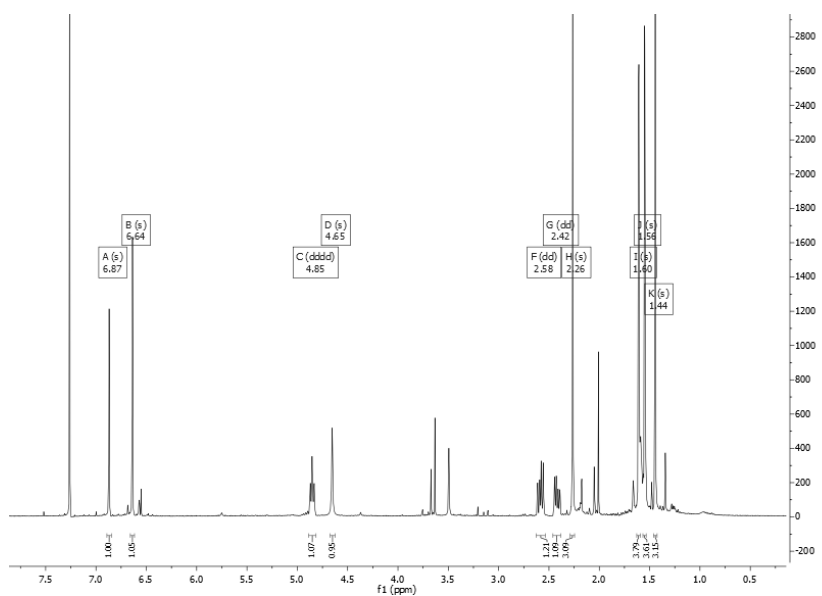
Appendix 68 - ^{1}H-NMR spectrum for compound **16** (400 MHz, CDCl$_3$).

160
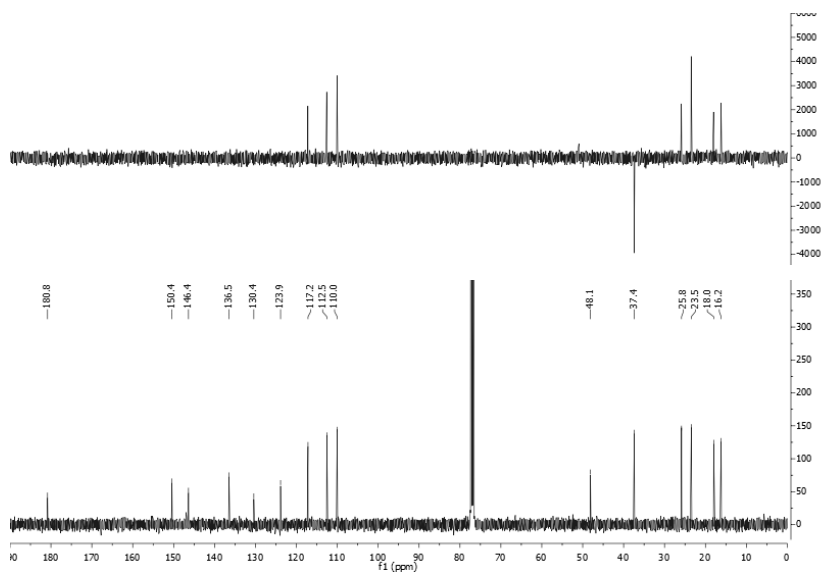
Appendix 69 - DEPT and ^{13}C-NMR spectra for compound **16** (100 MHz, CDCl$_3$).
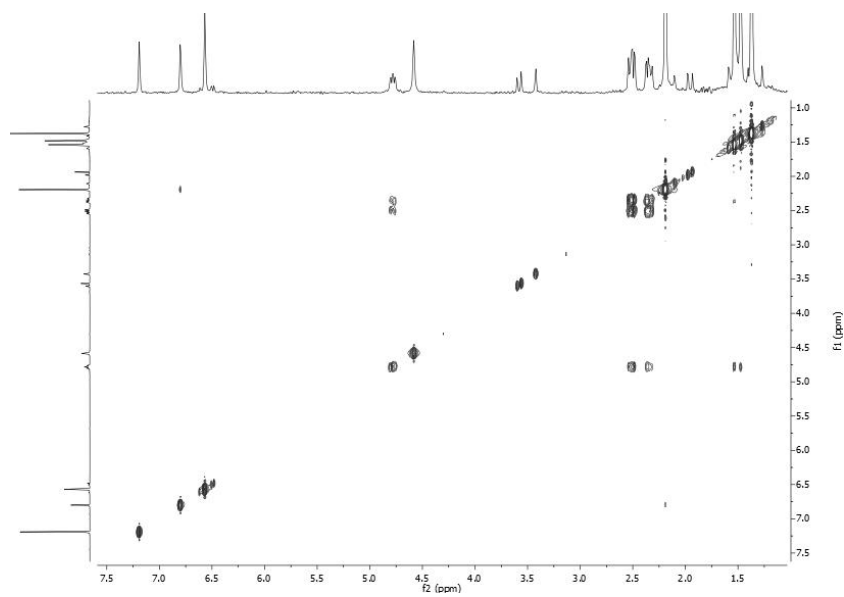
Appendix 70 - *g*-COSY spectrum for compound **16** (400 MHz, CDCl$_3$).
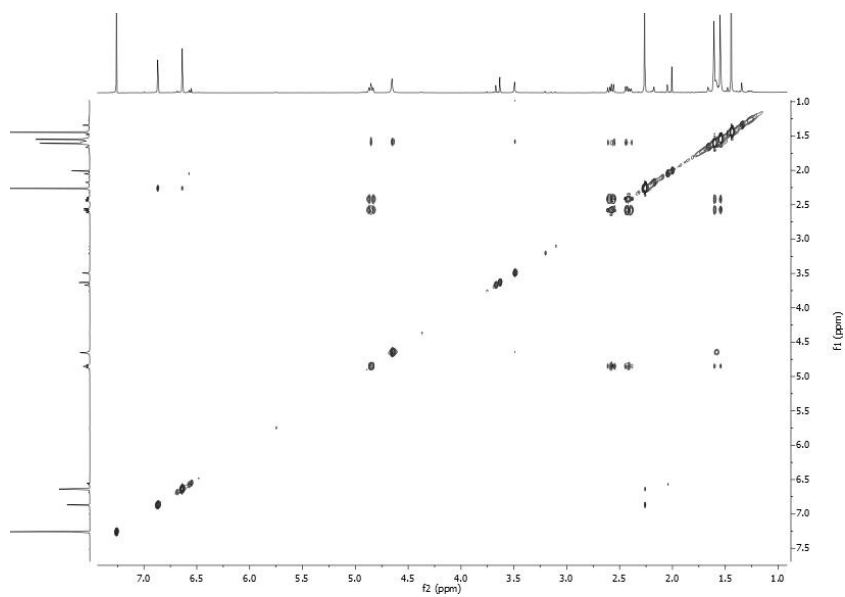
Appendix 71 - TOCSY spectrum for compound **16** (400 MHz, CDCl$_3$).
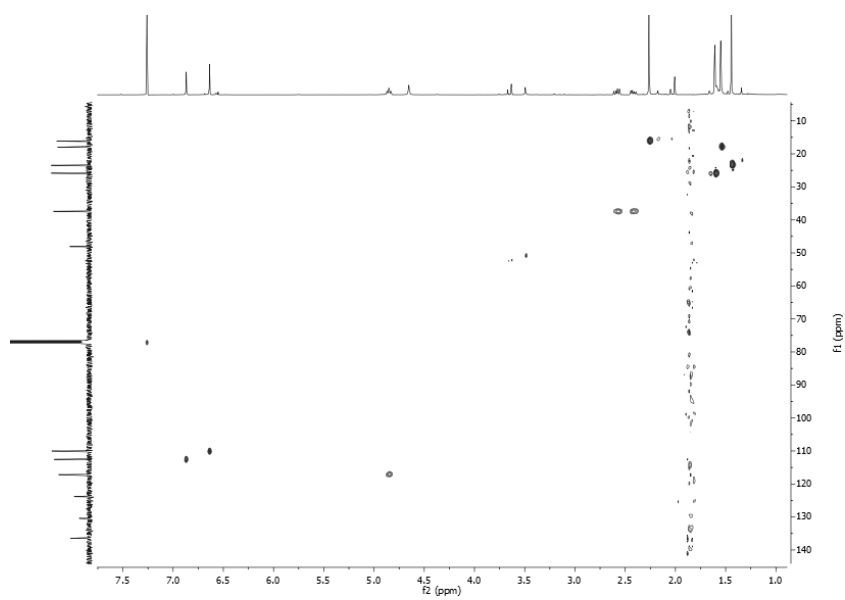
Appendix 72 - *g*-HSQC spectrum for compound **16** (400 MHz, CDCl$_3$).

162
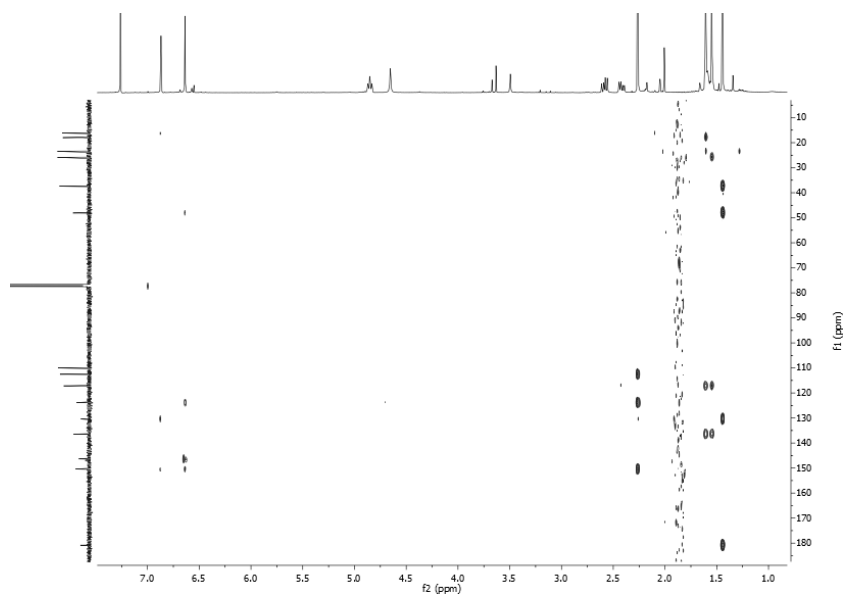
**Appendix 73 -** *g*-HMBC spectrum for compound **16** (400 MHz, CDCl₃).
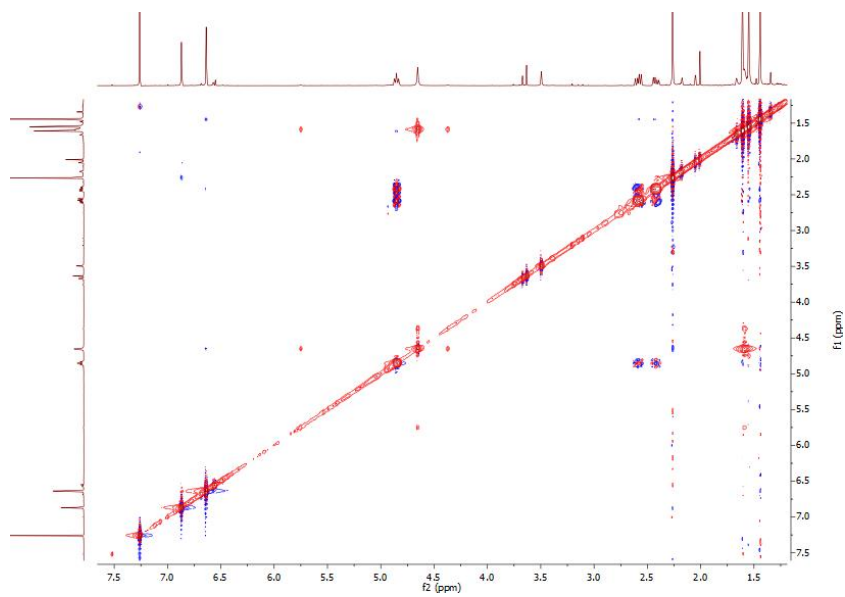
**Appendix 74 -** NOESY spectrum for compound **16** (400 MHz, CDCl₃).
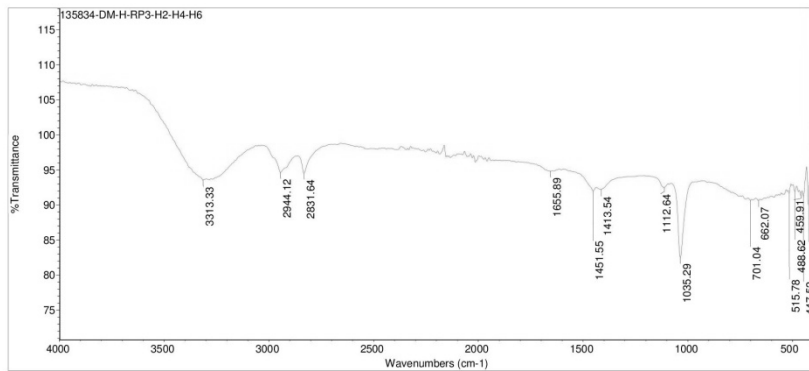
Appendix 75 - IR spectrum for compound **16** (MeOH).
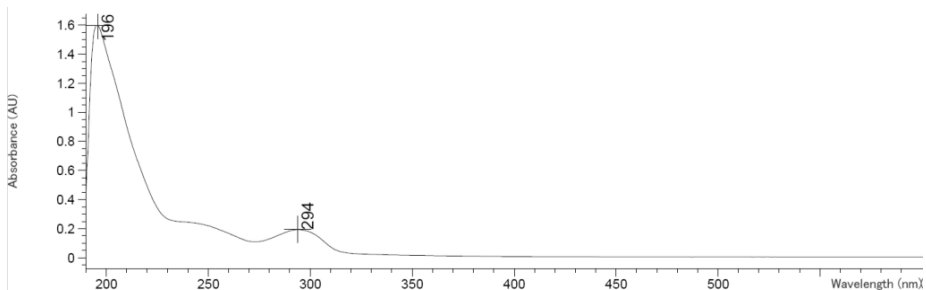
Appendix 76 - UV spectrum for compound **16** (MeOH).
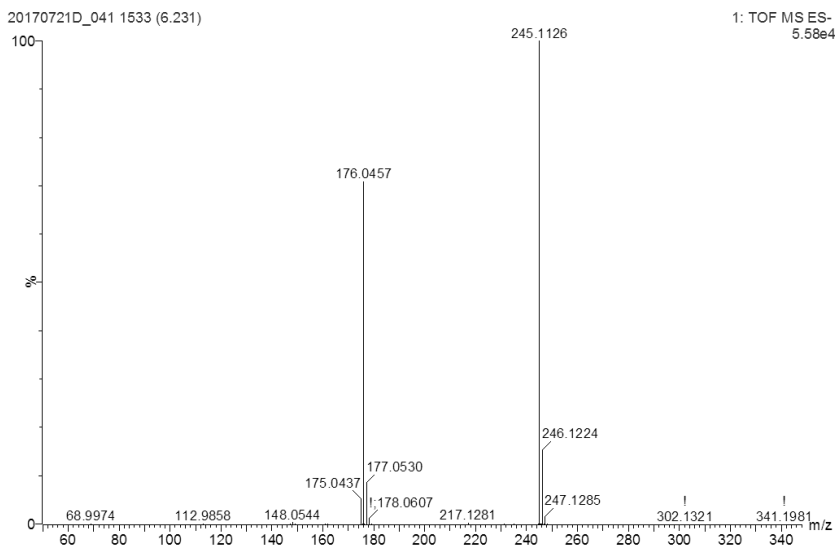
Appendix 77 - HRESIMS spectrum for compound **16**.
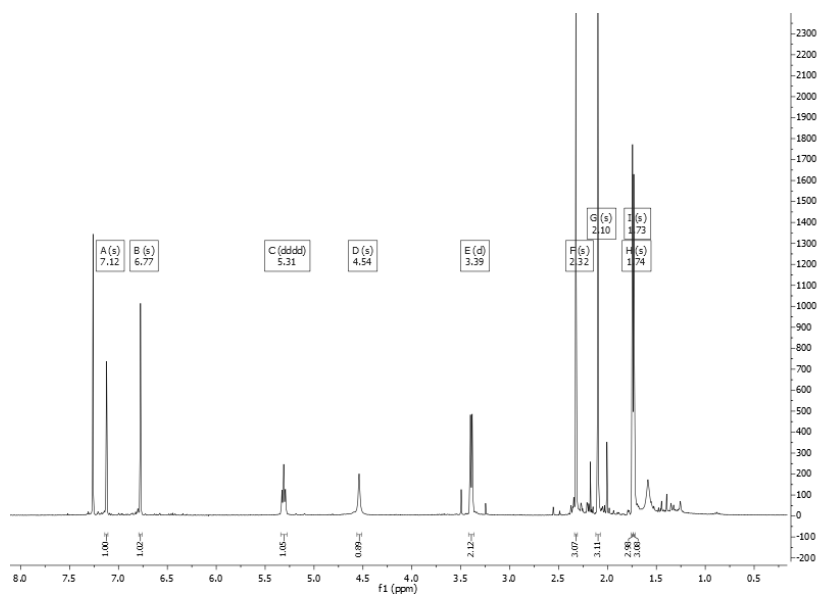
Appendix 78 - ^{1}H-NMR spectrum for compound **17** (400 MHz, CDCl$_3$).
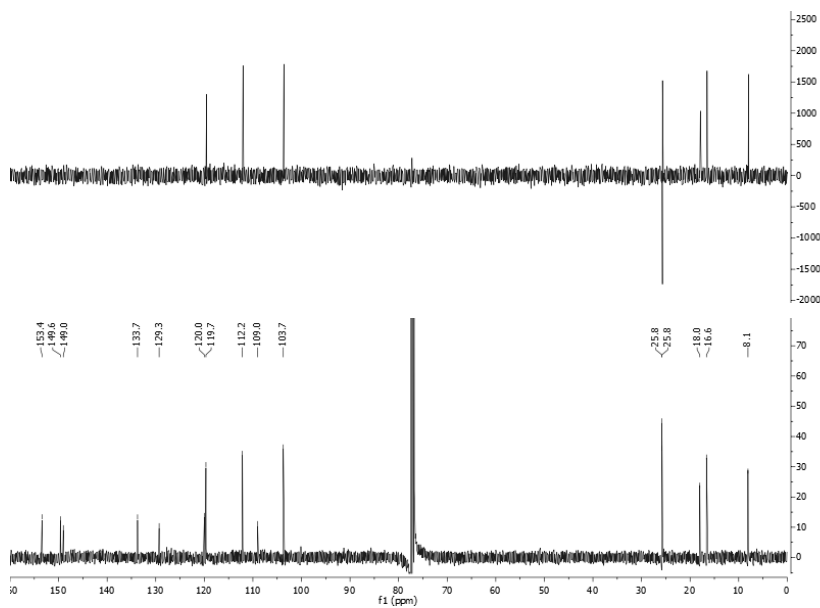
Appendix 79 - DEPT and ^{13}C-NMR spectra for compound **17** (100 MHz, CDCl$_3$).
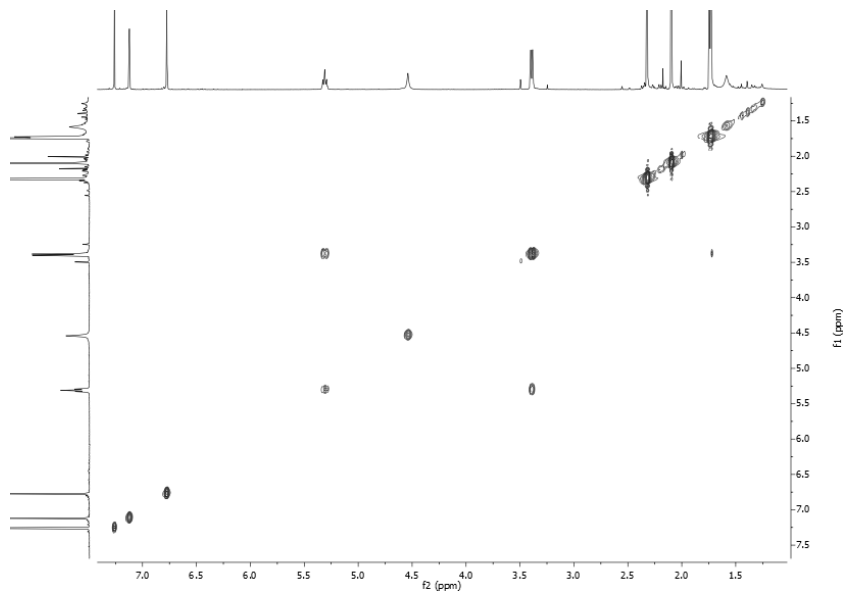
Appendix 80 - g-COSY spectrum for compound **17** (400 MHz, CDCl$_3$).
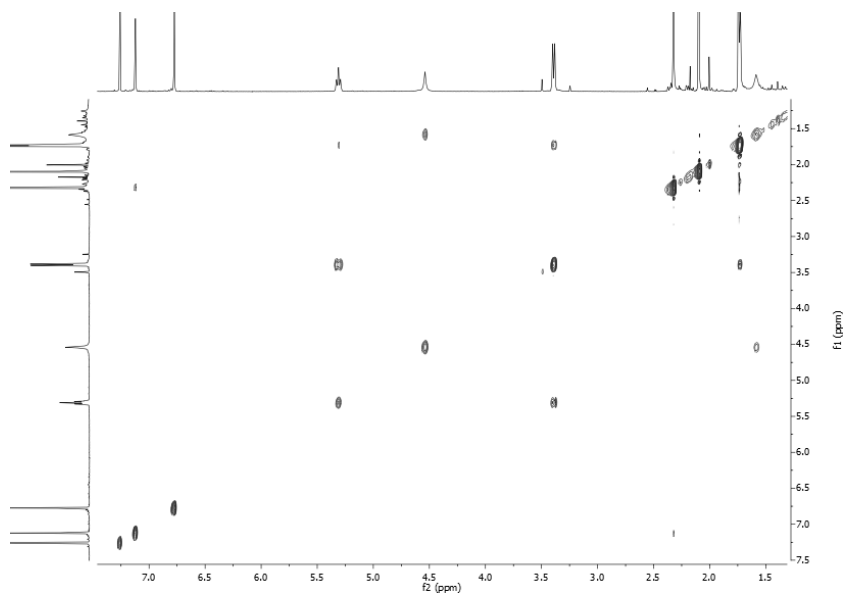
Appendix 81 - TOCSY spectrum for compound **17** (400 MHz, CDCl$_3$).
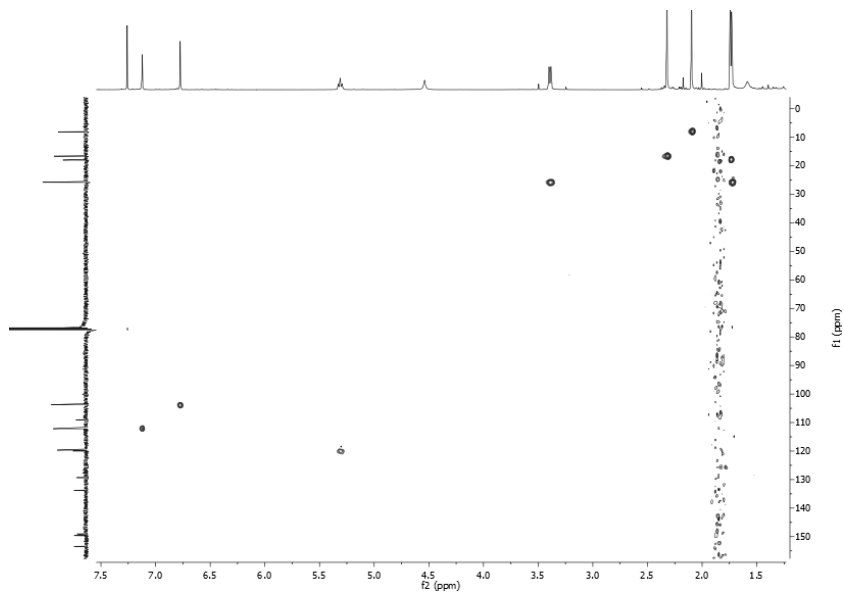
Appendix 82 - *g*-HSQC spectrum for compound **17** (400 MHz, CDCl₃).
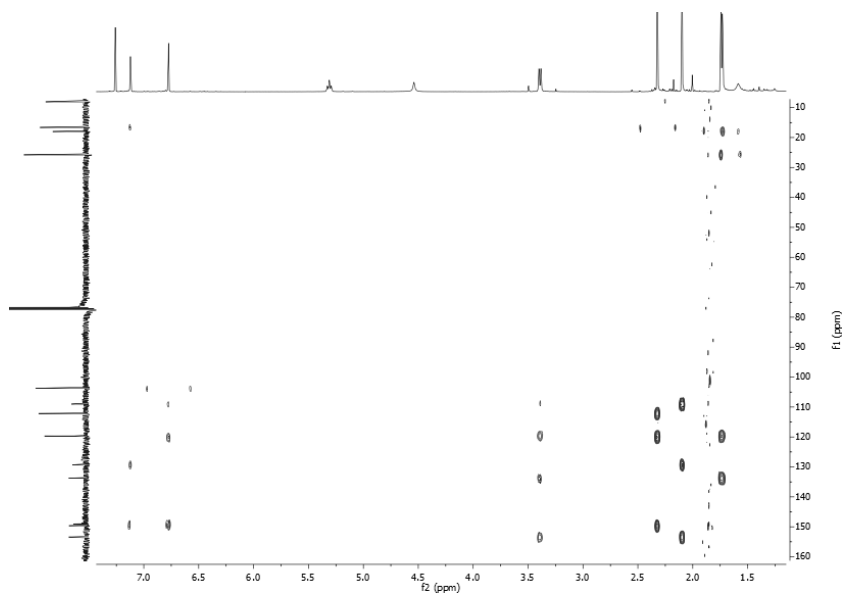
Appendix 83 - *g*-HMBC spectrum for compound **17** (400 MHz, CDCl₃).

167
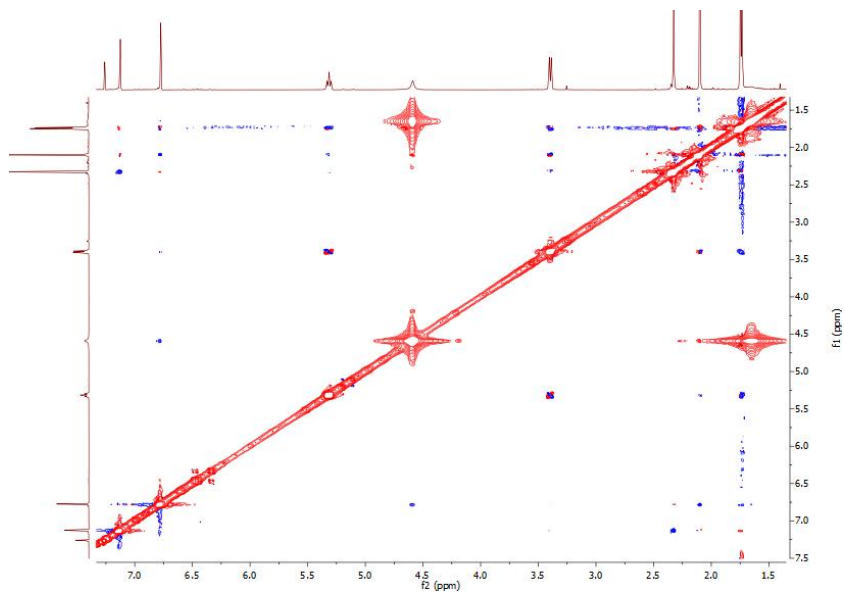
Appendix 84 - NOESY spectrum for compound **17** (400 MHz, CDCl$_3$).
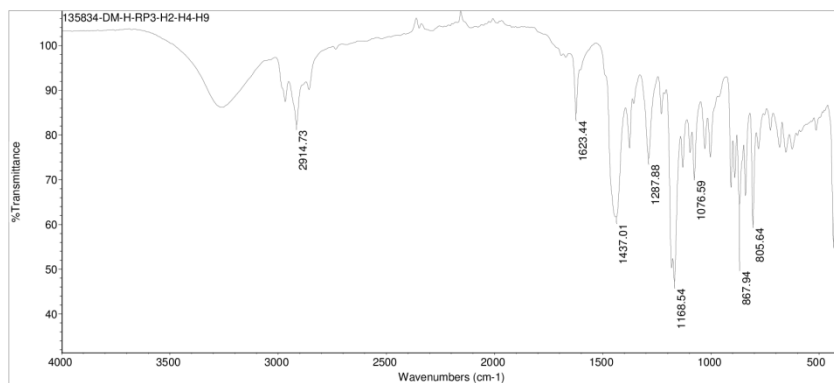
Appendix 85 - IR spectrum for compound **17** (neat).
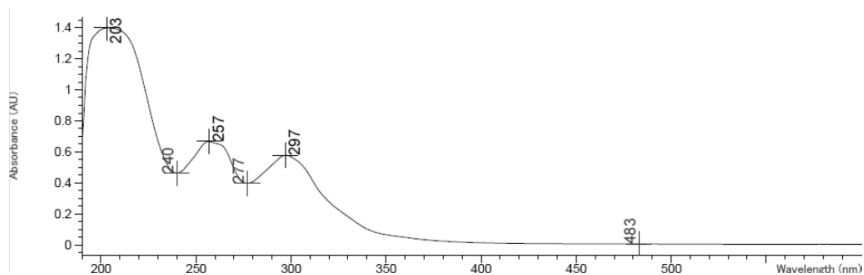
Appendix 86 - UV spectrum for compound **17** (MeOH).
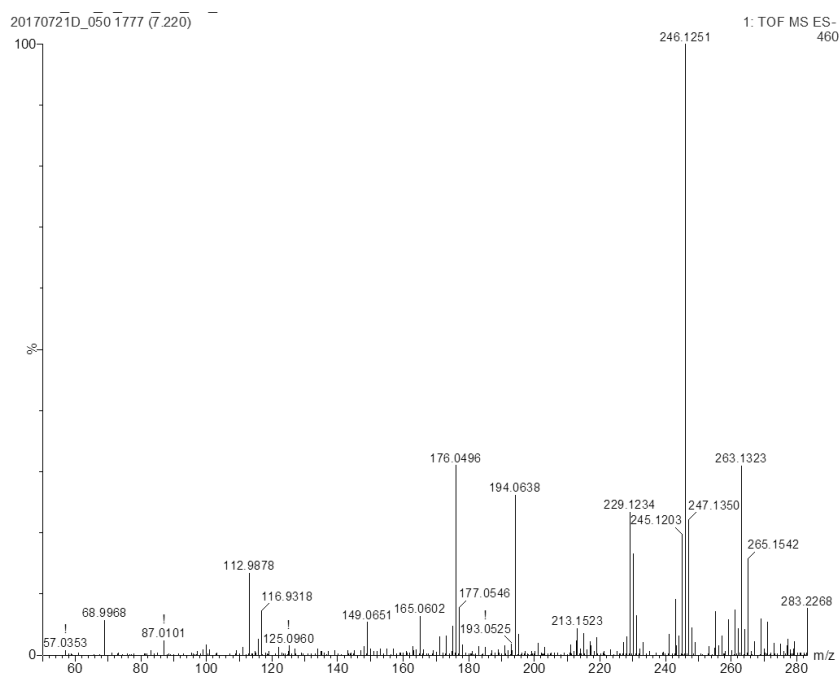
Appendix 87 - HRESIMS spectrum for compound **17**.
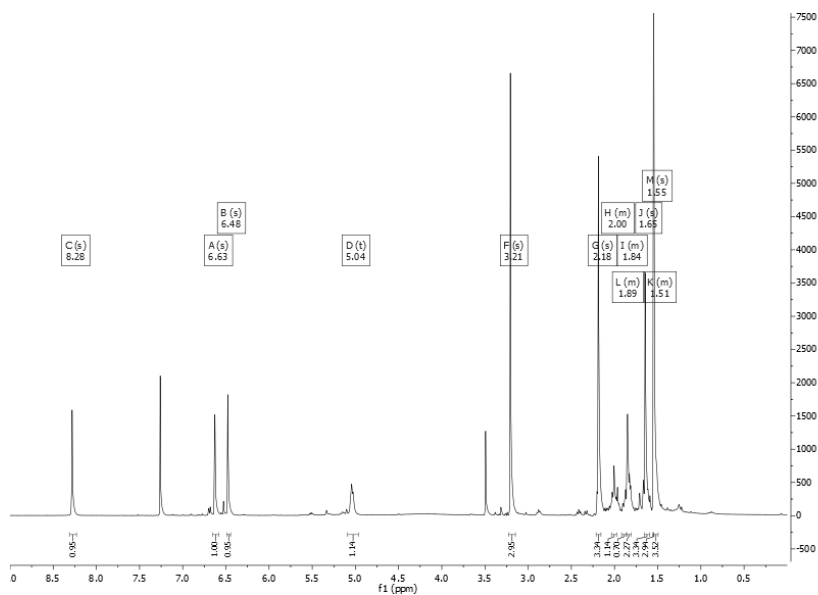
Appendix 88 - ^{1}H-NMR spectrum for compound **18** (400 MHz, CD$_3$OD).
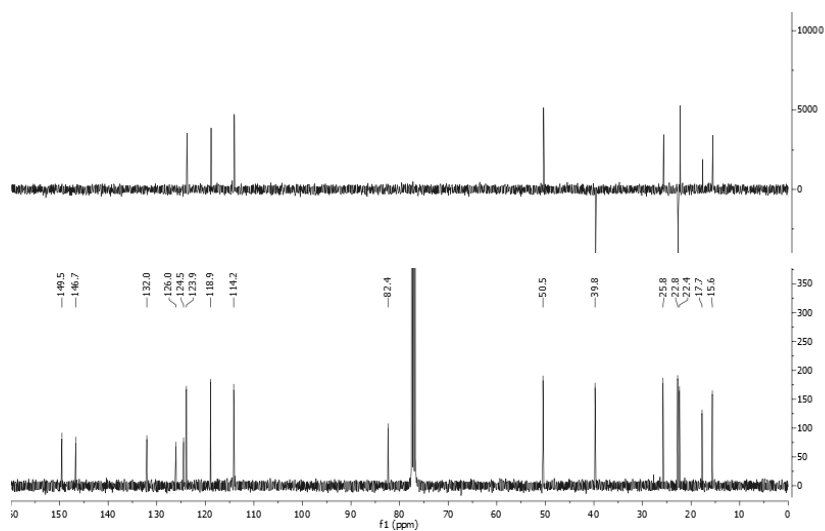
Appendix 89 - DEPT and ^{13}C-NMR spectra for compound **18** (100 MHz, CD$_3$OD).
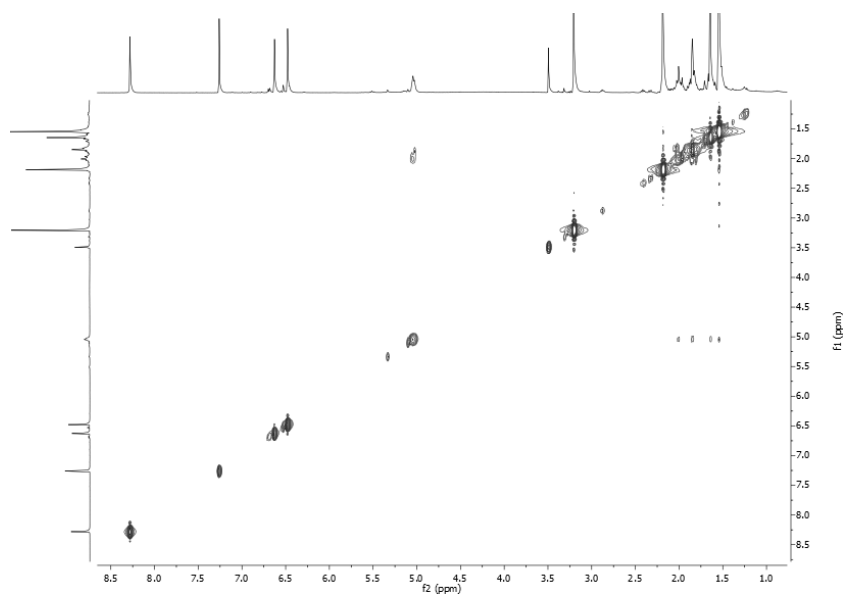
Appendix 90 - *g*-COSY spectrum for compound **18** (400 MHz, CD$_3$OD).
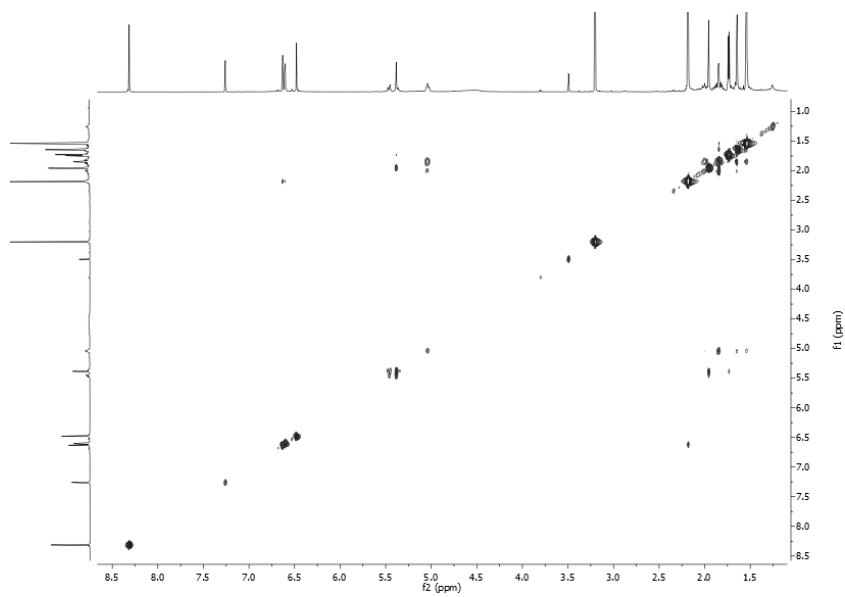
Appendix 91 - TOCSY spectrum for compound **18** (400 MHz, CD$_3$OD).

171
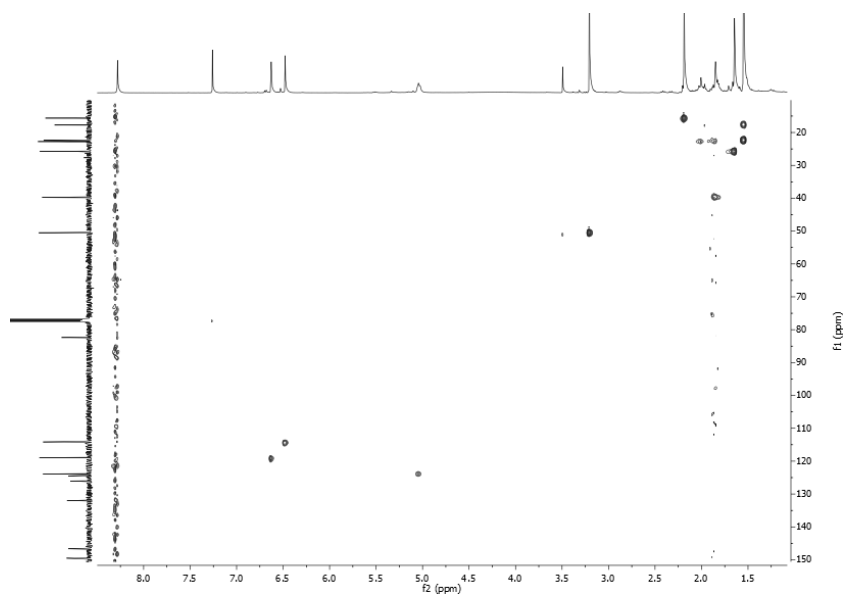
Appendix 92 - *g*-HSQC spectrum for compound **18** (400 MHz, CD₃OD).

Appendix 93 - *g*-HMBC spectrum for compound **18** (400 MHz, CD₃OD).

Appendix 94 - NOESY spectrum for compound **18** (400 MHz, CD$_3$OD).
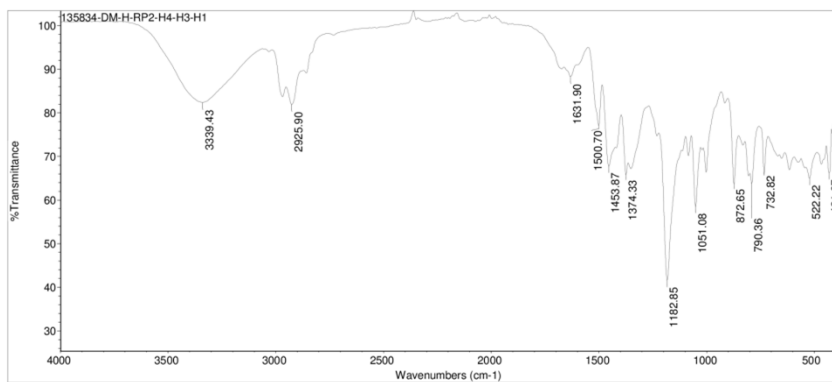
Appendix 95 - IR spectrum for compound **18** (MeOH).
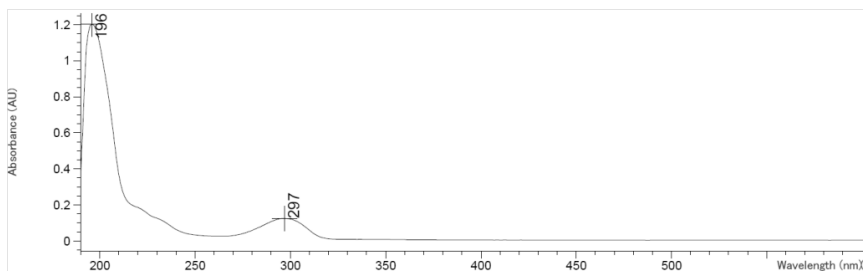
Appendix 96 - UV spectrum for compound **18** (MeOH).
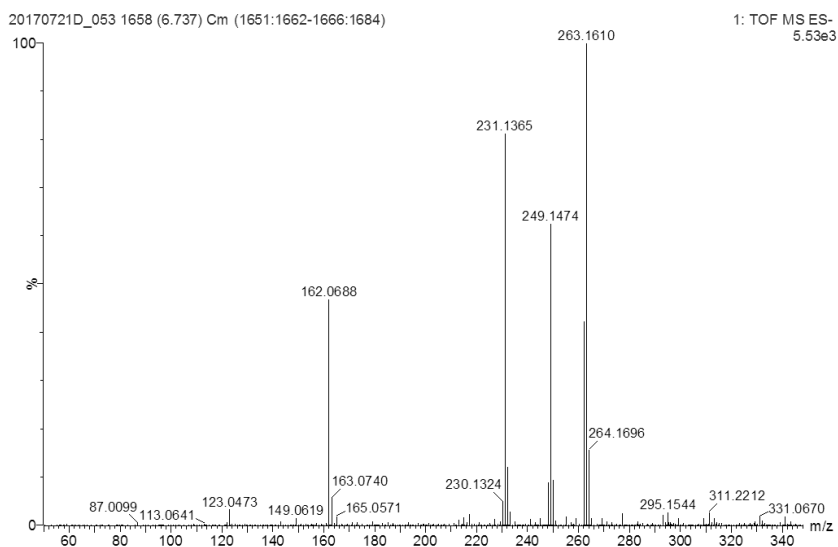
Appendix 97 - HRESIMS spectrum for compound **18**.

Appendix 98 - ^{1}H-NMR spectrum for compound **19** (400 MHz, CDCl$_3$).

Appendix 99 - DEPT and ^{13}C-NMR spectra for compound **19** (100 MHz, CDCl$_3$).

Appendix 100 - *g*-COSY spectrum for compound **19** (400 MHz, CDCl$_3$).

Appendix 101 - TOCSY spectrum for compound **19** (400 MHz, CDCl₃).
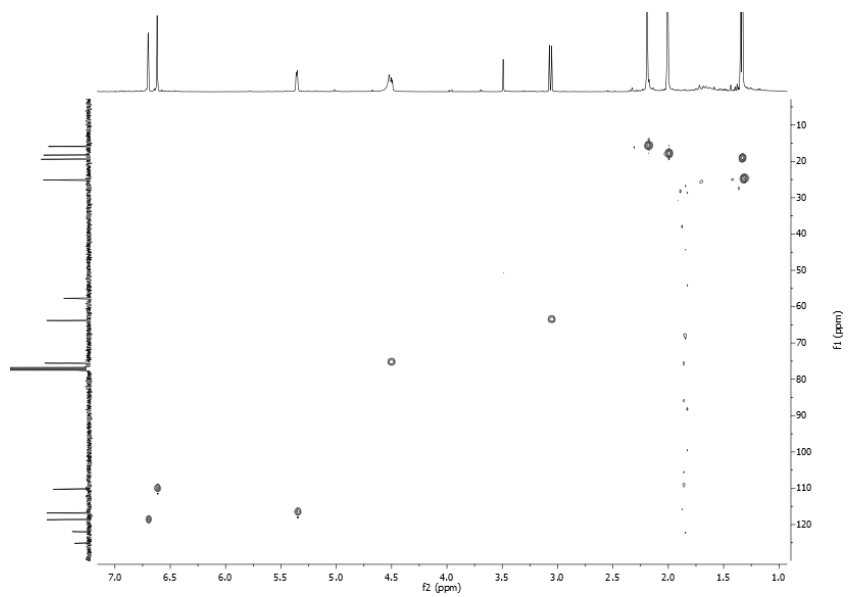
Appendix 102 - *g*-HSQC spectrum for compound **19** (400 MHz, CDCl₃).

176

Appendix 103 - *g*-HMBC spectrum for compound **19** (400 MHz, CDCl₃).

Appendix 104 - NOESY spectrum for compound **19** (400 MHz, CDCl3).

Appendix 105 - IR spectrum for compound **19** (MeOH).

Appendix 106 - UV spectrum for compound **19** (MeOH).

Appendix 107 - HRESIMS spectrum for compound **19**.
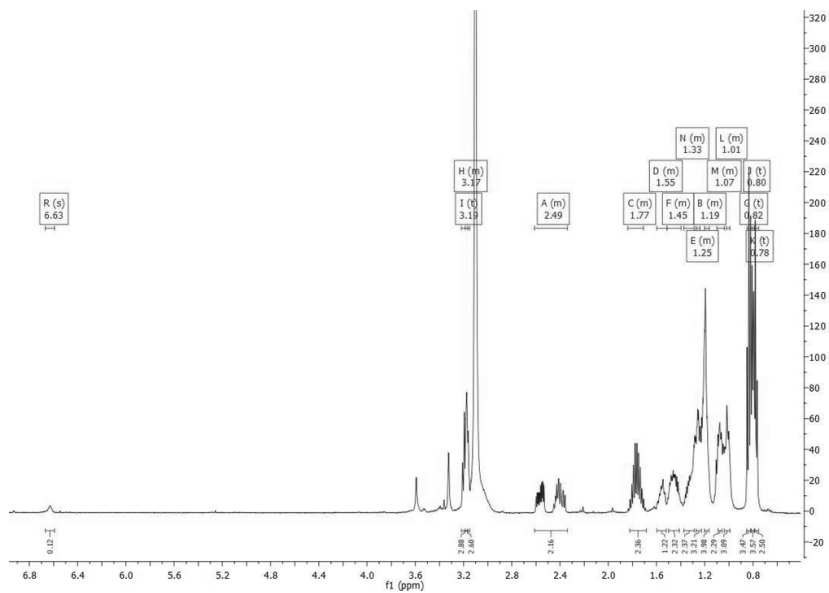
Appendix 108 - ^{1}H-NMR spectrum of **fluvirucinin C$_1$** (500 MHz, CDCl$_3$/CD$_3$OD).
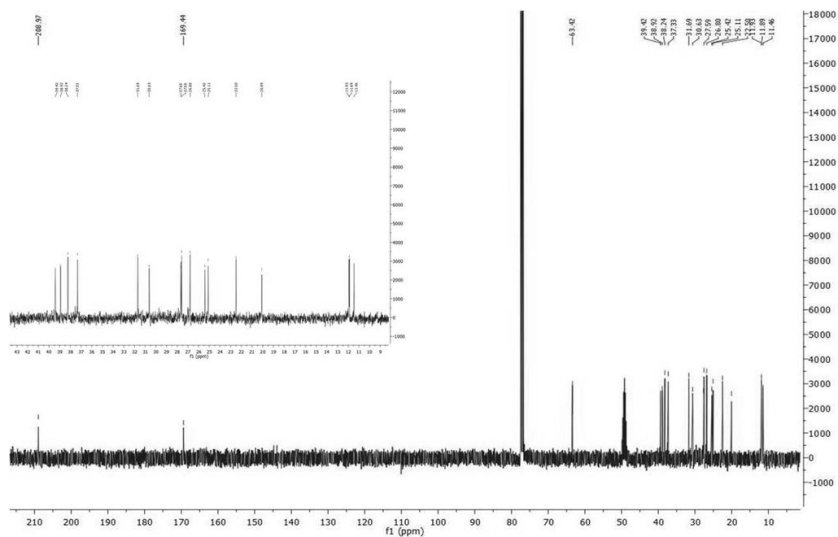
Appendix 109 - ^{13}C-NMR spectrum of **fluvirucinin C$_1$** (100 MHz, CDCl$_3$/CD$_3$OD).
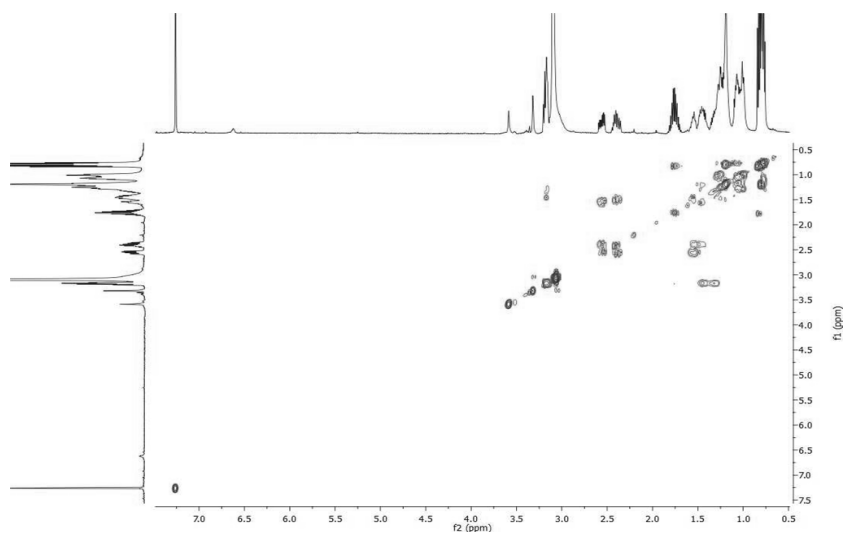
Appendix 110 - *g*-COSY spectrum of **fluvirucinin C$_1$** (500 MHz, CDCl$_3$/CD$_3$OD).
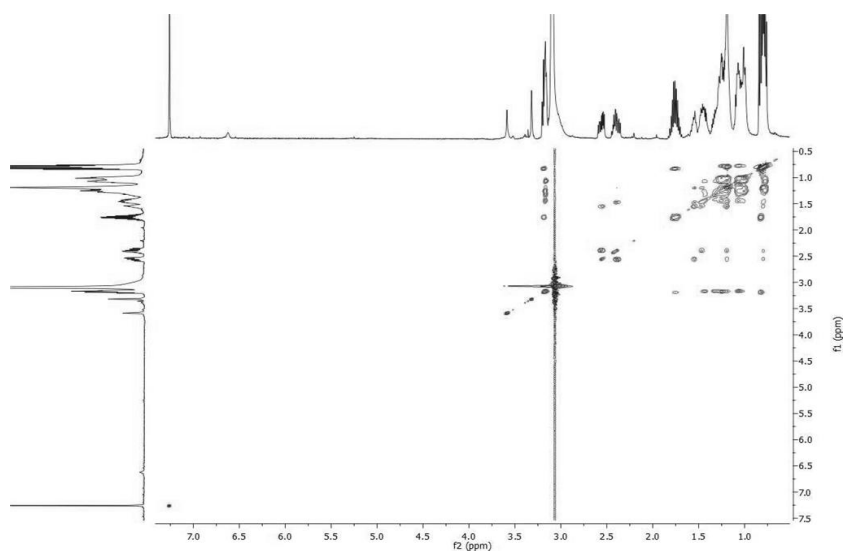
Appendix 111 - TOCSY spectrum of **fluvirucinin C$_1$** (500 MHz, CDCl$_3$/CD$_3$OD).
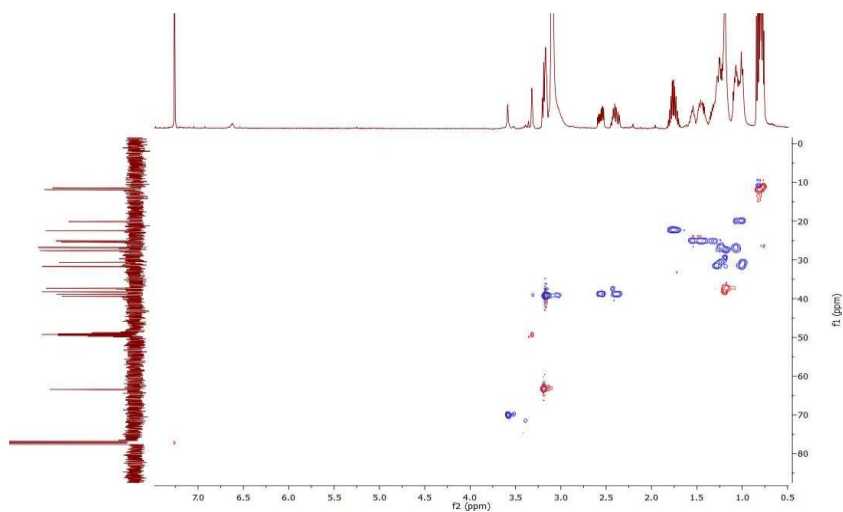
Appendix 112 - *g*-HSQC spectrum of **fluvirucinin C$_1$** (500 MHz, CDCl$_3$/CD$_3$OD).
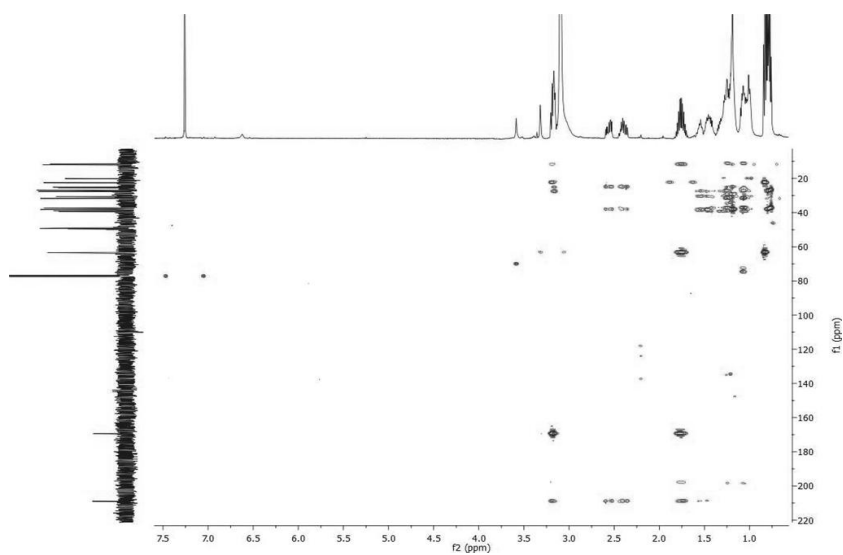
Appendix 113 - *g*-HMBC spectrum of **fluvirucinin C$_1$** (500 MHz, CDCl$_3$/CD$_3$OD).

181
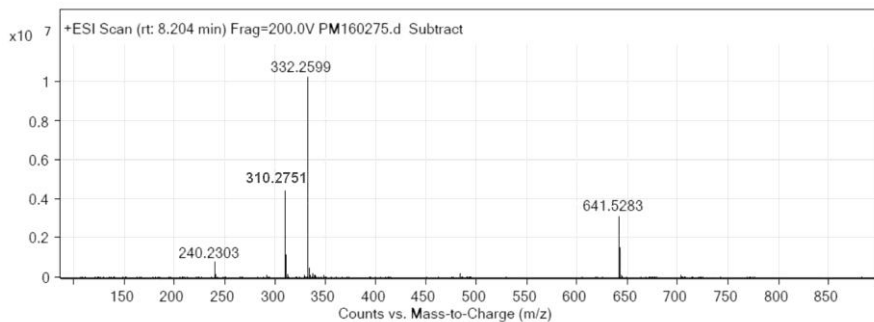
Appendix 114 - HRESIMS spectrum of **fluvirucinin C₁**.
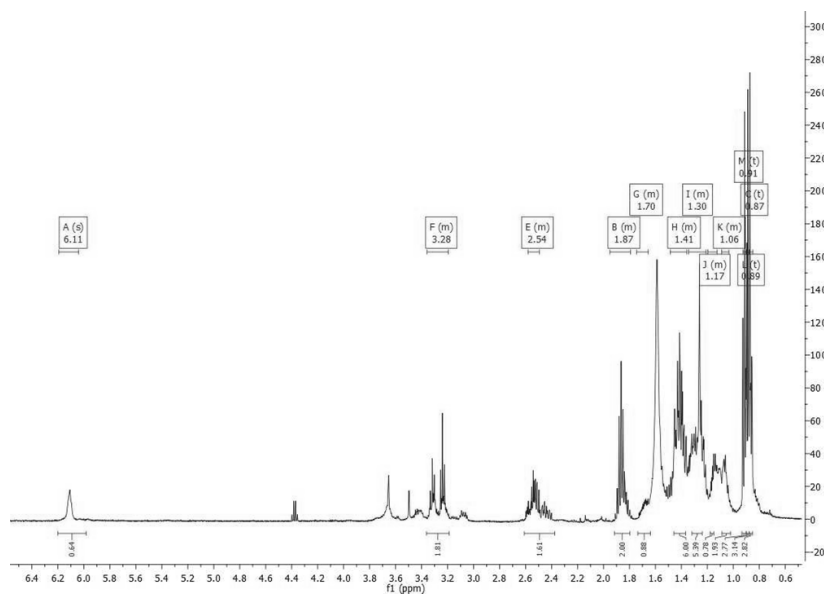
Appendix 115 - ¹H-NMR spectrum of **fluvirucinin C₂** (500 MHz, CDCl₃).

182

Appendix 116 - ^{13}H-NMR spectrum of **fluvirucinin C$_2$** (100 MHz, CDCl$_3$).

Appendix 117 - *g*-COSY spectrum of **fluvirucinin C$_2$** (500 MHz, CDCl$_3$).
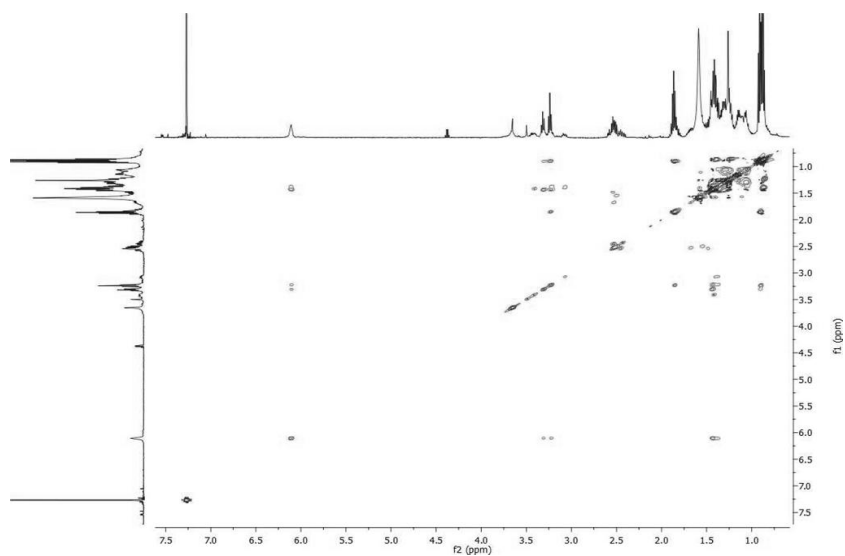
Appendix 118 - TOCSY spectrum of **fluvirucinin C₂** (500 MHz, CDCl₃).
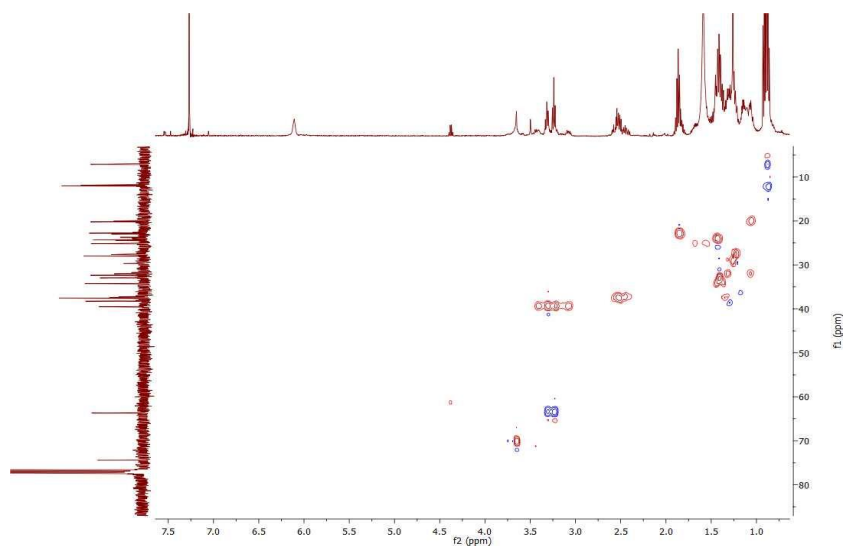
Appendix 119 - *g*-HSQC spectrum of **fluvirucinin C₂** (500 MHz, CDCl₃).
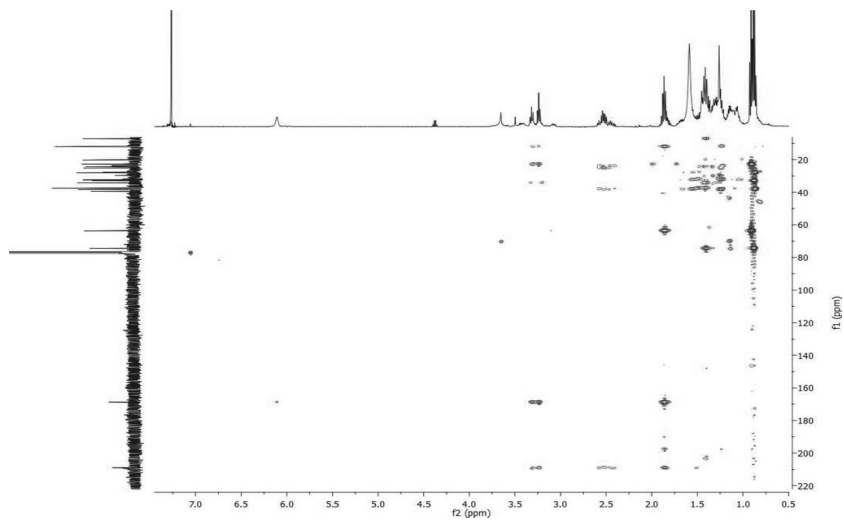
Appendix 120 - *g*-HMBC spectrum of **fluvirucinin C₂** (500 MHz, CDCl₃).
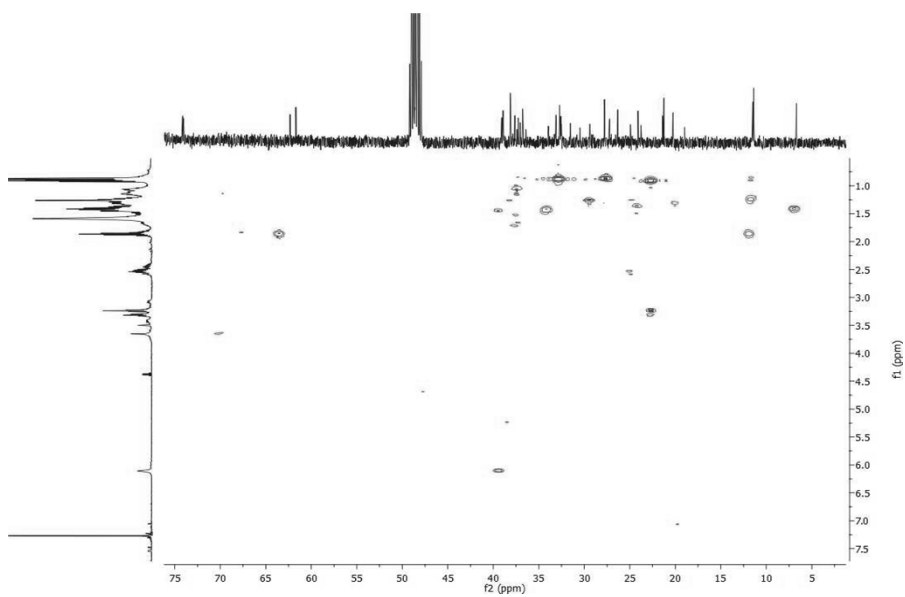
Appendix 121 - H2MBC spectrum of **fluvirucinin C₂** (500 MHz, CDCl₃).

185
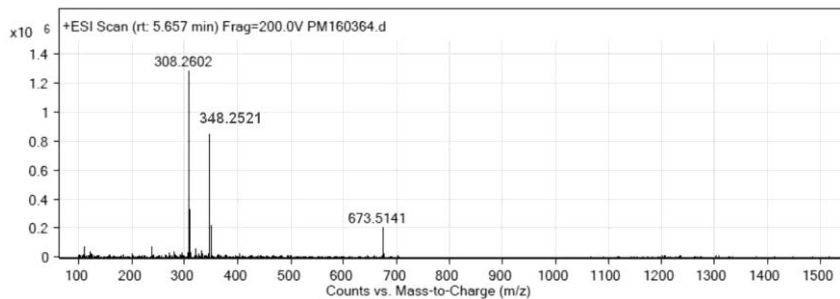
Appendix 122 - HRESIMS spectrum of **fluvirucinin C₂**.
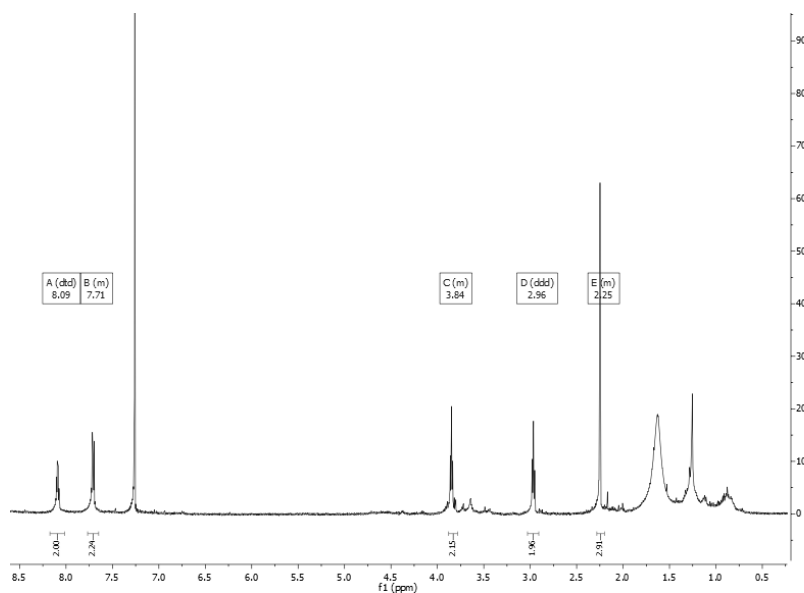
Appendix 123 - ¹H-NMR spectrum of **compound 22** (500 MHz, CDCl₃).
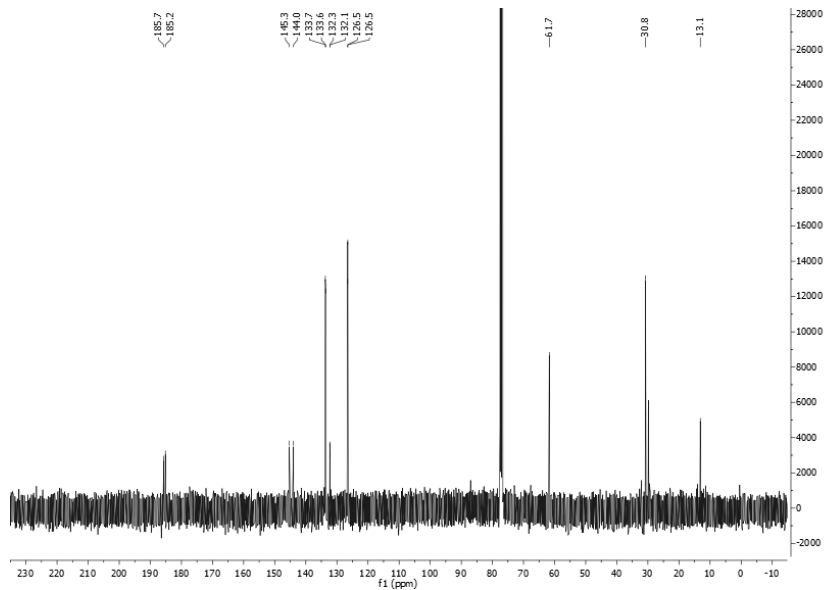
Appendix 124 - ^{13}C-NMR spectrum of **compound 22** (100 MHz, CDCl$_3$).
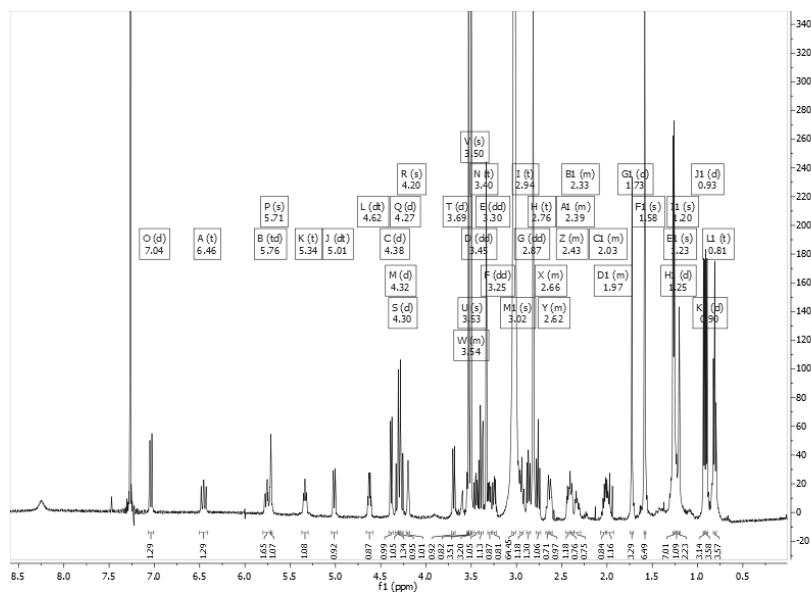
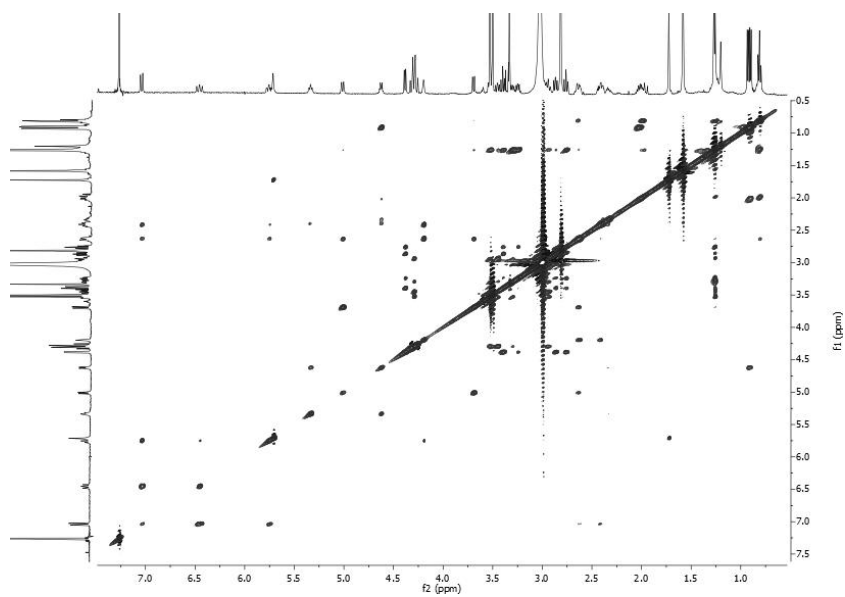**Appendix 125 -** ^{1}H-NMR spectrum of **mangrolide A** (500 MHz, CDCl$_3$/CD$_3$OD).
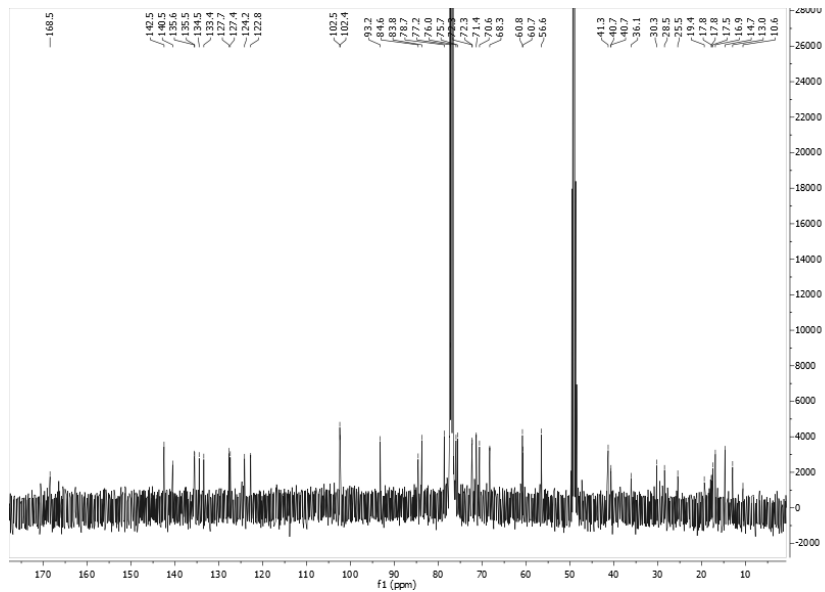
Appendix 126 - ^{13}C-NMR spectrum of **mangrolide A** (100 MHz, CDCl$_3$/CD$_3$OD).
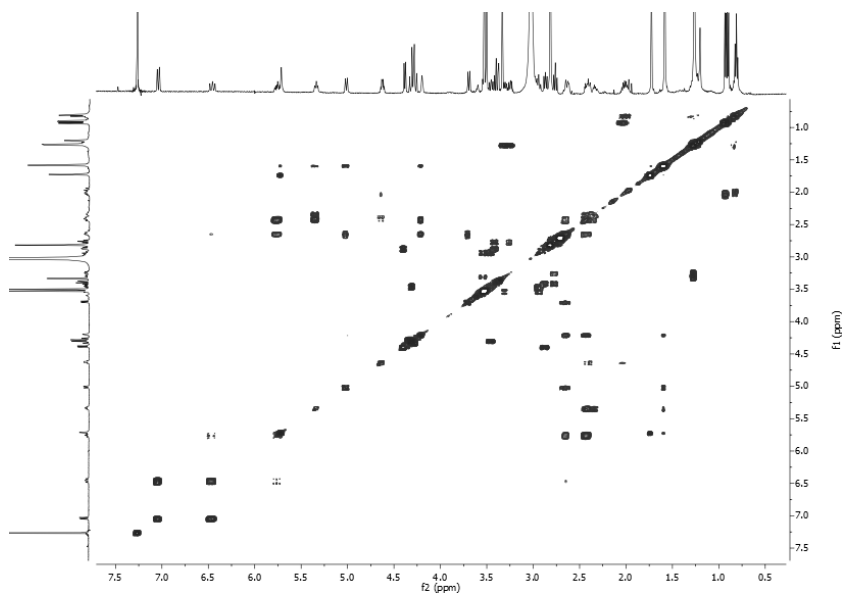
Appendix 127 - *g*-COSY spectrum of **mangrolide A** (500 MHz, CDCl$_3$/CD$_3$OD).
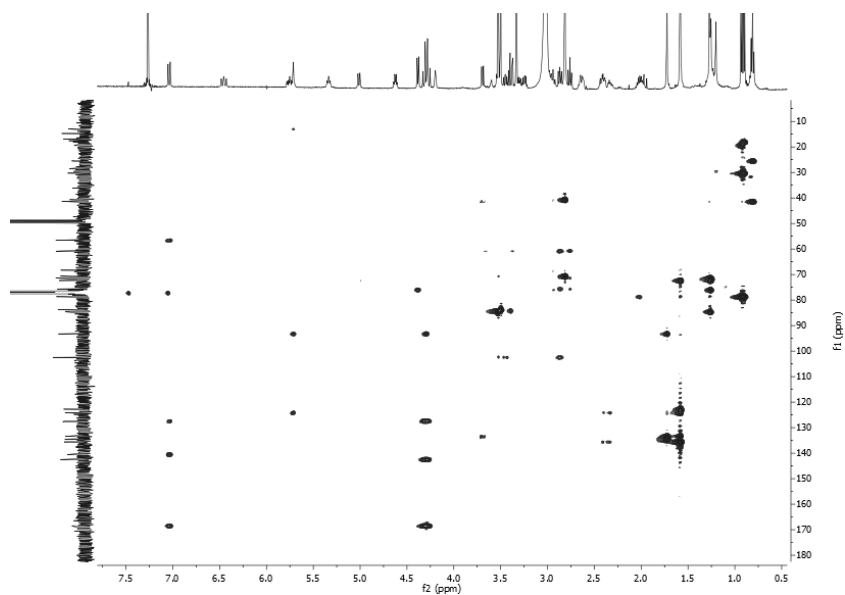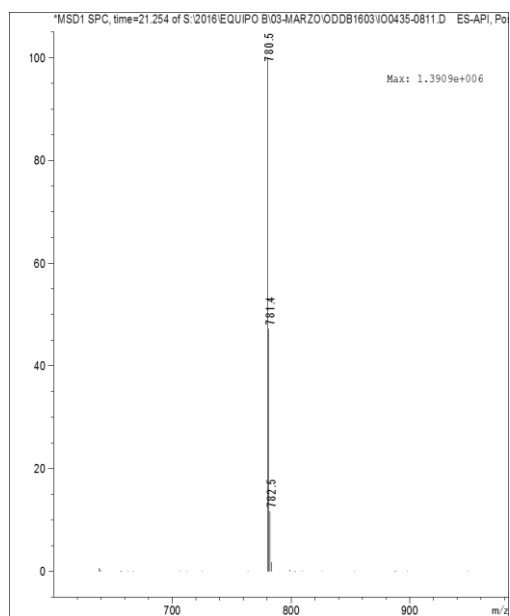
Appendix 128 - TOCSY spectrum of **mangrolide A** (500 MHz, CDCl$_3$/CD$_3$OD).
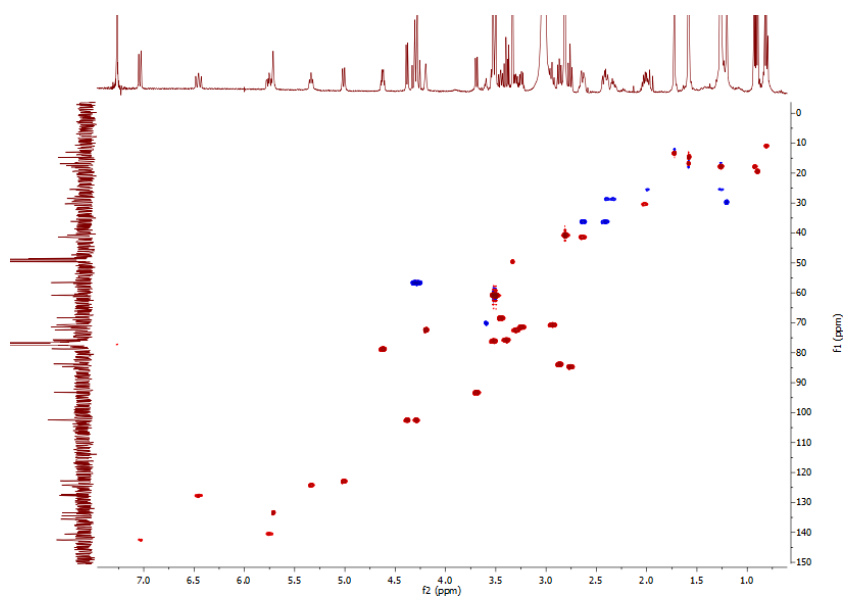
Appendix 129 - *g*-HSQC spectrum of **mangrolide A** (500 MHz, CDCl$_3$/CD$_3$OD).

Appendix 130 - *g*-HMBC spectrum of **mangrolide A** (500 MHz, CDCl$_3$/CD$_3$OD).

Appendix 131 - ESIMS spectrum of **mangrolide A**.